Zeitschrift für Geophysik

Probleme des Gesteins- und Paläomagnetismus

Veröffentlicht werden Originalarbeiten aus dem gesamten Gebiet der Geophysik und aus den Grenzgebieten in deutscher, englischer oder französischer Sprache. Außerdem erscheinen mehrmals im Jahr auf Einladung hin verfaßte Übersichtsartikel.

Für kurze Mitteilungen, bei denen Interesse an raschem Erscheinen besteht, gibt es neben den normalen Veröffentlichungen die „Briefe an den Herausgeber" (ohne Zusammenfassung). Sie werden nach Möglichkeit im nächsten Heft gebracht.

Jede Originalarbeit beginnt mit einer deutschen und einer englischen oder französischen Zusammenfassung. Bei deutschsprachigen Aufsätzen und Briefen werden Titel der Arbeit und Abbildungsunterschriften zusätzlich in englischer oder französischer Sprache gebracht.

Die Autoren erhalten 50 Sonderdrucke ihrer Arbeit kostenlos. Weitere Exemplare können vom Verlag gegen Berechnung geliefert werden. Eine Honorierung der Beiträge erfolgt nicht.

Es wird gebeten, die Manuskripte in Maschinenschrift mit handschriftlich eingetragenen Formeln druckfertig einzureichen und gesondert eine „Anweisung für den Setzer" beizufügen, aus der zu ersehen ist, wie kursiver, gesperrter oder fetter Satz und griechische, gotische oder einander ähnliche Typen und Zeichen kenntlich gemacht sind (z.B. durch farbige Unterstreichung). Die Vorlagen für die Abbildungen sollen reproduktionsfertig (Tuschzeichnung) möglichst im Maßstab 2:1 eingesandt werden.

Die Zitate sollen entsprechend folgendem Beispiel angefertigt werden:

Im Text: Bei der ersten Zitierung [JUNG, MENZEL und ROSENBACH 1965], bei jeder folgenden Zitierung [JUNG et al. 1965]. Im Literaturverzeichnis: JUNG, K., H. MENZEL und O. ROSENBACH: Gravimetermessungen im Nördlinger Ries. Z. Geophys. 31, 7—26, 1965.

Manuskripte sind zu senden an Prof. Dr. WALTER DIEMINGER, Max-Planck-Institut für Aeronomie, 3411 Lindau/Harz.

Anschrift der *Deutschen Geophysikalischen Gesellschaft:*

2 Hamburg 13, Binderstr. 22.   Postscheckkonto: Hamburg 55983

Bank: Neue Sparcasse, Hamburg 24/11528

Aufgenommen werden nur Arbeiten, die weder im In- noch im Ausland veröffentlicht wurden und die der Autor auch anderweitig nicht zu veröffentlichen sich verpflichtet. Mit der Annahme des Manuskriptes geht das ausschließliche Nutzungsrecht an den Verlag über.

INHALTSVERZEICHNIS

Vorwort

Die in diesem Sonderheft der Zeitschrift für Geophysik erschienenen Artikel basieren auf Vorträgen, die bei einem Kolloquium über „Probleme des Gesteins- und Paläomagnetismus" vom 15. bis 17. Dezember 1970 im Institut für Angewandte Geophysik der Universität München gehalten worden waren. Der Charakter der Veranstaltung war weniger der einer wohlorganisierten Tagung mit einer Einladung aller daran interessierten Wissenschaftler, als der einer recht kurzfristig geplanten und improvisierten Arbeitsbesprechung. Der Diskussion der einzelnen Vorträge wurde deshalb besonders viel Zeit gewidmet.

Die Anregung zu dieser Arbeitstagung gaben die angekündigten Besuche von zwei Wissenschaftler-Gruppen aus dem Ausland. Dies wurde zum Anlaß genommen, noch einige weitere auf dem Gebiet des Gesteins- und Paläomagnetismus in Mitteleuropa tätige Arbeitsgruppen auf das Treffen aufmerksam zu machen und zu Vorträgen einzuladen.

In über 20 Vorträgen und Diskussionsbeiträgen berichteten die einzelnen Gruppen über ihre neuesten Ergebnisse auf dem Gebiet des Gesteins- und Paläomagnetismus, tauschten Erfahrungen aus und gaben sich gegenseitig Anregungen zur Fortführung individueller und gemeinsamer Projekte. Die Skala der Themen reichte dabei von der Herstellung synthetischer Titanomagnetite und Chromspinelle und der Interpretation ihrer strukturellen und magnetischen Eigenschaften, über Probleme der Stabilität der remanenten Magnetisierung und Fragen der Entmagnetisierung, über die Anwendung dieser Ergebnisse auf paläomagnetische Messungen an Gesteinen unterschiedlichen Alters bis zu Fragen im Zusammenhang mit der Interpretation der Anomalien des Magnetfeldes im Bereich der mittelozeanischen Rücken.

Den Herausgebern der Zeitschrift für Geophysik sind wir zu großem Dank verpflichtet für die Möglichkeit, die Vorträge rasch in einem Sonderheft publizieren zu können. Herrn Prof. Dr. G. ANGENHEISTER vom Institut für Angewandte Geophysik der Universität München danken wir für seine Unterstützung bei der Organisation des Kolloquiums.

München, den 31. März 1971

<div align="right">

H. SOFFEL
N. PETERSEN

</div>

Cation Distribution in Titanomagnetites

U. BLEIL, München[1])

Summary: The theories and models proposed in literature for the cation distribution in the titanomagnetite spinel lattice are briefly reviewed and compared with present measurements of the saturation magnetization and data of previous workers. It can be shown that only temperature dependent arrangements give suitable agreement with these experimental results. The tendency of the different cations to preferentially occupy certain lattice sites (Fe^{3+}: tetrahedral sites, Ti^{4+}: octahedral sites) is changed with increasing temperature towards a more statistic distribution. An attempt was made to describe the ionic configuration in thermodynamic equilibrium state by means of an activation energy ΔE related to the Fe^{3+}—Fe^{2+} interchange between both sublattice sites. However, satisfactory agreement can only be obtained by assuming that ΔE is not a constant but includes distribution-sensitive components and consequently depends on composition as well as on temperature.

Zusammenfassung: In einer Übersicht werden die bislang veröffentlichten Modelle und Theorien zur Verteilung der Kationen im Spinellgitter der Titanomagnetite den Ergebnissen eigener Messungen der Sättigungsmagnetisierung und Literaturwerten gegenübergestellt. Der Vergleich zeigt, daß ausschließlich temperaturabhängige Anordnungen geeignet sind, die experimentellen Resultate hinreichend zu erklären. Die Grundtendenz der einzelnen Ionentypen, bevorzugt bestimmte Gitterplätze einzunehmen (Fe^{3+}: Tetraederplätze, Ti^{4+}: Oktaederplätze), ändert sich mit steigender Temperatur in Richtung auf eine mehr statistische Verteilung. Der Versuch, die thermischen Gleichgewichte gesetzmäßig mit Hilfe einer nur von der Probenzusammensetzung abhängigen Aktivierungsenergie zu beschreiben, erweist sich als unzureichend; vielmehr müssen auch solche Energieterme berücksichtigt werden, die ihrerseits von der jeweiligen Besetzung der Gitterplätze und damit von der Temperatur bestimmt sind.

1. Introduction

The most abundant ferrimagnetic substances in igneous rocks are titanomagnetites derived from magnetite (Fe_3O_4) by substitution of Ti^{4+} ions for Fe^{3+} ions, together with a change in ionozation of an Fe^{3+} ion to an Fe^{2+} ion. The gradual addition of titanium to magnetite finally produces ulvöspinel (Fe_2TiO_4). At high temperature there exists a complete solid solution series between these two end members [AKIMOTO, KATSURA and YOSHIDA 1957] of the general formula:

$$x\,Fe_2TiO_4\,(1-x)\,Fe_3O_4 \equiv Ti_xFe_{3-x}O_4; \quad 0 \leq x \leq 1 \tag{1}$$

---
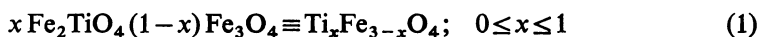
[1]) Dipl.-Phys. U. BLEIL, Institut für Angewandte Geophysik der Universität München, 8 München 2, Richard-Wagner-Straße 10.

In order to discuss their crystallographic and magnetic properties the first major consideration is the cation distribution.

2. Crystallographic and magnetic structure

The crystal structure is known to be of spinel type characterized by a face-centred, cubic close-packed arrangement of oxygen ions with metal ions fitting into the interstices and forming two sublattices. In tetrahedral (A) sites cations are surrounded by a tetrahedron of oxygen ions while in octahedral (B) sites six oxygen ions surround each cation. The unit cell contains eight molecules of $MeMe_2{}^*O_4$ where Me and Me* represent cations of one or more kinds in any proportion on A and B sites respectively. The distribution of cations in a single spinel containing only two types of metal ions may be

a) 'normal', with one Me in the A sites and two Me* in the B sites, that is in the usual notation $Me[Me^*{}_2]O_4{}^{2-}$
b) 'inverse' $Me^*[Me^*Me]O_4{}^{2-}$
c) 'intermediate' $Me_a Me^*{}_{1-a}[Me_{1-a}Me^*{}_{1+a}]O_4{}^{2-}$; $0 \leq a \leq 1$.

The end members of the titanomagnetite solid solution series are both inverse spinels [Bragg 1915; Barth and Posnjak 1932]:

$$Fe^{3+}[Fe^{3+}Fe^{2+}]O_4^{2-} \quad \text{magnetite} \tag{2}$$

$$Fe^{2+}[Fe^{2+}Ti^{4+}]O_4^{2-} \quad \text{ulvöspinel} \tag{3}$$

Regarding the intermediate members the problem consists in distributing (see equ. (1)—(3)) the xTi^{4+}, $(2-2x)Fe^{3+}$ and $(1+x)Fe^{2+}$ ions between two types of site, one of which can hold two ions the other holding one ion.

The highest entropy would be gained for a completely random arrangement:

$$Fe^{3+}_{\frac{2+2x}{3}}Fe^{2+}_{\frac{1+x}{3}}Ti^{4+}_{\frac{x}{3}}\left[Fe^{3+}_{\frac{2(2-2x)}{3}}Fe^{2+}_{\frac{2(1+x)}{3}}Ti^{4+}_{\frac{2x}{3}}\right]O_4^{2-} \tag{4}$$
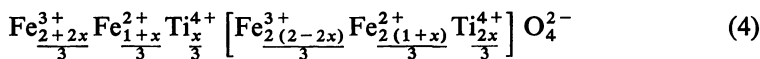
i. e. the general formula of titanomagnetites is given by:

$$Fe^{3+}_{(2-2x)a}Fe^{2+}_{(1+x)b}Ti^{4+}_{xc}\left[Fe^{3+}_{(2-2x)(1-a)}Fe^{2+}_{(1+x)(1-b)}Ti^{4+}_{x(1-c)}\right]O_4^{2-} \tag{5}$$
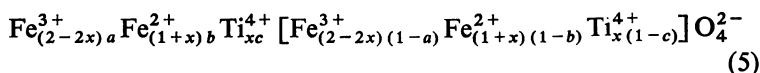
where a, b and c are the distribution parameters of Fe^{3+}, Fe^{2+} and Ti^{4+} respectively.

Assuming that the major magnetic interaction is of Neel $A-B$ antiferromagnetic type, in large magnetic fields at low temperatures all elementary atomic moments of sublattice A should align themselves antiparallel to those of sublattice B. Furthermore, as the ferrigmagnetic spinels may be considered to be essentially ionic, the atomic

moments of Fe^{3+} and Fe^{2+} are given to be 5 and 4 BOHR magnetons respectively. Thus the saturation magnetic moments μ will be the difference between the two sublattice moments and closely related to the distribution of cations:

$$\mu = 2(7-3x) - 20a(1-x) - 8b(1+x) \tag{6}$$

VERWEY and HEILMANN [1947] noted that most cations show a certain preference for either A or B sites, which depends primarily on charge and size of the ions. According to them Ti^{4+} has a strong tendency for octahedral, Fe^{3+} for tetrahedral sites. BLASSE [1964] who investigated several spinel systems containing Ti^{4+}, Fe^{3+}, Mg, Co and Li has found that Ti^{4+} always occupied B sites. Analysing neutron diffraction patterns of both polycrystalline materials and single crystals ISHIKAWA, AKIMOTO and SYONO [1964] proved within an error of 1% that this was also true for titanomagnetites. However GORTER [1957] reported that in the system $NiFe_2O_4$—$Ni_{1.5}FeTi_{0.5}O_4$ a fraction of Ti^{4+} also occured in tetrahedral sites and FORSTER and HALL [1965] suggested from neutron diffraction data that Fe_2TiO_4 is not a completely inverse spinel. They found only $0.92\ Ti^{4+}$ in octahedral sites working on a polycrystalline sample. In spite of the latter two results, the hypothesis concerning cation distribution of titanomagnetites were with one exception derived on the basis that Ti^{4+} is exclusively located in octahedral sites. Regarding equation (5) c would then become zero.

The total number of A sites per formula unit equals 1:

$$(2-2x)a + (1+x) = 1$$

substituting for b in (5) and (6) yields the equations:

$$Fe^{3+}_{(2-2x)a}Fe^{2+}_{1-(2-2x)a}[Fe^{3+}_{(2-2x)(1-a)}Fe^{2+}_{x+(2-2x)a}Ti^{4+}_x]O^{2-}_4 \tag{7}$$

$$\mu = (1-x)(6-4a) \tag{8}$$

Setting $a = 0.5$:

$$Fe^{3+}_{1-x}Fe^{2+}_x[Fe^{3+}_{1-x}Fe^{2+}_1Ti^{4+}_x]O^{2-}_4 \tag{7a}$$

$$\mu = 4 - 4x \tag{8a}$$

this arrangement is schematically represented in Fig. 1. It was proposed by AKIMOTO [1954]. The individual cations in both sites vary linearly between the concentrations found in the two end members and the saturation magnetization behaves in a similar way (see Fig. 3, 4). A second model (Fig. 2) is due to NEEL [1955] and CHEVALLIER, BOLFA and MATHIEU [1955]. They take into account the preference of Fe^{3+} for tetra-
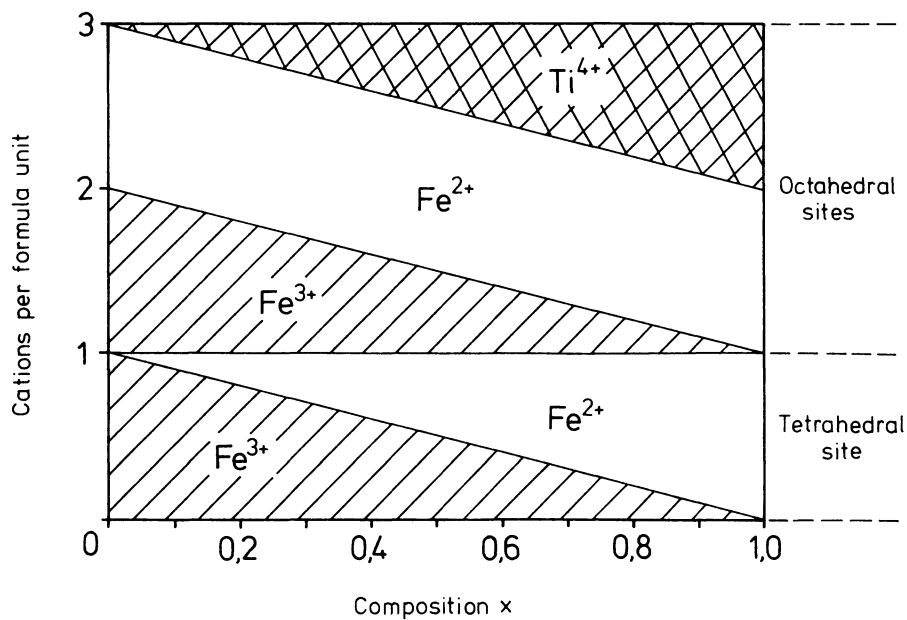
Fig. 1: Schematic cation distribution of the AKIMOTO model (after STEPHENSON 1969).
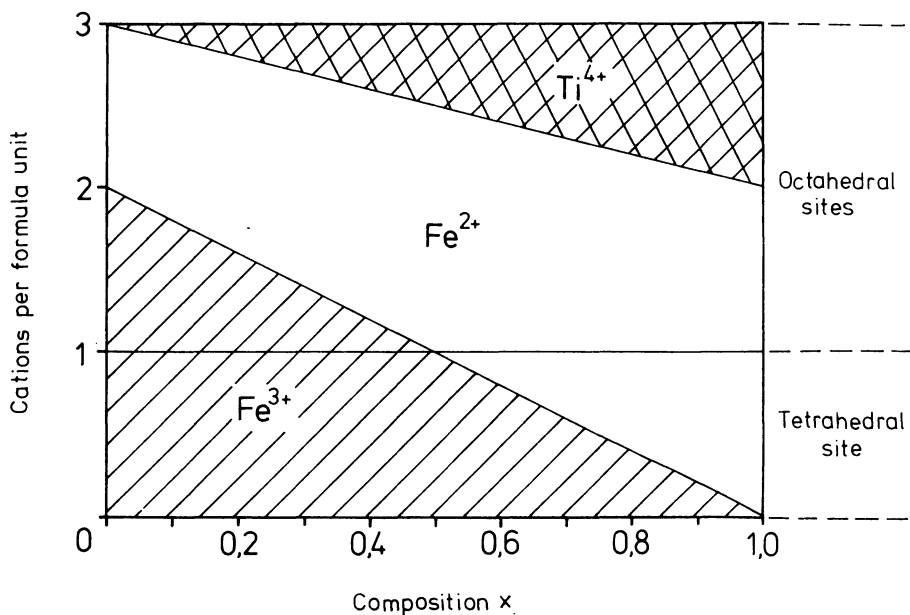
Fig. 2: Schematic cation distribution of the NEEL/CHEVALLIER model (after STEPHENSON 1969).
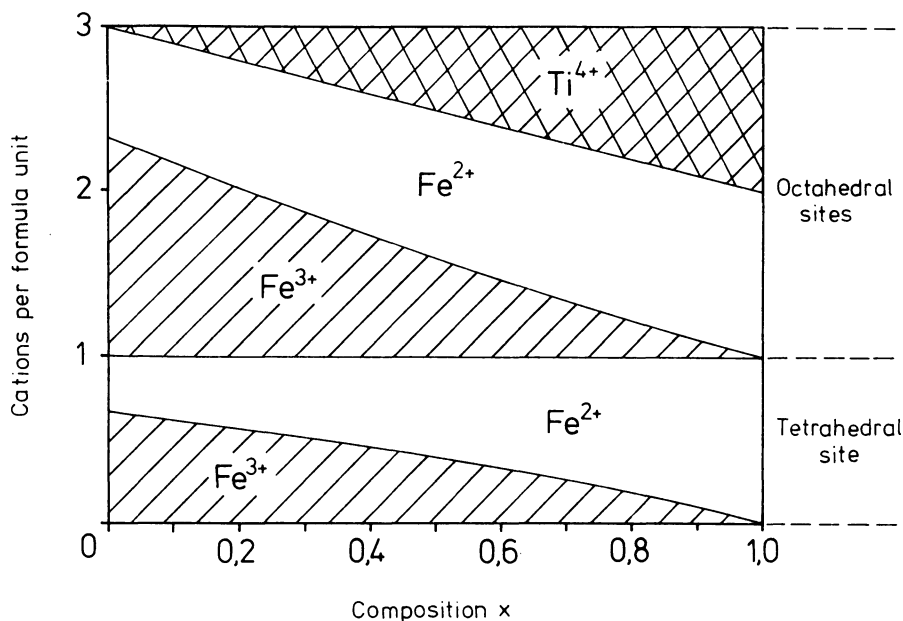
Fig. 3: Schematic cation distribution in which the ferrous-ferric ratio in both A and B sites is the same over the whole range of composition.

hedral sites; over the whole range of composition all available Fe^{3+} ions are supposed to be located in the A site:

$$Fe^{3+}_{2-2x} Fe^{2+}_{2x-1} \left[Fe^{2+}_{2-x} Ti^{4+}_{x} \right] O^{2-}_{4} \quad \text{for } x \geq 0.5 \text{ i.e. } a = 1$$

$$Fe^{3+}_{1} \left[Fe^{3+}_{1-2x} Fe^{2+}_{x+1} Ti^{4+}_{x} \right] O^{2-}_{4} \quad \text{for } x \leq 0.5 \text{ i.e. } a = \frac{1}{2-2x} \quad (7\,b)$$
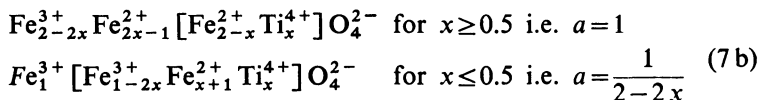
$$\mu = 2 - 2x \text{ for } x \geq 0.5$$
$$\mu = 4 - 6x \text{ for } x \leq 0.5 \quad (8\,b)$$

A cation distribution in which the ferrous—ferric ion ratio in both A and B sites is the same over the whole range of composition corresponds to $a = 1/3 - x$ (see Fig. 3):

$$Fe^{3+}_{\underset{3-x}{2-2x}} Fe^{2+}_{\underset{3-x}{1+x}} \left[Fe^{3+}_{\underset{3-x}{(2-2x)(2-x)}} Fe^{2+}_{x+\frac{2-2x}{3-x}} Ti^{4+}_{x} \right] O^{2-}_{4} \quad (7\,c)$$
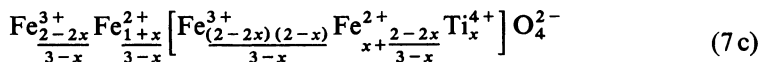
$$\mu = \frac{6x^2 + 20x - 14}{3-x} \quad (8\,c)$$

Equation (7c) represents the most 'random' distribution provided that the Ti^{4+} ions are fixed in B sites.

3. Experimental data

Experimentally observed values of μ which can be compared with these models were first given by AKIMOTO et al. [1957]. Their measurements have been made on synthetic samples of polycrystalline material by means of a magnetic balance. Using the ceramic method of BARTH and POSNJAK [1932] in which mixtures of Fe_2O_3, TiO_2 and iron powder are sealed in silica tubes, heated at $1150\,^0C$ for six hours and quenched from this temperature to retain a single phase, they prepared samples of the entire range of composition. The intensity of saturation magnetization at $0\,^0K$ (Fig. 4) was estimated by extrapolating the thermomagnetic curves determined between CURIE temperature and room temperature in a field of about 3000 Oe. In 1962 AKIMOTO presented similar data without specifying experimental conditions. As the results
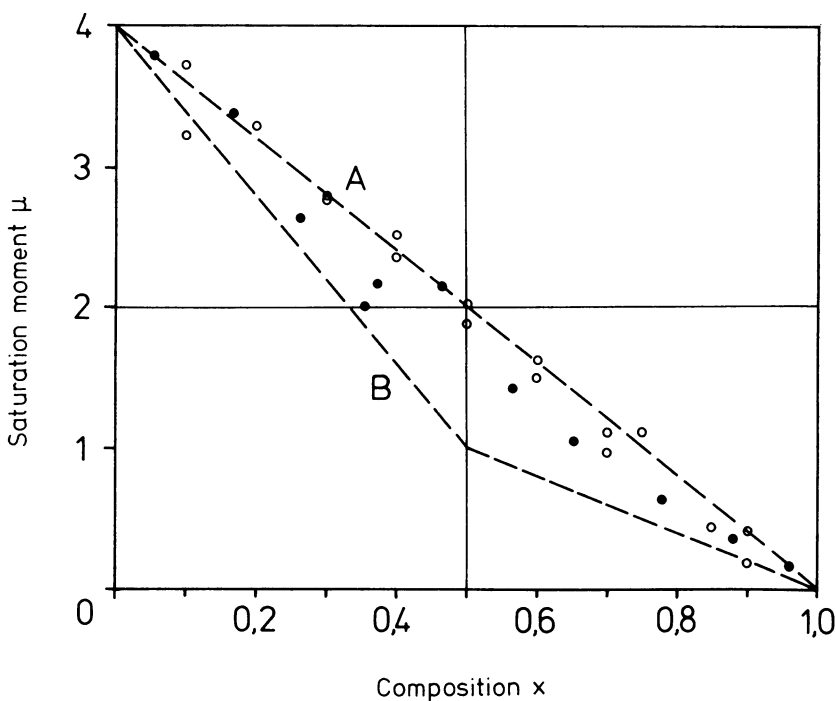
Fig. 4: Saturation moment (BOHR magnetons) as function of composition for AKIMOTO model (A) and NEEL/CHEVALLIER model (B). The experimental results are those of AKIMOTO et al. [1957]: full circles, and STEPHENSON [1969]: open circles.

deviated from both theories the authors concluded that some Ti^{4+} occupies A sites. This was first suggested by GORTER [1957] who modified the NEEL/CHEVALLIER model to:

$$Fe^{3+}_{1-a^*}Ti^{4+}_{a^*}\left[Fe^{3+}_{1-2x+a^*}Fe^{2+}_{1-x}Ti^{4+}_{x-a^*}\right]O^{2-}_4 \qquad (9\,a)$$
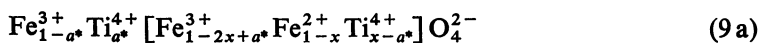
$$\mu = 4 - 6x + 10\,a^* \qquad (10\,a)$$

for $x \geq 0.5$ i.e. $a = \dfrac{1-a^*}{2-2x}$; $b=0$; $c = \dfrac{a^*}{c}$

and

$$Fe^{3+}_{2-2x}Fe^{2+}_{2x-1-a^*}Ti^{4+}_{a^*}\left[Fe^{2+}_{2-x+a^*}Ti^{4+}_{x-a^*}\right]O^{2-}_4 \qquad (9\,b)$$
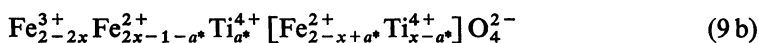
$$\mu = 2 - 2x + 8\,a^* \qquad (10\,b)$$

for $x \leq 0.5$ i.e. $a=1$; $b = \dfrac{2x-1-a^*}{1+x_j}$; $c = \dfrac{a^*}{x}$
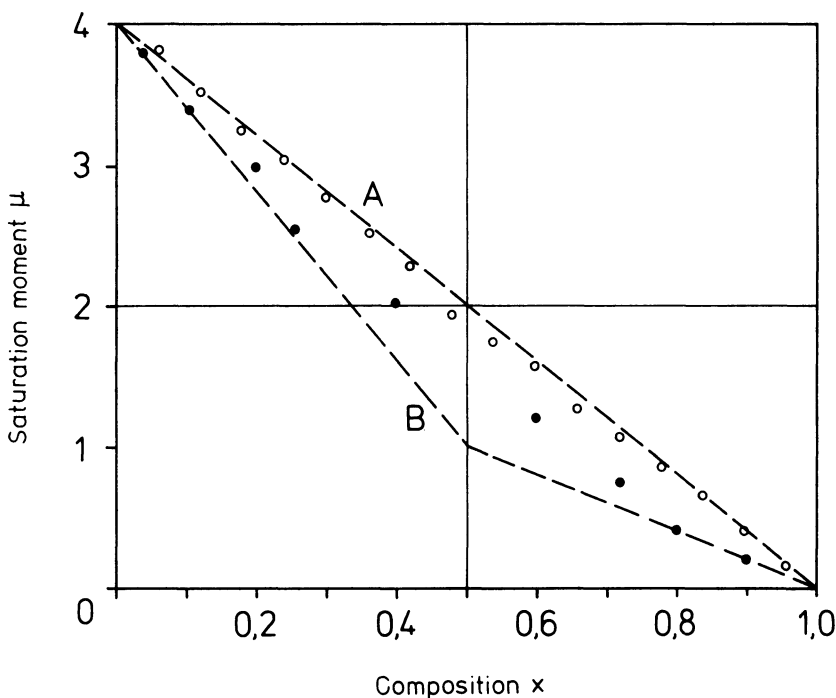
Fig. 5: Saturation moment (BOHR magnetons) as function of composition for AKIMOTO model (A) and NEEL/CHEVALLIER model (B). The experimental results are those of O'REILLY and BANERJEE [1965]: full circles, and present values: open circles.

O'REILLY and BANERJEE [1965] repeated these measurements. The specimens were synthesized by the same sintering process at $1100\,^0$C but a vibrating sample magneto-meter was used for the experiments. In the maximum available field of 30000 Oe the saturation magnetization could be measured down to liquid nitrogen temperature and then extrapolated to $0\,^0$K (Fig. 5). Here too, as the experimental results agreed with neither of the existing models, they postulated a new model in which the titano-magnetite solid solution series is devided into three regions:

I $0 \leq x \leq 0.2$

$$Fe_1^{3+}\,[Fe_{1-2x}^{3+}\,Fe_{x+1}^{2+}\,Ti_x^{4+}]\,O_4^{2-} \qquad\qquad \text{i.e. } a = \frac{1}{2-2x} \qquad (11\,a)$$

II $0.2 \leq x \leq 0.8$

$$Fe_{1.2-x}^{3+}\,Fe_{x-0.2}^{2+}\,[Fe_{0.8-x}^{3+}\,Fe_{1.2}^{2+}\,Ti_x^{4+}]\,O_4^{2-} \quad \text{i.e. } a = \frac{1.2-x}{2-2x} \qquad (11\,b)$$

III $0.8 \leq x \leq 1.0$

$$Fe_{2-2x}^{3+}\,Fe_{2x-1}^{2+}\,[Fe_{2-x}^{2+}\,Ti_x^{4+}]\,O_4^{2-} \qquad\qquad \text{i.e. } a = 1 \qquad (11\,c)$$
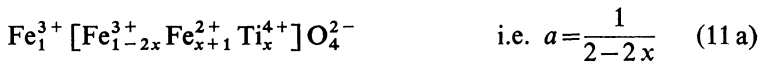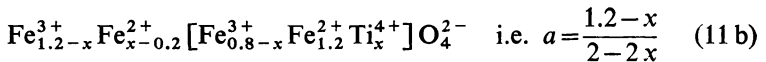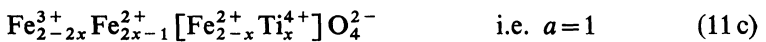
Thus Ti^{4+} is located only in octahedral sites. In regions I and III similar to the NEEL/ CHEVALLIER model, Fe^{3+} shows a complete preference for tetrahedral sites, whereas between $x = 0.2$ and $x = 0.8$ this preference is appreciable reduced.

STEPHENSON [1969] presented for the first time experimental data of titanomagnetite single crystals. The specimens were grown by a modification of BRIDGMAN technique in a carbon dioxide—hydrogen atmosphere and quenched from temperatures just below their melting points. He determined the saturation magnetization (Fig. 4) in a field of 3000 Oe at $77\,^0$K and assumed that the values are nearly equal to those at $0\,^0$K and that the magnetic moment of pure magnetite is 4 BOHR magnetons.

The present results (Fig. 5) were obtained from experiments on polycrystalline samples prepared at $1300\,^0$C by a sintering procedure involving controlled atmo-spheres. Appropriate mixtures of Fe_2O_3 and TiO_2 were kept at this temperature for two periods each 4 to 5 hours with crushing and pressing between the heating cycles and were reduced to spinel single phases in flowing gas made up from CO_2 and H_2. The exact composition of atmospheres required for the desired oxygen partial pressure were taken from the detailed $FeO-Fe_2O_3-TiO_2$ phase diagram reported by TAYLOR [1961]. A magnetic balance was used for the measurements down to liquid nitrogen temperature the maximum field strength employed reaching about 14000Oe. Further details will be given elsewhere.

4. Temperature dependent cation distribution

In comparing the experimental results it is apparent that despite the appreciable scatter a significant increase of saturation magnetization values is produced by increasing the quenching temperature. This assumes that the state of thermodynamic equilibrium at high temperature can be preserved down to room temperature by quenching. Such a quenching temperature effect was first mentioned for the titano-magnetites by STEPHENSON [1969] and has also been found for some other ferrites. Thus the tendency of the cations to be placed in a ordered distribution due to their preference for certain sites is in some cases weak enough to be changed with temperature. NEEL [1948] has shown that in ferrites containing only bivalent and trivalent ions the distribution parameter y varies with temperature according to the BOLTZMANN law:

$$(1+y)/(1-y)^2 = \exp(-E/kT) \tag{12}$$

where y and $(1-y)$ are the fractions of bivalent ions on tetrahedral and on octahedral sites, E is the energy involved in the interchange of a bivalent ion to an A site and a trivalent ion to a B site. PAUTHENET and BOCHIROL [1951] confirmed these ideas. They found working on Mg and Cu ferrites E/k to be 1220^0K and 1540^0K. Similarly STEPHENSON [1969] has given an equilibrium distribution for titanomagnetites:

$$\frac{m_0 \cdot n_t}{n_0 \cdot m_t} = \exp(-\Delta E/kT) \tag{13}$$

where m_t, m_0 are the number of Fe^{3+} ions, n_t, n_0 the number of Fe^{2+} ions in the A sites and in the B sites respectively. ΔE, the energy required to transfer a tetrahedral Fe^{3+} ion to the B site together with an octahedral Fe^{2+} ion to the A site, is positive since Fe^{3+} prefers the tetrahedral site. Beside Ti^{4+} being fixed in the B sites the model is further restricted by:

a) the octahedral sites can only accept a maximum of one Fe^{3+} ion,
b) the number of Fe^{2+} ions in octahedral sites which are available for interchange is $1-m_0$.

Substituting for m_0, n_0, m_t and n_t in (13) yields a quadratic equation for a, whose solutions are:

$$a = 1 - \frac{1}{2-2x}\left[\frac{1-3\gamma}{2(1-\gamma)} - x \pm \sqrt{\left(\frac{1+\gamma}{2(1-\gamma)}\right)^2 - x(1-x)}\right] \tag{14}$$

where $\gamma = \exp(-\Delta E/kT)$. With $T \to \infty$: $\gamma \to 1$ the positive solution of (14) is $a = 0.5$ i. e. the AKIMOTO model (7a) represents the completely disordered state. It also can be shown that for $T \to 0$: $\gamma \to 0$ the two solutions are $a = 1$ and $a = 1/2-2x$ i. e. the cation distribution of the most ordered state corresponds to the NEEL/CHEVALLIER model (7b).

Inserting (14) into equation (8) gives:

$$\mu = 2\left[1 + \frac{1-3\gamma}{2(1-\gamma)} - 2x \pm \sqrt{\left(\frac{1+\gamma}{2(1-\gamma)}\right)^2 - x(1-x)}\right] \tag{15}$$

Thus the magnetic moment of any titanomagnetite is clearly defined, provided that thermodynamic equilibrium was attained and preserved to room temperature. From the experimental results of AKIMOTO et al. [1957]—1150°C quenching temperature— the activation energy ΔE was determined to be 0.21 eV. The theoretical magnetic moments calculated on the basis of this value for a composition $x = 0.5$ as a function of quenching temperatures are shown in Fig. 5 (open circles). At 1300°C μ reaches 1.63 BOHR magnetons whereas the present data indicate that $\mu = 1.92$ and thus $\Delta E = 0.04$ eV. The theoretical temperature dependence calculated from these figures is also plotted in Fig. 6 (full circles).
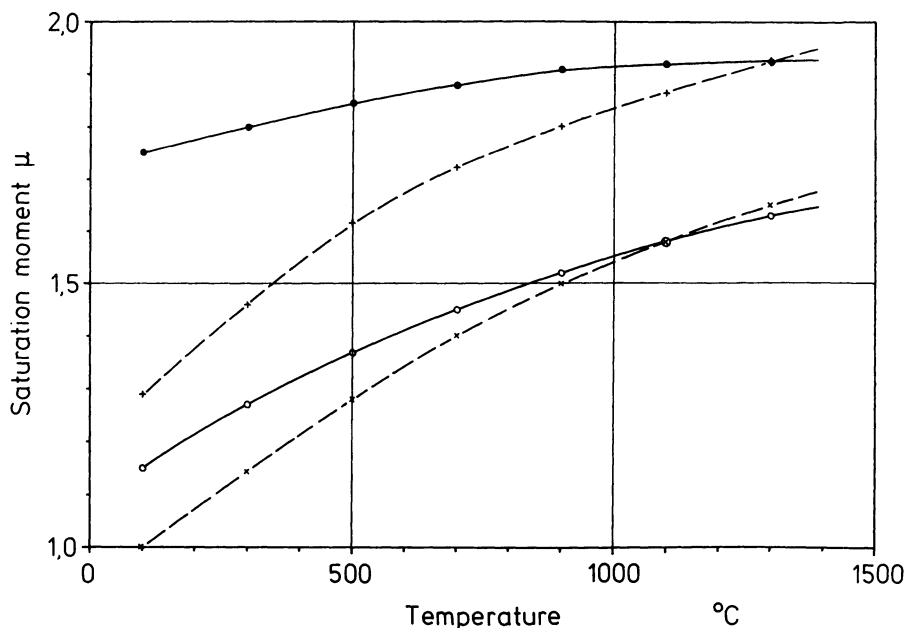
Fig. 6: Theoretical temperature dependence of saturation moment (BOHR magnetons) for a composition $x = 0.5$ obtained by substituting the experimental results of O'REILLY and BANERJEE [1965] in equation (15): open circles, and in equation (18): crosses, lower dashed line. Present results give substituted in equation (15) the full circles and together with equation (18) the crosses, upper dashed line.

The fact that these curves are not coincident is thought partly to be due to the special assumptions STEPHENSON [1969] made in deriving his theory. As the cation distribution of pure magnetite does not depend on the quenching temperature he concluded that either the diffusion is so rapid that Fe^{2+} ions can not be 'frozen' on A sites by quenching or E in (12) is so large that even at high temperatures only a very small amount of Fe^{2+} ions occupies tetrahedral sites. The latter idea is equivalent to a steeply increasing activation energy when the composition parameter x decreases. Consistent with the results observed for the titanomagnetites KRIESSMAN and HARRISON [1956] found a similar behavior in magnesium-manganese ferrites. Obviously associated with the number of Fe^{3+} in octahedral sites ΔE should be a function of the other cations as well as a function of their concentration and distribution. Therefore the conclusion that octahedral sites can only accept a maximum of one Fe^{3+} ion and the number of Fe^{2+} ions on B sites available for interchange is limited to $1-m_0$, which may be perfectly justified for magnetite, will not be valid in the remainder of the solid solution series.

Further evidence arises from the somewhat surprising fact that these suppositions lead to a ΔE which would be the same for every titanomagnetite. The Fe^{3+}-Fe^{2+} interaction schematically represented by a reaction

$$Fe_A^{3+} + Fe_B^{2+} \rightleftarrows Fe_B^{3+} + Fe_A^{2+} \tag{16}$$

involves only the transfer of one electron. A once disordered state would consequently soon be rearranged at room temperature if both lattice sites are energetically equivalent. This cannot be true for the iron ions of different valency on A and B sites, since the experiments prove energies of transfer comparable to those found for the exchange of Fe^{3+} with Mg^{2+} and Fe^{3+} with Cu^{2+}. A detailed study would also have to distinguish sites not surrounded by the same ionic configuration, i. e. the present method determines only an average value for ΔE.

Without the above restrictions equation (13) yields:

$$a = \frac{3 - 2x + x\gamma}{2(2 - 2x)(1 - \gamma)} \pm \sqrt{\left(\frac{3 - 2x + x\gamma}{2(2 - 2x)(1 - \gamma)}\right)^2 - \frac{1}{(2 - 2x)(1 - \gamma)}} \tag{17}$$

Substituting this in (8) gives:

$$\mu = \frac{3 - 4x - 6\gamma + 5\gamma x}{1 - \gamma} \pm \sqrt{\left(\frac{3 - 2x + x\gamma}{1 - \gamma}\right)^2 - \frac{8(1 - x)}{1 - \gamma}} \tag{18}$$

It can be shown that when $T \to 0$, $\gamma \to 0$ (17) is solved by $a = 1$ and $a = 1/2 - 2x$. Thus the NEEL/CHEVALLIER model (7b) corresponds to the completely ordered state,

ΔE
eV

0,6

0,4

0,2

0

0,2   0,4   0,6   0,8   1,0
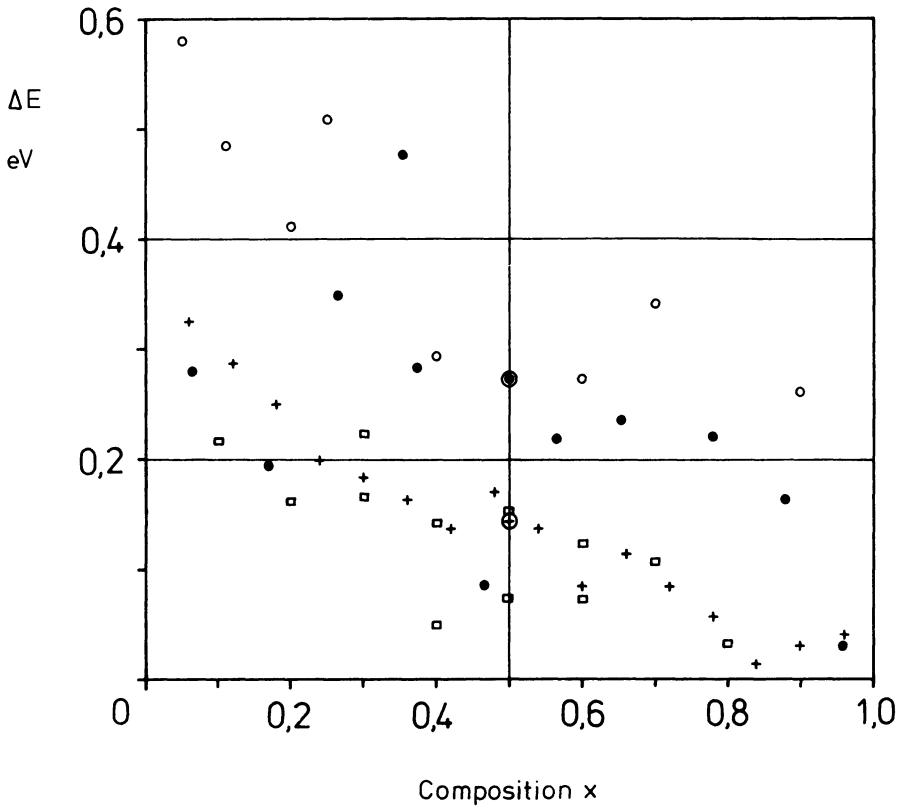
Composition x

Fig. 7: Activation energies ΔE (eV) as function of composition calculated from equation (17) for the experimental data of (o) O'REILLY and BANERJEE [1965], (●) AKIMOTO et al. [1957], (□) STEPHENSON [1969] and (+) present results.

whereas from the AKIMOTO model (7a) it follows $x = \gamma$ and for $T \to \infty$, $\gamma \to 1$ when disorder is greatest a distribution represented by (7c) will be attained. The activation energies derived from (18) for all experimental data available are plotted in Fig. 7. In spite of a high scatter the expected increase of ΔE with decreasing composition parameter x is clearly observed for every measurement. On the other hand the agreement for different quenching temperatures still remains poor since high values would be related to low temperatures and vice versa. The theoretical temperature dependence of the magnetic moments μ for $x = 0.5$ calculated on average values (see Fig. 7) at $1100^{0}C$ and $1300^{0}C$ are shown in Fig. 6 (crosses, broken lines).

The remaining discrepancies may lie in the obvious experimental difficulty in achieving true equilibrium conditions and also in the rate of quenching. Further possibilities arise however, these are:

a) despite the results of ISHIKAWA et al. [1964] some Ti^{4+} occupies A sites and similar to equation (16) at high temperatures the reactions:

$$Fe^{3+}_A + Ti^{4+}_B \rightleftarrows Fe^{3+}_B + Ti^{4+}_A \tag{19}$$

$$Fe^{2+} + Ti^{4+}_B \rightleftarrows Fe^{2+}_B + Ti^{4+}_A \tag{20}$$
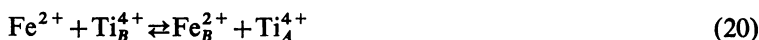
have to be considered and/or

b) ΔE involves distribution-sensitive components such as MADELUNG energy, bonding energy, magnetic exchange energy [CALLEN, HARRISON and KRIESMAN 1954] and consequently should itself depend on temperature.

If this latter assumption is made some useful information can be gleaned from Fig. 7, but it is not possible to distinguish between the different contributions.

5. Conclusions

The temperature dependent cation distribution for the titanomagnetite solid solution series [STEPHENSON 1969] is confirmed by low temperature measurement of the saturation magnetic moments of synthetic samples. In order to allow consistent interpretation of the experimental results the assumption has to be made that the activation energy ΔE which describes the ionic configuration at different temperatures is not a constant. A detailed analysis of all experimental data available indicates an appreciable increase of ΔE from ulvöspinel to magnetite which is independent of the particular preparation techniques used. Thus, as the activation energies include distribution sensitive components they also depend on temperature in agreement with experiment. The exact form of ΔE as function of composition and temperature remains uncertain because of the high scatter in the data. This may primarily be due to the obvious experimental difficulty in preparing appropriate samples and the different methods of measuring and determining the magnetic moments.

At present it is not possible to say what distribution one can expect in natural samples. If a thermodynamic equilibrium state for 300^0K was reached, an arrangement similar to the NEEL/CHEVALLIER model will be found. However, at temperatures below about 1000^0C the values of ΔE related to specimens with low ulvöspinel contents (see Fig. 7) are perhaps comparable to those for magnetite. Naturally occuring samples with a composition $x < 0.5$ will consequently be very stable and thus a cation distribution near the experimental values at 1100^0C is 'frozen' in even when they are slowly cooled down and/or when they are of geological age.

As an ionic reordering changes the spontaneous magnetization of the two sublattices, this effect is of special interest from the geophysical point of view. A mechanism that involves the possibility for the weaker sublattice to become the stronger one by transition from a disordered to ordered arrangement could produce a reversed rema-

nence in geological times. The above results indicate however that such a behavior can not be expected for stoichiometric titanomagnetites: the octahedral sublattice moment remains always greater than the tetrahedral. In natural titanomagnetites which contain a certain amount of impurities of Mg^{2+} and Al^{3+} a new situation arises [VERHOOGEN 1956]. Here a reversal of magnetization may be possible; this is also true for samples which were oxidized to a certain degree without losing their spinel structure.

Acknowledgement

References

AKIMOTO, S.: Thermo-magnetic study of ferromagnetic minerals contained in igneous rocks, J. Geomag. Geoelect. 6, 1—14, 1954

AKIMOTO, S.: Magnetic properties of $FeO-Fe_2O_3-TiO_2$ system as a basis of rock magnetism, J. Phys. Soc. Japan 17, Suppl. B-1, 706—710, 1962

AKIMOTO, S., T. KATSURA, and M. YOSHIDA: Magnetic properties of the $Fe_2TiO_4-Fe_3O_4$ system and their change with oxidation, J. Geomag. Geoelect. 9, 165—178, 1957

BARTH, T. F. W., and E. POSNJAK: Spinel structures: with and without variant atom equipoints, Z. Krist. 82, 325—341, 1932

BLASSE, G.: Crystal chemistry and some magnetic properties of mixed metal oxides with spinel structure, Philips Res. Repts. Suppl. 3, 1—139, 1964

BRAGG, W. H.: The structure of the spinel group of minerals, Phil. Mag. 30, 305—315, 1915

CALLEN, H. B., S. E. HARRISON, and C. J. KRIESSMAN: Cation distribution in ferrospinels. Theoretical, Phys. Rev. 103, 4, 851—856, 1956

CHEVALLIER, R., J. BOLFA, and S. MATHIEU: Titanomagnétites et ilménites ferromagnétiques, Bull. Soc. franc. Min. Crist. 78, 307—346, 1955

FORSTER, R. H., and F. O. HALL: A neutron and X-ray diffraction study of ulvöspinel, Fe_2TiO_4, Acta Cryst. 18, 857—862, 1965

GORTER, E. W.: Chemistry and magnetic properties of some ferrimagnetic oxides like those occuring in nature, Adv. Phys. 6, 336—361, 1957

HAUPTMAN, Z., and A. STEPHENSON: A technique for growing ulvöspinel single crystals from the melt, J. scient. Instrum. 2, 1, 1236—1237, 1968

ISHIKAWA, Y., Y. SYONO, and S. AKIMOTO: Neutron diffraction study of $Fe_3O_4-Fe_2TiO_4$ series, Ann. Prog. Rep. Rock Mag. Group Japan, 14—20, 1964

KRIESSMAN, C. J., and S. E. HARRISON: Cation distribution in ferrospinels. Magnesium-manganese ferrites, Phys. Rev. 103, 4, 857—860, 1956

NEEL, L.: Propriétés magnétiques des ferrites; ferrimagnétisme et antiferromagnétisme, Ann. Phys. 3, 137—198, 1948

NEEL, L.: Some theoretical aspects of rock magnetism, Adv. Phys. 4, 191—243, 1955

O'REILLY, W., and S. K. BANERJEE: Cation distribution in titanomagnetites $(1-x)$ Fe_3O_4 $x Fe_2TiO_4$, Phys. Lett. 17, 237—238, 1965

PAUTHENET, R., and L. BOCHIROL: Aimantation spontanée des ferrites, J. Phys. Radium 12, 249—251, 1951

STEPHENSON, A.: The temperature dependent cation distribution in titanomagnetites, Geophys. J. R. astr. Soc. 18, 199—210, 1969

TAYLOR, R. W.: An experimental study of the system $FeO-Fe_2O_3-TiO_2$ and its bearing on mineralogical problems, Thesis, Pennsylvania State University, 1961

VERHOOGEN, J.: Ionic ordering and selfreversal of magnetization in impure magnetites, J. Geophys. Res. 61, 201—209, 1956

VERWEY, E. J. W., and E. HEILMANN: Physical properties and cation arrangement of oxides with spinel structures, J. chem. Phys. 15, 174—180, 1947

The Preparation and Unmixing
of Cation Deficient Titanomagnetites

W. O'Reilly[1]) and P. W. Readman[1,2]), Newcastle

Summary: Cation deficient titanomagnetites were prepared by pregrinding sintered titano-magnetites in a water slurry followed by oxidation in air at temperatures $< 300^0$C. It is found that, below about 300^0C, all compositions represented by points in the $Fe_3O_4-Fe_2TiO_4$ $-Fe_2TiO_5-Fe_2O_3$ quadrilateral of the $FeO-TiO_2-Fe_2O_3$ ternary diagram may exist as spinels.

The cell edge and Curie temperature have been determined and plotted as contours on the ternary diagram.

The stability of these materials on heating above 300^0C in evacuated capsules has also been studied. γ Fe_2O_3 produced by oxidation of pre-ground Fe_3O_4 inverts to α Fe_2O_3, but the presence of Ti^{4+} ions in all other cation deficient spinels results in a variety of unmixing products depending on the composition of the spinel phase before inversion. The spinel constituent has been identified using the cell edge and Curie temperature contours. Titanium appears to be ineffective in stabilising the cation deficient structure.

Zusammenfassung: Es wurden Titanomagnetite mit einer Kationen-Defektstruktur herge-stellt, indem in Wasser vorgemahlene gesinterte Titanomagnetite in Luft bei Temperaturen $< 300^0$C oxidiert wurden. Es wurde gefunden, daß unterhalb 300^0C alle die Phasen, die im ternären System $FeO-TiO_2-Fe_2O_3$ durch die Verbindungslinien $Fe_3O_4-Fe_2TiO_4-$ $Fe_2TiO_5-Fe_2O_3$ eingeschlossen werden, als Spinelle existieren können. Die Linien gleicher Curie Temperatur und Gitterkonstante wurden für das ternäre System erarbeitet und die Stabilität der Spinelle mit Kationen-Defektstruktur gegen Erwärmung über 300^0C in eva-kuierten Kapseln untersucht. Maghemit (γ Fe_2O_3), der durch Erhitzen von gemahlenem Fe_3O_4 gewonnen worden war, invertiert dabei zu Hämatit (α Fe_2O_3). Die Anwesenheit von Ti^{4+}-Ionen in den anderen Spinellen mit Kationen-Defektstruktur hat eine Reihe von Entmi-schungsprodukten zur Folge, die von der chemischen Zusammensetzung der Spinellphase vor ihrer Inversion abhängen. Die Spinellphasen wurden dabei durch ihre Gitterkonstante und Curie Temperatur identifiziert. Titan scheint dabei keinen Einfluß auf die Stabilität der Kationen-Defektstruktur zu besitzen.

[1]) Dr. W. O'Reilly and P. W. Readman, Department of Geophysics and Planetary Phy-sics, School of Physics, The University of Newcastle upon Tyne, Newcastle upon Tyne, NE1 7RU, U. K.

[2]) Present address: Laboratoire d'Electrostatique et de Physique du Métal, C. N. R. S., Cédex 166, 38-Grenoble, France.

1. Introduction

The oxidation of titanomagnetites $Fe_{3-x}Ti_xO_4$ ($0 < x < 1$) to non-stoichiometric (cation deficient) titanomagnetites of general formula $Fe_aTi_b\square_cO_4$ ($a + b + c = 3$ and $\square$ represents a vacant lattice site) is a process which takes place in submarine and continental basalts. The reaction has recently been shown to take place in the laboratory when sintered titanomagnetites are preground in a water slurry prior to oxidation [SAKAMOTO, INCE and O'REILLY 1968] followed by oxidation in air. Maghemite, γ Fe_2O_3, which is a special case of cation deficient titanomagnetite, ($a = \frac{8}{3}$, $b = 0$, $c = \frac{1}{3}$) is unstable if heated above about 350^0C, inverting irreversibly to hematite α Fe_2O_3.

The purpose of the work to be described in the present paper is first to make a systematic study of the mechanism of oxidation of wet ground titanomagnetites to cation deficient spinels, to determine the range of compositions over which they may be formed and to study the kinetics of the reaction using thermogravimetric and magnetic analysis. The second objective is to investigate the unmixing of the cation deficient spinel oxidation products to more stable intergrowths of the same bulk chemical composition and to see what, if any, stabilizing influence titanium has on the spinel structure. The inversion mechanism and products will also be more complicated than the relatively simple $\gamma \rightarrow \alpha$ Fe_2O_3 transformation and the effect of the composition of the initial spinel on the unmixing products is to be investigated. A more complete description of these experiments may be found in READMAN and O'REILLY [1970].

2. Preparation of samples and reaction kinetics

2.1 Preparation of samples

Sintered titanomagnetites were preground in a water slurry prior to oxidation in air in a thermobalance. X ray line broadening measurements yielded a particle size of the order of 1000 Å after broadening due to strain had been taken into account. The composition of the oxidation product was determined from the observed weight increase and by chemical analysis. Single phase materials were formed throughout the Fe_3O_4—Fe_2TiO_4—Fe_2TiO_5—Fe_2O_3 quadrilateral of the FeO—TiO_2—Fe_2O_3 ternary diagram. The cell size decreased with increasing oxidation parameter (figure 1). The intensity of the (111) reflection fell dramatically with increasing oxidation and this may provide a means of distinguishing between naturally occurring stoichiometric and oxidized materials having the same cell edge. Superstructure lines corresponding to 5:1 and in some cases 3:1 ordering of cations and vacancies were observed.

A differential thermogravimetric (DTG) analysis was made on preground samples with a range of x values. The DTG curves were characterized by a major peak centred at about 250^0C. For samples with $x > 0.2$ a second (smaller) peak was observed at about 360^0C. This is attributed to the limited availability for oxidation of Fe^{2+} on

the tetrahedral sites of the structure, which does not oxidize in the time available in the lower temperature range. The DTG curves of coarse ground samples show a major peak at about 450°C and only a minor peak at 250°C indicating only limited formation of cation deficient spinel, perhaps as a surface layer.

2.2 Reaction Kinetics

The progress of the reaction may be investigated by measuring mass as a function of time during isothermal runs in the thermobalance in the temperature range 200°C to 300°C. The reaction should be described by an order, n given by $dm/dt = Km^n$ where m is the mass of the sample and K is the reaction constant, which will depend
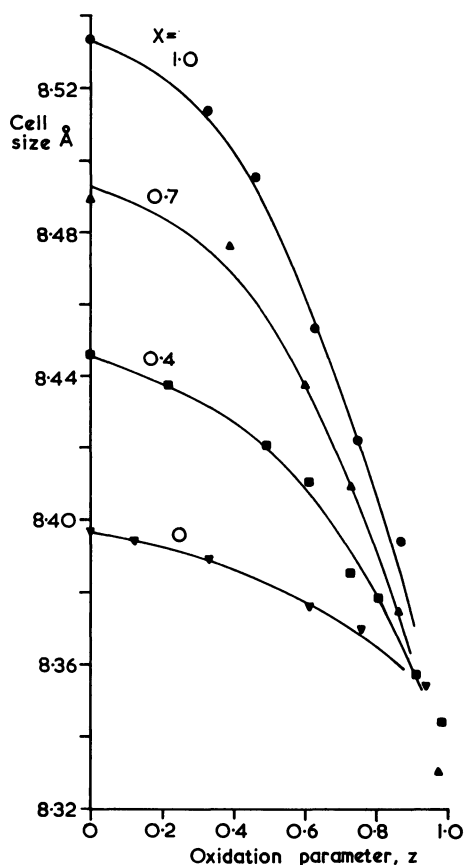
Fig. 1: Variation of extrapolated cell edge for titanomagnetites $x = 0$, 0.4, 0.7 and 1.0 as a function of oxidation parameter z. The similar values for high z come from the fact that the ionic radii of Ti^{4+} and Fe^{3+} are about the same.

on the temperature following the ARRHENIUS relationship $K = K_0 \exp(-Q/kT)$. For the initial stages of the reaction the order was found to be 3, but this decreased and approached unity with increasing degree of oxidation. The initial value is thought to be in error due to internal heat generation in the sample and if an order of $n = 1$ is assumed, the temperature variation of the reaction constant gives activation energies of $Q = 1.5$, 1.4 and 1.2 eV/molecule for $x = 0$, 0.2 and 0.4 respectively.

Over geological time a similar process may take place at moderate temperatures. The time constant for the oxidation of the samples used in the present study would be of the order of 10^6 years at $300\,^0$K. This could be regarded as a lower limit for titanomagnetites occurring naturally in rocks.

The oxidation can also be followed by observing the time dependence of magnetization at the oxidation temperature. This method is not as reliable as measuring weight change because the magnetic moment is not related to the chemical composition in a simple manner. The activation energy determined from magnetization-time curves are in agreement with those obtained gravimetrically for $x = 0$ and 0.2. For $x = 0.4$ the agreement is poor, the values determined gravimetrically and magnetically being 1.2 and 0.8 eV/molecule respectively. For high x values the magnetization-time curves are too complicated to be interpreted in terms of time constants and activation energies.

3. Inversion of non-stoichiometric titanomagnetites

The inversion ("unmixing") of cation deficient titanomagnetites was observed by heating the oxidized samples, sealed in evacuated quartz capsules, from room temperature to about $600\,^0$C in a magnetic balance. The inversion is shown by a decrease in magnetization for samples with a low initial x value, and an increase in magnetization for samples with a high initial x value. The resulting assemblage was X-rayed after cooling to room temperature and the constituent phases identified. The spinel component of the intergrowth was identified from the CURIE temperature measured during the inversion run and cell edge determination. The CURIE temperature and cell edge contours on the FeO—TiO$_2$—Fe$_2$O$_3$ ternary diagram (figures 2 and 3) were those obtained from synthetic cation deficient samples prepared as described in section 2.

The general conclusions about the nature of the inversion products are summarised in figure 4 which shows the dependence of components of the final intergrowth on the position of the initial cation deficient spinel. When heated in evacuated capsules, samples in zones 1, 2 and 3 of figure 4 invert to an intergrowth of two phases: a spinel phase richer in iron than the original titanomagnetite and a rhombohedral phase. In zone 1 the rhombohedral phase is very near to ilmenite in composition and the spinel phase a near stoichiometric titanomagnetite which can be located by extending a line from the point representing FeTiO$_3$ through the point representing the cation deficient spinel to intersect the titanomagnetite join. Passing through zones 2 and 3 the rhombohedral phase becomes less titanium rich and approaches hematite in composition. The spinel phase is near to magnetite in composition with possibly a small
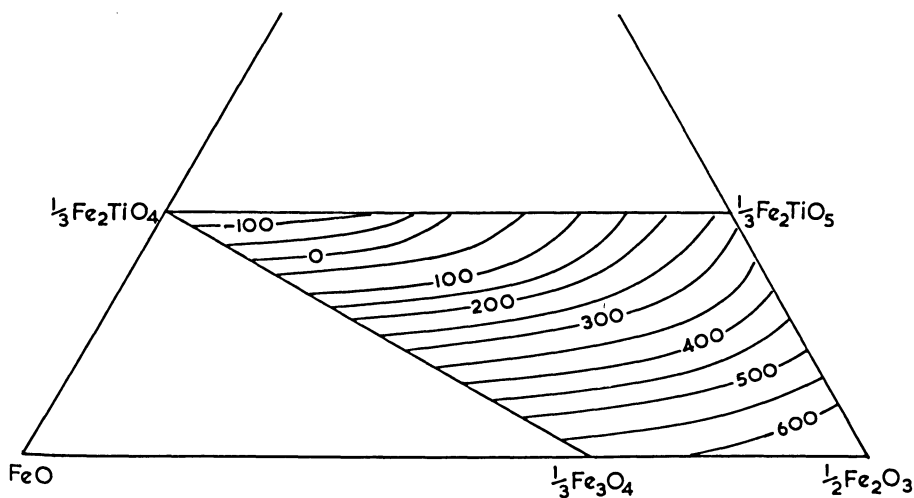
Fig. 2: Contours of constant CURIE temperatures (^{0}C) for cation deficient spinel oxides in the $Fe_3O_4-Fe_2TiO_4-Fe_2TiO_5-Fe_2O_3$ quadrilateral of the $FeO-TiO_2-Fe_2O_3$ ternary diagram.
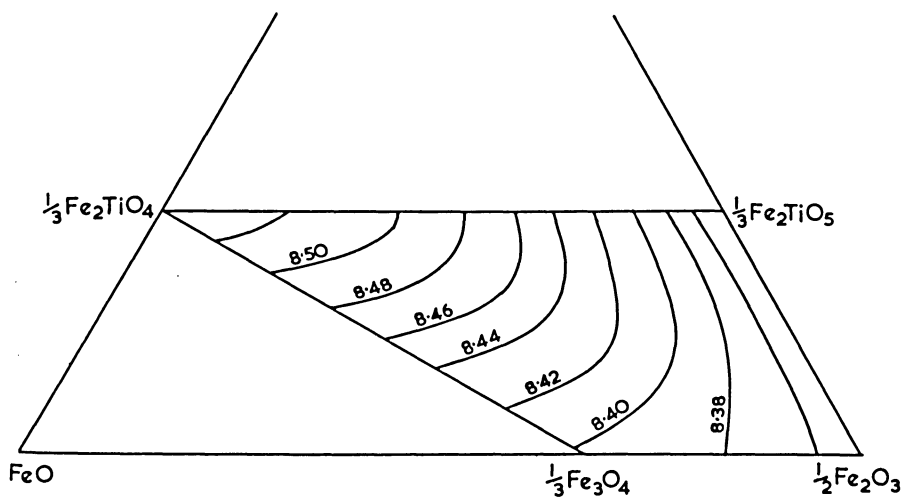
Fig. 3: Contours of constant extrapolated cell edge (Å) of cation deficient spinels in the $Fe_3O_4-Fe_2TiO_4-Fe_2TiO_5-Fe_2O_3$ quadrilateral.

quantity of titanium and vacancies. Cation deficient spinels located in zones 4 and 5 invert to an intergrowth of three components. Any remaining Fe^{2+} forms an iron rich spinel near to magnetite. In zone 4 the other components are anatase, TiO_2, and hematite, and in zone 5 pseudobrookite, Fe_2TiO_5, and hematite.

The inversion mechanism consists in a reorganization of the crystal structure accompanied by the translation of ions to form the separate phases. The γ $Fe_2O_3 \rightarrow \alpha$ Fe_2O_3 transformation is relatively simple as the spinel and corundum structures are similar. Here, from the type of inversion product observed, we can list the relevant structures in order of increasing incompatibility with the original spinel structure: spinel-rhombohedral-orthorhombic-tetragonal.

4. Conclusions

The technique of DTG analysis directly confirms that pregrinding of sintered titanomagnetites makes possible the synthesis of cation deficient titanomagnetites
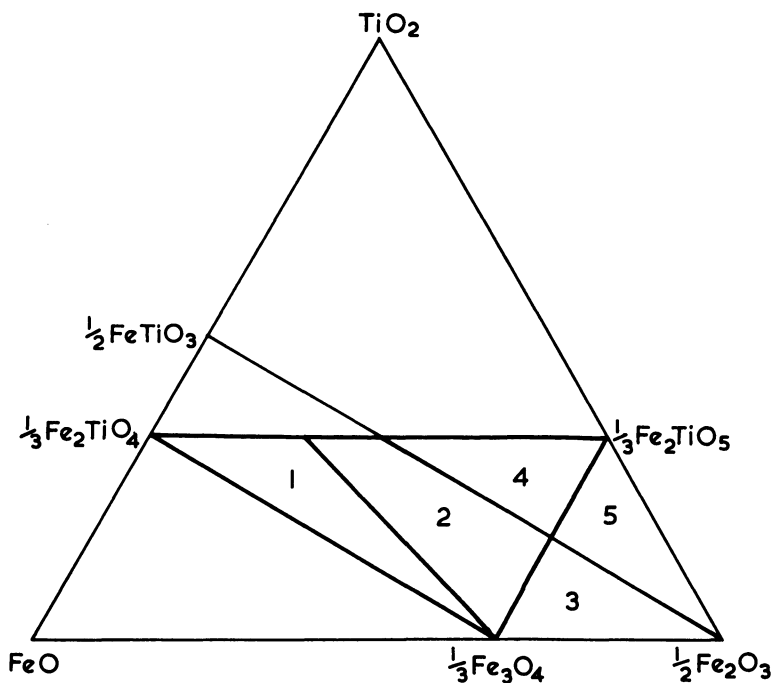
Fig. 4: Summary of inversion of cation deficient spinels to stable intergrowths of the same bulk chemical composition. The inversion products are: zone 1, Ilmenite + titanomagnetite; zones 2, 3 Iron rich spinel + hemoilmenite decreasing in Ti content on passing through zones 2 to 3; zone 4, Iron rich spinel + hematite + anatase; zone 5, Iron rich spinel + hematite + pseudobrookite.

and that the oxidation characteristics of coarse ground samples are quite different to the wet ground samples. It has also been shown that the present wet ground samples would be appreciably oxidized at room temperature over a period of 10^6 years. This could be regarded as a lower limit for titanomagnetites occuring naturally in rocks. It has been found that all compositions in the $Fe_3O_4-Fe_2TiO_4-Fe_2TiO_5-Fe_2O_3$ quadrilateral of the $FeO-TiO_2-Fe_2O_3$ ternary diagram may exist as spinels.

All cation deficient spinels in this system invert irreversibly to multiphase intergrowths without change in bulk chemical composition on heating above the range $350-400^0C$. Any stabilizing effect of Ti ions must be offset by the higher vacancy concentrations. The inversion products depend on the initial location of the cation deficient spinel on the ternary diagram and are summarized in figure 4. A rhombohedral phase is always formed and, for highly oxidized samples, pseudobrookite or anatase are found.

Acknowledgements

References

READMAN, P. W. and W. O'REILLY: The synthesis and inversion of non-stoichiometric titanomagnetites, Phys. Earth Planet. Interiors, 4, 121—128, 1970

SAKAMOTO, N., P. I. INCE and W. O'REILLY: The effect of wet grinding on the oxidation of titanomagnetites, Geophys. J. R. astr. Soc., 15, 509—515, 1968

Oxidation Processes in Titanomagnetites

P. W. Readman[1,2]) and W. O'Reilly[1]), Newcastle

Summary: The processes by which titanomagnetites oxidize in nature to multi- and single phase products are reviewed. Existing models for the cation distribution in non-stoichiometric titanomagnetites are modified and tested by measurements of saturation magnetization of synthetic samples. The results indicate that, in the spinel structure, the inherent availability for oxidation of tetrahedrally sited Fe^{2+} ions is about 20% of the availability of octahedrally sited Fe^{2+} ions.

Zusammenfassung: Es wird eine Übersicht über die Prozesse gegeben, nach denen sich aus Titanomagnetiten in der Natur- ein und mehrphasige Oxydationsprodukte bilden. Die bestehenden Modelle für die Verteilung der Kationen in nicht stöchiometrischen Titanomagnetiten wurden abgeändert und durch die Messung der Sättigungsmagnetisierung synthetischer Proben überprüft. Es zeigte sich dabei, daß in Spinellstrukturen die Neigung zur Oxydation der Fe^{2+}-Ionen auf Tetraederplätzen nur etwa 20% derjenigen der Fe^{2+}-Ionen auf Oktaederplätzen beträgt.

1. Introduction

The oxidation of titanomagnetites, $Fe_{3-x}Ti_xO_4$ $(0 < x < 1)$, in igneous rocks is currently of great interest. The phenomenon not only poses interesting problems in physical chemistry but may also have wide ranging implications in the field of geophysics. It has been suggested, for example, that the iron-titanium oxide mineral system may possibly be useful in geothermometry and geobarometry studies. Furthermore, oxidized titanomagnetites may also play a rôle in the interpretation of magnetic anomalies in the region of the mid-oceanic ridges [Creer, Petersen and Petherbridge, 1970]. It may also be possible that the oxidation of titanomagnetites produces a self-reversal of the natural remanent magnetization (NRM) of rocks. The importance of the oxidation of titanomagnetites to stability of NRM and the validity of paleomagnetic and paleointensity studies is quite obvious. Finally there has been much discussion about the possible correlation between polarity of NRM and degree of oxidation of the magnetic minerals as determined by ore microscope observations.

[1]) P. W. Readman and Dr. W. O'Reilly, Department of Geophysics and Planetary Physics, School of Physics, The University of Newcastle upon Tyne, Newcastle upon Tyne, NE1 7RU, U. K.

[2]) Present address: Laboratoire d'Electrostatique et de Physique du Métal, C. N. R. S., Cédex 166, 38-Grenoble, France.

The object of the present paper is first to review the various possible ways in which titanomagnetites oxidize and, secondly, to discuss in detail one of the oxidation processes. This is the production of non-stoichiometric (cation deficient) titanomagnetites. The mechanism by which the titanomagnetites become increasingly non-stoichiometric has been studied at the atomic level by the measurement at liquid helium temperature of saturation magnetization of synthetic samples oxidized in the Laboratory.

2. Review of Oxidation Processes in Titanomagnetites

2.1 Magnetite

The oxidation of magnetite, Fe_3O_4, which may be regarded as a special case of the oxidation of titanomagnetites, has received much attention because of the technological application of the oxidation products.

Under suitable conditions, magnetite may oxidize to maghemite, $\gamma\ Fe_2O_3$ which also has the spinel structure, and may be re-written as $Fe^{3+}_{8/3}\square_{1/3}\ O^{2-}_4$ indicating that some lattice positions normally occupied in stoichiometric spinels are now vacant. A complete $Fe_3O_4-\gamma\ Fe_2O_3$ solid solution exists, and partial oxidation of Fe_3O_4 produces a member of this series. On heating to about $400\,^0C$ (the exact temperature depending on the history of the sample) or by the application of a hydrostatic pressure of about 150 bars at room temperature, maghemite inverts irreversibly to hematite, αFe_2O_3, of corundum structure. Similarly members of the $Fe_3O_4-\gamma\ Fe_2O_3$ series unmix to an intergrowth of spinel and corundum phases without change in bulk chemical composition.

An alternative process is the direct oxidation of magnetite to hematite. Partial oxidation results in the formation of a skin of hematite around the grains and a core of composition along the $Fe_3O_4-\gamma Fe_2O_3$ series. The conditions under which alternative processes take place have been discussed by e. g. COLOMBO, FAGHERAZZI, GAZZARINI, LANZAVECCHIA and SIRONI [1968] and GALLAGHER, FEITNECHT and MANNWEILER [1968].

2.2 Titanomagnetites

We may expect that the oxidation of titanomagnetites broadly follows the same pattern as that for magnetite, one process being the production of non-stoichiometric titanomagnetites ($Fe_aTi_b\square_c\ O_4$, $a + b + c = 3$) with the alternative of the formation of a multi-phase oxidation product.

a) Non-stoichiometric titanomagnetites.

The natural occurence of non-stoichiometric titanomagnetites (titanomaghemites) in continental basalts has been established by chemical analysis [AKIMOTO and KATSURA, 1959] and by the combination of ore microscope, electronprobe and CURIE point analysis [SANVER and O'REILLY, 1970; CREER and PETERSEN, 1969; CREER and

IBBETSON, 1970]. OZIMA and LARSEN [1970] have reported their presence in submarine basalts. This presumably indicates that the rocks have spent prolonged periods in the temperature range 100—300°C but not exceeding about 350°C [READMAN and O'REILLY, 1970; see also this volume] if results from laboratory experiments can be extrapolated to naturally occurring materials. The presence of residual magmatic liquids and gases, or even atmospheric oxygen, may produce highly oxidizing conditions in a body cooling slowly through this temperature range. A second possibility is that the burial of lavas by subsequent flows to a depth of the order of 1000 metres results in the formation of secondary minerals under hydrothermal conditions indicating temperatures as high as 300°C [see e. g. ADE-HALL, KHAN, DAGLEY and WILSON 1968]. Considering the stabilizing effect of water on the spinel structure, highly nonstoichiometric titanomagnetites may be produced in buried lavas provided the temperature and pressure do not exceed the point where unmixing to a stable multiphase intergrowth would result. A third possibility is that, in the case of submarine basalts, sea water may act as an oxidizing agent and produce a degree of oxidation increasing with distance from the mid-oceanic ridges.

b) Multiphase oxidation products.

A titanium rich titanomagnetite is usually formed under the conditions of oxygen pressure and temperature existing in basaltic melts. If the basalt is cooled rapidly the titanomagnetite is preserved as a single phase, but in a slowly cooled self-buffering body an intergrowth of a spinel phase, progressively richer in iron, and a rhombohedral phase, progressively richer in titanium, is formed [BUDDINGTON and LINDSLEY, 1964]. This process forms the initial part of the so-called deuteric oxidation which is the basis of the optical scale for the classification of basalts of BLACKETT, WILSON and their co-workers. When the redistribution of iron and titanium has taken place at temperatures above about 600°C the rocks are reliable for paleomagnetic work. However oxidation may also take place at lower temperatures also producing a multiphase oxidation product. Hematite and rutile may result in the highly oxidizing conditions which arise if atmospheric oxygen has access to the magnetic minerals. A similar intergrowth can be produced by the inversion or "unmixing" of a nonstoichiometric titanomagnetite but this may be distinguishable by the presence of an iron rich spinel phase formed from any residual Fe^{2+} ion and possibly the presence of anatase. Although the direction of NRM in such rocks may be passed on faithfully through successive generations of minerals, their use for paleointensity studies clearly demands caution.

3. Mechanism of Formation of cation deficient Spinels

3.1 Evaluation and modification of existing mechanisms

The cation distribution which is observed in cation deficient titanomagnetites depends upon the cation distribution in the original titanomagnetites and on the

oxidation process itself. One model (Model 1) for the cation distribution in non-stoichiometric titanomagnetites has been suggested by VERHOOGEN [1962]. In this model it is assumed that all available Fe^{3+} is located in tetrahedral sites. This takes into account the so-called preference of Fe^{3+} for tetrahedral sites which is basically due to the reduction of the total lattice energy brought about by the formation of covalent bonds.

A second model (Model 2) [O'REILLY and BANERJEE, 1966] takes account of the observed initial cation distribution and the oxidation process, which essentially results from the ionization of the adsorbed oxygen atoms by the extra electrons of the Fe^{2+} ions diffusing through the crystal. The process is therefore controlled by diffusion rates and the preparation of samples with high diffusion rates provides the key to the formation of cation deficient oxidation products. In titanomagnetites Fe^{2+} ions occur on both sublattices of the structure in contrast to magnetite which has Fe^{2+} on octahedral sites only. The diffusion rates of ions in the two sublattices are not equal as ions in octahedral sites are ionically bound whereas those in tetrahedral sites are more strongly bound due to covalency. O'REILLY and BANERJEE [1966] approximated the mobility of tetrahedrally sited Fe^{2+} ions to zero and, on the assumption that Ti^{4+} ions and vacancies were located only in octahedral sites, were able to predict the variation of cation distribution with increasing degree of non-stoichiometry. This results in a two stage reaction in which tetrahedrally sited Fe^{2+} is only attacked after octahedrally sited Fe^{2+} has been exhausted.

Both of these models are open to criticism. The preference of Fe^{3+} for tetrahedral sites is not necessarily the dominant factor and may be partially overcome by the lowering of the electrostatic energy of the lattice obtained with Fe^{2+} in tetrahedral sites, as is found in stoichiometric titanomagnetites. In the O'REILLY-BANERJEE mechanism the new tetrahedral sites created at the surface must be occupied by Fe^{2+} and Fe^{3+} in the same ratio as in the original tetrahedral sites in the interior. This is artificial but is a necessary consequence of the zero mobility of tetrahedral site Fe^{2+} ions if a uniform single phase material is to be formed. Secondly, it is only a first approximation to assume that no tetrahedral site oxidation takes place. Third, for high degrees of oxidation, when only tetrahedral site Fe^{2+} is being oxidized, it may be possible for some vacancies to remain in tetrahedral sites.

We now propose a third mechanism (Model 3) containing the important features of both models. Consider the adsorption and ionization of each oxygen atom. This results in the creation, on average, of $1/4$ new tetrahedral sites and $1/2$ new octahedral sites which must be partially filled with cations. Those most likely to fill the new sites are the Fe^{2+} which have diffused to the surface and transformed to Fe^{3+} ions during the ionization of the oxygen atom. Because of the low mobility of tetrahedral site Fe^{2+}, these ions will come from the octahedral sublattice leaving octahedral site vacancies. The preference of Fe^{3+} for tetrahedral sites results in the newly created tetrahedral sites being filled with Fe^{3+} ions and each new octahedral site filled by, on average, $5/6$ Fe^{3+} and $1/6$ vacancy. In effect, a skin of maghemite is formed,

possibly with some Fe^{2+} and Ti^{4+} ions on octahedral sites. The interior of the sample and the skin rapidly become homogeneous within the octahedral sublattice due to migration of vacancies and Fe^{3+} ions into, and Fe^{2+} and Ti^{4+} ions out of, the interior. At the same time the cation population of the tetrahedral sublattice is made homogeneous by the movement of electrons from the interior, which is equivalent to moving Fe^{2+} from, and Fe^{3+} into, the interior. Electron hopping between tetrahedral sites contributes to the conductivity of certain ferrites and has an activation energy of 0.2 to 0.3 eV [VERWEY, HAAJMAN and ROMEIJN, 1947]. This is considerably smaller than the observed activation energy of the oxidation reaction ($\sim$1 eV) and electron hopping should therefore make an effective contribution to the process. It must be pointed out that electron hopping alone cannot account for oxidation as local charge balance would not be maintained. Translation of electrons by hopping in tetrahedral sites only contributes to the process if accompanied by translation of ions in octahedral sites. Ionic diffusion is therefore the rate limiting process.

The final modification (Model 4) to produce a model taking into account all the shortcomings of the original two models can now be made. The assumption that tetrahedral site Fe^{2+} ion mobility is zero can now be replaced by a factor describing the relative probability of oxidation of Fe^{2+} ions in the two sublattices. This factor will be the product of relative concentrations of the two kinds of Fe^{2+} ion together with a parameter which describes the inherent relative availability of the Fe^{2+} ions depending on their mobility arising from ionic and/or electronic diffusion.

3.2 Experimental evidence for models—saturation magnetization

In principle, at least, the cation distribution of a magnetic spinel oxide can be inferred from measurement of saturation magnetization at low temperature, assuming spin-only values for ionic moments and a NÉEL AB type ferrimagnet.

The general formula for a stoichiometric titanomagnetite is

$$Fe^{2+}_{(1+x)} Fe^{3+}_{(2-2x)} Ti^{4+}_x O^{2-}_4 \quad (0 < x < 1)$$
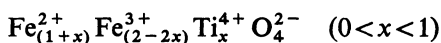
and the degree of oxidation may be defined by an oxidation parameter z ($0 < z < 1$) given by

$$Fe^{2+} + \frac{z}{2} O \rightarrow (1-z) Fe^{2+} + z Fe^{3+} + \frac{z}{2} O^{2-}$$
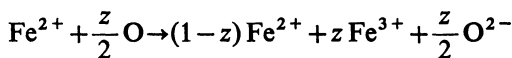
Every 4 oxygen ions in the original sample becomes $4 + z/2\,(1 + x)$ in the oxidized sample, and the number of formula units in the sample increases by a factor $1/R$ where $R = 8/[8 + z\,(1 + x)]$. The general formula for the cation distribution in an oxidized titanomagnetite may therefore be written as

$$Fe^{3+}_{1-\delta} Fe^{2+}_{\delta} [Fe^{3+}_{(2-2x+z+zx)\,R-1+\delta} Fe^{2+}_{(1+x)\,(1-z)\,R-\delta} Ti^{4+}_{xR} \square_{3\,(1-R)}] O^{2-}_4$$
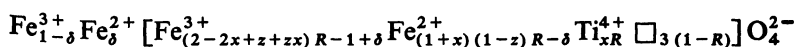
Where δ is simply defined as the number of Fe^{2+} ions per formula unit in tetrahedral sites and it is assumed that Ti^{4+} and vacancies are in octahedral sites only. The saturation moment is then

$$n_{(B-A)} = [(14-6x + xz + z) R + 2\delta - 10]\mu_B$$

per formula unit, assuming spin-only values. For a given composition (x, z) the distribution is therefore described completely by δ and each of the four models discussed above are characterized by the variation of δ with z which is as follows:

(a) Model 1 (VERHOOGEN). The original model is not compatible with the observed cation distribution in stoichiometric titanomagnetites. For the present purpose the model is slightly modified by taking the initial observed distribution and assuming that all new Fe^{3+} is created at the expense of tetrahedral Fe^{2+} and is placed on tetrahedral sites. This gives

$$\delta = [\delta_0 - (1+x)z] R \quad \text{for} \quad z < \delta_0/(1+x)$$

where δ_0 is the initial value of δ for the stoichiometric titanomagnetite and

$\delta = 0$ for higher z values.

This model is represented by curves 1 in the figures 2—4.

(b) Model 2 (O'REILLY and BANERJEE)

$$\delta = \delta_0 \text{ for } z < \frac{8(1+x-\delta_0)}{(1+x)(8+\delta_0)}$$

$\delta = (1 + x)(1-z) R$ for higher z values.

This model is represented by curves 2 in the figures 2—4.

(c) Model 3 (zero mobility tetrahedral Fe^{2+}—Fe^{3+} tetrahedral site preference— tetrahedral electron hopping).

$$\delta = \delta_0 R \text{ for } z < 1 - \frac{\delta_0}{(1+x)}$$

$\delta = (1+x)(1-z) R$ for higher z values.

This model is represented by curves 3 in the figures 2—4.
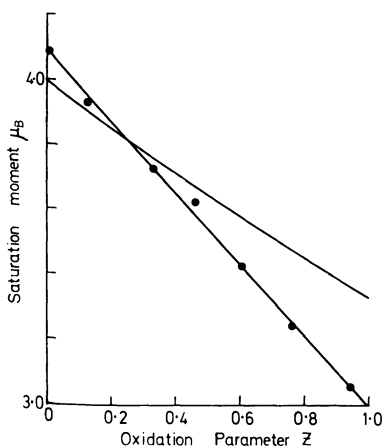
Fig. 1
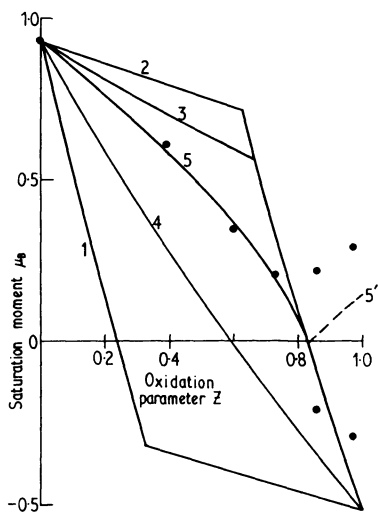
Fig. 3
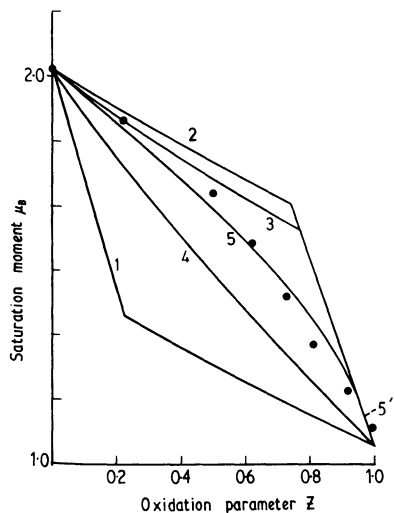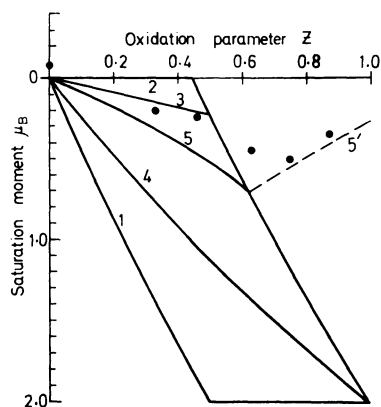
Fig. 2   Fig. 4

Fig. 1: Spontaneous magnetization (μ_B) as a function of oxidation (z) for the $Fe_3O_4-Fe_2O_3$ series produced by oxidation of wetground sintered Fe_3O_4. The line shows the variation expected theoretically if all vacancies are in octahedral sites of the spinel structure.

Fig. 2: Spontaneous magnetization (μ_B) as a function of oxidation (z) for oxidized wet ground $Fe_{2.6}Ti_{0.4}O_4$. Lines 1 to 5 represent magnetization predicted by models (see text).

Fig. 3: Spontaneous magnetization (μ_B) as a function of oxidation (z) for oxidized wet ground $Fe_{2.3}Ti_{0.7}O_4$.

Fig. 4: Spontaneous magnetization (μ_B) as a function of oxidation (z) for oxidized wet ground Fe_2TiO_4. It is assumed that experimental points represent an A-sublattice predominant moment.

(d) Model 4 (finite availability of tetrahedral Fe^{2+}).

The number of new Fe^{3+} formed by the oxidation of Fe^{2+} is $z(1+x)R$ per formula unit. If f is the fraction of these formed from oxidation of tetrahedral Fe^{2+} ions then, assuming that the hopping mechanism is also operating

$$\delta = [\delta_0 - fz(1+x)]R$$

f is the product of a concentration factor $f_{conc} = \delta/(1+x)(1-z)R$, which is the ratio of the number of Fe^{2+} ions in tetrahedral sites to the total number of Fe^{2+} ions and a factor α which describes the inherent availability of tetrahedral Fe^{2+} for oxidation. Substituting for f_{conc}

$$\delta = \delta_0(1-z)R/(1-z+\alpha z)$$

When $\alpha = 0$, tetrahedral Fe^{2+} has zero mobility and Model 3 results. When $\alpha = 1$, tetrahedral and octahedral Fe^{2+} are equally available, $f = f_{conc}$, and

$$\delta = \delta_0 R(1-z)$$

This is represented by curves 4 in the figures 2—4.

The reaction may be one or two stage depending on the value of x, δ_0 and z. In general the first stage ends at

$$z = \frac{1}{1-\alpha}[1-\delta_0/(1+x)]$$

This model has been plotted in the figures 2—4 (curves 5) for $\alpha = 0.2$ for which the first stage ends at $z = 0.97$, 0.84 and 0.63 for $x = 0.4$, 0.7 and 1.0 respectively.

(e) Experimental evidence.

The method of preparation results in the formation of fine grain materials ($\sim$1000 Å from X-ray line broadening, taking strain-broadening into account) which are single domain and difficult to saturate magnetically. Further difficulties arise from the possible presence of surface non-exchange coupled material. The experimental points obtained at 4.2^0K in a maximum field of 15 kOe are thus the product of suitable extrapolations. Data for compositions $x = 0$ (magnetite), 0.4, 0.7 and 1.0 (ulvöspinel) are shown in figures 1, 2, 3 and 4.

A good fit to the data is given by Model 4 (curve 5) in which the inherent availability of tetrahedral Fe^{2+} has been set empirically at 20% of the octahedral Fe^{2+} availability. For ulvöspinel, the agreement is not so good as with electron hopping (curve 3) without tetrahedral oxidation. However this compound is complicated by having a low moment in which orbital contributions may be more important than spin-only values of ionic moments.

The agreement in the higher oxidation stages is less good particularly for $x = 1.0$. First, it is impossible to distinguish between A and B sublattice predominant moments by magnetostatic means. Secondly, oxidation is proceeding exclusively by the oxidation of tetrahedrally sited Fe^{2+} and it may be that it is not possible for Fe^{3+} ions from the octahedral sublattice to fill the vacancies as fast as they are produced. Tetrahedral vacancies decrease the A sublattice moment therefore reducing the moment of highly oxidized ulvöspinel. The formation of a maghemite ($Fe_{8/3} \square_{1/3} O_4$) skin in the second stage produces $1/3 \square$ in octahedral sites and leaves up to $8/3 \square$ in tetrahedral sites depending on the rate at which these may be filled by diffusion of Fe^{3+} from octahedral sites. Curves $5'$ in the figures 2—4 represent a model in which vacancies are formed in the ratio $8:1$ in tetrahedral and octahedral sites in the second stage of oxidation. However, once the possibility of tetrahedral site vacancies is considered the saturation moment no longer provides a unique solution to the cation distribution problem and other, more powerful, techniques must be employed.

Acknowledgements

References

ADE-HALL, J. M., M. A. KHAN, P. DAGLEY, and R. L. WILSON: A detailed opaque petrological and magnetic investigation of a single tertiary lava flow from Skye-Scotland, Geophys. J. R. astr. Soc. 16, 375—388, 1968

AKIMOTO, S., and T. KATSURA: Magnetochemical study of the generalized titanomagnetite in volcanic rocks, J. Geomag. Geoelectr. 10, 69—90, 1959

BUDDINGTON, A. F., and D. H. LINDSLEY: Iron titanium oxides and synthetic equivalents, J. Petrology 5, 310—357, 1964

COLOMBO, U., G. FAGHERAZZI, F. GAZARRINI, G. LANZAVECCHIA, and G. SIRONI: Mechanism of low temperature oxidation of magnetites, Nature 219, 1036—1037, 1968

CREER, K. M., and J. D. IBBETSON: Electron microprobe analyses and magnetic properties of non-stoichiometric titanomagnetites in basaltic rocks, Geophys. J. R. astr. Soc. 21, 485—511, 1970

CREER, K. M., and N. PETERSEN: Thermochemical magnetization in basalts, Z. Geophys., 35,, 501—516, 1969

CREER, K. M., N. PETERSEN, and J. PETHERBRIDGE: Partial self-reversal of remanent magnetization and anisotropy of viscous magnetization in basalts, Geophys. J. R. astr. Soc., 21, 471—483, 1970

GALLAGHER, K. J., W. FEITNECHT, and U. MANNWEILER: Mechanism of oxidation of magne-
tite to γ-Fe$_2$O$_3$, Nature 217, 1118—1121, 1968

O'REILLY, W., and S. K. BANERJEE: Oxidation of titanomagnetites and self reversal, Nature,
211, 26—28, 1966

OZIMA, M., and E. LARSON: Low- and high-temperature oxidation of titanomagnetite in
relation to irreversible changes in the magnetic properties of submarine basalts, J. Geophys.
Res. 75, 1003—1017, 1970

READMAN, P. W., and W. O'REILLY: The synthesis and inversion of non-stoichiometric
titanomagnetites, Phys. Earth Planet. Interiors 4, 121—128, 1970

SANVER, M., and W. O'REILLY: The identification of naturally occurring non-stoichiometric
titanomagnetites. Phys. Earth Planet. Interiors 2, 166—174, 1970

VERHOOGEN, J.: Oxidation of iron-titanium oxides in igneous rocks, J. Geol. 70, 168—181,
1962

VERWEY, E. J. W., P. W. HAAJMAN, and F. C. ROMEIJN: Physical properties and cation
arrangement of oxides with spinel structure, J. Chem. Phys. 15, 174—180, 1947

A Method for Identifying
Naturally Occuring Titanomagnetites

M. Prévot, Saint-Maur[1])

Summary: A method of calculation of the cell edge *a* of titanomagnetites, based on the concept of invariance of the distance "anion-cation" is briefly described. For members of the solid solution series between magnetite and ulvöspinel the lattice parameter measured by previous workers from synthetic materials is in good agreement with the theoretical values which can be calculated, with this method, by using the Akimoto model of cation distribution. The curves of equal lattice parameter for oxidized titanomagnetites can also be calculated if the mechanism of oxidation is known. The curves obtained by assuming that all the Fe^{3+} ions which appear during oxidation process are located in octahedral sites show that the decrease of *a*, as oxidation proceeds, is much less important than claimed by Akimoto and al. Cell edge calculations can also be used to determine the degree of oxidation of iron in naturally occuring titanomagnetites, even if they are relatively rich in "minor" elements. A few examples are given, showing that oxidation degrees deduced by this method for titanomagnetites and titanomaghemites from a porphyritic basalt are supported by petrological and thermomagnetic data.

Zusammenfassung: Es wird eine Methode der Bestimmung der Gitterkonstante *a* von Titanomagnetiten beschrieben, die von der Unveränderlichkeit der Entfernung Anion—Kation ausgeht. Unter der Voraussetzung der Gültigkeit des Modells von Akimoto für die Kationen-Verteilung wurden die theoretisch zu erwartenden Gitterkonstanten für die Mischreihe Magnetit—Ulvöspinell berechnet. Die Werte stimmen gut mit denen überein, die andere Autoren durch Messungen an synthetischen Proben dieser Mischreihe erhalten hatten. Bei oxydierten Titanomagnetiten können Linien gleicher Gitterkonstanten berechnet werden, wenn der Oxydations-Mechanismus bekannt ist. Wenn man annimmt, daß alle bei der Oxydation gebildeten Fe^{3+}-Ionen Oktaederplätze besetzen, so ist die Abnahme von *a* mit steigendem Oxydationsgrad geringer als von Akimoto et al. angenommen worden war. Die Gitterkonstanten natürlicher Titanomagnetite können auch vor Bestimmung des Oxydationsgrades dieser Minerale verwendet werden, selbst wenn diese reich an Fremdzonen sind. Einige Beispiele zeigen die Übereinstimmung der Ergebnisse für den Oxydationsgrad von Titanomagnetiten und Titanomaghemiten nach der hier beschriebenen Methode und auf Grund petrographischer Daten und thermomagnetischer Kurven.

1. Introduction

Iron titanium oxides of spinel structure are the more common magnetic minerals in igneous rocks. They are usually called "titanomagnetites", in spite of the fact that

[1]) Michel Prévot, Laboratoire de Géomagnétisme, 4, avenue de Neptune, 94—Saint-Maur (France).

this word was first strictly reserved to the members of the solid solutions series lying between magnetite and ulvöspinel. To avoid any confusions, the following expressions will be used in this paper:

—*pure titanomagnetite* (or stoichiometric titanomagnetite): members of the solid solution series between Fe_3O_4 and Fe_2TiO_4.

—*true titanomagnetite*: titanomagnetite which differs from a pure titanomagnetite only by subsituting "minor" elements such as Al, Mg, Mn and Cr. This group and the previous one are *non-oxidized titanomagnetites*, characterized by the absence of any vacant site in the spinel lattice.

—*oxidized titanomagnetite*: titanomagnetite with some vacant lattice sites. It can be pure or contain minor elements.

—*true equivalent titanomagnetite*: the true titanomagnetite which has the same cation ratios as a given oxidized titanomagnetite.

—*pure equivalent titanomagnetite*: the pure titanomagnetite corresponding to a given true one by replacing the minor elements by iron.

Naturally occuring titanomagnetites are pure titanomagnetites or, more often, oxidized titanomagnetites with minor elements. The determination of the chemical composition of these minerals by the usual macrochemical analysis is difficult because their small size make their separation from the whole rock very critical. Consequently, the electron probe X-ray micro-analyser is generally used, though the Fe^{3+}/Fe^{2+} ratio cannot be determined with this instrument. An indirect method is therefore needed to calculate this ratio.

The method generally used is based on the fact that the lattice parameter a and the CURIE temperature θ_c depend on the oxidation of iron. Unfortunately, the variation of a and θ_c with the Fe^{3+}/Fe^{2+} ratio is not well established. Moreover, the minor elements always present in naturally occuring titanomagnetites have an influence on the values of a and θ_c.

Two attempts have yet been made to draw the contours of equal values of CURIE temperature and cell edge for oxidized titanomagnetites in the $FeO-Fe_2O_3-TiO_2$ ternary diagram. AKIMOTO and al. [1957] constructed these curves on the basis of measurements on synthetic samples heated in air. OZIMA and LARSON [1970] have shown that oxidation products obtained by the Japanese workers are not pure oxidized titanomagnetites but a mixture of several oxides. Thus, their curves cannot be of any use to our purpose. From the values of a and θ_c they collected in literature, ZELLER and BABKINE [1965] deduced other curves of equal a or θ_c. The data utilized being dispersed, and not uniformly distributed in the area between Fe_3O_4, Fe_2TiO_4, $FeTiO_3$ and Fe_3O_3, their curves are not defined with precision, except near the join $Fe_3O_4-Fe_2TiO_4$. Therefore it is difficult to use them for a quantitative study.

Molecular contents of minor elements is often about 5% in naturally occuring titanomagnetites and can sometimes be much higher (up to 15%) especially in tita-

nium-poor titanomagnetites. The effect of minor elements, which is to diminish both a and θ_c, is often neglected. In fact it is rarely unimportant. For example, in the case of magnetite, the substitution of a 3 % molecular content of Al_2O_3 leads to values of a and θ_c respectively smaller by 0.02 Å and 15°C than those for pure magnetite [POUILLARD, 1949].

Noting the absence of any reliable experimental results for oxidized titanomagnetites, SANVER and O'REILLY [1970] proposed a method for identifying naturally occuring titanomagnetites. This method is essentially based on an empirical calculation of the CURIE temperature (O'REILLY, 1968]. This calculation being a crude one, its application to the determination of the degree of oxidation of iron in titanomagnetites cannot give accurate results.

The method of determination of the Fe^{3+}/Fe^{2+} ratio proposed here is based on a new method of calculation of the cell edge of titanomagnetites. It can be applied to oxidized titanomagnetites even if rich in "minor" elements.

2. Method of cell edge Calculation

This method is based on the concept of invariance of the distance "anion-cation" and on some geometrical properties of the spinel structure.

2.1 Invariance of the distance "anion-cation"

It has been shown by POIX [1965] that any cation can be characterized by a distance anion-cation which depends only on its oxidation state and its coordination degree. This rule, discovered when studying orthotitanates and stannates of spinel structure has been verified for minerals of spinel, perovskite or $\alpha NaFeO_2$ structure. In particular the distances "metal-oxygen" have been calculated for many elements [POIX, 1965, 1969] and are known with a precision which is probably better than 0.01 Å, except for the distance "vacancy-oxygen".

2.2 Geometrical properties of the spinel structure

Let $\alpha = (Me_1-O)_4$ and $\beta = (Me_2-O)_6$ be the distances cation-oxygen corresponding respectively to cations Me_1 located in tetrahedral sites and to cations Me_2 located in octahedral sites. It can be shown (POIX, 1965; PRÉVOT et POIX, 1971] that α and β are given by:

$$\alpha = a\sqrt{3}\left(\frac{1}{8}+\delta\right) \tag{1}$$

$$\beta = a\left(\frac{1}{16}-\frac{\delta}{2}+3\delta^2\right)^{1/2} \tag{2}$$

where a is the cell edge and δ is a parameter given by $\delta = u - {}^3/_8$ (u being the oxygen parameter).

The cell edge is thus expressed by:

$$a = 2.0995\,\alpha + (5.8182\,\beta^2 - 1.4107\,\alpha^2)^{1/2} \qquad (3)$$

In the case of titanomagnetites, each site is generally occupied by several cations, so that α and β in the equation (3) are given by:

$$\alpha = \frac{\Sigma\,x_i\,\alpha_i}{\Sigma\,x_i} \qquad (4)$$

where x_i is the number of cations with a given α_i

$$\beta = \frac{\Sigma\,y_i\,\beta_i}{\Sigma\,y_i} \qquad (5)$$

where y_i is the number of cations with a given β_i.

3. Application to synthetic titanomagnetites

3.1 Adjustment of the distances "metal-oxygen"

From the values given by POIX [1965], it is possible to calculate the cell edge of magnetite, ulvöspinel and maghemite. It was found that calculated cell edges are not in perfect accordance with experimental data [PRÉVOT and POIX, 1971], suggesting that the distances "metal-oxygen" are, in the system investigated here, slightly different from those proposed by POIX [1965]. An adjustment is then necessary. As magnetite, ulvöspinel and maghemite are the only minerals whose cell edge and cation distribution are both known, it is not possible, at the present time, to calculate the corrected values for the six distances "metal-oxygen" we have to consider. Using equations (1) to (5) several sets of adjusted values can be obtained, which fulfil the two following conditions:

—(i) cell edges for magnetite, ulvöspinel and maghemite must be equal to 8.396 Å, 8.535 Å and 8.34 Å respectively.

—(ii) the corrections must not be too large. It can be assumed that the corrected distances should not be different from the POIX [1965] values by more than 1 %.

A set of such adjusted values is given in table I. Let us notice that it has been shown previously [PRÉVOT and POIX, 1971] that, for a given compound whose chemical composition is between Fe_3O_4, Fe_2TiO_4, $FeTiO_3$ and Fe_2O_3, the calculated cell edge is about the same (± 0.002 Å) whatever the set of adjusted values used. Thus, the choice of the adjusted distances "metal-oxygen" is not critical; but it must be made, obviously, by using the equations mentioned above.

Table I
Distances metal-oxygen for titanomagnetites (in Å)

Cations	4-fold coordination	6-fold coordination
Fe^{2+}	2.024	2.130
Fe^{3+}	1.855	2.026
Ti^{4+}	—	1.944
Valency	—	2.216
Al^{3+}	1.777	1.898
Mg^{2+}	1.990	2.106
Mn^{2+}	2.041	2.220
Cr^{3+}	—	1.987
V^{3+}	—	2.022

3.2 Cell edge calculations for titanomagnetites

By using the method of calculation presented here, PRÉVOT and POIX [1971] calculated the cell edge of pure and oxidized titanomagnetites. Their results can be summarized as follows:

For pure titanomagnetites, whose general formula is $xFe_2TiO_4(1-x)Fe_3O_4$, the calculated values of a are in good agreement with experimental data if the AKIMOTO model of cation distribution is assumed. With the O'REILLY and BANERJEE model, and especially with the NÉEL and CHEVALLIER model, the calculated values are less than to the experimental ones. If we consider the shape of the theoretical curves it is clear however that none of the proposed distributions can explain exactly the totality of the experimental results. But, from a practical point of view, we may consider that, for such cell edge calculations, the AKIMOTO model is suitable: experimental data and theoretical curve coincide for $x > 0.4$ and, if for $0.1 < x < 0.4$ the theoretical curve is above experimental values, the difference is less than 0.005 Å.

The AKIMOTO model being assumed for pure titanomagnetites, curves of equal lattice parameter for oxidized titanomagnetites can be calculated if the mechanism of oxidation is known. The bonding for tetrahedral sites cations being covalent, and the bonding in octahedral sites probably almost purely ionic [O'REILLY, 1969], we may assume that oxidation process takes place only at the expense of octahedral sites iron. The theoretical curves of equal lattice parameter, obtained for oxidation of octahedral sites only, correspond approximately, in the $FeO-Fe_2O_3-TiO_2$ ternary diagram, to the area between Fe_3O_4, Fe_2TiO_4, $FeTiO_3$ and Fe_2O_3. In this region, theoretical results show that a decreases when oxidation increases. The diminution is much less important than it was claimed by AKIMOTO and al., which is probably due to mistake in their experiments (OZIMA and LARSON, 1970]. Let us notice however that if some of the ferric ions produced during oxidation process were located in the tetrahedral sites, the calculated cell edge should diminish more.

4. Identification of naturally occuring titanomagnetites

4.1 Basic assumptions

Cell edge calculations for naturally occuring titanomagnetites can be made if are known: the cation distribution for true titanomagnetites; the location of Fe^{3+} ions which appear during oxidation process; the values of the distances "metal-oxygen" for minor elements; and the location of these elements.

(i) The cation distribution for true titanomagnetites is probably near the AKIMOTO model. Indeed, ZELLER and BABKINE have shown that for naturally occuring non oxidized titanomagnetites the lattice parameter varies linearly with x. The theoretical curve calculated by using the AKIMOTO model being approximately a straight line, this distribution can be assumed for cell edge calculations.

(ii) From theoretical and experimental data, we may deduce that Fe^{3+} ions which appear during oxidation process are probably located in octahedral sites. The bondings between anions and cations are probably the same in natural and in synthetic titano-magnetites. So, we are entitled to think that, in that case also, oxidation will take place largely at the expence of octahedral Fe^{2+} and the cation population of tetra-hedral sites will remain constant. Thus, Fe^{3+} produced by oxidation will be located in octahedral sites only. This deduction has been verified experimentally by POIX, PRÉVOT and MERGOIL [1971] for a highly oxidized titanium-rich titanomagnetite. The pure equivalent titanomagnetite of the studied mineral had an ulvöspinel content equal to 90% and was thus characterized by quite a small number of tetrahedral Fe^{3+} ions (0.1 according to the AKIMOTO model). The naturally oxidized titanomagne-tite should consequently contain Fe^{3+} almost exclusively in octahedral sites, which has been verified by determining, from a careful study of the X-ray diffraction pattern, the u parameter and the reflectivities of the octahedral and tetrahedral populations.

(iii) The values of the distances "metal-oxygen" for minor elements can be taken equal to the POIX values. Indeed, for these elements, whose content is very low with respect to the Fe content, it is not necessary to adjust the values of their distances. So, we can use the POIX values (table I).

(iv) The location for the more common minor elements in naturally occuring titanomagnetites may be assumed as follows, from many observations on spinels: Al^{3+} and Cr^{3+} in octahedral sites, Mn^{2+} in tetrahedral and Mg^{2+} in both octahedral and tetrahedral sites.

4.2 Method for determining the degree of oxidation of iron

The assumptions mentioned above allow us to calculate the lattice parameter of any naturally occuring titanomagnetite whatever its "impurities" contents and its degree of oxidation are. Details of calculation have been given previously [PRÉVOT and POIX, 1971]. The error about the value of the calculated lattice parameter should not be greater than 0.005 Å.

Let z be an oxidation parameter ($0 \leq z \leq 1$) which is the fraction of the total original Fe^{2+} ions in the equivalent titanomagnetite converted to Fe^{3+} [O'REILLY and BANERJEE, 1966]. Calculation of z for naturally occuring titanomagnetites needs the following successive operations to be made:

1—measurement of the *mean* metallic ion contents of the titanomagnetite population. It can be done easily by using an electron probe X-ray micro-analyser. But it is obvious that, to obtain mean values, these analyses must be made for numerous titanomagnetite grains.

2—measurement of the cell edge a of the titanomagnetite.

3—calculation of the cell edge a_0 of the true equivalent titanomagnetite and comparison with the observed value a.

If a_0 is equal to a, it may be concluded that the titanomagnetite is not oxidized.

If a is less than to a_0, the titanomagnetite is oxidized. Let us notice that the difference must be at least equal to 0.005 Å to be significant. It is then possible to calculate the degree of oxidation needed to obtain a calculated lattice parameter equal to the observed value.

1.3 Examples

This method has been applied by PRÉVOT and MERGOIL [1971] to study the chemical composition of various titanomagnetite or titanomaghemite populations in a porphyritic basalt.

The first population studied consisted of phenocrysts of titanomagnetites which are poor in titanium (the pure equivalent titanomagnetite contains a percentage of ulvöspinel equal to 40 %) and relatively rich in aluminium and magnesium. They are included, together with pyrrhotite grains, in phenocrysts of clinopyroxene which crystallized previous to eruption. The phenocrysts of titanomagnetites thus also crystallized intratellurically, when the oxygen fugacity was low, and they can be expected to be true titanomagnetites. This deduction, based on petrological considerations, has been verified by using the method exposed above. It was found that the calculated cell edge a_0 for the true equivalent titanomagnetite, equal to 8.401 Å, was not significantly different from the measured value ($a = 8.404$ Å). So, these titanomagnetites are really true titanomagnetites.

The same phenocrysts of clinopyroxene are also present in the projections which lie under and above the lava flow. There, the phenocrysts of titanomagnetites included in the clinopyroxene are often partially maghemitized. As previously observed in another case [PRÉVOT and al., 1968], the metallic ion contents are not exactly the same for the patches of titanomaghemite and for the original, unaltered, titanomagnetite. This must be accounted for by a differential diffusion rate of the different cations. In particular, the titanium does not appear to diffuse significantly. For these titanomaghemites, a_0 (8.364 Å) is greater than a (8.33 Å). The calculated oxidation parameter z is equal to 0.62, which means that this mineral is an highly oxidized titano-
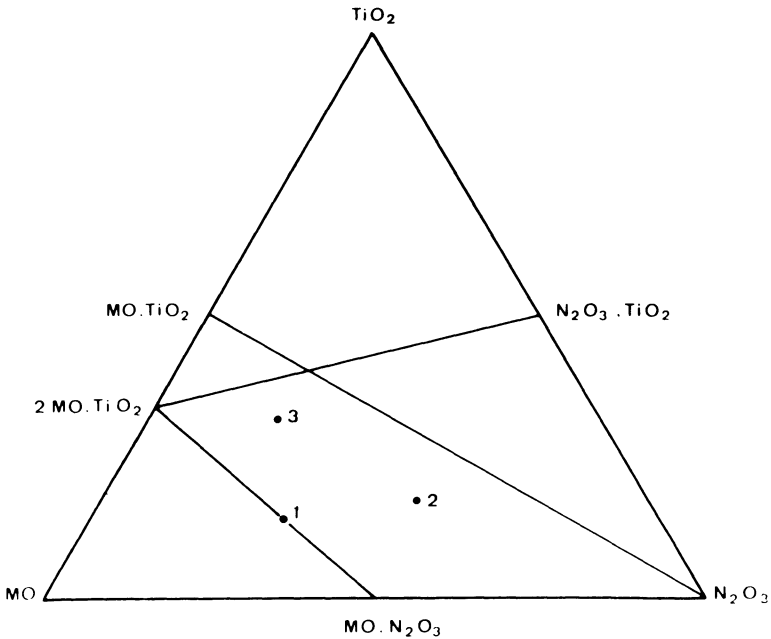
Fig. 1: Chemical composition of the three titanomagnetite and titanomaghemite populations. 1, phenocrysts of titanomagnetite included in clinopyroxene; 2, titanomaghemite patches in the previous crystals; 3, microcrysts of titanomaghemite from the ground-mass. M is the total number of bivalent ions, N the total number of trivalent ions.

magnetite (fig. 1). As generally observed for such compounds, the mineral was destroyed by heating above a few hundred degrees and its Curie point could not be measured.

The microcrysts of titanomagnetites in the groundmass have a reflectivity power superior to the one of the first population and may be called titanomaghemites. They are quite rich in titanium (the content in ulvöspinel of the pure equivalent titano-magnetite is equal to 88%) and poor in aluminium and magnesium. a_0 (8.484 Å) is greater than a (8.449 Å) and the calculated oxidation parameter z is equal to 0.32 (fig. 1). The Curie temperature being about 215^0C, this value of z seems plausible.

5. Conclusion

Cell edge calculations seems to be a good method to determine the oxidation para-meter of naturally occuring titanomagnetites. The method proposed here can be applied to any titanomagnetite, even if it contains an important percentage of "im-purities". The results obtained with this method for titanomagnetites or titanomaghe-mites from a porphyritic basalt are in accordance with petrological and thermomag-netic data.

References

AKIMOTO, S., T. KATSURA and M. YOSHIDA: Magnetic properties of $TiFe_2O_4$—Fe_3O_4 system and their change with oxidation. J. Geomagn. Geoelectr., 9, 4, 165—178, 1957

CHEVALLIER, R., J. BOLFA and S. MATHIEU: Titanomagnétites et ilménites ferromagnétiques. Bull. Soc. franç. Minér. Crist., 78, 307—346 and 365—399, 1955

NEEL, L.: Some theoretical aspects of rock-magnetism. Phil. Mag. Sup., 4, 191—242, 1955

O'REILLY, W.: Application of neutron diffraction and MÖSSBAUER effect to rock magnetism; in The application of modern physics to the earth and plenatary interiors, p. 479—484, 1969

O'REILLY, W. and S. K. BANERJEE: Oxidation of titanomagnetites and self-reversal. Nature, 211, 5044, p. 26—28, 1966

OZIMA, M. and E. E. LARSON: Low- and high-temperature oxidation of titanomagnetite in relation to irreversible changes in the magnetic properties of submarine basalts. J. Geophys. Res., 75, 5, p. 1003—1018, 1970

POIX, P.: Sur une méthode de détermination des distances cation-oxygène dans les oxydes mixtes à structure spinelle, application des valeurs à quelques cas particuliers. Bull. Soc. Ch. Fr., p. 1085—1087, 1965

POIX, P.: Table générale des distances caractéristiques "métal-oxygène" en coordinance 6. C. R. Acad. Sc., 268, p. 1139—1140, 1969

POIX, P., M. PRÉVOT and J. MERGOIL: Localisation du fer ferreux dans une titaniomagnétie naturelle riche en titane fortement oxydée. In press.

POUILLARD, E.: Sur le comportement de l'alumine et de l'oxyde de titane vis-à-vis des oxydes de fer. Thèse, Paris, 1949

PRÉVOT, M., G. RÉMOND and R. CAYE: Etude de la transformation d'une titanomagnétite en titanomaghémite dans une roche volcanique. Bul. Soc. fr. Minér. Cristal., 91, 65—74, 1968

PRÉVOT, M. and J. MERGOIL: Variation de la composition chimique des titanomagnétites au cours de la cristallisation d'un basalte porphyrique. In press

PRÉVOT, M. and P. POIX: Un calcul du paramètre cristallin des titanomagnétites oxydées. J. Geomagn. Geoelect. In press, 1971

SANVER, M. and W. O'REILLY: Identification of naturally occuring non-stoichiometric titano-magnetites. Phys. Earth Plan. Inter., 2, 166—174, 1970

ZELLER, C. and J. BABKINE: Mise en évidence d'une loi reliant le paramètre cristallin au chimisme des titanomagnétites. C. R. Acad. Sc., 250, 1375—1378, 1965

Magnetic and X-Ray Diffraction Measurements of the Synthetic Spinel System $FeFe_2O_4$— $MgFe_2O_4$— $NiFe_2O_4$

R. Pucher, Hannover[1])

Summary: The main purpose of this study was to measure the magnetic properties of ferrites searching for nonlinearities within solid solution series. The ternary system $FeFe_2O_4$— $MgFe_2O_4$— $NiFe_2O_4$ has been chosen since the end members show distinctly different magnetic parameters. The synthetic samples were made by the hydrothermal high pressure method. The measurements indicate that neither for specific saturation magnetization nor for Curie temperature and lattice parameter the change is linear for all of the three binary solid solution series. Curie temperature has a maximum near $Ni_{0.8}Fe_{0.2}Fe_2O_4$ with $T_c = 595\,^0C$ and a minimam near $Ni_{0.3}Fe_{0.7}Fe_2O_4$ with $T_c = 490\,^0C$. Specific saturation magnetization measured at $20\,^0C$ shows a minimum near $Ni_{0.5}Fe_{0.5}Fe_2O_4$ with $J_s = 34.6$ Gcm^3 g^{-1} and a maximum with $J_s = 77.0$ Gcm^3 g^{-1} near $Ni_{0.75}Mg_{0.25}Fe_2O_4$. Except near $Ni_{0.75}Mg_{0.25}Fe_2O_4$ with $a_0 = 8.384$ Å there is no remarkable irregularity for the lattice parameter.

Zusammenfassung: Ziel dieser Untersuchung von synthetischen Ferriten war die Beantwortung der Frage, ob sich die magnetischen Eigenschaften innerhalb von Mischreihen immer streng linear ändern. Das ternäre System $FeFe_2O_4$— $MgFe_2O_4$— $NiFe_2O_4$ wurde für die vorliegende Studie gewählt, weil dessen Endglieder deutlich verschiedene magnetische Parameter haben. Die synthetischen Proben wurden mit Hilfe der hydrothermalen Hochdruckmethode hergestellt. Die Messungen ergaben, daß die Änderung weder der spezifischen Sättigungsmagnetisierung noch der Curie-Temperatur und der Gitterkonstante für alle drei binären Mischreihen streng linear ist. Die Curie-Temperatur hat nahe $Ni_{0.8}Fe_{0.2}Fe_2O_4$ mit $T_c = 595\,^0C$ ein Maximum und mit $T_c = 490\,^0C$ nahe $Ni_{0.3}Fe_{0.7}Fe_2O_4$ ein Minimum. Die spezifische Sättigungsmagnetisierung, gemessen bei Raumtemperatur, zeigt ein relatives Minimum in der Nähe von $Ni_{0.5}Fe_{0.5}Fe_2O_4$ mit $J_s = 34.6$ Gcm^3 g^{-1} und ein Maximum mit $J_s = 77.0$ Gcm^3 g^{-1} nahe $Ni_{0.75}Mg_{0.25}Fe_2O_4$. Für die Gitterkonstante wurden außer mit $a_0 = 8.384$ Å bei $Ni_{0.75}$-$Mg_{0.25}Fe_2O_4$ keine deutlich nichtlinearen Änderungen gemessen.

Introduction

At present the magnetic influence of minor components like MgO, MnO, Al_2O_3 or Cr_2O_3 in magnetite is under discussion in rock magnetism. Although the magnetic properties of magnesium ferrite $MgFe_2O_4$ are known [Smit and Wijn 1962], those of the solid solution series Mg-ferrite $MgFe_2O_4$—magnetite $FeFe_2O_4$ have not yet been completely measured [Benard and Chauron 1937]. Except for ore, fairly pure

---

[1]) Dr. Rudolf Pucher, Niedersächsisches Landesamt für Bodenforschung, 3 Hannover-Buchholz, Stille-Weg 2

Mg-ferrite is rare [RAMDOHR 1952]. In nature the members of the series $MgFe_2O_4$—$FeFe_2O_4$ near magnetite are frequent and therefore important in rock magnetism.

In case of linear change of the magnetic parameters within a solid solution series the parameters of a member with a fixed composition could be computed from the parameters of the end members. Since this is in general not the case, members of natural solid solution series have to be synthesized and studied.

In order to estimate the nonlinearity of magnetic parameters for some inverse ferrites, samples of ternary solid solution series have been synthesized for which the end members show distinctly different magnetic parameters. The system $FeFe_2O_4$—$MgFe_2O_4$—$NiFe_2O_4$ was chosen since the saturation magnetization of $NiFe_2O_4$ is much lower and the CURIE temperature is higher than for magnetite (see table 1).

Experimental Method

The preparation of the samples was done by the hydrothermal high pressure method. The starting materials, hematite Fe_2O_3, iron Fe, nickel oxide NiO, and magnesium oxide MgO, were mixed stoichiometrically, sealed in gold capsules and put into a pressure vessel with confining pressure of 1500—2000 bars at a tempera-ture of 650^{0}C for two days. With these experimental conditions the grain size of the samples ranges from 2 μ to 20 μ. To provide a better chemical contact of the mixture and to mobilize the reaction of the phases, a liquid had to be added to the starting mixture. The best results were obtained when using 1 normal oxygen free HCl as a liquid.

The saturation magnetization J_s was determined by measuring the upper part of the hysteresis loop within nine steps for increasing magnetic intensity up to 5.10^3 Oe at room temperature. Then the paramagnetic influence was subtracted by a graphic method. For calibration magnetite was used.

As second parameter the CURIE temperature T_c was measured. For its determina-tion a high frequency unit [HILLEBRAND 1966] was used which applies a method of FRAUENBERGER [1955] and PETERSEN [1967] of measuring the Hopkinson maximum of the initial susceptibility close below the CURIE point. Depending on the steepness of its curve the accuracy of the T_c determination is $\pm 2^0$—5^{0}C. To prevent oxidation of the sample the measurements were carried out in purified N_2 atmosphere.

For the X-ray diffraction measurements the K_a-radiation of an Fe-tube with Mn-filter was used. To obtain the lattice parameter a_0 with an accuracy as high as possible an inner standard and a very low measuring speed were applied. The a_0 values of figure 3 have an accuracy of $\pm 10^{-3}$ Å.

Results and Discussion

In order to outline the nature of this study, a brief description of the spinel structure will be given. The general formula of an oxide spinel is XY_2O_4. The spinel structure

can be described as a face-centered cubic lattice of oxygen ions with cations in inter-
stices. The spinel lattice contains tetrahedral (A site) and octahedral (B site) inter-
stices with four and six oxygen atoms respectively as nearest neighbours. In the unit
cell there are 64 A sites and 32 B sites. Only eight A sites and 16 B sites are occupied.
We are dealing with "inverse 2—3 spinels" in which X is divalent and Y trivalent.
A spinel is called "inverse" if the occupied A sites contain only trivalent cations
with the formula Y (XY) O_4. In the "normal" spinels the occupied A sites contain
only divalent cations.

The magnetic moments of the A sites are antiferromagnetically coupled with those
of the B sites. If the resultant magnetic moment of one of the two ferromagnetic
sublattices is unequal zero, the "ferrimagnetic" state arises. This theory, due to NÉEL
[1948], is confirmed by neutron diffraction. But for many cases this model does not
explain the experimental data. According to NÉEL's [1948] theory, the interaction of
different pairs of cations are AA < BB ≪ AB. The bonding of the spinels is ruled
by coupling of antiparallel electron spins, not so much by the electrostatic valences

Table 1

ferrite	lattice parameter a_0 (Å)	saturation magnetization at 20°C (Gcm³ g⁻¹)	CURIE temperature (°C)
$FeFe_2O_4$	8.394	92.0	576
$NiFe_2O_4$	8.358	50.4	585
$MgFe_2O_4$	8.397	41.9	438

Table 2

ferrite	cation distribution [ ]: octahedral B sites		ion radii (5) trivalent	divalent
$FeFe_2O_4$	$Fe^{III} [Fe^{II}Fe^{III}]O_4$	(1)	0.67 Å	0.83 Å
$NiFe_2O_4$	$Fe^{III} [Ni^{II}Fe^{III}]O_4$	(2)	0.67 Å	0.78 Å
$MgFe_2O_4$	$Mg_{0.1}{}^{II}Fe_{0.9}{}^{II}[Mg_{0.9}{}^{III}Fe_{1.1}{}^{III}]O_4$	(3, 4)	0.67 Å	0.78 Å

(1) SHULL, WOLLAN, and KOEHLER [1951]
(2) HASTINGS and CORLISS [1953]
(3) BACON and ROBERTS [1953]
(4) CORLISS, HASTINGS, and BROCKMAN [1935]
(5) SMIT and WIJN [1962]
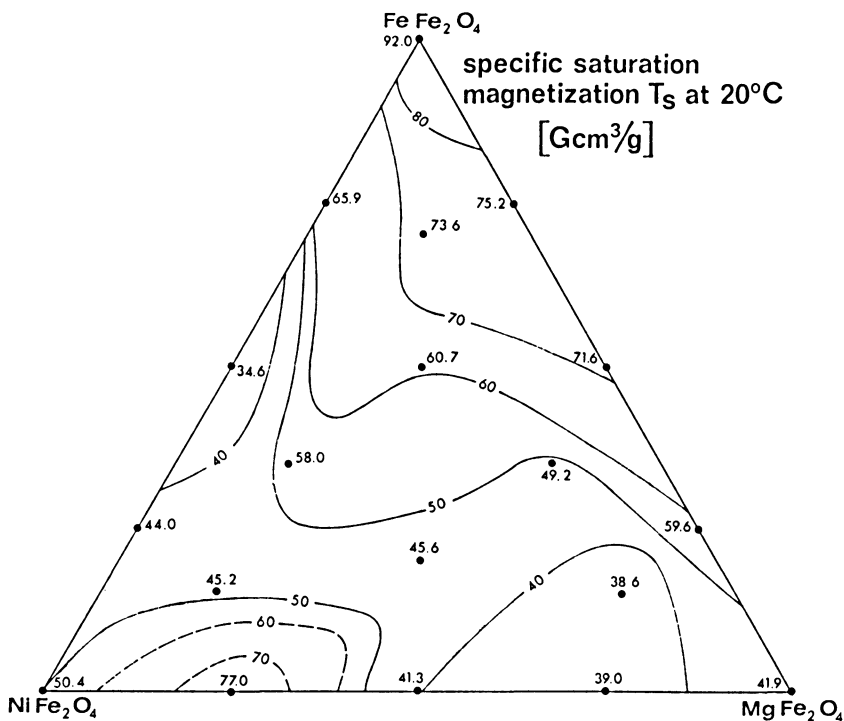
Fig. 1: Specific saturation magnetization measured at room temperature for magnetic field intensity up to $5 \cdot 10^3$ Oe.

Points in figures 1, 2, and 3 indicate the composition of the synthetized samples, the numbers nearby give the value of the parameter.

of the cations. The coordination of the ions is a result of the electron configuration in the lattice and is not remarkably influenced by the radii of the cations or ratio of the radii of interstices and radii of the cations [FRÖLICH 1964, p. 40.] From the fact that lattice situations and electron states influence each other, LÖFFLER [1964] derived a theory for interpretations of the magnetic behaviour of the oxide spinels with 3d transition metals. Besides many other points, the occupation of the electron orbitals has much influence on the type of bond and the interaction strength. A large over-lapping of orbitals with increased probability of electron occurrence results in strong interactions. The lattice symmetry influences the angular dependence of the electron orbitals. Whereas for the magnetization of spinels, ions as carrier of magnetic mo-ments are responsible, the CURIE temperature is ruled by indirect AB interactions [LÖFFLER, FRÖLICH, STILLER 1965]. STILLER and FRÖLICH [1964] showed that for the solid solution series magnetite-ulvospinel the CURIE temperature is ruled completely by AB interactions of the Fe^{3+} ions.

Cation distribution of magnetite, Mg-ferrite, and Ni-ferrite which is derived from neutron diffraction measurements is summarized in table 2. Magnetite and Ni-ferrite are completely inverse. Cation distribution of Mg-ferrite indicates that its crystal structure is only partly inverse. In table 2 ion radii of the cations also are summarized.

In this paper a calculation of cation configuration and magnetic properties of the investigated solid solutions shall not be tried. The measurements of saturation magnetization, CURIE temperature, and lattice parameter shall be presented without theoretical interpretation.

Figures 1, 2, and 3 show the result of our measurements. The changes of the parameters are not always linear. But the irregularities are not simply correlated. The behaviour of the center solid solution of this ternary system is fairly equivalent to the interpolated value of the three end members.

Saturation magnetization: The saturation magnetization of the different binary solid solution series shows both linear and nonlinear transitions between the end members of the series. The value for MgFe₂O₄ is considerably different from that of SMIT and WIJN [1962, p. 180]. Probably the way of preparation of the samples causes
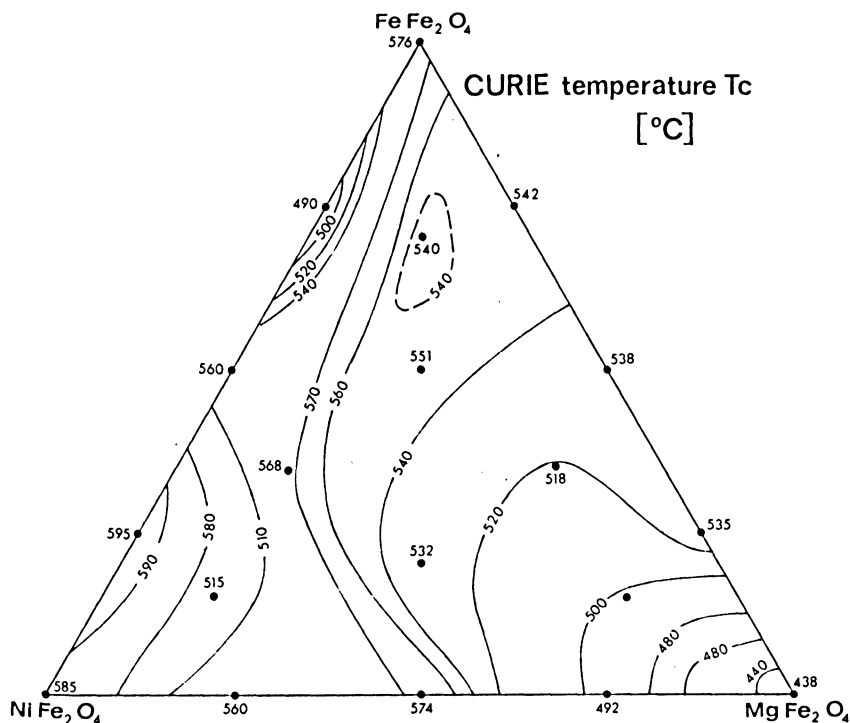
Fig. 2: CURIE temperature distribution of the ternary system $FeFe_2O_4 - MgFe_2O_4 - NiFe_2O_4$.
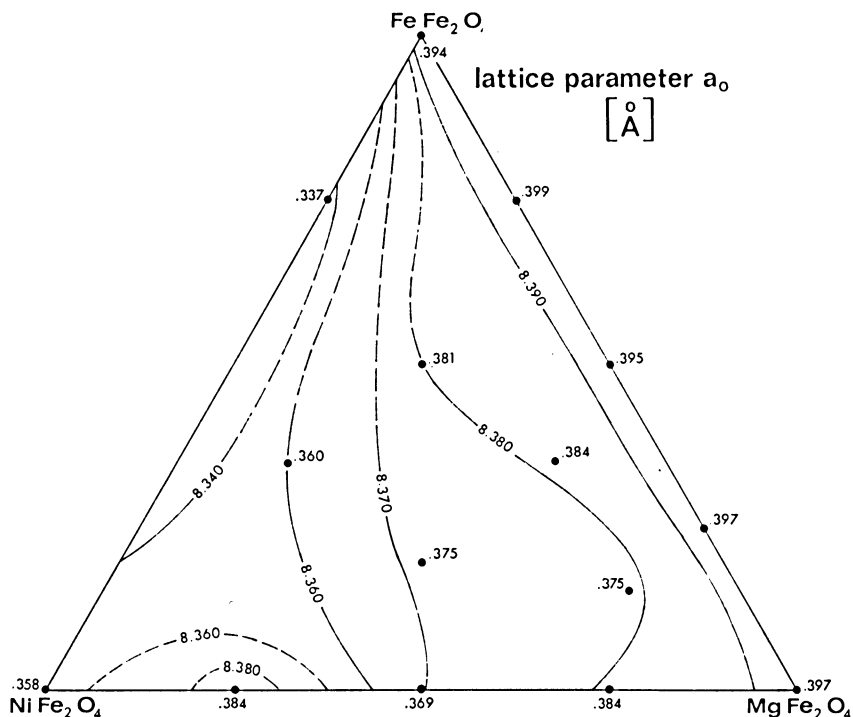
Fig. 3: Distribution of the lattice parameter a_0 of the system $FeFe_2O_4-MgFe_2O_4-NiFe_2O_4$.

a different magnetic behaviour of the partly normal Mg-ferrite as has already been observed [PAUTHENEST and BOCHIROL 1951]. The measurements yielded a maximum of $J_s = 77.0$ Gcm^3 g^{-1} near $Ni_{0.75}Mg_{0.25}Fe_2O_4$, and a minimum of $J_s = 34.6$ Gcm^{3}g^{-1} near $Ni_{0.5}Fe_{0.5}Fe_2O_4$.

CURIE *temperature:* In the same manner as saturation magnetization the change of the CURIE temperature is not quite linear for any of the three binary solid solution series. Our results for the series $FeFe_2O_4-NiFe_2O_4$ are in contradiction to those of BENARD et al. [1937]. Their measurements show a linear change of the CURIE temperature.

Lattice parameter: The lattice parameter of the series magnetite—Mg-ferrite is almost constant. For the other two binary series the nonlinearities are also small except for the area near $Ni_{0.75}Mg_{0.25}Fe_2O_4$ with a higher lattice parameter. Probably the reason of the remarkable deviation from VEGARD's law which postulates a linear change of the lattice parameter within a solid solution series is inhomogeneity of the synthesized phase. Since this anomaly is indicated by only one sample, this irregularity need not be real.

In view of rock magnetism it may be said that in first approximation the values of magnetic parameters of a solid solution of different spinels are the sum of the end members proportional to the contents only if inverse spinels are exclusively involved. Otherwise the values can change unexpectedly. The same may be said of substitution by cations of more than three valences.

In addition the values for solid solutions in natural rocks will change as a result of partial oxidation. The density of vacancies will increase [SCHMIDBAUER 1969]. A second mechanism during partial oxidation or alteration is diffusion of some cations out of the spinel crystal. If the residual system is an inhomogeneous solid solution, spinel exsolution can happen and can change the magnetic behaviour of this rock [PUCHER 1969].

Acknowledgements

References

BACON, G. E., and F. F. ROBERTS: Neutron Diffraction Studies of Magnesium Ferrite-Aluminate Powders. Acta Cryst. 6, 57—62, 1953

BÉNARD, J., and G. CHAUDRON: Préparation de ferrites par substitution des ions ferreux dans la magnétite. Compt. rend. 204, 766—768, 1937

CORLISS, L. M., G. M. HASTINGS and F. G. BROCKMAN: A Neutron Diffraction Study of Magnesium Ferrite. Phys. Rev. 90, 1013—1018, 1935

FRAUENBERGER, F.: Über eine Hochfrequenzmethode für metallkundliche Untersuchungen an magnetischen Legierungen. Z. Metallk. 46, 749—751, 1955

FRÖLICH, E.: Der physikalische Zustand der Gesteine und seine Auswirkungen auf das magnetische Verhalten der Erdkruste. Abh. Nr. 34 Geomagnet. Institut Potsdam, Akademie-Verlag Berlin, 1964

HASTINGS, J. M., and L. M. CORLISS: Neutron Diffraction Study of Zinc Ferrite and Nickel Ferrite. Rev. Mod. Phys. 25, 114—119, 1953

HILLEBRAND, O.: Zur Messung einiger magnetischer Eigenschaften von künstlichen Eisen-Titan-Oxyden. Dipl.-Arbeit Math. Nat., Univ. Göttingen, 1966

LÖFFLER, H., F. FRÖLICH and H. STILLER: Interpretation of Changes in CURIE temperature Observed in Rocks. Geophys. J. R. astr. Soc. 9 (5), 411—422, 1965

LÖFFLER, H.: Eine phänomenologische Theorie zur Erklärung des magnetischen Verhaltens der Spinelltyp-Oxyde der 3d-Übergangsmetalle. Abh. Nr. 34 Geomagnet. Institut Potsdam, Akademie-Verlag Berlin, 1964

NEEL, L.: Propriétes magnétiques des ferrites: Ferrimagnétisme et antiferromagnétisme. Ann. Phys., Paris 3, 137, 1948

PAUTHENST, R., and L. BOCHIROL: Aimantation Spontané des Ferrites. Journ. Phys. Radium 12, 249—251, 1951

PETERSEN, N.: A High-Frequency Method for the Measurement of CURIE Temperature of Ferrimagnetic Minerals, in: Methods in Paleomagnetism. Elsevier Publ. Comp., Amsterdam 1967

PUCHER, R.: On the Oxidation and Reduction of Natural Magnetites. Geophys. J. R. astr. Soc. 18, 489—497, 1969

RAMDOHR, P.: Neue Beobachtungen am Bühl-Eisen. Sitzungsber. Akad. Wiss. Berlin Nr. 5, 1952

SCHMIDBAUER, E.: Magnetic Properties of Oxidized Fe-Cr-Spinels. Z. Geophys. 35, 475—484, 1969

SHULL, C. G., E. O. WOLLAN and W. C. KOEHLER: Neutron Scattering by Ferromagnetic Minerals. Phys. Rev. 84, 912—921, 1951

SMIT, J., and H. P. J. WIJN: "Ferrite". N. V. Philips Gloeilampenfabrieken, Eindhoven (Holland), 1962

STILLER, H., and F. FRÖLICH: Studies on Rack Forming Magnetic Minerals. Z. Geophys. 30 (1), 13—22, 1964

On the Strength of Exchange Interactions
in Titanomagnetites and its Relation to Self-Reversal
of Magnetization

A. SCHULT, München[1])

Summary: When in titanomagnetites a cation deficient spinel phase is produced by oxidation, the ratio of the sublattice magnetizations at $0°K$ M_A/M_B should increase with increasing oxidation degree. For $M_A/M_B > 1$ self-reversal of magnetization is possible. The sequence of "anomalous" $M_S(T)$ curve types (spontaneous magnetization versus temperature curves which appear for $M_A/M_B \approx 1$) is determined by the sign of the magnetic exchange interactions and the composition range in which these curve types occur is determined by the strength of the interactions.—It can be estimated by the aid of the molecular field theory and the pressure dependence of the CURIE temperatures of the titanomagnetites that the exchange interaction in the B-sublattice is positive and relatively strong. It follows from NÉEL's theory that the sequence of the $M_S(T)$ curve types will be $Q \rightarrow P \rightarrow L \rightarrow N \rightarrow Q$ with increasing oxidation degree and the composition ranges for these curve types will be large. This is in agreement with determinations of the composition of natural titanomagnetites and their corresponding $M_S(T)$ curve types. Self-reversal of magnetization can only occur when the oxidation degree and the titanium content are extremely high.

Zusammenfassung: Wird bei der Oxidation von Titanomagnetiten eine Spinellphase mit Kation-Defekt-Struktur gebildet, sollte das Verhältnis der Untergitter-Magnetisierungen bei $0°K$ M_A/M_B zunehmen und bei einem bestimmten Oxidationsgrad gleich 1 werden. Für $M_A/M_B > 1$ ist Selbstumkehr der Magnetisierung möglich. Die Reihenfolge von „anomalen" $M_S(T)$ Kurven-Typen (spontane Magnetisierung als Funktion der Temperatur, „anomale" Typen treten für $M_A/M_B \approx 1$ auf) wird bestimmt durch das Vorzeichen der Austausch-wechselwirkungen; die Variationsbreite der chemischen Zusammensetzung, in der diese Kurven-Typen auftreten, wird durch die Stärke der Wechselwirkungen bestimmt. Mit Hilfe der Molekular-Feld-Theorie und der Druckabhängigkeit der CURIE Temperaturen der Titano-magnetite kann gezeigt werden, daß die Austauschwechselwirkungen im B-Untergitter positiv und relativ groß sind. Es folgt damit aus der NÉELschen Theorie, daß die Reihenfolge der $M_S(T)$ Kurven-Typen mit zunehmendem Oxidationsgrad $Q \rightarrow P \rightarrow L \rightarrow N \rightarrow Q$ ist und die Variationsbreite der Zusammensetzung, für die diese $M_S(T)$ Kurven auftreten, groß ist. Dies stimmt überein mit Messungen der chemischen Zusammensetzung von natürlichen Titano-magnetiten mit entsprechenden $M_S(T)$ Kurven-Typen. Selbstumkehr der Magnetisierung kann deshalb nur auftreten, wenn der Oxidationsgrad und der Titangehalt der Titanomagne-tite extrem hoch sind.

[1]) Dr. AXEL SCHULT, Institut für Angewandte Geophysik der Ludwig-Maximilians-Uni-versität München, 8 München 2, Richard-Wagner-Straße 10, Germany.

1. Introduction

It is known that under certain conditions titanomagnetites $(1-x) \cdot Fe_3O_4$-$x \cdot Fe_2$-TiO_4 can form a cation deficient spinel phase by oxidation. As the vacancies are probably confined to B-sites only (octahedral sites) a change from a B-sublattice predominant magnetization (the "normal" case for titanomagnetites) to an A-sublattice (tetrahedral sublattice) predominant magnetization is possible (for $x > 0.5$) thus producing self-reversal of magnetization. This means that with increasing oxidation degree the ratio of the sublattice magnetizations at 0^0K M_A/M_B increases, reaching unity at a certain oxidation state and increases further. This has been discussed by several authors [e. g. VERHOOGEN 1962, O'REILLY et al. 1967, SAKAMATO et al. 1968, SCHULT 1965, 1968].

It follows from NÉEL's [1948] theory that at the stage where $M_A/M_B \approx 1$ the spontaneous magnetization versus temperature curves $M_S(T)$ have anomalous shapes which are classified in different curve types (P-type with a hump, L-type with vanishing magnetization at 0^0K, N-type with a compensation temperature, Q-type is a "normal" $M_S(T)$ curve). The change of the shape of the $M_S(T)$ curves as function of M_A/M_B is determined by the sign and the strength of the magnetic exchange interactions which can be described by J_{AA}, J_{BB} and J_{AB} (exchange interactions in the A- and B-sublattices and between the A- and B-sublattice, respectively).—It is the purpose of this paper to give some estimations of the exchange interactions in titanomagnetites and the behaviour of the shape of the $M_S(T)$ curves for different oxidation degrees.

2. Exchange interactions in titanomagnetites

Using the notation of NÉEL [1948] the exchange interactions J_{AB}, J_{BB}, J_{AA} are linearly related to the molecular field coefficients n, $n\beta$, and $n\alpha$ respectively. We assume now that J_{AA} is negligible small with respect to J_{AB} and J_{BB} i. e. $\alpha \approx 0$. This has been proved by theoretical and experimental results for ferrites by BLASSE [1964] and several other authors.

Then it follows directly from NÉEL's [1948] theory that the $M_S(T)$-curve is of the P-type for M_A/M_B values between 1 and $(1-\beta)$ and of the N-type for M_A/M_B between 1 and $(1 + \beta)$. For $M_A/M_B = 1$ the $M_S (T)$ curve is of the L-type and for all other M_A/M_B values of the Q-type (see Fig. 1). From the sequence of the different $M_S(T)$ curves as a function of M_A/M_B the sign of β can be determined and from the concentration range in which the curves change their shape the magnitude of β (see Fig. 1) can be deduced.

The situation for the titanomagnetites is shown in Fig. 2. The M_A/M_B ratio as a function of x was deduced from the cation distribution given by O'REILLY et al. [1965]. The $M_S(T)$ curves are of the Q-type for $x < 0,6$ and of the P-type for $x > 0,6$ according to AKIMOTO et al. [1957]. Again it is assumed that $\alpha \approx 0$. For $x = 0.6$ where the Q-type changes to the P-type curve follows $M_A/M_B = 1-\beta$ (see Fig. 1 and 2). From the cation distribution for $x = 0.6$ according to O'REILLY et al. [1965]

$$Fe_{0,4}^{2+} Fe_{0,6}^{3+} (Fe_{1,2}^{2+} Fe_{0,2}^{3+} Ti_{0,6}^{4+}) O_4$$
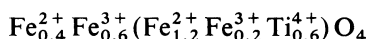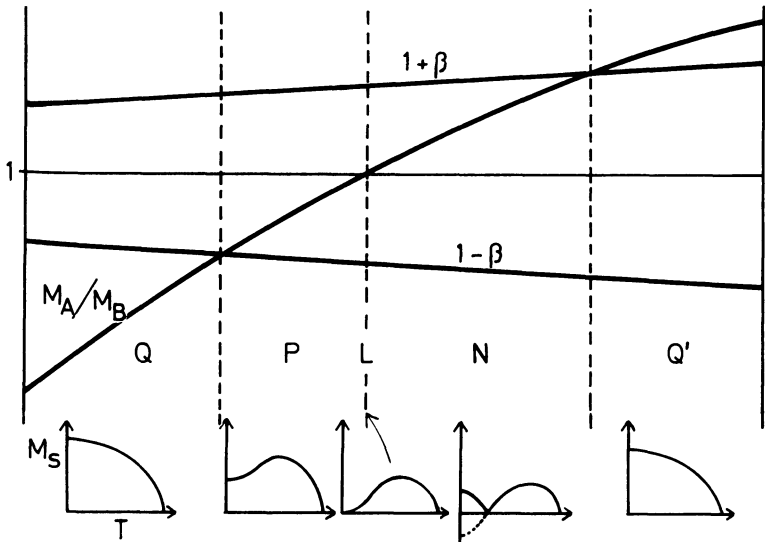
Fig. 1: Change of types of $M_S(T)$ curves—given at the bottom of the figure—as a function of M_A/M_B. The abscissa denotes a variation in chemical composition. (e. g. substitution of paramagnetic ions by diamagnetic ions in the B-sublattice). For increasing M_A/M_B the sequence of the $M_S(T)$ curve types is $Q \to P \to L \to N \to Q'$ for β positive (as shown in the figure) and $Q \to N \to L \to P \to Q'$ for β negative. If β is large the composition ranges of P- and N-type curves are also large and vice versa.
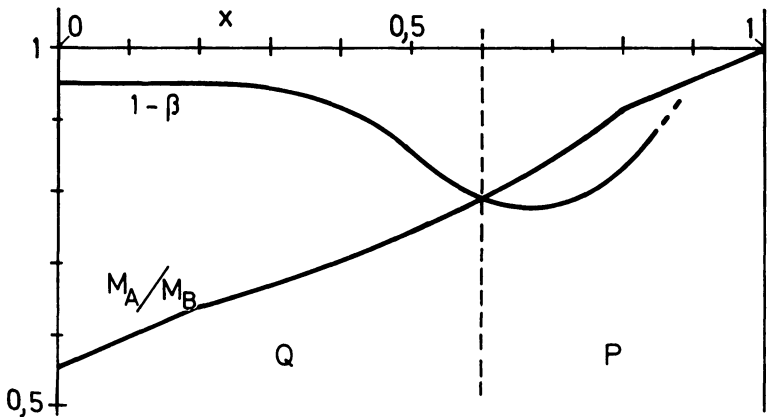
Fig. 2: Behaviour of M_A/M_B, $1-\beta$ and types of $M_S(T)$ curves as a function of x for titano-magnetites $(1-x) \cdot Fe_3O_4 - x \cdot TiFe_2O_4$.

one finds $M_A/M_B = 0.79$ and $\beta = +0.21$. With the conversion from the molecular field coefficients to the exchange interaction ratio we get $J_{BB} = -0.42\ J_{AB}$ (J_{BB} positive).

For magnetite it was shown by GLASSER et al. [1963] on both experimental and theoretical grounds that $J_{BB} \approx -0.1\ J_{AB}$ (J_{BB} positive). With the conversion to the molecular field coefficient we get $\beta = +0.05$. This value was used to draw the $1-\beta$ curve in Fig. 2. The increase of β for $x > 0.4$ will be discussed later.

Another aproach to estimate the exchange interactions may be possible by the measurement of pressure dependence of the CURIE temperature of titanomagnetites. The strength of exchange interactions depends critically upon interatomic distances. As the exchange interactions are related to the CURIE temperature T_c the variation of T_c with pressure provides a measure for dependence of the exchange interactions upon interatomic distances and under certain assumptions a measure for the interactions itself.
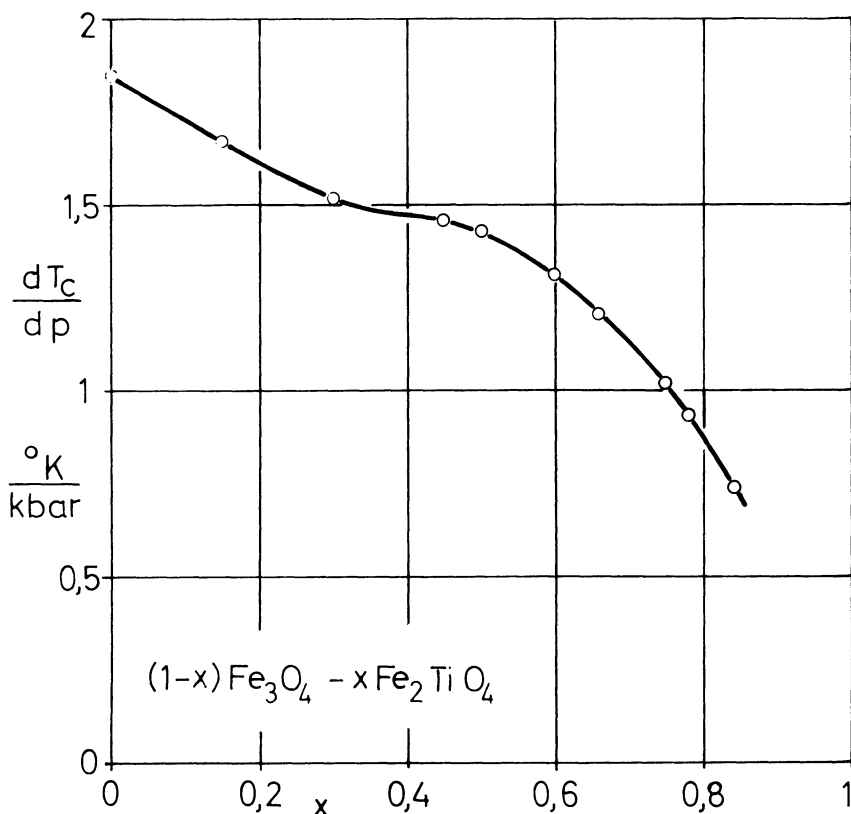
Fig. 3: Shift of the CURIE temperature dT_c/dp as a function of the composition of the titano-magnetites according to SCHULT [1970]

The pressure dependence of the CURIE temperatures of synthetic titanomagnetites has been investigated by SCHULT [1970]. The CURIE temperatures increase linearly with pressure. The slopes dT_c/dp for various x are shown in Fig. 3.

It is uniformly suggested that the CURIE temperature is a linear function of the exchange interactions J_{ij}.

$$T_c = \sum_{ij} A_{ij} J_{ij} . \tag{1}$$

The A_{ij} are constants. The exchange interactions vary with volume (i. e. with inter-atomic distances). The variation can be described by the so-called "magnetic GRÜN-EISEN parameter" [BLOCH 1966]:

$$\gamma_m = \frac{d \ln T_c}{d \ln V} = \frac{d T_c}{dp} \frac{dp}{T_c} \frac{V}{dV} = d \ln \sum_{ij} A_{ij} J_{ij} / d \ln V . \tag{2}$$

dV/Vdp is the isothermal volume compressibility near the CURIE temperature. These values are not available. We have adopted therefore the uniform value $5,5 \pm 0,3 \cdot 10^{-4}/$ kbar, the compressibility of magnetite at room temperature [see SCHULT 1970]. It can be assumed that the compressibility is not drastically different from this value for the titanomagnetites at their CURIE temperatures. The values of γ_m determined by equation (2) are shown in Fig. 4.
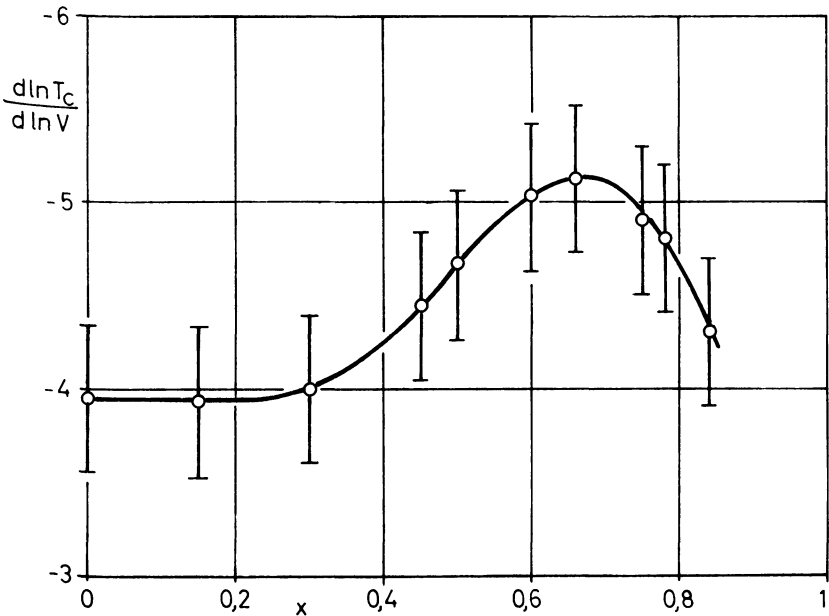
Fig. 4: Magnetic GRÜNEISEN parameter $\gamma_m = d \ln T_c / d \ln V$ as a function of the composition of the titanomagnetites $(1-x) \cdot Fe_3O_4 - x \cdot TiFe_2O_4$.

A quantitative interrelationship between T_c and the various exchange interactions in Fe_3O_4 was given by KOUVEL [1956]:

$$kT_c \approx 4\sqrt{2}\,J_{AB}\sigma_A\sigma_B - \frac{4}{3}J_{AA}\sigma_A^2 - 2J_{BB}\sigma_B^2 \tag{3}$$

where

$$\sigma_A^2 = S_A(S_A+1), \qquad \sigma_B^2 = S_B(S_B+1). \tag{4}$$

k is the BOLTZMANN constant. S_A and S_B are the average spins of electrons associated with the iron moments on A- and B-sites, respectively. S_A amounts to 5/2 because the A-sites are occupied by Fe^{3+} ions. The average value for S_B can be written (Fe^{2+} and Fe^{3+} ions): $S_B = 1/2\,(4/2 + 5/2) = 2,25$. Assuming now again that J_{AA} is negligible small with respect to J_{AB} and J_{BB} equation (3) reduces to

$$kT_c \approx 4\sqrt{2}\,J_{AB}\sigma_A\sigma_B - 2J_{BB}\sigma_B^2. \tag{5}$$

The exchange interactions are assumed to depend only on volume but not necessarily in the same way. Derivating equation (5) in the same way as equation (2) yields after some substitutions:

$$\gamma_m = \frac{d\ln T_c}{d\ln V} = \frac{d\ln J_{AB}}{(1-1/a)\,d\ln V} - \frac{d\ln J_{BB}}{(a-1)\,d\ln V} \tag{6}$$

with

$$a = \frac{4\sqrt{2}\,\sigma_A\sigma_B J_{AB}}{2\,\sigma_B^2 J_{BB}}. \tag{7}$$

J_{AB} is an indirect exchange interaction between cations via an oxygen ion whereas it is evident from theoretical and experimental investigations that J_{BB} is a direct cation-cation interaction [BLASSE 1964, GOODENOUGH 1966]. BLOCH [1966] has shown that in simple ferrites, oxides and garnets the indirect exchange interactions vary as the $-10/3$ power of the volume (i. e. $d\ln J_{AB}/d\ln V = -3.33$ or $\gamma_m = -3.33$ in simple compounds with any other than the indirect exchange interactions negligible). The direct exchange interactions are much stronger dependent on the interatomic distances (GOODENOUGH 1966]. We assume therefore that the relative large γ_m found for titanomagnetite series (see Fig. 4) is related to the strong (positive) direct exchange interactions J_{BB}.

SCHWOB [1969] assumed that the direct exchange interactions are inverse proportional to the square of the cubic crystalline-field splitting of the ion energy levels. By the aid of paramagnetic resonance spectra measurements WALSH [1961, 1965] determined for iron ions that the cubic crystalline-field splitting is proportional to the -21 power of the interatomic distances. This implies that the direct exchange interaction J_{BB} should vary as the -14 power of the volume. We set therefore in

equation (6) for $d \ln J_{BB} / d \ln V = -14$. Under the assumption that σ_A and σ_B are independent of pressure and with $J_{BB} = -0.1 \, J_{AB}$ for magnetite after GLASSER et al. [1963] equation (6) yields $\gamma_m = -3.7$ which is in agreement with the measured value of about -4 within the experimental errors.

With the approximation that the relation for the CURIE temperature given in equation (5) is also valid for the titanomagnetites, equation (6) yields with $J_{BB} = -0.42 \, J_{AB}$ for $x = 0.6$ (see above) $\gamma_m = -4.6$ which is again in agreement with the measured value of about -5 (for $x = 0.6$) within the experimental errors.

Generally it can be said that the behaviour of the exchange interactions in titano-magnetites deduced from the high pressure measurements is consistent with the results available from other investigations. We therefore assume that β in Fig. 2 varies as a function of x qualitatively in the way as γ_m in Fig. 4.

3. Discussion

The consequences of the relative large and positive β (strong J_{BB} interaction) for the behaviour of the $M_S(T)$ curves with increasing oxidation degree of titanomagne-tites and by this for self-reversal models can be characterized as follows:

As β is positive the sequence of the $M_S(T)$ curve types for increasing degree of oxi-dation (increasing M_A/M_B ratio) is $Q \to P \to L \to N \to Q'$ (see Fig. 1, for the moment the abscissa is a measure of the oxidation degree. Q' denotes a $M_S(T)$ curve with A-sublattice predominant at any temperature below the CURIE temperature. A com-plete "irreversible" self-reversal of magnetization takes place when the composition is shifted over the border N/Q'.) The relative large β—particularly for $x > 0,5$ — implies that the concentration range in which the $M_S(T)$ curves change their shape is also large (see Fig. 1). This deduced relation of chemical composition to a corresponding $M_S(T)$ type curve is consistent with the measured composition and $M_S(T)$ type curves of natural titanomagnetites as shown in Fig. 5.

It must be kept in mind, however, that the slope of the M_A/M_B curve in Fig. 1 (as a function of the degree of oxidation) determines the extension of the chemical composition of the different types of $M_S(T)$ curves as shown in Fig. 5 as well. The slope depends on the cation distribution which is not exactly known and we do not intend to discuss this problem here. After all it can be assumed that the composition range with the Q'-type $M_S(T)$ curve—if there is any—is relatively far away form the Fe_3O_4—Fe_2TiO_4 join as it is indicated in Fig. 5.

The titanomagnetites in the hypothetical Q'-range should be highly cation deficient and should have a high titanium content ($x > 0.9$). Until now it has not been defi-nitely shown that they exist, neither for synthetic nor for natural titanomagnetites.

If the highly cation deficient titanomagnetites in the Q'-region exist it would be more likely that also the somewhat less cation deficient titanomagnetites in the N-region exist. The N-type titanomagnetites have been found rarely but only with
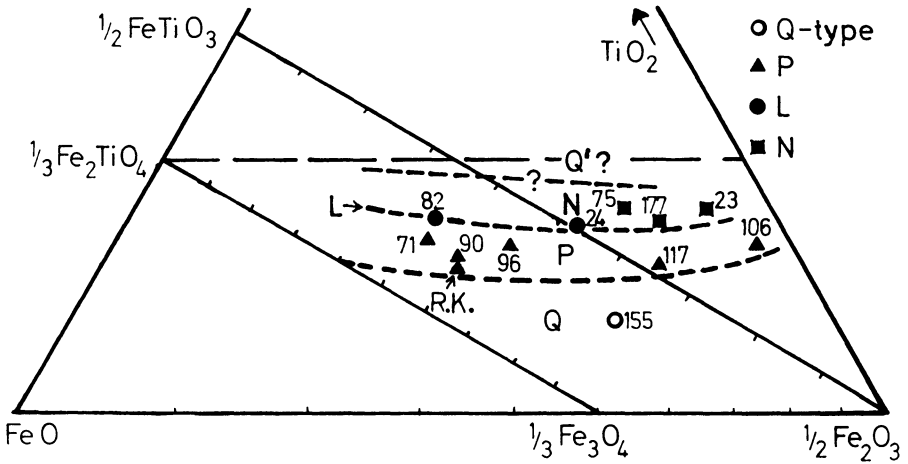
Fig. 5: Chemical composition of natural (cation deficient) titanomagnetites in basalts deter-
mined with a microprobe (Fe/Fe + Ti ratio, horizontal line in this diagram), from
the CURIE temperature of the sample, and the CURIE temperature-composition relation
of cation deficient titanomagnetites given by READMAN and O'REILLY [cit. in CREER
et al. 1970]. The numbers refer to the number of the samples. The $M_S(T)$ curves are
given in SCHULT [1965, 1968]. R. K. according to CREER et al. [1969]. Probable bor-
ders between different types of $M_S(T)$ curves are indicated with broken lines. This
diagram is a new calculation (with some new composition determinations) of a similar
diagram given by SCHULT [1968, 1970]. The CURIE temperature-composition relation
given by AKIMOTO et al. [1957] was no longer used.

compensation temperatures below room temperature [SCHULT 1965, 1968]. This
means that these titanomagnetites are located in the N-range closer to the P-range
than to the Q'-range. The higher cation deficient titanomagnetites (with high titanium
content) in the N-range near the Q'-range should have a compensation temperature
above room temperature, but these titanomagnetites have not been found until now,
despite of an enormous number of existing measurements of $M_S(T)$ curves and
remanence versus temperature curves above room temperature. On the other hand
the composition range of these N-type titanomagnetites should be fairly large because
of the strong J_{BB} interaction; in case of their existence one should eventually find
them.

Acknowledgement

References

AKIMOTO, S., T. KATSURA, and M. YOSHIDA: Magnetic properties of Fe_2TiO_4—Fe_3O_4 system and their change with oxidation, J. Geomagn. Geoelec. 9, 165—178, 1957

BLASSE, G.: Crystal chemistry and some magnetic properties of mixed metal oxides with spinel structure, Philips Res. Rept. Suppl. 3, 1—139, 1964

BLOCH, D.: The 10/3 law for the volume dependence of superexchange, J. Phys. Chem. Solids 27, 881—885, 1966

CREER, K. M., and J. D. IBBETSON: Electron microprobe analyses and magnetic properties of non-stoichiometric titanomagnetites in basaltic rocks, Geophys. J. 21, 485—511, 1970

CREER, K. M., and N. PETERSEN: Thermochemical magnetization in basalts, Z. Geophys. 35, 501—516, 1969

GLASSER, W. L., and F. J. MILFORD: Spin Wave spectra of magnetite, Phys. Rev. 130, 1783—1789, 1963

GOODENOUGH, J. B.: Magnetism and the chemical bond, J. Wiley and Sons, New York 1966

KOUVEL, J. S.: Specific heat of a magnetite crystal at liquid helium temperatures, Phys. Rev. 102, 1489—1490, 1956

NÉEL, L.: Propriétés magnétiques des ferrites: ferrimagnétisme et antiferrimagnétisme, Ann. Phys. 3, 137—198, 1948

O'REILLY, W., and S. K. BANERJEE: Cation distribution in titanomagnetites $(1-x) \cdot Fe_3O_4$-$x \cdot Fe_2TiO_4$, Phys. Letters 17, 237—238, 1965

—: The mechanism of oxidation in titanomagnetites: a magnetic study, Mineral. Mag. 36, 29—37, 1967

SAKAMOTO, N., P. I. INCE, and W. O'REILLY: The effect of wet-grinding on the oxidation of titanomagnetites, Geophys. J. 15, 509—515, 1968

SCHULT, A.: Über die Umkehr der remanenten Magnetisierung von Titanomagnetiten in Basalten, Beitr. Mineral. Petrog. 11, 196—216, 1965

—: Self-reversal of magnetization and chemical composition of titanomagnetites in basalts, Earth Planet. Sci. Lett. 4, 57—63, 1968

—: Effect of pressure on the CURIE temperature of titanomagnetites $[(1-x) \cdot Fe_3O_4$-$x \cdot TiFe_2O_4]$, Earth Planet. Sci. Letters 10, 81—86, 1970

SCHWOB, P.: Die magnetischen Eigenschaften der Europium-Chalkogenide unter hydrostatischem Druck, Phys. Kondens. Materie 10, 186—218, 1969

VERHOOGEN, J.: Oxidation of iron-titanium oxides in igneous rocks, J. Geol. 70, 168—181, 1962

WALSH, W. M.: Effect of hydrostatic pressure on the paramagnetic resonance spectra of several iron group ions in cubic crystals, Phys. Rev. 122, 762—771, 1961

—: Temperature-dependence crystal field and hyperfine interactions, Phys. Rev. 139, A 1338 to 1350, 1965

Notes on the Correlation between Petrology and Magnetic Properties of Basaltic Rocks

R. B. Hargraves[1]) and N. Petersen[1, 2]), Princeton

Summary: The bulk magnetic properties of basaltic rocks (intensity of NRM J_n, susceptibility χ, Curie point T_c) are dominated by the primary Fe-Ti oxides, although there may be some contribution from ferrimagnetic phases produced by alteration of and exsolution from silicates. At solidus temperatures ($\sim 1000\,^0$C), the primary oxide assemblage is restricted to titanomagnetite with between 40 and 85 mol % ulvospinel (T_c 300 ^{0}C to $-50\,^0$C) and ferrian ilmenite with between 80 and 97 mol % ilmenite (T_c $-50\,^0$C to $-200\,^0$C). Environment of crystallization and cooling rate are major interrelated factors influencing subsequent changes in mineralogy and resulting magnetic properties as follows:

(i) Rapid cooling, as in thin flows, borders of dikes/sills: initially fine grained oxide assemblage may be quenched, but extremely vulnerable to environmental contamination, with attendant high T oxidation resulting in pseudobrookite-hematite-rutile assemblage. Generally high Q ratio ($J_n/\chi \cdot H$), T_c up to 670 ^{0}C).

(ii) Slow, closed-system cooling, as in plutons, thick sills/dikes, or center of thick flows: favors subsolidus equilibration with oxidation of titanomagnetite to low titanium magnetite/ilmenite intergrowths. Low temperature exsolution of residual ulvospinel from magnetite, or titanomaghemitization (γFe_2O_3) may take place. In general low Q ratio, T_c around 550 ^{0}C. The potential exists at intermediate temperatures for extreme oxidation by differential diffusion of hydrogen.

The spectrum covered by these extremes includes most natural basaltic rocks.

Zusammenfassung: Träger der magnetischen Eigenschaften von Gesteinen mit basaltischem Chemismus sind hauptsächlich die primären Fe-Ti-Oxyde. Sie bestimmen Eigenschaften wie natürliche remanente Magnetisierung J_n, Suszeptibilität χ und Curie-Temperatur T_c, obwohl ein gewisser Beitrag auch von sekundären, durch Oxydations- und Entmischungsprozesse in den Silikaten gebildeten ferrimagnetischen Phasen geliefert werden kann. Bei der Solidus-Temperatur des Gesteins ($\sim 1000\,^0$C) ist die Zusammensetzung der primären Fe-Ti-Oxyde beschränkt auf Glieder der Titanomagnetit-Mischreihe mit 40 bis 85 mol% Ulvöspinell (T_c 300 bis $-50\,^0$C) und Glieder der Ilmenit-Hämatit-Mischreihe mit 80 bis 97 mol% Ilmenit (T_c -50 bis $-200\,^0$C).

Umgebungsbedingungen während des Kristallisationsvorganges und Abkühlungsgeschwindigkeit sind die wichtigsten (miteinander korrelierten) Faktoren, welche subsequente Ver-

---

[1]) Prof. Dr. R. B. Hargraves and Dr. N. Petersen, Department of Geological and Geophysical Sciences, Princeton University, Princeton, N. J., USA.

[2]) Permanent address: Institut für Angewandte Geophysik der Universität München, 8 München 2, Richard-Wagner-Straße 10.

änderungen der mineralogischen und daraus resultierenden magnetischen Eigenschaften folgendermaßen beeinflussen:

(i) Hohe Abkühlungsgeschwindigkeit, wie in dünnen Ergüssen und Randzonen von ober-flächennahen Gängen: Die primären Fe-Ti-Oxyde behalten auf Grund des Abschreckungs-vorganges oft ihre ursprüngliche Zusammensetzung (niedrige CURIE-Temperatur), sind ande-rerseits jedoch äußerst anfällig gegen eine umgebungsbedingte Kontamination und damit zusammenhängende Hochtemperatur-Oxydation, was zur Bildung von Pseudobrookit-Hämatit-Rutil führen kann. Gewöhnlich hoher Q-Faktor $(J_n/\chi \cdot H)$ und im Fall extremer Oxydation CURIE-Temperaturen bis zu 670 °C.

(ii) Geringe Abkühlungsgeschwindigkeit bei konstantem Gesamtchemismus (abgeschlosse-nes System), wie in Plutonen, mächtigen Gängen und mittleren Partien von dicken Ergüssen: Subsolidus-Oxydation von Titanomagnetit zu Magnetit/Ilmenit-Verwachsungen. Tieftempe-ratur-Entmischung des noch im Magnetit verbliebenen Ulvöspinnels oder Titanomaghemit-Bildung möglich. Im allgemeinen niedriger Q-Faktor, T_c um 550 °C. Bei mittleren Tem-peraturen besteht die Möglichkeit zu extremer Oxydation durch differentielle Diffusion von Wasserstoff.

Die Mehrzahl der basaltischen Gesteine findet sich dazwischenliegend zwischen den beiden extremen Fällen (i) und (ii).

Introduction

Two major types of basalt magma are distinguished by petrologists: tholeitic and alkalic [YODER and TILLEY 1962]. Although rocks derived from these liquids may occur in intimate association, the flood basalts of the continents, and the abyssal basalts of the ocean floors (both associated with rifts) are predominantly tholeitic. Alkalic basalts, and their more undersaturated derivatives, on the other hand, are more characteristic of central volcanic complexes forming the high oceanic islands, and the volcanism associated with the stable continental areas. Together with pre-dominant andesite, both basalt types may occur associated in island arcs, and conti-nental border/trench terrains [KUNO 1966].

The chemical difference between these basalt parent-magmas is slight but subtle, and manifest most clearly in their late stage derivatives, which are quartz normative in the case of tholeite, and nepheline normative, from the alkali olivine basalts. Volumetrically, alkali olivine basalts are subsidiary, but inasmuch as they characterize the superstructure of oceanic islands [ENGEL, ENGEL and HAVENS 1965] they have been studied and sampled out of all proportion to their true abundance. Likewise on continents the wide distribution of central volcanic complexes has overemphasized their relative importance.

Experimental petrology, in recent years has clarified the relationship between these magma types, and their mode of origin [GREEN 1970; O'HARA 1968; ITO and KENNEDY 1968]. With respect to magnetic properties, the most significant difference is that alkali olivine basalt magma tends to contain more volatiles [YODER and TILLEY 1962], and may show more subsolidus alteration.

Emplacement of basaltic rocks

Although most basalt magma generated within the earth is extruded on to the surface of the earth as lava flows, these may vary considerably in thickness and extent, depending upon such factors as viscosity, temperature, composition and local environment and topography. In addition, substantial volumes of magma, do not quite reach the surface, but consolidate as dykes and sills, of thickness up to 10^3 meters, in both oceanic and continental crust. Finally, colossal pools of basaltic magma, up to 10,000 meters deep were the beginning of the gravity-stratified bodies such as the Stillwater and Bushveld Igneous Complexes.

The size of the magma body largely dictates the rate of crystallization, and the degree of phase equilibrium which might be attained during cooling. In addition, the environment of consolidation (extrusive versus intrusive) influences the likelihood, and extent of interaction between magma and/or host rock and the atmosphere or hydrosphere. Provided the magma is juvenile, the primary mineral phase assemblage (excluding glass in quenched lavas) at the basalt solidus ($\sim 1000\,°C$) is similar regardless of whether the magma crystallized at depth or on surface. The final assemblage when cold, however, depends critically on the environment and rate of cooling.

The magnetic properties of basaltic rocks are imparted mainly by the contained Fe (or Fe-Ti) oxides, the sulfides and chromites playing only a very minor role. These minerals may occur as primary accessories, which survive cooling from above $1000\,°C$; others may be produced by exsolution of Fe-Ti oxides from silicate; or by oxidation of paramagnetic Fe^{2+} present in pyroxenes and olivines. Additional Fe-Ti oxide may be released on devitrification of residual glass. Of the average 10% FeO $+$ Fe_2O_3 in basaltic rocks (not including the extreme differentiates of the gravity stratified sheets) about 20 to 50% is usually contained in the primary Fe-Ti oxide accessories. These minerals dominate the bulk magnetic properties (susceptibility, saturation magnetization, CURIE points, etc., and the initial Natural Remanent Magnetization* prior to demagnetization) regardless of the subsolidus petrologic history. With particular respect to magnetic properties, these accessory oxides will be described, and their changes in response to diverse possible petrologic histories will be reviewed.

Composition of the primary Fe—Ti oxides at the basalt solidus

The primary Fe-Ti oxides which crystallize from basaltic magmas above $1000\,°C$ are members of the magnetite (Fe_3O_4)—ulvospinel (Fe_2TiO_4) and ilmenite ($FeTiO_3$)—hematite (α-Fe_2O_3) solid solution series. Based on measurements of the oxygen fugacity associated with basaltic magmas [FUDALI 1965, PECK and WRIGHT 1966], and the experimental work of BUDDINGTON and LINDSLEY [1964], CARMICHAEL and NI-

---

*The stable component of remanence may reside in minute or submicroscopic oxide grains in the silicate [EVANS and McELHINNY 1969, HARGRAVES and YOUNG 1969], but the initial NRM is imposed by primary Fe-Ti oxides.

CHOLLS [1967] predicted that the stable oxide assemblage should be titaniferous magnetite (titanomagnetite) with between 50 and 80 mol % ulvospinel and ferrian ilmenite with between 80 and 99 mol % ilmenite. Actual microprobe measurements of the primary Fe-Ti oxide composition in basalt are in good agreement with these predictions (Fig. 1). These data were obtained from either homogeneous grains of
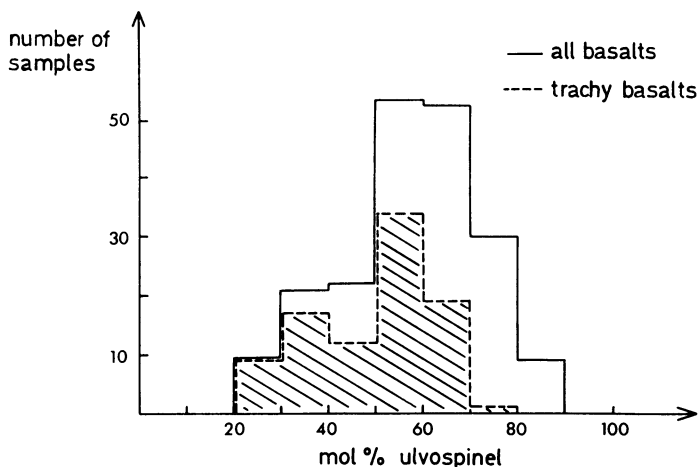
Fig. 1: Composition of the primary titanomagnetite grains in basalts from different localities. The results are based on microprobe analyses by SMITH [1967], ANDERSON [1968] and CREER and IBBETSON [1970]. The trachybasalts are plotted separately.

titanomagnetite and ferrian ilmenite or on finely exsolved grains for which the bulk composition could be averaged. In these it is assumed that only the oxygen content and not the iron-titanium ratio has changed. The range of composition measured is between about 40 and 85 mol % ulvospinel in titanomagnetites and between 80 and 97 mol % ilmenite in ferrian ilmenites. Within these data there seems to be the following trend: With decreasing basicity of the rock the content of ulvospinel in titanomagnetite and the content of ilmenite in ferrian ilmenite is decreasing.* In general however, little is known as to whether or not there exists a correlation between different types of basalts, (tholeites, and alkali basalts) and the titanium content of their primary titanomagnetites and ferrian ilmenites.

The range of CURIE temperatures that corresponds to the above outlined composition of the primary ore minerals lies between about -50 and $300\,^\circ$C for the titanomagnetites and between -50 and $-200\,^\circ$C for the ferrian ilmenites (see table 1).

---

*This is illustrated in Fig. 1 where the trachybasalts are plotted separately. Their titanomagnetites have a distinctly lower ulvospinel content. A lower temperature of crystallization may contribute to this trend.

Table 1: Range of CURIE temperatures and Q-ratios for basalts containing primary titano-magnetites and ferrian ilmenites.

Composition	CURIE Temperature	Q-factor at room Temperature
titanomagnetites 40 to 85 mol% ulvospinel	300 to $-50\,^0C$	10 to 100
ferrian ilmenites 80 to 99 mol% ilmenite	-50 to $-200\,^0C$	

CARMICHAEL and NICHOLLS [1967] draw from these data the important conclusion that all rocks of basaltic composition with a CURIE temperature higher than 300°C must have undergone subsequent alteration of their magnetic oxides.

Petrologic Histories

The principal factors that dominate any variations in the primary Fe-Ti oxides are physical environment and cooling rate on the one hand and changes of the original chemical composition of the magma on the other. These factors will be discussed first with respect to two possible extremes:

1) The magma crystallizes and cools entirely as a closed system.

2) The cooling magma complex is open to contamination by meteoric water and/or air.

Following this the general case will be reviewed.

1) The first situation is approximated by gabbros and the central part of thick dikes and sills, all representing bodies with very low cooling rate. But it may also be approximated in situations where the magma cools down very fast, as in the chilled border zones of dikes and sills or even in border zones of lavas that have been quenched.

1a) In a magma body which behaves as a closed system, and cools very rapidly the composition of the primary ore minerals is frozen in. They therefore preserve a composition as outlined above, between 40 and 85 mol % ulvospinel for the titanomagnetites and 80 to 99 mol % ilmenite for the ferrian ilemenites.

As a result of rapid cooling, the size of the ore grains in the rocks of this category is relatively small, from submicroscopic to a few tens of microns. This range is close to the critical diameter for single-multidomain transition in homogeneous titano-magnetite grains (1 μ, according to SOFFEL 1968). As the grains are homogeneous the coercivity in these rocks will be determined primarily by the actual size of the ore grains.

Many of the dredged ocean floor basalts fall into this category. As their primary ore grains frequently have sizes close to 1 μ, they therefore possess high coercivities. This is reflected in the high values for their Q-factor (ratio of remanent magnetization to magnetization induced by the ambient earth magnetic field) as reported for example by ADE-HALL [1965] and DE BOER, SCHILLING and KRAUSE [1970].

In table 1 composition of the primary ore grains, CURIE temperature and Q-factor of rocks falling into this category are summarized.

The titanomagnetite and ferrian ilmenite mineral assemblage in these rocks is not in equilibrium with air [VERHOOGEN 1962]. Their equilibrium oxygen fugacity is extremely small, and at elevated temperatures in air the original titanomagnetites and hemoilmenites tend to oxidize, which causes distinct changes in the magnetic properties. This has frequently been observed during heat treatment on such rocks in the laboratory [e. g. BEWERSDORFF 1961, MEITZNER 1963]. The very early stages of oxidation take place on a submicroscopic scale and are therefore overlooked if oxidation is judged only from ore-microscopic observations. Magnetic properties like CURIE temperature and coercive force however are very sensitive to these submicroscopic changes [CREER and PETERSEN 1969].

1b) Closed system cooling very slowly.

Here the composition of the primary ore minerals will gradually change if the cooling rate is slow enough to allow them to readjust their composition to remain in equilibrium with the environment. As demonstrated by BUDDINGTON and LINDSLEY [1964] this is caused by the fact that the temperature variation of the oxygen fugacity of the primary iron-titanium-oxides—titanomagnetite and ferrian ilmenite—does normally not coincide with the actual variation of oxygen fugacity with temperature prevailing in the rock. The latter is determined by reaction between ferrous and ferric iron present both in the Fe-Ti oxides and in the silicate minerals, and by volatile components. The actual oxygen fugacity will then depend on the mass portions of these three components.

The variation with temperature of the oxygen fugacity in a cooling rock body has been directly measured [SATO and WRIGHT 1966] or calculated by several authors [ANDERSON 1968, CARMICHAEL and NICHOLLS 1967, BUDDINGTON and LINDSLEY 1964] with slightly different results. In order to illustrate the principle of this process of compositional change in the primary Fe-Ti oxides we simplify the problem by taking the temperature variation of oxygen fugacity of the quartz/fayalite/magnetite (QFM) buffer as representative for an average basalt. When precipitating from the silicate melt at about 1050 °C, titanomagnetite with 60 mol % ulvospinel (Usp60:Mt40) and ferrian ilmenite with 90 mol% ilmenite (Ilm90) are in equilibrium with the environmental oxygen fugacity represented by the QFM-buffer. However, after cooling down to 600 °C, Usp10:Mt90 coexisting with Ilm96 are now the phases in equilibrium with the QFM-buffer. This means during cooling down from 1050 °C to 600 °C the primary Usp60:Mt40 was gradually oxidized to Usp10:Mt90 becoming poorer in

titanium and simultaneously forming lamellae of Ilm97. The primary Ilm90 was gradually reduced to Ilm97 becoming enriched in titanium and so simultaneously forming lamellae of Usp10:Mt90 (Fig. 2).
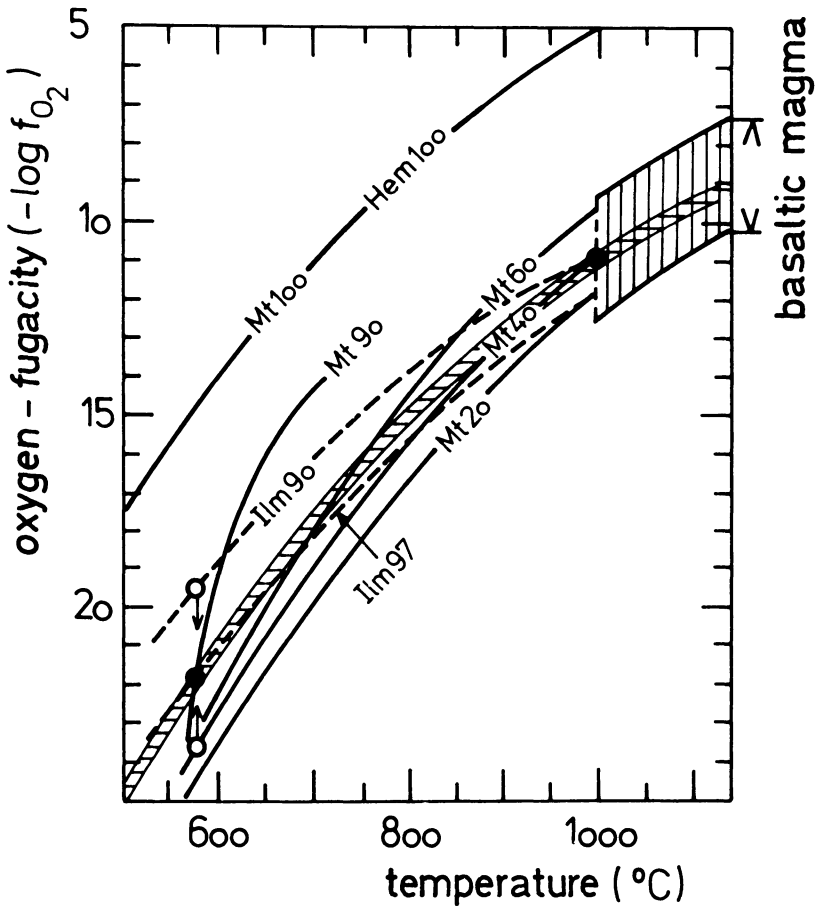
Fig. 2: Oxygen fugacities plotted against temperature. The vertically dashed area represents the range of oxygen fugacities in basaltic magmas [from CARMICHAEL and NICHOLLS 1967]. The horizontally dashed curve gives the temperature variation of oxygen fugacity of the fayalite-magnetite-quartz buffer. The curves labelled Mt and Ilm are the equilibrium oxygen fugacities of different members of the magnetite-ulvospinel (Mt) and the ilmenite-hematite (Ilm) solid solution series [from BUDDINGTON and LINDSLEY 1964]. The two filled circles indicate the composition of the Fe-Ti oxides in equilibrium with the fayalite-magnetite-quartz buffer at 1000° and 600°C; open circles see text.

1b—i) Intersection with the solvus curve.

At temperatures below 600 °C another process may come into operation: Exsolution of titanomagnetite (in our example of Fig. 3 it will be Usp10:Mt90 at 600 °C) into ulvospinel and magnetite [VINCENT et al. 1957]. It is difficult to say which of the two processes, oxidation or exsolution, will dominate below 600 °C; possibly both of them take place simultaneously.
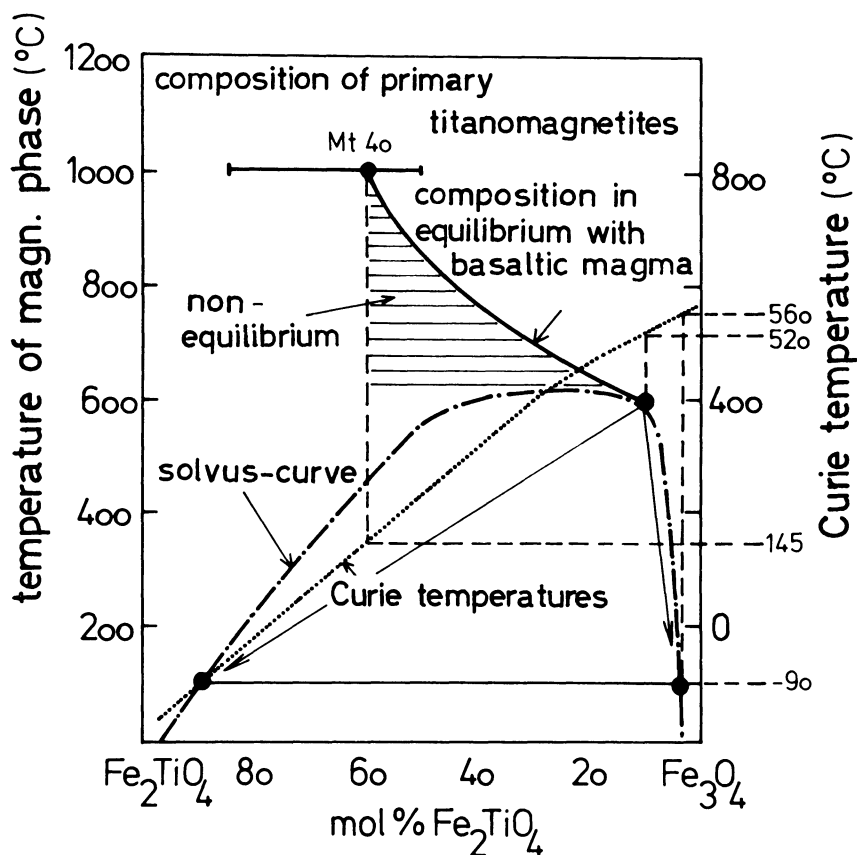
Fig. 3: Influence of the solvus curve (dash-dot) of the titanomagnetite solid solution series on composition and CURIE temperature. Thick horizontal bar represents the range of compositions of primary titanomagnetites in basaltic rocks at 1000 °C. Thick solid curve indicates the compositions of titanomagnetite in equilibrium with a fayalite-magnetite-quartz buffer when cooling down to 600 °C (obtained from Fig. 2). The horizontally dashed area gives the possible compositions between the two extremes of equilibrium composition and unchanged (due to rapid cooling) original composition. Solvus curve adapted from VINCENT et al. [1957].

Although the solvus curve of the ilmenite-hametite solid solution series has its crest at a higher temperature compared to the titanomagnetite solid solution series, the primary composition of the rhombohedral phase is close to the ilmenite end and unlikely to intersect the hematite-ilmenite solvus [CARMICHAEL 1961].

This process of oxidation (and reduction if ferrian ilmenite is present) and exsolution will strongly influence the magnetic properties of the rock. Whereas the CURIE temperature of the primary phases Usp60:Mt40 and Ilm90 would be about 150°C and —130°C respectively, after cooling, CURIE temperatures of about 560°C for almost pure magnetite, —100°C for ulvospinel and about —180°C for Ilm97 (see Fig. 3) are to be expected. As the magnetite phase will dominate magnetically the whole process results in an increase of CURIE temperature and saturation magnetization. This is a highly simplified model as the actual temperature variations of the oxygen fugacity may be much more complicated. However, that it approximates the situation in many cooling basalts is well demonstrated in the example of the Alae and Makaopuhi lava lakes, Hawaii [GROMMÉ, WRIGHT and PECK 1969]. The CURIE temperatures predicted here also agree well with values measured on different gabbros [see for example CHEVALLIER, MATHIEU and VINCENT 1954; HARGRAVES and YOUNG 1969].

The stability of any remanent magnetization will also be influenced by the oxidation-reduction and exsolution process. As the fairly coarse primary ore grains of the rocks falling into this category will be subdivided by the formation of nonmagnetic lamellae (at room temperature) the coercivity of an ore grain is not simply a function of its actual size but of its internal structure. The process of subdivision will increase the coercivity [PETERSEN 1966, LARSEN et al. 1969]. There is some argument, however, as to whether the stable remanence in gabbros is located actually in the coarse exsolved ore grains or in minute ore particles (single domain grains) exsolved from the silicate crystals [HARGRAVES and YOUNG 1969, EVANS, McELHINNY and GIFFORD 1968].

2) Extreme oxidation of the primary Fe-Ti oxides by contamination of the cooling magma with air and/or surface water.

Complete oxidation results in the alteration of all the primary Fe-Ti oxides to a mixture of hematite (α-Fe_2O_3), rutile (TiO_2) (and anatase) and pseudobrookite (Fe_2TiO_5), these minerals being the stable Fe-Ti oxide assemblage in air [VERHOOGEN 1962]. This extreme is relatively rarely realized in nature. It is approximated in some lava flows and in most cases only in special zones of the flows.

Three factors are involved in the oxidation of a lava flow; (a) the accessibility of oxygen from air or water (this is mainly determined by the physical from of the flow, the frequency of joints, etc.) (b) the rate of cooling and (c) the possibility of development of zones of high oxygen fugacity by differential diffusion of hydrogen (this latter effect will be discussed in the following chapter).

Different opinions exist as to where the zones of highest oxidation of the primary Fe-Ti oxides are normally located. The investigations of WATKINS and HAGGERTY

[1967] on 13 Icelandic lava flows show the zones of highest oxidation near the center of the flows. They attribute this high oxidation to differential diffusion of hydrogen relative to oxygen and water (see next section). On the other hand measurements by ANGENHEISTER and TURKOWSKY [1964] on bore cores through several basalt flows from the Vogelsberg area, West Germany, indicate the zones of maximum oxidation are near the surface suggesting the importance of contamination with air for maximum oxidation of the flows. The physical nature of the surface of the flow (vesicular or smooth) may be the decisive factor in this context. It is interesting to note that in the case of the Makaopuhi lava lake (smooth surface) only slight contamination with air is observed and this is confined to the uppermost 30 cm [GROMMÉ et al. 1969].

The magnetic properties of the completely oxidized Fe-Ti oxides are distinctly different from the unoxidized or little oxidized. Rutile and pseudobrookite are non-magnetic whereas hematite has a weak ferrimagnetism with a saturation magnetization a factor about 200 less than that of magnetite and a CURIE temperature of 670 °C. The zones of extreme oxidation in lava flows are therefore normally characterized by low intensity of magnetization, on the one hand and high stability of its remanence on the other, as hematite is able to carry a very stable remanent magnetization despite its weak ferrimagnetism. The CURIE temperatures in these zones of highest oxidation range between 600 and 680 °C indicating that often titanohematite is present beside pure hematite.

The General Case

The bulk of basaltic rocks are best described as intermediate between the two rather idealized cases discussed in 1 and 2. However at the present stage of investigation very little can be reliably predicted concerning the correlation between mineralogy and magnetic properties in the more uncertain natural situation.

In an attempt to catalogue the effects that may be responsible for the development of these intermediate cases, we distinguish between three factors:

a) Partial contamination with air and or surface water.

b) Development of zones of high oxygen fugacity by differential diffusion of hydrogen.

c) Enrichment of the volatile component within the melt during the crystallization process.

All three factors are correlated with the cooling rate.

a) The possibility of contamination is relevant to extrusive lavas and has essentially been discussed in the extreme case. If the oxidation of the primary Fe-Ti oxides due to contamination has not been completed at higher temperatures, but goes on at temperatures below 600 °C, a metastable, cation deficient spinel phase, titanomaghemite may be formed.

Titanomaghemite has been found in many lava flows [AKIMOTO and KUSHIRO 1960, SASAJIMA 1961], and contributes substantially to the magnetic properties of these lavas as it is strongly magnetic, comparable to magnetite. The magnetic properties of the titanomaghemites are complicated and not yet fully understood [PETERSEN 1966, O'REILLY and BANERJEE 1967]. Its structure and magnetic properties seem to be dependent on the temperature of oxidation: at low temperatures (below 200 °C) single phase titanomaghemite being formed [READMAN and O'REILLY 1970], whereas at somewhat elevated temperatures at least two unidentified magnetic phases, closely intergrown, may be produced. In the latter case self reversal of remanent magnetization has been observed [CREER, PETERSEN and PETHERBRIDGE 1970]. The phenomenon of two antiparallel polarities of natural remanent magnetization within one single lava flow as observed by DOMEN [1968] can probably be attributed to these multiphase titanomaghemites.

b) It was suggested by OSBORN [1959] that zones of high oxygen fugacity may develop in the interior parts of cooling dikes and lavas by differential diffusion of hydrogen: while hydrogen escapes relatively rapidly toward the surface, oxygen and water molecules cannot diffuse easily through the basalt. This preferential escape of hydrogen induces further thermal decomposition of water and can generate locally high oxygen fugacities.

SATO and WRIGHT [1966] have directly measured such zones of high oxygen fugacities in holes drilled through the crust of Makaopuhi lava lake, Hawaii. They inferred that the differential escape of H_2 relative to H_2O and O_2 was significant only between about 550 °C and 800 °C. Below 550 °C there is no significant diffusion of any gas species and above 800 °C there is no diffusion rate difference. GROMMÉ et al. [1969] concluded that a minimum thickness of basalt was needed in order for it to act as a semipermeable membrane (about 3 m). These data suggest that the semipermeable membrane effect is likely to operate only in dikes or lava flows thicker than about 6 m. Another possible conclusion is that this effect is unlikely to be responsible for the formation of titanomaghemite, as it is restricted to temperatures above about 500 °C.

There is little information as to the effect on magnetic properties of oxidation due to this semipermeable membrane effect. SATO and WRIGHT [1966] state that the zone of exceptionally high oxygen fugacity in the Makaopuhi lava lake is related to a zone of highly altered basalt with markedly high magnetic susceptibility. Further, more detailed magneto-mineralogical investigations on samples from the Makaopuhi lava lake by GROMMÉ et al. [1969] show that the Fe-Ti oxide minerals in these zones are pseudobrookite (representing a very high oxidation state of the Fe-Ti oxides), hemo-ilmenite and magnetite; the latter being responsible for the high magnetic susceptibility and the CURIE temperature of the rock of 580 °C.

c) It has been pointed out [OSBORN 1959, HAMILTON and ANDERSON 1967] that as crystallization of a water-undersaturated magma proceeds, the partial pressure of water rises as the amount of melt decreases. As a dike crystallizes from the edge

inwards the volatiles become progressively concentrated in the residual melt. The center parts of the dike must therefore have crystallized under higher pH_2O than their counterparts in the margins. This process, possibly combined with differential diffusion of hydrogen (as discussed under b) would result in a relative increase of pO_2. That this process can take place in nature has been demonstrated on an ultrabasic dike (thickness 10m) by GIBB and HENDERSON [1971]. However no data on the variation of magnetic properties are reported.

All three factors a, b and c: contamination with air, outward diffusion of hydrogen and enrichment of the volatile phase during crystallization may be operative in thick lava flows and lava lakes. In dikes and sills only factors b and c will normally be effective. The interplay of these factors may cause a systematic variation of the oxidation state of the primary Fe-Ti oxides that should be reflected in the magnetic properties of the rock. The systematic variation of natural remanent magnetization in lava flows has been demonstrated by different authors [HATHERTON 1954, ANGENHEISTER and TURKOWSKY 1964, ADE-HALL et al. 1968, SCHENK 1970]. Similar variations of different magnetic properties in a sill have been reported by KADZIALKO-HOFMOKL [1969]. However quantitative correlations of cooling history, composition of Fe-Ti oxides and magnetic properties are still lacking.

Conclusion

The bulk magnetic properties of basaltic rocks (intensity of natural remanent magnetization J_n, susceptibility χ, CURIE temperature T_c) are dominated by the primary Fe-Ti oxides, although there may be some contribution from ferrimagnetic phases produced by alteration of and exsolution from silicates. At solidus temperatures ($\sim 1000\,°C$) the primary oxide assemblage is restricted to titanomagnetite with between 40 and 85 mol % ulvospinel (T_c 300 °C to $-50\,°C$) and ferrian ilmenite with between 80 and 97 mol % ilmenite (T_c $-50\,°C$ to $-200\,°C$). Environment of crystallization and cooling rate are major interrelated factors influencing subsequent changes in mineralogy and resulting magnetic properties as follows:

Rapid cooling (fine grain) is consistent with thin extrusives, or the chilled borders of shallow intrusives. The initial mineralogy may be quenched, but in such environment the rock is extremely vulnerable to oxidation by air, water, or country rock—leading to substantial changes in mineralogy and magnetic properties. The Q ratio is generally high; CURIE point is low if unoxidized, but may be very high, however, if extremely oxidized.

Slow cooling is consistent with plutons, sills and dikes, and the center of thick flows. Crystallization and cooling is usually as in a closed system, with maintenance of phase equilibrium down to temperatures approaching 700 °C. Primary spinel phase oxidizes to magnetite/ilmenite intergrowths. If fO_2 in bulk assemblage remains buffered, exsolution of residual ulvospinel from magnetite may take place; reaction with residual trapped volatiles sometimes causes maghemitization. Such rocks gene-

Table 2: Correlation between petrology and magnetic properties of basaltic rocks.

| | Gabbros | Dolerite Dikes and Sills | | Basalts | | |
| | | Border | Center | Thin | Thick | |
					Border	Center
Cooling rate	slow	fast	slow	quench	quench	intermediate
Volatile Components	juvenile closed system	probably juvenile	juvenile	contamination, oxidation	probably oxidized by contamination and H_2 diffusion	possibly contaminated, oxidation by H_2 diffusion
Subsolidus Fe-Ti Oxide relations	equilibrated down to 700 °C	may be quenched from 1000 °C	varying subsolidus equilibration, may undergo low T oxidation	primary assemblage quenched. Possibly some high T oxidation	high T oxidation of primary assemblage, some low T oxidation	may be primary assemblage varying subsolidus oxidation, exsolution etc.
Phases	usp10:Mt90 titanomagnetite; possibly minor exsolved ulvo-spinel; Ferrian ilmenite	ulvospinel rich magnetite; ferrian ilmenite	titaniferous magnetite or titanomaghemite; ferrian ilmenite	usp80,Mt20; with ilmenite; pseudobrookite, hematite rutile	pseudobrookite, hematite, rutile relic titanomagnetite	magnetite-ulvo-spinel/ilmenite intergrowths, titanomaghemite
Q	0.5 to 5 (medium)	5 to 15 (medium to high)	0.5 to 5 (medium)	10 to 100 (high)	10 to 100 (high)	5 to 15 (medium to high)
T_c (dominant)	550 °C	0° to 550 °C	550 °C	0° to 670 °C	0° to 670 °C	0° to 55 °C

rally have low Q ratio, and CURIE temperatures up to that of pure magnetite. In this environment, the potential exists at intermediate temperatures for differential diffusion and escape of hydrogen leading to highly oxidized assemblages.

In general the mineralogy and magnetic properties of basaltic rocks are represented by some intermediate between these possible extremes.

Table 2 summarizes the results discussed in this paper.

Acknowledgments

References

ADE-HALL, J. M.: The magnetic properties of some submarine oceanic lavas, Geophys. J., 9, 85—94, 1965

ADE-HALL, J. M., M. A. KHAN, P. DAGLEY, R. L. WILSON: A detailed opaque petrological and magnetic investigation of a single Tertiary lava flow from Skye, Scotland, I, II, III. Geophys. J. 16, 375—415, 1968

AKIMOTO, S., I. KUSHIRO: Natural occurrence of titanomaghemite and its relevance to the unstable magnetization of rocks, J. Geomagn. Geoelectr., 11, 94—110, 1960

ANDERSON, A. T.: The oxygen fugacity of alkaline basalt and related magmas, Tristan da Cunha, Am. J. Sci., 266, 704—727, 1968

ANGENHEISTER, G., C. TURKOWSKY: Die Verteilung der induzierten und natürlichen remanenten Magnetisierung innerhalb einiger Basaltlagen des Vogelsberges, Boll. Geofis. teor. ed appl., 6, 285—295, 1964

BEWERSDORFF, A.: Der Einfluß der Entmischung auf remanente Magnetisierung von Titanomagnetiten, Z. Geophys., 27, 215—256, 1961

BUDDINGTON, A. F., D. H. LINDSLEY: Iron-titanium oxide minerals and synthetic equivalents, J. Petrol. 5, 310—357, 1964

CARMICHAEL, C. M.: The magnetic properties of ilmenite hematite crystals. Proc. Roy. Soc., London, series A, 263, 508—530, 1961

—: Paper III, IAGA Meeting, Madrid 1969

CARMICHAEL, C. M., J. NICHOLLS: Iron-titanium oxides and oxygen fugacities in volcanic rocks, J. Geophys. Res., 72, 4665—4687, 1967

CHEVALLIER, R., S. MATHIEU, E. A. VINCENT: Iron-titanium oxide minerals in layered gabbros of the Skaergaard intrusion, East Greenland, Part II. Magnetic properties. Geochim. et Cosmochim. Acta 6, 27—34, 1954

CREER, K. M., J. D. IBBETSON: Electron microprobe analyses and magnetic properties of non-stoichicmetric titanomagnetites in basaltic rocks. Geophys. J., 21, 485—511, 1970

CREER, K. M., N. PETERSEN: Thermochemical magnetization in basalts, Z. Geophys. 35, 501—516, 1969

CREER, K. M., N. PETERSEN, J. PETHERBRIDGE: Partial self-reversal of remanent magnetization and anisotropy of viscous magnetization in basalts, Geophys. J., 21, 471—483, 1970

DE BOER, J., J.-G. SCHILLING, D. C. KRAUSE: Reykjanes ridge: implications of magnetic properties of dredged rock, Earth Planet. Sci. Letters, 9, 55—60, 1970

DOMEN, H.: An experimental study on the unstable natural remanent magnetization of rocks as a palaeomagnetic fossil, Bull. Fac. Edn. Yamagchi Univ., 18, 1—31, 1968

ENGEL, A. E., C. G. ENGEL, R. G. HAVENS: Chemical characteristics of oceanic basalt and the upper mantle. Bull. Geol. Soc. Am. 76, 719—734, 1965

EVANS, M. E., M. W. MCELHINNY: An investigation of the origin of stable remanence in magnetite-bearing igneous rocks. J. Geomagn. Geoelectr., 21, 757—773, 1969

EVANS, M. E., M. W. MCELHINNEY, A. C. GIFFORD: Single domain magnetite and high coercitivies in a gabbroic intrusion, Earth Planet. Sci. Letters, 4, 142—146, 1968

FUDALI, F. R.: Oxygen fugacities of basaltic and andesitic magmas, Geochim. et Cosmochim. Acta, 29, 1063—1075, 1965

GIBB, F. G. F., C. M. B. HENDERSON: The magnetic oxygen fugacity of an ultrabasic dyke, Contr. Min. Petr. 30, 119—124, 1971

GREEN, D. H.: A review of experimental evidence on the origin of basaltic and nephelinitic magmas. Phys. Earth Planet. Interiors 3, 221—235, 1970

GROMMÉ, C. S., T. L. WRIGHT, D. L. PECK: Magnetic properties and oxidation of iron-titanium oxide minerals in Alae and Makaopuhi lava lakes, Hawaii, J. Geophys. Res., 74, 5277—5293, 1969

HAMILTON, D. L., ANDERSON, G. M.: Effects of water and oxygen pressures on the crystallization of basaltic magmas. In: Vol. 1 of Basalts, The POLDERVAART treatise on rocks of basaltic composition (H. H. HESS and A. POLDERVAART, eds.) New York: John WILEY & Sons 1967

HARGRAVES, R. B., W. M. YOUNG: Source of stable remanent magnetism in Lambertville diabase, Am. J. Sci., 267, 1161—1177, 1969

HATHERTON, T.: The permanent magnetization of horizontal volcanic sheets. J. Geophys. Res. 59, 223—232, 1954

ITO, K., G. C. KENNEDY: Melting and phase relations in the plane tholeite-lherzolite-nepheline basanite to 40 kilobars with geological implications. Contr. Min. Petr. 19, 177—211, 1968

KADZIALKO-HOFMOKL, M.: The relations between magnetic properties and differentiation processes for dolerite intrusion from Schnellbach (Thuringia). Materialy i Prace ZG PAN, 35, 3—33, 1969

KUNO, H.: Lateral variation of basalt magma type across continental margins and island arcs. Bull. Volcanologique 29, 195—222, 1966

—: Differentiation of basalt magmas, in "Basalts, the POLDERVAART treatise on rocks of basaltic composition" edited by H. H. HESS and A. POLDERVAART, vol. 2, 623—688, 1968

LARSON, E., Mituko OZIMA, Minoru OZIMA, T. NAGATA, D. STRANGWAY: Stability of remanent magnetization of igneous rocks. Geophys. J., 17, 263—292, 1969

Meitzner, W.: Der Einfluß von Entmischung und Oxydation auf die magnetischen Eigenschaften der Titanomagnetite in Basalten bei 250°C und 350°C, Contr. Min. Petr., 9, 320—352, 1963

O'Hara, M. J.: The bearing of phase-equilibria studies in synthetic and natural systems on the origin and evolution of basic and ultrabasic rocks. Earth. Sci. Reviews 4, 69—134, 1968

O'Reilly, W., S. K. Banerjee: The mechanism of oxidation in titanomagnetites: a magnetic study, Min. Mag. 36, 29—37, 1967

Osborn, E. F.: Role of oxygen pressure in the crystallization and differentiation of basaltic magma. Am. J. Sci. 257, 609—647, 1959

Peck, D. L., T. L. Wright: Experimental studies of molten basalt in situ: a summary of physical and chemical measurements on recent lava lakes of Kilauea volcano, Hawaii, Geol. Soc. Am. 1966 Ann. Meeting Abstr., 158—159, 1966

Petersen, N.: Beobachtung einiger mineralogischer und magnetischer Eigenschaften dreier Basaltproben nach unterschiedlicher thermischer Behandlung, J. Geomagn. Geoelectr., 18, 463—479, 1966

Readman, P. W., W. O'Reilly: The synthesis and inversion of non-stoichiometric titanomagnetites, Phys. Earth Planet. Interiors, 4, 121—128, 1970

Sasajima, S.: γ-Titanohematites in nature and the role they play in rock-magnetism. J. Geomagn. Geoelectr. 12, 190—215, 1961

Sato, M., T. L. Wright: Oxygen fugacities directly measured in magmatic gases. Science, 153, 1103—1105, 1966

Schenk, E.: Zur Problematik der Deutung paläomagnetischer Messergebnisse auf Grund von Untersuchungen an den Basalten des Paläovulkans Vogelsberg in Hessen. Z. Geophys. 36, 356—385, 1970

Smith, P. J.: Electron probe microanalysis of optically homogeneous titanomagnetites and ferrian ilmenites in basalts of palaeomagnetic significance, J. Geophys. Res., 72, 5087—5100, 1967

Soffel, H.: Die Bereichsstrukturen der Titanomagnetite in zwei tertiären Basalten und die Beziehung zu makroskopisch gemessenen magnetischen Eigenschaften dieser Gesteine, Habilitationsschrift, Naturwiss. Fak. Univ. München, 1968

Soffel, H., P. Supalak: Paläomagnetische Messungen am Basalt des Parkstein bei Weiden (Bayern), Z. Geophys., 34, 287—296, 1968

Verhoogen, J.: Oxidation of iron-titanium oxides in igneous rocks, J. Geol. 70, 161—181, 1962

Vincent, E. A., J. B. Wright, R. Chevallier, S. Mathieu: Heating experiments on some natural titaniferous magnetites. Min. Mag. 31, 624—655, 1957

Watkins, N. D., S. E. Haggerty: Primary oxidation variation and petrogenesis in a single lava, Contr. Min. Petr., 15, 251—271, 1967

Wilson, R. L., S. E. Haggerty, N. D. Watkins: Variation of palaeomagnetic stability and other parameters in a vertical traverse of a single Icelandic lava, Geophys. J., 16, 79—96, 1968

Yoder, H. S., C. E. Tilley: Origin of basalt magmas: an experimental study of natural and synthetic rock systems. J. Petr. 3, 342—532, 1962

Geophysical Interpretation of Remanent Magnetization in Oxidized Basalts

K. M. Creer, Newcastle[1])

Summary: The possible models of self-reversal of remanent magnetization of basalts and its importance for Geophysics are briefly reviewed under the aspect of recent results of investigations on the magnetic properties of cation deficient Fe-Ti spinels, which can be produced from stoichiometric titanomagnetites by oxidation. Heating experiments in air on continental and oceanic basalts show that the daughter products with different Curie temperatures and other magnetic properties than the mother phase can acquire a thermoremanence or thermo-chemical remanent magnetization opposite to the previous TRM direction due to mainly magnetostatic interactions. This can lead to a reduction of the initial TRM intensity and in some cases to an inversion of the primary TRM direction.

Zusammenfassung: Die möglichen Modelle der Selbstumkehr der remanenten Magnetisierung von Basalten und ihre Bedeutung für die Geophysik werden kurz dargestellt. Auf Grund von neueren Untersuchungen der magnetischen Eigenschaften von Fe-Ti-Spinellen mit Kationen-Defektstruktur, die aus töchiometrischen Titanomagnetiten durch Oxydation hervorgehen, werden die bisherigen Modelle kritisch beurteilt. Erhitzungsversuche in Luft an kontinentalen und ozeanischen Basalten ergaben, daß die aus den primär in den Basalten gebildeten Titano-magnetiten hervorgehenden Tochterprodukte mit anderen Curie-Temperaturen und magneti-schen Eigenschaften als die Mutterphase infolge magnetostatischer Wechselwirkungen eine zur ursprünglichen Thermoremanenz entgegengerichtete Thermoremanenz oder thermo-chemische Remanenz erwerben können. Dies führt zu einer Verringerung, in manchen Fällen zu einer Inversion der Richtung der ursprünglich bei der Entstehung des Gesteins gebildeten Thermoremanenz.

1. Introduction

There is now little room for doubt about the reality of reversals of polarity of the geomagnetic field. Three lines of evidence have led to this firm conclusion. (a) The polarity time scale (e.g. see Cox, Doell & Dalrymple, 1968) constructed for the past 4 My from combined palaeomagnetic and K-Ar radiometric observations appears to be valid for all parts of the earth's surface. (b) The resolution of this polarity time scale has been improved by measurements of the continuous geomagnetic field record contained in cores of sediment extracted from the sea floor (e.g. see Ninkovich,

---

[1]) Prof. Dr. K. M. Creer, Department of Geophysics and Planetary Physics, School of Physics, The University of Newcastle upon Tyne, Newcastle upon Tyne, NE1 7RU, U.K.

OPDYKE, HEEZEN & FOSTER, 1967). (c) The successful use of this polarity time scale in the interpretation of magnetic anomalies obtained on traversing the ocean rift systems and the consequent deduction of geophysically acceptable rates of sea-floor spreading, e.g. see VINE (1968).

While a decade ago it seemed possible, even probable, that all reversed NRM in igneous rocks might be attributable to intrinsic properties of the rocks, it is now generally supposed that the various mechanisms of self-reversal such as those put forward by NÉEL (1955) have been of little importance in nature. For instance, the self-reversing Haruna dacite [ISHIKAWA & SYONO 1963] contains hemo-ilmenites in which superexchange interactions occur between different phases which exist because the cation distribution between the two sub-lattices is actually in the process of change from a state of disorder to one of order. Hemo-ilmenites are not usually found in basalts or diabases which are the most widely used rock types in which oxidized titanomagnetites are the principal carriers of RM. NÉEL [1955] also suggested that N-type ferrimagnetic minerals similar to lithium ferrite might occur in nature, but none have been discovered.

However, the idea that self-reversal of RM is of some importance geologically is not dead. In this paper we shall examine the extent to which reversed RM, or at least partial reversal of NRM been impressed during oxidation of primary titanomagnetites, as suggested, for example, by VERHOOGEN (1962).

A suggestion, that there is a statistical bias towards reversed polarity of RM with increasing degree of oxidation has been made by some research workers after magnetic and petrological studies of large numbers of samples of Cenozoic basalts, e.g. WILSON & WATKINS (1967). This correlation is not clear cut, for other workers have failed to detect it in rock formations they have studied, e.g. LARSON & STRANGWAY (1968), ADE-HALL & WATKINS (1970). Six oxidation classes have been defined petrologically to describe the extent of deuteric oxidation, i.e. oxidation which took place during the initial cooling as opposed to slow oxidation at ambient temperatures. Bearing in mind that no magnetic or petrologic differences have been detected between basalts of different polarity belonging to the same oxidation class, it would seem reasonable to attribute the reversed NRM to reversed polarity of the geomagnetic field when the rocks cooled. It follows that the oxygen fugacities within basaltic magmas which were erupted and which cooled while the geomagnetic field was in a reversed mode, should have been somewhat higher than in similar magmas which erupted while the field was in a normal mode (WILSON & WATKINS, 1967). It is hard to accept this conclusion because the geomagnetic field originates within the earth's liquid core while volcanic eruptions originate within the lithosphere or uppermost mantle and no good reasons why the two phenomena should be interdependent are evident.

To resolve this paradox we should ask whether some essential and critical chemical or petrological features of these basalts have been missed and to answer this question we can do no better than start by asking ourselves how much we actually know about the processes of oxidation in titanomagnetites. This is one of the main themes of this

symposium. Many workers in rock magnetism still quote the results of the pioneer Japanese studies (AKIMOTO, KATSURA & YOSHIDA, 1957) in which the CURIE temperatures and saturation magnetizations of synthetic sintered titanomagnetites were followed as they were progressively oxidized to what were thought to be homogeneous and cation deficient spinel structures with unchanged Fe/Ti ratio. However, it is now accepted (OZIMA & LARSON 1969), that the oxidation products described by AKIMOTO et al. (1957) were not homogeneous but that unmixing to a Fe rich spinel phase and a Ti rich rhombohedral phase, albeit on a very fine scale had occurred. This illustrates the well known fact that two types of oxidation product can be obtained from stoichiometric titanomagnetites, and an up to date account of the oxidation process as it occurs in synthetic samples under laboratory conditions will be presented at this symposium by READMAN and O'REILLY.

The shape of the solvus of the magnetite-ulvöspinel solid solution series tells us that homogeneous titanomagnetite grains of the composition usually found in basalts, see Fig. 1 for range of x values, have been produced by rapid cooling. This deduction from laboratory experiment is confirmed by the geological observation that they are only found in the outer parts of sub-aerial basalt flows or in submarine basalts which must have undergone a very rapid quenching. Thus these homogeneous titanomagnetites are not stable at ambient temperatures, although the rate of unmixing, if it can take place at all, must be very slow. Can we extrapolate the results of experiments in which the activation energy of unmixing produced at a few hundreds of degrees Celsius (CREER, IBBETSON & DREW, 1970) in laboratory times, to infer what happens more slowly in nature at ambient temperatures and geological times? The validity of such extrapolations is pertinent to the geophysical conclusions which may be drawn from the rock magnetic measurements.

Thus the geophysicist may enquire about the composition of the phases produced in nature by slow oxidation at ambient temperatures. Are cation deficient spinels
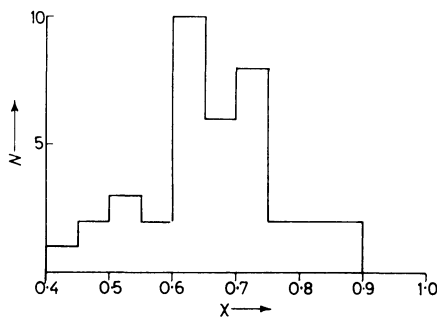
Fig. 1: Histogram showing frequency of values of x determined by microprobe analysis, in the molecular formula $(1 - x) Fe_3O_4 \cdot Fe_2TiO_4$. Impurity cations, Al, Mg, Cr, Mn (see Table 1) are taken to have replaced in the calculations of x.

formed or has unmixing occured on a submicroscopic scale, or may both daughter phases coexist with the mother phase? In any of these cases, the oxidized titanomagnetite grains would be placed in class 1 as a result of observation under the ore microscope. It is possible to define a range of degrees of low grade oxidation within class 1 depending on the shape of the thermomagnetic curve as discussed in section 3.

What of the magnetic interactions between mother and daughter phases? These are of considerable importance in paleointensity studies of the geomagnetic field so that it is essential to detect rocks in which a chemical magnetization has been produced during nucleation of the daughter phase and to find out whether its direction and intensity were controlled by a past geomagnetic field alone, by a magnetic interaction field of internal origin or by the resultant of two such fields of nearly equal strength. Submarine basalts are also progressively oxidized with time (HAGGERTY & IRVING, 1970) and we must enquire how this has affected their original RM and whether it may sometimes preclude the use of magnetic anomaly traverses across the sea floor rift systems to deduce rates of sea floor spreading. This is further discussed in section 7 below.

Considering how complex the NRM of rocks which have undergone oxidation can be, one might ask, with some justification, whether the effects of oxidation could have rendered invalid the historical record of the geomagnetic field built up from rock magnetic studies. The answer is a clear and unequivocal 'no'. Fortunately it was realized, when the earliest paleomagnetic studies on igneous rocks were made, that basalts containing ore grains with fine exsolution lamellae of magnetite and ilmenite, indicative of deuteric oxidation, possessed the most stable NRM: such basalts had high CURIE points above 500 °C and strong resistance to alternating field demagnetization. Rocks with these characteristics were consequently selected for paleomagnetic studies, and it is estimated that more than about 90 % of the data used to establish the most important results, viz. the polarity-time scale for the past 4 My, Cenozoic geomagnetic pole positions and field intensities, have been derived from such rocks.

Deuteric oxidation has usually resulted in the formation of exsolution lamellae several microns thick so that it is recognisible under the ore microscope. Such exsolved Fe-Ti oxide grains underwent a considerable oxidation during their initial cooling, so they are much less apt to undergo further oxidation at ambient temperatures than homogeneous Ti rich titanomagnetite grains. We are principally concerned here with changes in the latter induced by oxidation.

2. Composition and cation deficiency of natural titanomagnetites

NAGATA [1961] noted in his textbook on rock magnetism that natural 'titanomagnetites' are somewhat oxidized, their representative points on the $TiO_2—FeO—Fe_2O_3$ compositional diagram lying exclusively to the higher oxygen content side of the ideal titanomagnetite line. The homogeneity of the minerals studied was tested by X-ray analysis and their composition found by wet chemical analysis.
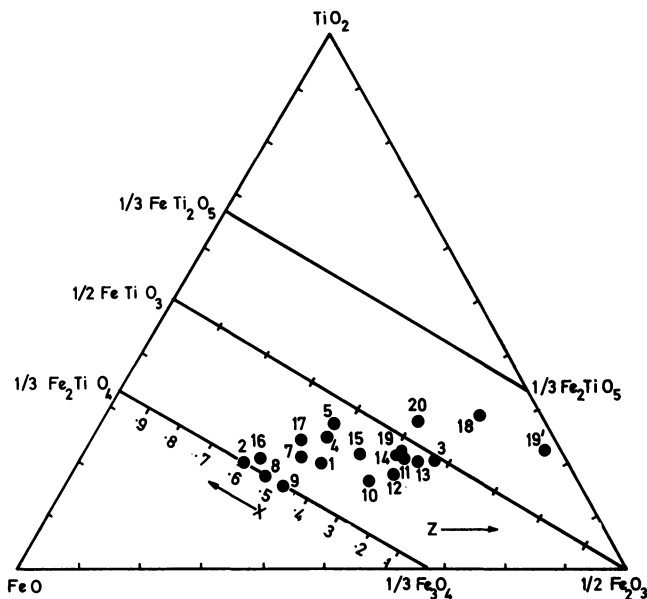
Fig. 2: Compositions of apparently homogeneous spinel type Fe-Fi oxide grains determined from electron-microprobe and CURIE temperature measurements.

It is nowadays more convenient to analyse the chemical composition with an electron microprobe. There are difficulties, however, in the determination of oxygen in the presence of titanium because the K absorption edge of the former at 23.3 Å is in the same region as the L absorption edge of the latter. In default of direct measurement of the oxygen content, the degree of oxidation of optically homogeneous 'titano-magnetites' may be determined by calculating the elevation of their CURIE points, as indicated by their thermomagnetic curves, above the values expected for stoichio-metric members of the $(1-x)\,Fe_3O_4 \cdot x\,Fe_2TiO_4$ solid solution series. The composi-tions illustrated in Fig. 2 are the points of intersection of the lines of Fe/Ti ratio determined by microprobe analysis (CREER & IBBETSON, 1970) and the CURIE point isotherms obtained from experimental determinations on pure synthesized cation deficient titanomagnetites, READMAN & O'REILLY (1970), but corrected for impurity cations. Titanomagnetites in Cenozoic basalts usually contain an appreciable amount of Al and Mg. Although the effects of impurity cations on the CURIE point of magnetite, $(x = 0)$ have been studied (FRÖLICH, LÖFFLER & STILLER, 1965) data for the impure titanomagnetites $(x \neq 0)$ are lacking, so the depression of the CURIE points throughout the series have been assumed to be the same as for $x = 0$.

There is another method of estimating the CURIE points of impure titanomagnetites. O'REILLY (1968) and SANVER & O'REILLY (1970) have described an empirical method

Table 1: Chemical analysis and observed and calculated Curie temperatures of numerous basalts.

Country of Origin	Sample Number	molecular formula						Curie temperature (°C)	
		Fe	Mg	Al	Mn	Cr	Ti	calculated	observed
Argentina	117	1.98	0.12	0.15	0.02	0.04	0.69	63	— 520
	118	1.91	0.16	0.11	0.02	0.00	0.78	4	— 550
	139	2.01	0.22	0.14	0.02	0.08	0.52	183	250, 550
	152	1.94	0.14	0.16	0.02	0.00	0.72	40	200, 550
	203	2.02	0.23	0.14	0.02	0.01	0.58	134	300, 530
	293	2.01	0.21	0.14	0.02	0.01	0.62	107	200, —
	376	1.98	0.24	0.15	0.02	0.01	0.60	117	225, —
	T33	1.98	0.17	0.07	0.02	0.00	0.74	37	125, —
	T34	1.95	0.18	0.15	0.02	0.00	0.68	66	350, —
Turkey	A57	2.13	0.06	0.07	0.02	0.00	0.70	74	275, 540
	A41	2.04	0.15	0.12	0.02	0.00	0.66	87	300, 500
	A106	2.14	0.10	0.07	0.02	0.02	0.64	113	300, —
	D123	2.11	0.05	0.07	0.02	0.00	0.74	40	300, —
	D127	1.99	0.10	0.04	0.00	0.00	0.85	— 41	150, —
	G143	2.15	0.05	0.05	0.02	0.01	0.72	64	300, —
	H122	2.04	0.13	0.06	0.02	0.01	0.74	43	120, —
	T91	2.18	0.04	0.10	0.04	0.00	0.64	113	180 to 500
	K27	1.90	0.28	0.24	0.02	0.00	0.55	135	150, —
	BT31	2.01	0.05	0.05	0.03	0.00	0.85	— 27	230, 520
Azores	FL1F1	2.03	0.22	0.16	0.03	0.00	0.54	159	350, 470
	FL2A1	2.11	0.66	0.10	0.04	0.00	0.69	76	300, 560
	FL2A2	2.12	0.06	0.09	0.03	0.00	0.69	78	250, 530
	FL2B4	1.99	0.14	0.08	0.02	0.00	0.74	38	400, 670
	FL2D2	1.93	0.16	0.14	0.03	0.00	0.73	34	— 520
	FL7A5	2.04	0.06	0.06	0.02	0.00	0.81	— 2	150, 540
Germany	RK	2.02	0.18	0.29	0.02	0.03	0.46	198	250, —
Aden	H21A	2.05	0.13	0.15	0.02	0.00	0.64	98	150, —
Bulgaria	B1	2.05	0.17	0.29	0.02	0.01	0.46	198	300, —
	B3	1.79	0.25	0.32	0.02	0.02	0.61	82	250, —
	B6	1.99	0.28	0.17	0.03	0.02	0.52	167	300, —
	B9	1.93	0.11	0.24	0.02	0.10	0.60	117	260, —
	B10	2.01	0.06	0.24	0.02	0.00	0.66	75	220, —
Pacific Islands	TP38A	1.94	0.10	0.13	0.02	0.00	0.80	— 9	200, 480
Japan	JG3	2.02	0.10	0.07	0.02	0.01	0.77	22	250, —
Canary Islands	ICb	1.87	0.24	0.24	0.02	0.00	0.62	89	200, 530
	IC16	2.03	0.16	0.12	0.04	0.01	0.64	100	200, —
	IC1	2.42	0.06	0.05	0.03	0.04	0.39	294	— 500
	IC3	1.88	0.26	0.18	0.03	0.02	0.63	89	150, —
Reykjanes Ridge	V25D1	2.20	0.09	0.10	0.02	0.01	0.58	151	150, —

Table 2: Estimated and measured CURIE temperatures of impure Fe-Ti spinels in various basalts.

| Origin | Rock No. | Estimated T_c | | Measured T_c of oxidized natural samples |
| | | AB interaction | extrapolation from $x = 0$ | |
		ordered	disordered	
Germany	RK	$-63\,°C$	$-38\,°C$	$193\,°C$	$250\,°C$
Bulgaria	B1	$-53\,°C$	$+17\,°C$	$206\,°C$	$300\,°C$
Argentina	T33	$-103\,°C$	$-88\,°C$	$15\,°C$	$100-150\,°C$
Argentina	293	$-88\,°C$	$-68\,°C$	$95\,°C$	$180-250\,°C$
Turkey	A41	$-23\,°C$	$-18\,°C$	$67\,°C$	$300\,°C$
Turkey	H122	$-98\,°C$	$-88\,°C$	$10\,°C$	$120\,°C$
Azores	FL2A2	$-108\,°C$	$-63\,°C$	$57\,°C$	$250\,°C$
Pacific Islands	TP38A	$-133\,°C$	$-123\,°C$	$-27\,°C$	$200\,°C$
Reykjanes Ridge	V25D1	$-21\,°C$	$+52\,°C$	$134\,°C$	$200\,°C$

for calculating the relative strength of the AB interactions of Fe^{2+} and Fe^{3+} ions in materials with the spinel structure. Since the AB interaction energy equals the thermal energy at the CURIE temperature, the ratio between values of the latter for two substances of similar chemical composition may be taken to be roughly the same as that between the calculated AB interactions. Thus the CURIE points of titanomagnetites doped with Al^{3+} and Mg^{2+} may be estimated by comparing their AB interaction strengths with those of the pure titanomagnetite with the same molecular proportion of Ti^{4+}. Application of this method requires a knowledge of the cation distribution. We may consider two possibilities, taking account of the strong preference of Ti^{4+} for the octahedral B sites: we may either (i) distribute the Al^{3+} and Mg^{2+} randomly on the single A site and $(2 - x)$ B sites per formula unit or (ii) place the Al^{3+} and Mg^{2+} in B sites in preference, if necessary to Fe^{2+} and Fe^{3+}. There is some justification for (ii) considering the cation arrangement of $MgFe_2O_4$ (almost inverse) and the result that Al^{3+} replaces Fe^{3+} in B sites rather than in A sites when substituted into $NiFe_2O_4$ (also an inverse ferrite), SMIT & WIJN (1959). In both models (i) and (ii) we start with a distribution of Fe^{2+} and Fe^{3+} as in the O'REILLY & BANERJEE (1966) model for pure titanomagnetites.

We then find that the estimated CURIE temperatures for the disordered structures (model i) are somewhat lower than for the ordered structures (model ii). Both estimates are considerably lower than those obtained by extrapolating FRÖLICH et al's (1965) data from $x = 0$ as illustrated for a representative group of samples in Table 2. We stress that the differences between the last estimate (col. 5) and the measured (col. 6) have been used to estimate the degree of oxidation of the natural samples illustrated in Fig. 2. The values listed in cols. 3 and 4, Table 2 appear rather low, although the differences between the estimated CURIE points corresponding to the distribution of

Al^{3+} and Mg^{2+} are probably significant. The consequences of this and ot the different
spontaneous magnetizations calculated for the two distributions will be discussed
elsewhere (CREER & STEPHENSON, 1971, in preparation).

3. Laboratory oxidation of continental basalts containing optically homogeneous titano-magnetites

CREER & PETERSEN (1969) studied the evolution of thermomagnetic curves with
progressively longer heat treatments in air at 400 °C. In Fig. 3 the results for the Rauher
Kulm basalt, which are quite typical of many similar basalts studied, are illustrated.
Two changes are identified: (a) a steady increase in the initial CURIE temperature and
(b) the growth of a new magnetic phase with a CURIE point of about 520 °C. The first
observation, (a), is attributed to the oxidation of the mother titanomagnetite phase to
a progressively more cation deficient spinel structure maintaining the initial Fe/Ti
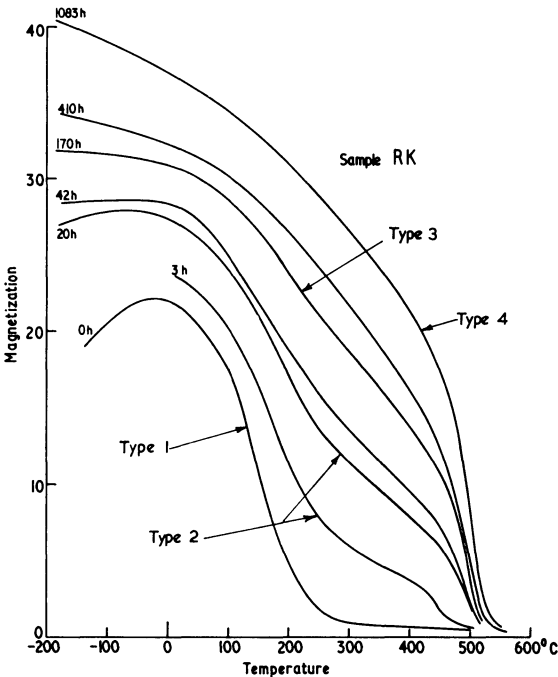
Fig. 3: Evolution of shapes of thermomagnetic curve with progressive heat treatment in air at
400 °C of a basalt from Argentina containing Fe-Ti spinel type grains which remained
apparently homogeneois throughout and to belong to oxidation class 1. Thus apparently
unoxidized grains can be graded on the basis of the shapes of the thermomagnetic curves.

ratio. (Note that the mother phase is a Q-type ferrite, although it is apparently P-type in fields of less than 10 Koe (Fig. 4).) The second observation (b), may be attributed to an unmixing of the cation deficient phase into an iron rich ferrimagnetic daughter phase with the new high CURIE temperature of about 520 °C and a titanium rich phase with CURIE point below room temperature. In some other basalts, the CURIE point of the Fe rich phase ranges in value up to about 560 °C, possibly depending on the amount of Mg and Al impurity. The grains appeared optically homogeneous even after over 1000 hours heating at 400 °C. Yet the magnetic properties had been completely transformed, suggesting that if unmixing had occured, it must have been on a submicroscopic scale.

Measurement of the time constants τ, (several minutes to hours) for isothermal unmixing at temperatures in the range 360° to 430 °C in a basalt from the Azores (FL2a2 and FL7a5) allow the calculation of the activation energy for this process. It is 0.5 eV (CREER, IBBETSON & DREW, 1970). Extrapolation to an ambient tempera-
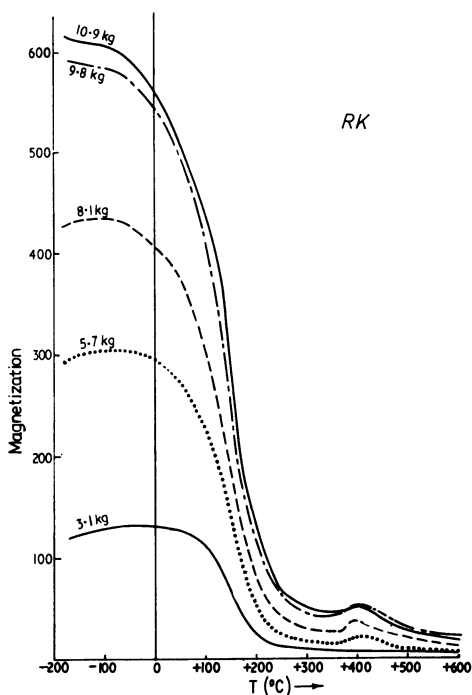
Fig. 4: Magnetization vs temperature curves in different applied field strength. In fields of a few kilo-oersteds the curves exhibit an apparent P-type behaviour. But the titanomagnetite, β (0.45) contained in this rock, the Rauher Kulm basalt, is really a Q-type ferrite as demonstrated by the shape of the J_s (T) curve in 10 kOe.

ture of 300°K yields a time constant of about 3 My for the same process. However the time constant of the reaction at a given temperature in the vicinity of 400°C can be decreased by a factor 10 by grinding the rock more finely. Conversely the time constant for the bulk rock could be much higher at any given temperature than that for the small chips of rock on which the experiments were carried out. While the activation energy fixes the slope of the $\ln \tau$ vs T^{-1} line, the actual position of the line depends on the availability of oxygen, because unmixing only occurs when sufficient vacancies have been introduced into the titanomagnetite structure.
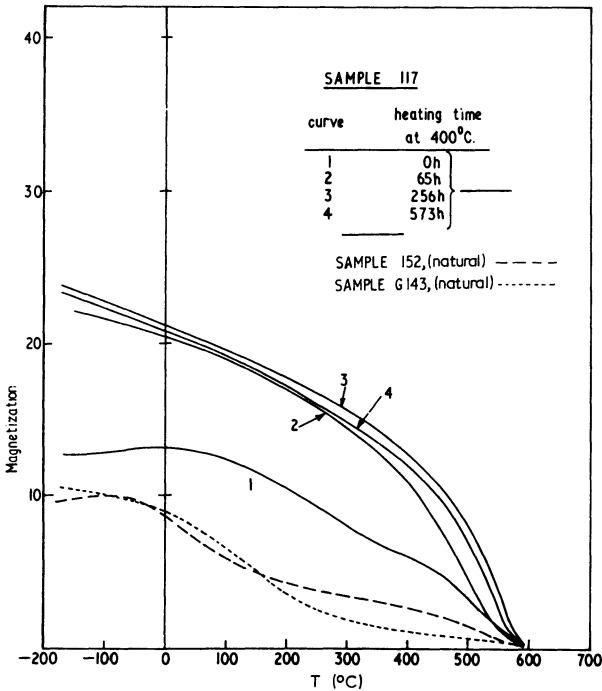
Fig. 5: Thermomagnetic curves of untreated samples which are deduced to have undergone oxidation at ambient temperatures naturally.

Studies of the shapes of the thermomagnetic curves of many untreated, i.e. natural, rocks containing apparently homogeneous titanomagnetites and comparison with their Fe/Ti ratios determined from microprobe analysis suggest that both processes, (a) and (b) have occurred naturally (Fig. 5). The degree of oxidation and the extent of unmixing may be estimated from the shape of the J_s (T) curve. It is convenient to classify 4 types (Fig. 3).

4. Magnetic interactions between mother and daughter phases

There appears to be a weak magnetic interaction between mother and daughter phases corresponding to an internal field of 0.1 to 0.15 oe in the rocks studied after heat treatment at 400 °C in the laboratory.

The daughter phase produced after unmixing of the cation deficient titanomagnetite, first nucleates, then grows successively through grain sizes corresponding to super-paramagnetic, viscous and stably magnetized single domain grains.

A chemical magnetization can be produced in the largest grains, which fall in the last category, i.e. the heatings in air are carried out in a weak magnetic field, e.g. in the geomagnetic field of about 0.44 oe. On cooling the rock subsequently, in zero field, any remaining mother phase (now a cation deficient titanomagnetite) acquires a remanence in the internal magnetic field (Fig. 6). HAVARD & LEWIS (1965) found this

B1
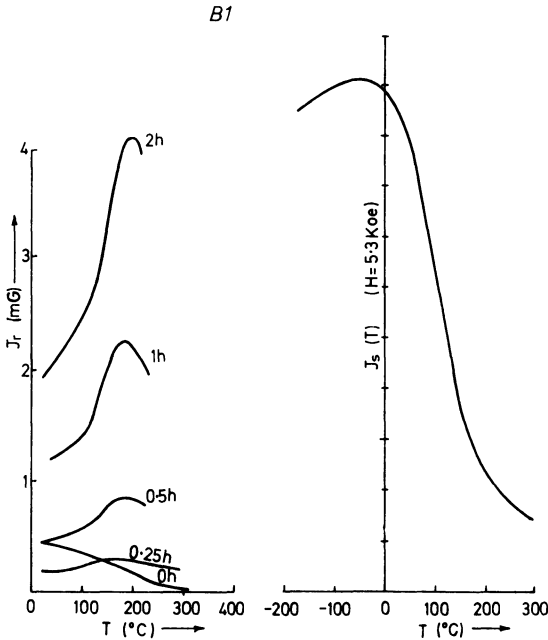
Fig. 6: Temperature variation of remanence of partially oxidized and unmixed titanomagnetite grains in a Bulgarian basalt which had been given a chemical remanence by heating in air for the stated times at 400°C. Note how the lower blockage temperature (where $J_r(T)$ is maximum) increases with time of heating due to progressive oxidation of the mother titanomagnetite phase to a cation deficient daughter phase. The chemical magnetization resides in an iron rich phase which is produced by unmixing of some of the cation deficient phase. The curve on the right is the $J(T)$ curve of the virgin sample in 5.3 koe.
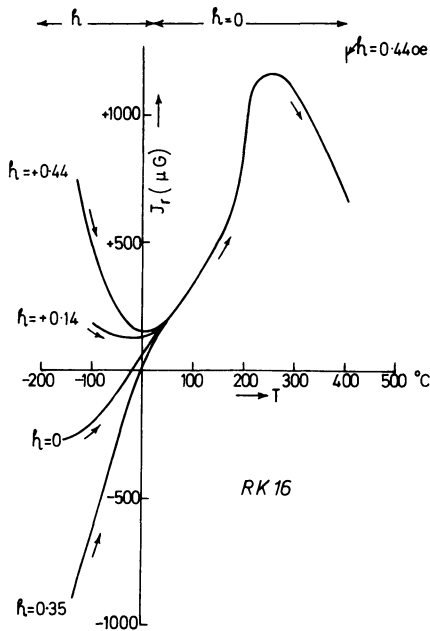
Fig. 7: Temperature variation of remanence of Rauher Kulm basalt, RK after cooling to li-
quid nitrogen temperature in different magnetic fields as stated and warming up to
room temperature beneath an astatic magnetometer. The sample, which initially con-
tained homogeneous titanomagnetite, had been heated in air for 240 hr at 400° in a
field of 0.44 oe and then cooled to room temperature in zero field.

so be several tenths of an oersted both in Indian Deccan Trap lavas and in synthetic
samples with $x = 0.5$. CREER, PETERSEN & PETHERBRIDGE (1970) measured an inter-
action field of 0.14 oe affecting the growth of viscous magnetization at room tempera-
ture in partially oxidized samples of the Rauher Kulm basalt. Similarly, by cooling
below room temperature in different weak applied fields, some of the smaller grains
which are superparamagnetic at room temperature become blocked in and CREER &
PETHERBRIDGE (1971, in preparation), have observed interaction fields of between 0.1
and 0.15 oe in partially oxidized Rauher Kulm and Bulgarian basalts (Fig. 7). LEWIS
(1968) has also observed this kind of interaction in synthetic titanomagnetites.

5. Oxidation of Submarine Basalts

So far we have discussed the oxidation of continental basalts, with the exception
perhaps of the Azores samples which might be regarded as sub-aerial eruptions of
basalts of submarine basalt composition.

In what respects, if at all, do submarine basalts differ form continental basalts. Because of the rapid cooling due to contact with sea water at approximately $0\,°C$, after eruption, submarine basalts are usually very fine grained and also they contain homogeneous titanomagnetite grains, like some chilled basalls originating from continental eruptions. But dredged submarine basalts do appear to contain more sulphides than continental basalts.

Because of their fine grain size, the NRM intensities of submarine basalts are considerably higher than those of continental basalts although the susceptibilities may be about the same. Hence their KÖNIGSBERGER ratios are higher (STACEY 1967) as shown in Table 3. There appear to be no fundamental differences in composition in the samples we have studied (Table 2).

The environment on the ocean floor is more highly oxidizing (VERHOOGEN 1962 and SVERDUP, JOHNSON & FLEMING, 1954) than that at many places on the continental surface, and chemical analysis of dredged samples shows them to be progressively more highly oxidized as the distance from the ocean rifts from which they were dredged increases (SCHILLING 1970, private communication), as illustrated in Fig. 8. Further evidence of oxidation is that there is a corresponding increase in CURIE temperature.
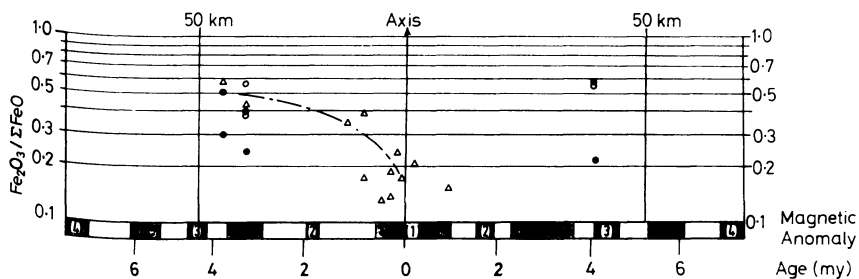
Fig. 8: Fe^{3+}/Fe^{2+} ratio in samples of basalt dredged from the floor of the Atlantic ocean at the distances shown from the central rift (after J.-G. SCHILLING).

What is the nature of the daughter phase in oxidized sea floor basalts? The presence of water is known to enhance the stability of the cation deficient spinel structure. So should we expect unmixing to have occurred in sea floor basalts at any stage of cation deficiency, even if the representative compositional point has crossed the ilmenite-hematite join?

OZIMA & OZIMA (1967) have observed a self reversal in the RM of three out of eight samples of basalts dredged from deep sea mounts in the Pacific Ocean. The initial CURIE temperature was $250\,°C$, indicative of the kind of material described in

Table 3: Magnetic properties of some continental and oceanic basalts.

Origin	Source	Age	Sample No.	$J_n(mG)$	$k(mG/oe)$	Q	$d(\mu m)$	H_{af}	$J_s(T)$	T_c	T_B	x	δ
Continental	Bulgaria		B1	0.5	3.3	0.33	100—2		Type 1	250°C	250°C	0.46	0.46
Continental	Germany		RK	6.0	3.2	4.2	50—2	40	Type 1	200°C	200°C	0.46	0.47
Oceanic	Reykjanes Ridge	Brunhes	V25D1	11.7	1.1	23.6	10	120	Type 1	200°C	180°C	0.58	0.19
Oceanic	Reykjanes Ridge	Brunhes	V25T13	12.5	0.8	34.8	2	200	Type 1	250°C	200°C	—	—
Oceanic	Carlsberg Ridge	Matuyama	5111.7	8.1	0.65	27.8	<1	—	Type 1	—	—	—	—
Oceanic	Carlsberg Ridge	30 My.	6252.10	3.8	0.8	10.6	1	—	Type 1	—	250°C	—	—

J_n intensity of NRM in mG

k weak field susceptibility in mG/oe

Q KÖNIGSBERGER ratio [J_n/kh] $h = 0.45$ oe

d mean grain size in microns

$J_s(T)$ saturation magnetization curve type (see Fig. 3)

H_{af} alternating field required to demagnetize RM to half the NRM intensity

T_c CURIE temperature

T_B Blockage temperature

x number of Ti^{4+} per formula unit of titanomagnetite

δ number of $(Mg^{2+} + Al^{3+})$ per formula unit of titanomagnetite

he analyses of Table 1. Normal TRM resulted when the samples were heated and ooled in the geomagnetic field from temperatures less than 300 °C but reversed RM was produced after heating the samples at 300—310 °C in air for about 10 minutes nd cooling in the geomagnetic field. This property of self reversal was lost after heat- ng some of the samples at 300° for 150 minutes. Thus it would appear that although he mechanism operating in these rocks is associated with metastable products of artial oxidation as in the Rauher Kulm and Bulgarian basalts (sections 3 and 4), it perates at lower temperatures and in shorter times suggesting that it may not be uite the same. The self reversal in these ocean floor basalts could not be suppressed y cooling in a field of 3600 oe which suggests, though does not prove, that the inter- ction is due to superexchange. The interaction in the Rauher Kulm and Bulgarian asalts is very weak, of the order of the geomagnetic field intensity and hence probably nagnetostatic. OZIMA & OZIMA (1967) suggested that the self reversal was due to a earrangement of cations rather than to oxidation because similar changes were pro- uced on heating in air and in 10^{-3} Torr. However, this reduced pressure is not low nough to suppress oxidation (VERHOOGEN, 1962).
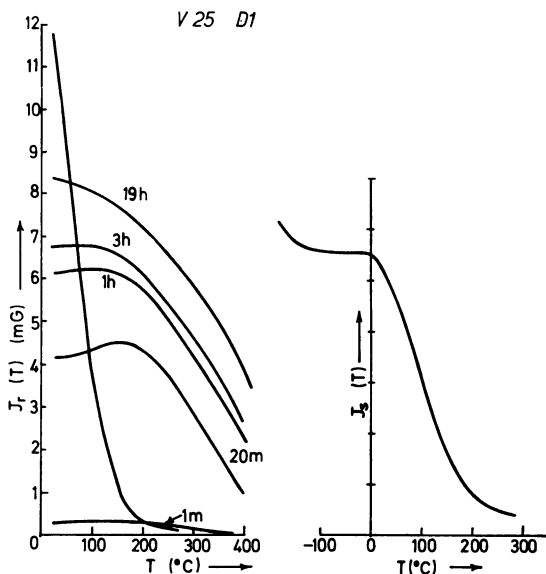
ig. 9: Temperature variation of remanence of a basalt from the vicinity of the Reykjanes Ridge. Curve (a) is for the previously untreated NRM, the other curves are for a chemical remanence acquired during heating in air for the stated times at 400 °C. Coolings and heatings below 400 °C were carried out in zero field. The curve on the right is the $J(T)$ curve in 10 koe for the virgin sample.

Basalts dredged from the ocean floor over the central magnetic anomaly along the Reykjanes Ridge (DE BOER, SCHILLING & KRAUSE, 1970) show evidence of weak magnetic interactions after quite short heat treatments at 400 °C. The temperature variations of remanence determined by heating and cooling in zero field under an astatic magnetometer of the natural sample and after heating for different times on a field of 0.42 Oe at 400 °C for several hours are shown in Fig. 9. The NRM of the sample had blocking and CURIE temperatures of about 170 °C in good agreement with the CURIE temperature estimated from the chemical composition, assuming stoichiometry of its titanomagnetites (Table 1). The presence of a weak magnetic interaction between a daughter phase with blocking temperature of about 500 °C and the parent phase is shown by the 'humped' shape of the curves. It is also evidenced by the different growth rates of viscous magnetization in directions (a) parallel to and (b) opposing the CRM (Fig. 10). These submarine basalts respond to heat treatment at 400 °C essentially in the same way as the continental basalts described earlier. However, there are two differences: (i) the oxidation proceeds much more quickly, in 20 hr rather than 1000 hr and (ii) the interaction between mother and daughter phases is much weaker, though it is still negative.
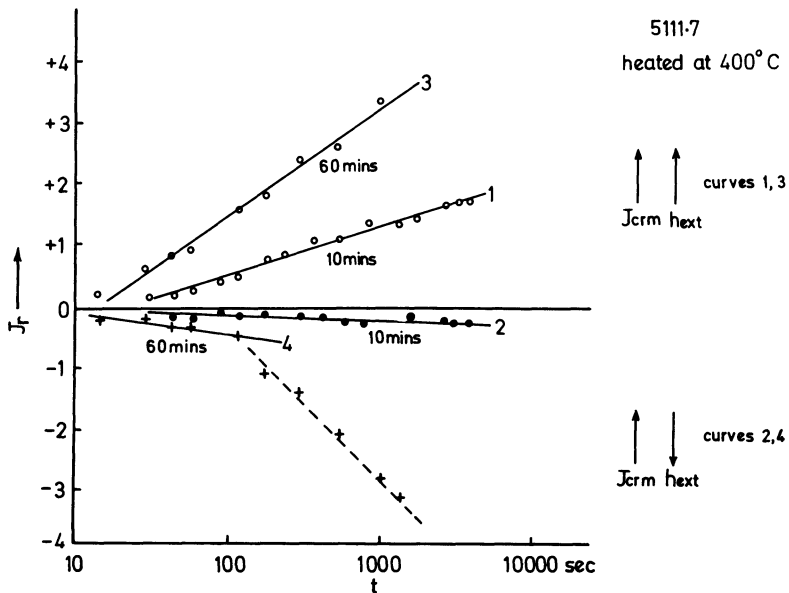
Fig. 10: The rates of growth of viscous magnetization differ according to whether the external field is applied (a) parallel or (b) antiparallel to the chemical magnetization of a laboratory heat treated (400°C, h = 0.44 oe) basalt from the Carlsberg Ridge (5111.7, J. A. CANN).

6. On the compositions of the unmixed phases

The oxidation of pure finely ground synthetic titanomagnetites yield a magnetic product with CURIE point between 500° and 580 °C and is a Fe rich titanomagnetite (READMAN & O'REILLY, 1970). But there are reasons for doubting whether this may be so in natural titanomagnetites in which the presence of Al and Mg impurities may help stabilize the cation deficient phase.
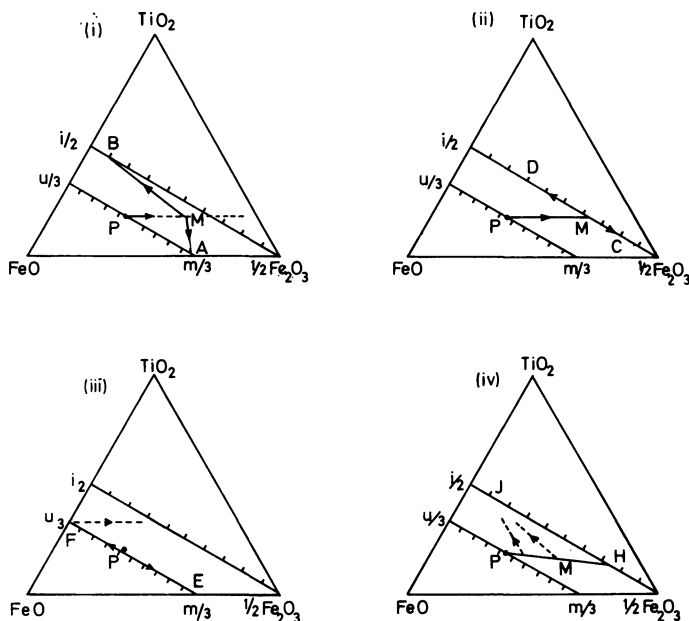
Fig. 11: Possible stages of oxidation and unmixing through which a parent titanomagnetite phase [β (0.55) is taken] passes. M is a metastable cation deficient phase, γ ($x\cdot$, n). A to J are the phases finally produced. See section 6.

We may list four possible sequences of oxidation and unmixing (Fig. 11). But before describing these, let us define a set of symbols by which we may conveniently represent the various phases.

(i) *stoichiometric titanomagnetites*. VERHOOGEN (1962) refers to these as the β **phase.** We identify a member of this solid solution series by β (x) where x is the molecular proportion of ulvöspinel in the molecular formula x Fe_2TiO_4 $(1 - x)$ Fe_3O_4.

(ii) *stoichiometric ilmenite-hematites*. These are normally known as the α phase. We shall denote a member of this solid solution series, y $FeTiO_3$ $(1 - y)$ Fe_2O_3, by α (y).

(iii) *cation deficient titanomagnetites.* We shall refer to all such compositions as the γ phase, and to a specific member by the symbol γ (x', n) where x' corresponds to x in the β series and is a measure of composition, and n is a measure of the number of vacancies. Following VERHOOGEN (1962) we define n as follows:

$$4\left[\mathrm{Fe}^{2+}_{1+x}\,\mathrm{Fe}^{3+}_{2-2x}\,\mathrm{Ti}^{4+}_{x}\,\mathrm{O}^{2-}_{4}\right]+n\,\mathrm{O}_2=\left(4+\frac{1}{2}\,n\right)\left[\mathrm{Fe}^{2+}_{a}\,\mathrm{Fe}^{3+}_{b}\,\mathrm{Ti}^{4+}_{c}\,\square_d\,\mathrm{O}^{2-}_{4}\right]$$
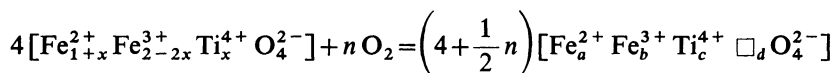
where $\square$ denotes a vacancy and :—

$a = 4\,(1 + x - n)/f$
$b = 8\,(1 - x + \frac{1}{2}\,n)/f$
$c = 4\,x/f$
$d = 3\,n/2\,f$
$f = 4 + \frac{1}{2}\,n$
for ulvöspinel; $x = 1$ and $0 < n < 2$
for magnetite; $x = 0$ and $0 < n < 1$

$n = 2/3$ corresponds to oxidation to the ilmenite-magnetite join. $n = 1$ corresponds to oxidation to the $\mathrm{FeTiO_3}-\mathrm{Fe_2O_3}$ join. Thus we shall refer to a titanomaghemite as γ (x', 1) where $x' = c = 8\,x/9$. The homogeneous γ (x', 1) phase would be produced by oxidation of β (x).

Four possible sequences of oxidation and unmixing are (see Fig. 11):

(I.) parent phase $P = \beta$ (x_0) is oxidized to a metastable phase $M = \gamma$ (x'_0, n), which unmixes to $A = \beta$ (x_1) which is Fe rich, plus $B = \alpha$ (y) which is Ti rich. The terminal CURIE temperatures of $\gtrsim$ 500°C after heating natural basalts at 400°C (section 3) show that $x_1 \lesssim 0.1$. However if impurity Al and Mg concentrate in A rather than B, the CURIE point would be depressed, and x_1 would be closer to 0. The variation in terminal CURIE point from basalt to basalt and in pure synthetic materials may be due to varying amounts of impurity in $A = \beta$ (x_1).

(II.) parent phase $P = \beta$ (x_0) is oxidized to a metastable cation deficient phase $M = \gamma$ (8 $x_0/9$, 1) which unmixes to a Fe rich γ-phase, $C = \gamma$ (x'_1, 1) and a Ti rich γ-phase $D = \gamma$ (x'_2, 1). The terminal CURIE temperature of $\gtrsim$ 500°C shows that $x'_1 \lesssim 0.33$. Phase D would be less stable than C because of the competing preferences of Fe^{2+} and Ti^{4+} for B sites. Hence D would probably invert to α (y_2), close to ilmenite in composition. The strong saturation magnetization of the heat treated basalts suggests that phase C, if the model is correct, has not inverted to an α-phase, perhaps being stabilized by the impurity Al and Mg cations found in natural samples.

(III.) The parent phase $P = \beta$ (x_0) might unmix to E and F, two β-phases. The Ti rich phase, F, would then oxidize and unmix following either models I or II.

(IV.) According to PETERSEN (1969), Ti would tend to migrate out of the cation deficient phase formed on oxidation of $P = \beta$ (x_0). Thus, the γ-phase would not follow a line of fixed Fe/Ti ratio parallel to the base line of the compositional triangle, but

slope down as shown, with increase of n. The Fe rich magnetic end member might thus be $H = C = \gamma (x'_1)$ with $x' \lesssim 0.33$. The other phase, J, would be a Ti rich α phase.

Experimental data favouring models (II) or (IV) are:

(i) Magnetic phases with CURIE points higher than 580°, that of magnetite, β (0) are occasionally observed e.g. in nature in a self reversing Japanese basalt by DOMEN (1969) and in the product of oxidation and unmixing of a synthetic titanomagnetite, β (0.8), Fig. 12, where the CURIE point is 620°C. See also Fig. 7 of READMAN and O'REILLY (1970).
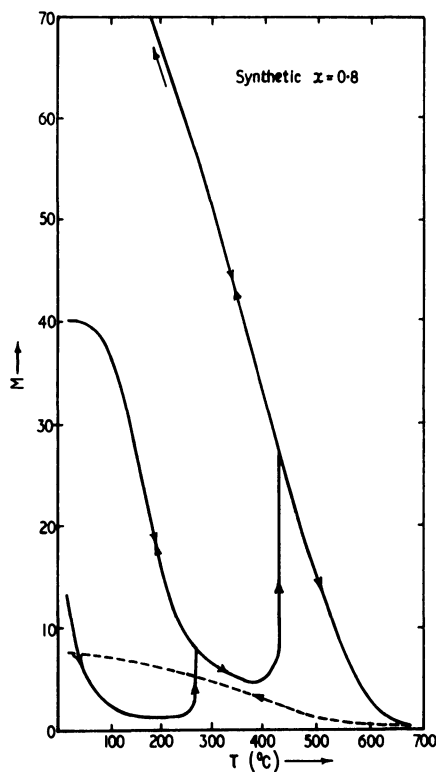
Fig. 12: $J_s (T)$ curve for a fine, wet-ground synthetic titanomagnetite, β (0.8). The first discontinuity at about 270°C is due to the formation of a cation deficient spinel phase which then unmixes at about 430°C. Note that the new magnetic phase has a CURIE point of over 600°C, so it cannot be magnetite, β (0). This is not completely stable at 680°C: When it is kept at this temperature for tens of minutes, it inverts to a less magnetic phase with a lower CURIE temperature (broken curve). Note that this does not appear to be hematite, α (0).

(ii) When samples of the Rauher Kulm basalt, having been stabilized after heating for over 1000 hr at 400 °C are heat treated in air at 600 °C or 700 °C for extended times, both the CURIE temperature and saturation magnetization decrease, Fig. 13. On model I only the decrease in saturation magnetization can be accounted for by oxidation of β ($x_1 \approx 0.1$) to hematite, α (y_1) with y_1 near 0. But no accompanying change in CURIE point would be observable because of the low saturation magnetization of hematite. On model (II) or (IV), phases $C = H = \gamma$ (x'_1, 1) might invert to the α phase with the same composition, but retaining an ordered cation structure with the Al and Mg on one of the magnetic sublattices. γ (0.33, 1) would invert to α (0.24) which has a CURIE temperature of about 460 °C. Thus we have a possible explanation of both the fall in CURIE temperature from about 520° to 460° and the reduction in saturation of magnetization observed in the Rauher Kulm basalt after heating at 600 °C—700 °C. The presence of Al and Mg in the impure titanomagnetites initially present in this rock may thus have a very strong influence on the nature of the oxidation products.

Fig. 13: Remanent magnetisation vs temperature curves for a sample of the Rauher Kulm basalt after prolonged heatings (6 h, 21 h, and 38 h) at 700 °C in air. Note how (a) the CURIE temperature falls to less than 500°C with prolonged heating and (b) the thermoremanence acquired on cooling to ambient temperature in h = 0.44 oe falls from 10.9 mG (after 6 h) to 3.3 mG (after 38 h).

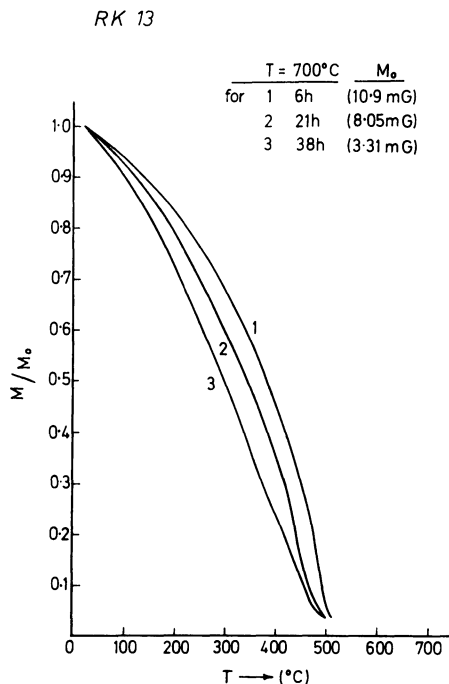## 7. Natural Occurrence of Self-reversal and partial self-reversals of RM possibly associated with oxidation processes

(a) Of the twenty compositions plotted in Fig. 2, it is interesting to note that only one, sample No. 18, a Quaternary basalt from Turkey, plots in the area of the Gorter triangle where self reversal could have occurred due to the redistribution of vacancies and cations on oxidation, assuming either the VERHOOGEN (1962) model or the O'REILLY and BANERJEE (1966) model.

(b) OZIMA and OZIMA (1967) attribute the self reversal they discovered in their sea floor basalt to cation migration without actually specifying any model. In fact their arguments against oxidation or unmixing being the cause are not very good because the large increase in spontaneous magnetization can be attributed to the low CURIE point of the parent phase and because 10^{-3} Torr is not sufficient to suppress oxidation, the partial pressure of oxygen in equilibrium with the magnetite to maghemite reaction being as low as $10^{-68.2}$ at ambient temperatures. This, they now accept (OZIMA and LARSON, 1969).

(c) DOMEN (1969) has discovered reversals of NRM within a single basaltic lava flow. The normally magnetized samples tend to have a single CURIE point of about $350\,°C$ while the reversely magnetized samples tend to have two CURIE points of about $110°$ and $520\,°C$. The material responsible for the normal remanence could then be $\gamma\ (x'_0, n)$; the CURIE point of $350\,°C$ is rather high for a homogeneous β phase (see Table 1). Let us suppose that $n = 1$ to simplify the discussion. Then the phase with CURIE point $350\,°C$ would be γ (0.44, 1) which would be the oxidation product of a parent phase β (0.55) with CURIE point $170\,°C$ (no longer present in the rock). We now adopt model II, section 6, and suppose that γ (0.44, 1) unmixes to two γ-phases which would be γ (0.31, 1) with CURIE point $520\,°C$ and γ (0.77, 1) with CURIE point $110\,°C$. If γ (0.77, 1) has already inverted it would have to be α (0.575) to have the observed CURIE point of $110\,°C$. There would have to be negative interaction between the parent phase and each of the daughter phases on unmixing to explain the self reversal. The presence of normally and reversely magnetized regions within the lava flow, even within hand sized chunks, indicates that the extent to which unmixing has occurred is very uneven.

(d) The intensity of the central anomaly over the rift axis is noticibly high compared with the intensity of the satellite anomalies (e. g. CARMICHAEL, 1970). A possible explanation is that unmixing has occurred in the constituent titanomagnetites. For, as in continental basalts, the interaction field in submarine basalts is negative (Fig. 8 and 9). Thus it will oppose the ambient field in rocks which were erupted in the present magnetic polarity interval, and any chemical magnetization will be small being induced by only a weak effective field, the resultant of the ambient and interaction fields (CREER et al., 1970). However in rocks erupted during the immediately preceding magnetic polarity interval (the Matuyama), will acquire a chemical magnetization in a strong resultant magnetic field which is opposed to the direction of the original NRM
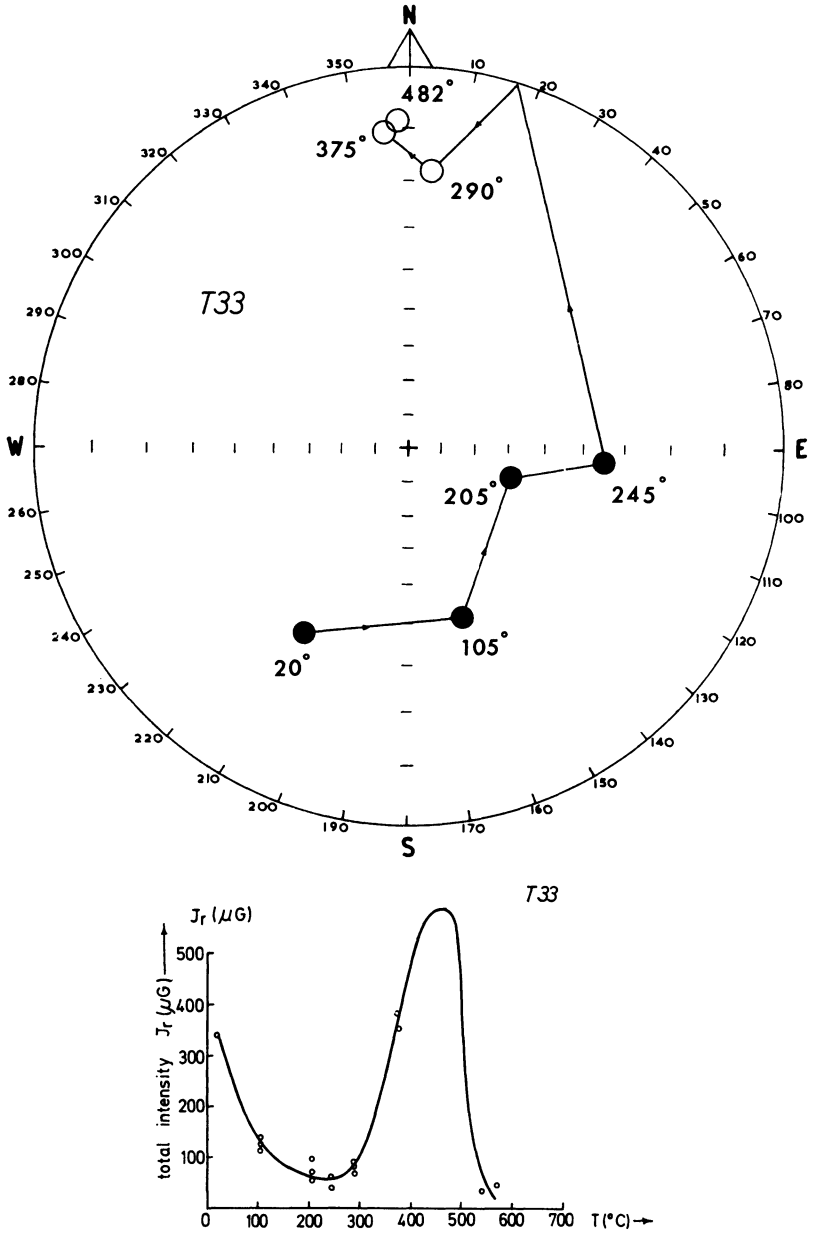
Fig. 14: Change of remanent magnetization of a Tertiary basalt sample, T33, from W.
Argentina during thermal demagnetization.
a) Vaniation of the direction, b) Variation of the intensity.
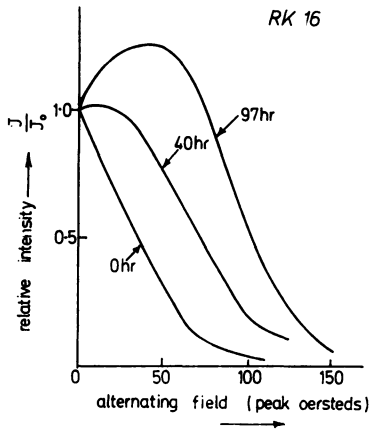
Fig. 15: Effect of progressive heating in air on the a.c. demagnetization behaviour of a basalt sample from Rauher Kulm, Germany.

which will thus be markedly reduced. The observation that the reduction in intensity takes place between the central and first satellite anomalies allows us to attach a time constant of about 1 My to the rate of oxidation and unmixing processes on the ocean floor. Otherwise the decrease in intensity of the anomalies would extend over several polarity epochs and not be so striking.

(e) The CRM acquired by heating above the CURIE temperature of the mother phase is aligned along the direction of a weak external field as illustrated in Fig. 14a and b for a Tertiary basalt, T33, from W. Argentina (see Table 1 for microprobe analyses). While the CRM grows most rapidly between about 300° and 400 °C (Fig. 14b), it appears to have started growing almost from the commencement of heating, judging from the rotation of the total remanent magnetization vector (Fig. 14a). Thus the chemical changes accompanying the acquisition of the secondary remanence can occur near the ambient. Magnetization parallel to the NRM has decayed to zero by about 245 °C. The CRM above 290 °C was parallel to the external field of 0.1 oe. This behaviour is typical of basalts containing homogeneous titanomagnetites initially. The secondary CRM is harder than the NRM and becomes progressively harder with time of heating at 400 °C as illustrated for a sample of Rauher Kulm basalt in Fig. 15.

References

ADE-HALL, J. M., and N. D. WATKINS: Absence of correlations between opaque petrology and natural remanence polarity in Canary Island lavas. Geophys. J. 19, 351—360, 1970

AKIMOTO, S., T. KATSURA, and M. YOSHIDA: Magnetic properties of $TiFe_2O_4 - Fe_3O_4$ systems and their change with oxidation: J. Geomagn. Geoelect. 9, 165, 1957

DE BOER, J., J.-G. SCHILLING, and D. C. KRAUSE: Reykjanes Ridge: implication of magnetic properties of dredged rock. Earth planet. Sci. Lett. 9, 55—60, 1970

CARMICHAEL, L. M.: The mid-Atlantic ridge near 45°N. Magnetic Properties and opaque mineralogy of dredged samples. Can. J. Earth. Sci. 7, 239, 1970

COX, A., R. R. DOELL, and G. B. DALRYMPLE: Radiometric time scale for geomagnetic reversals. Q. Jl. geol. Soc. Lond. 124, 53—66, 1968

CREER, K. M., and J. IBBETSON: Electron microprobe analyses and magnetic properties of non-stoichiometric titanomagnetites in basaltic rocks. Geophys. J. 21, 485—511, 1970

CREER, K. M., J. IBBETSON, and W. DREW: Activation energy of cation migration in titano-magnetites. Geophys. J. 19, 93—101, 1970

CREER, K. M., and N. PETERSEN: Thermochemical magnetisation in basalts. Z. Geophys. 35, 501—516, 1969

CREER, K. M., N. PETERSEN, and J. PETHERBRIDGE: Partial self reversal of remanent magnetization and anisotropy of viscous magnetization in basalts. Geophys. J. 21, 471—483, 1970

CREER, K. M., and J. PETHERBRIDGE: in preparation, 1971

CREER, K. M. and A. STEPHENSON: in preparation, 1971

DOMEN, H.: An experimental study on the unstable natural remanent magnetization of rocks as a palaeomagnetic fossil. Bull. Fac. Edn. Yamaguchi University 18, 1—31, 1969

FRÖLICH, F., M. LÖFFLER, and H. STILLER: Interpretation and changes in CURIE temperatures observed in rocks. Geophys. J. 9, 411—412, 1965

HAGGERTY, S. E., and E. IRVING: Trans. Amer. Geophys. Union 51, 273, abstract only, 1970

HAVARD, A. D., and M. LEWIS: Reversed partial thermomagnetic remanence in natural and synthetic titanomagnetites: Geophys. J. 10, 59—68, 1965

ISHIKAWA, Y., and Y. SYONO: Order-disorder transformation and reverse thermoremanent magnetism in the $FeTiO_3 - Fe_2O_3$ system. J. Phys. Chem. Solids. 24, 517—528, 1963

LARSON, S. E., and D. W. STRANGWAY: Discussion: Correlation of petrology and natural magnetic polarity in Colombia Plateau basalts: Geophys. J. 15, 437—441, 1968

LEWIS, M.: Some Experiments on Synthetic Titanomagnetites, Geophys. J. 16, 295—310, 1968

NAGATA, T.: Rock Magnetism. Maruzen, Tokyo, 1961

NEEL, L.: Some theoretical aspects of rock magnetism. Advances in Physics (Phil. Mag. Supple.) 4, 191—243, 1955

NINKOVICH, D., N. O. OPDYKE, B. C. HEEZEN, and J. H. FOSTER: Palaeomagnetic stratigraphy rate or deposition and tephrachronology in North Pacific deeplsea sediments. Earth & Planet. Sci. Lett. 1, 476—492, 1961

O'REILLY, W.: Estimation of the Curie temperatures of maghemite and oxidized titanomagnetites. J. Geomag. and Geoelect. 20, 381—386, 1968

O'REILLY, W., and S. K. BANERJEE: The mechanism of oxidation in titanomagnetites: a magnetic study. Min. Mag. 36, 29—37, 1966

OZIMA, M., and E. E. LARSON: Low and high temperature oxidation of titanomagnetite in relation to irreversible changes in the magnetic properties of submarine basalts, J. Geophys. Res. 75, 1003—1017, 1969

OZIMA, MITUKO, and MINORU OZIMA: Self reversal of remanent magnetization in some dredged submarine basalts. Earth Planet. Sci. Lett. 3, 213—215, 1967

PETERSEN, N.: Calculation of diffusion coefficient and activation energy of ritanium in titanomagnetites. Earth planet. Sci. Lett. 4, 175—178, 1969

READMAN, P. W., and W. O'REILLY: The synthesis and inversion of non-stoichiometric titanomagnetites. Phys. Earth. Planet. Int. 4, 121—128, 1970

SANVER, M., and W. O'REILLY: Identification of naturally occurring non-stoichiometric titanomagnetites. Phys. Earth. Planet. Int. 2, 166—174, 1970

SCHILLING, J.-G.: private communication, 1970

SMIT, J., and H. P. J. WIJN: Ferrites, Chapter VIII. Phillips Tech. Library, 369 pp., 1959

STACEY, F. D.: The KÖNIGSBERGER ratio and the nature of the thermo-remanence in igneous rocks, Earth and planet. Sci. Lett. 2, 67—68, 1967

SVERDUP, H. V., M. W. JOHNSON, and R. H. FLEMING: The Oceans, pp. 745—755, Prentice Hall Inc., New York, 1954

VERHOOGEN, J.: Oxidation of Fe-Ti oxides in igneous rocks. J. Geol. 70, 168—181, 1962

VINE, F. J.: Magnetic anomalies associated with mid-ocean ridges in The History of the Earth's Crust, ed. R. A. PHINNEY, Princeton Univ. Press 73, 1968

WILSON, R. L., and N. D. WATKINS: Correlation of petrclogy and natural magnetic polarity in Colombia Plateau basalts, Geophys. J. 12, 405—424, 1967

.

The Weak Ferromagnetism of Goethite (α—FeOOH)

I. G. Hedley, München[1])

Summary: The basic magnetic properties of both natural crystals and polycrystalline goethite have been investigated. A variable weak ferromagnetism was observed which lay only in the crystallographic c-direction and which disappeared above the Neel temperature at around 110°C. Chemical analysis revealed a correlation between the aluminium content and the size of the weak ferromagnetism. A simple model is suggested where the Al^{3+} replaces the Fe^{3+} in the lattice and the resultant spin imbalance gives rise to the observed ferromagnetism. An exchange anisotropy could possibly be present giving goethite a considerable magnetic hardness.

Zusammenfassung: Die wichtigsten magnetischen Eigenschaften von natürlichen Kristallen und polykristallinem Goethit wurden untersucht. Danach besitzt Goethit einen schwachen Ferromagnetismus unterschiedlicher Stärke in Richtung der kristallographischen c-Richtung, der oberhalb der Neel Temperatur bei etwa 110°C verschwindet. Die chemische Analyse ergab eine Korrelation zwischen dem Aluminiumgehalt der Proben und der Intensität des schwachen Ferromagnetismus. Es wird ein einfaches Modell vorgeschlagen, in dem Al^{3+} das Fe^{3+} im Gitter ersetzt, dadurch ein Ungleichgewicht in der Verteilung der Spinmomente bewirkt und so einen schwachen Ferromagnetismus (Defekt-Moment) hervorruft. Eine vorhandene Austausch-Anisotropie würde bei Goethit eine beträchtliche Stabilität der remanenten Magnetisierung bewirken.

1. Introduction

Goethite or Nadeleisenerz occurs widely as a mineral and is the principal constituent of sedimentary ironstones [James 1966]. It is the most stable form of the four iron oxyhydroxides (FeOOH) and it is formed by the weathering of iron minerals or by direct precipitation from iron bearing solutions. Produced from the alteration of iron silicates, goethite is thought to be an intermediate stage in the pigmentation of red beds [Walker 1967]. However, little is known of its magnetic properties. It has been practically ignored in paleomagnetic studies as until recently it was assumed that it could not carry a remanence.

2. Crystal structure

Goldsztaub [1935] showed that the structure is orthorhombic, space group Pbnm D^{16}_{2h}. The unit cell dimensions have recently been refined by Sampson [1969]

[1]) Dr. I. G. Hedley, Institut für Angewandte Geophysik der Universität München, 8 München 2, Richard-Wagner-Straße 10.
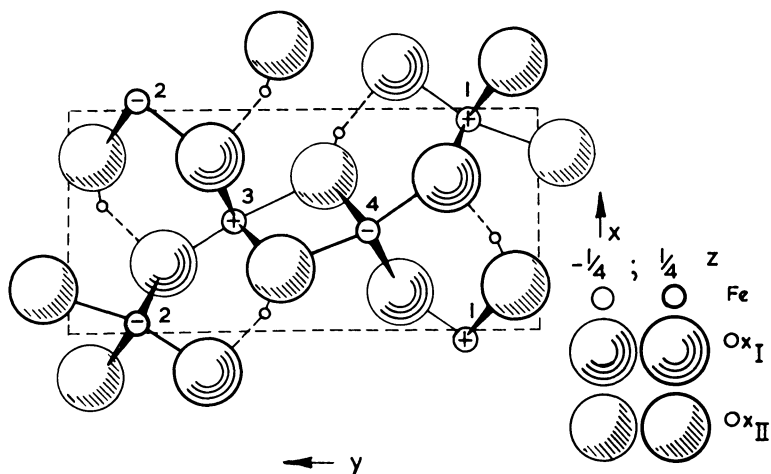
Fig. 1: Projection of goethite crystal structure on (001).

and were found to be the same for both the mineral and synthetic samples studied: $a = 4 \cdot 602 \pm 0 \cdot 003$; $b = 9 \cdot 992 \pm 0 \cdot 004$; and $c = 3 \cdot 021 \pm 0 \cdot 002$ Å. There are four FeOOH units in a unit cell and half of the octahedral sites in the hexagonal close packed lattice are filled with ferric ions. A projection of the crystal structure on the (001) plane is shown in Fig. 1.

3. Samples

Goethite has a very variable appearance ranging from powdery yellow ochre to shiny black single crystals. The general term limonite is often applied to material of an indefinite appearance which has not been identified. It usually consists largely of poorly crystallized goethite. However, the samples examined in the present study consisted of either single crystals or very well crystallized material.

4. Previous magnetic studies

Low temperature magnetic measurements [quoted by CREER 1961] show an almost temperature independent susceptibility of $29 \cdot 10^{-6}$ G $\cdot$ Oe$^{-1} \cdot$ cm$^3 \cdot$ g^{-1}, suggesting that goethite was antiferromagnetic. This was confirmed by the single crystal study of VAN OOSTERHOUT [1965] which revealed a classical antiferromagnetic behaviour with a c-axis spin orientation.

SZYTULA et al. [1966] have found peaks in the temperature dependence of the magnetic susceptibility at around 60°C which they interpret as a NEEL point. In the case of their mineral sample this peak was small and poorly defined. The NEEL point is usually poorly marked in the thermomagnetic curves of synthetic powders at around

130^{0}C [FORSYTH, HEDLEY and JOHNSON 1968]. The high NEEL point of 170^{0}C obtained by VAN OOSTERHOUT [1965] for a single crystal may be due to the error involved in the extrapolation of the low temperature data. However, the properties do seem variable as the many MÖSSBAUER measurements indicate NEEL temperatures which range from 67^{0}C to 130^{0}C. The MÖSSBAUER technique has also been used to confirm the antiferromagnetic spin axis direction by comparing the observed electric quadrupole splitting with that deduced for different spin models [VAN DER WOUDE and DEKKER 1966] and by using a single crystal together with a polarized γ-ray source [FORSYTH et al. 1968].

The actual spin structure has been determined by a powder neutron diffraction investigation [FORSYTH et al. 1968] and the spin ordering is shown in Fig. 2.

STRANGWAY, HONEA, MCMAHON and LARSON [1968] have shown that goethite can acquire a weak thermoremanence (TRM) when the mineral is field cooled through the NEEL point. This TRM varies from sample to sample and the authors conclude that it is due to unpaired spins produced by small grain size, or the presence of imperfections or impurities.

5. Magnetic measurements

The variation in the thermomagnetic behaviour is illustrated in Fig. 3 which shows typical curves for various samples of goethite.

The very broad maximum in susceptibility centred around the NEEL point of the synthetic material is possibly associated with the persistance of short range order above the magnetic disordering temperature. Such material is thought to be in a state of strain produced during synthesis [FORSYTH et al. 1968]. The decrease in susceptibility around 300^{0}C is caused by the dehydration to hematite. Massive samples of the mineral have similar thermomagnetic curves.
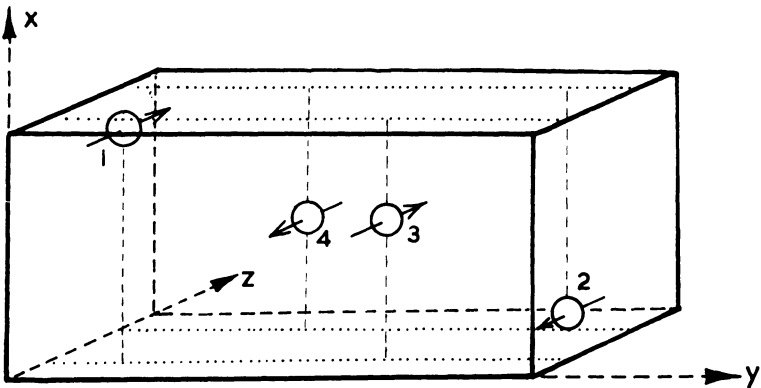

Fig. 2: Magnetic structure of goethite (FORSYTH et al., 1968) showing the relative orientation of the spins of the four ferric ions in a unit cell.
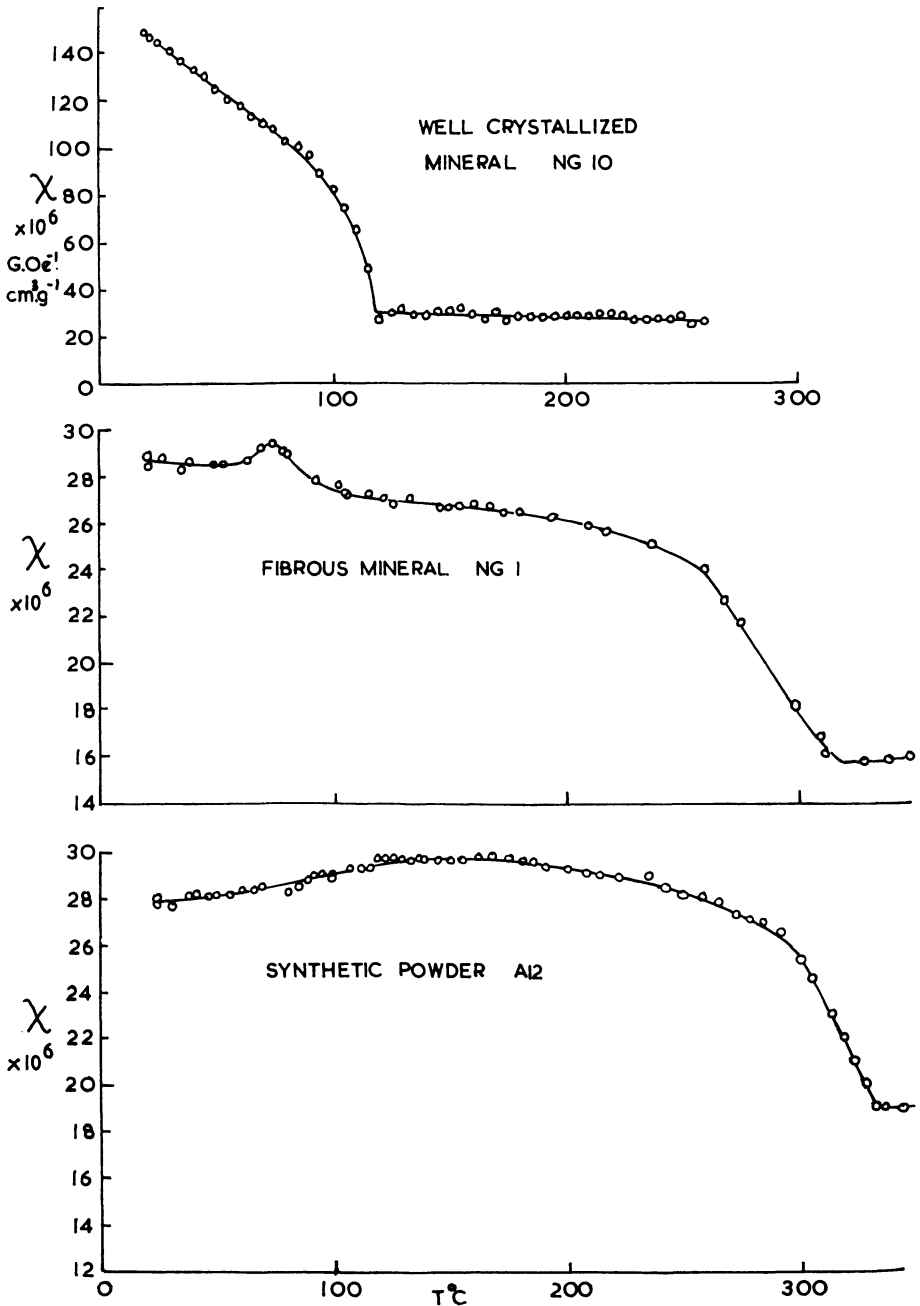
Fig. 3: Typical thermomagnetic curves for various types of goethite.
(N.B. Upper figure has different susceptibility scale.)

The peak at the NEEL point exhibited by the fibrous mineral is most probably a HOPKINSON type effect and is also seen in the thermomagnetic curves of hematite [CHEVALLIER 1951]. The NEEL point of these botryoidal samples, which are often poorly crystallized, is lower, only 60^0—90^0C.

In the case of the well crystallized mineral the steep drop in susceptibility is due to the disappearance of a weak ferromagnetism at temperatures in the region of the antiferromagnetic NEEL point which for these samples lies between 110—120^{0}C.

A magnetic study of single crystals is more informative and the weak ferromagnetism is seen to be highly anisotropic and to lie only along the crystallographic c-axis [001] which is also the antiferromagnetic spin axis (Fig. 4). The temperature variation
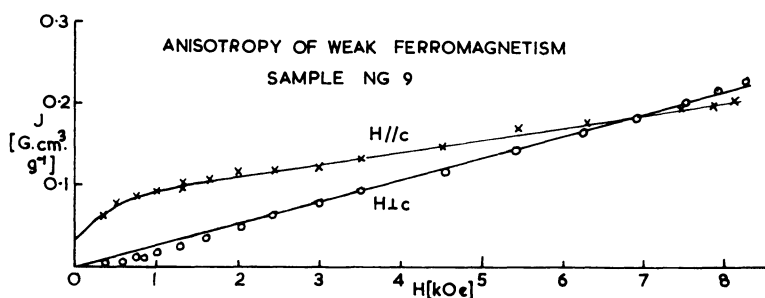
Fig. 4: Magnetization curves of a single crystal NG 9 (3) with the magnetic field parallel and perpendicular to the c-axis.

of the weak ferromagnetism and the antiferromagnetic susceptibility parallel and perpendicular to [001] for a crystal NG 9 from the Restormel Royal iron mine, Cornwall, is shown in Fig. 5 and the weak ferromagnetism is seen to disappear at the antiferromagnetic NEEL temperature.

The NEEL temperature of these magnetic crystals was variable (Table 1). The DTA technique as described by VOLLSTADT [1968] gave similar temperatures, Fig. 6.

The saturation value of the weak ferromagnetism at room temperature was highly variable ranging from 10^{-3} to 1 G $\cdot$ cm$^3 \cdot$ g^{-1} in the samples examined (Fig. 7) and the coercive force of this moment was typically a few hundred oersteds. However, samples of the fibrous mineral and synthetic powders were less magnetic and their saturation remanence was in the range 10^{-2} to 10^{-3} G $\cdot$ cm$^3 \cdot$ g^{-1}.

6. Discussion

STRANGWAY et al. [1968] have suggested that the TRM that is produced by cooling mineral samples comes from some spin imbalance source but the origin of this moment was not identified. It is not due to small crystal size in the goethites examined
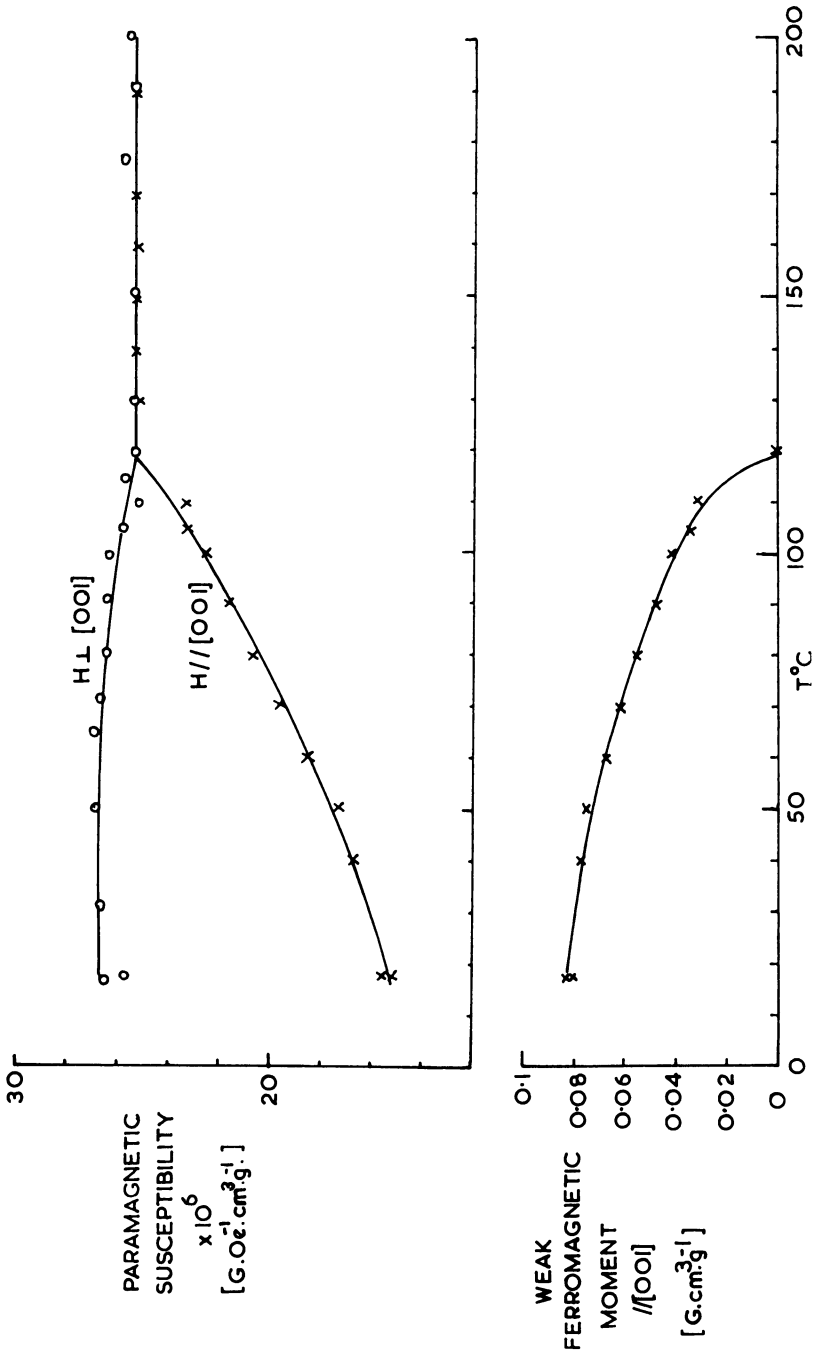
Fig. 5: Temperature dependence of the magnetic susceptibility and weak ferromagnetism in a natural single crystal NG 9 (3).

Table 1

Chemical and magnetic parameters of some natural goethite crystals

Sample	Source	Origin	Chemical Analysis weight % (Electron Microprobe)				Magnetic Parameters		
			Si	Al	Mg	Mn	J_s^2)	$T_N(°C)$ (magnetic)	$T_N(°C)$ (DTA)
NG 18	Royal Scottish Museum	Bottalack Mine, St. Just, Cornwall	0.16	0.53	0.11	0.06	1.00	110^0	114^0
NG 10	Oxford Museum	Restormel Mine, Cornwall	0.14	0.13	0.05	0.06	0.35	112^0	
NG 11	Oxford Museum	Restormel Mine, Cornwall	0.26	0.03	0.29	0.01	0.20	112^0	115^0
NG 9	British Museum BM 26884	Restormel Mine, Cornwall	0.22	0.03	0.08	0.10	0.08	117^0	
NG 23	Glasgow Museum	Lostwithiel, Cornwall	0.20	0.01	0.06	0.04	0.05	113^0	
NG 27	British Museum BM 1967/181	Crystal Peak Colorado, USA	{0.26 {0.69	0.03 0.005	0.07 0.01	0.01 0.01	0.01 ^{4})		
NG 1	Newcastle University, Geology Department	Red mine seam.^{1}) Staffs., England	0.87	0.01	0.05	0.18	0.01^3)	80^0	

^{1}) Polycrystalline material
^{2}) Saturation magnetization at room temperature in $G \cdot cm^3 \cdot g^{-1}$
^{3}) Saturation remanence at room temperature in $G \cdot cm^3 \cdot g^{-1}$
^{4}) British Museum (Natural History) analysis
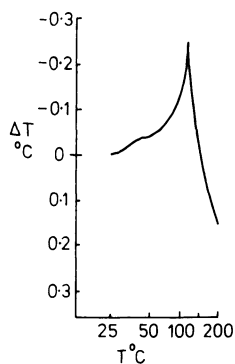
Fig. 6: DTA record for sample NG 11B measured on a CNRS Bureau de Liaison analyser. Sample weight 11.5 mg, heating rate $16 °C$/min, inert sample hematite. This particular sample showed the largest peak.

here because of their relative crystalline perfection. Similarly the disappearance of the weak ferromagnetism at the antiferromagnetic NEEL point rules out the possibility that it is due to some second phase such as magnetite or hematite. The observation that the anisotropic weak ferromagnetism is always parallel to the spin axis means that it cannot have a spin canting origin as in the case of hematite.

Furthermore, the great variability in the magnitude of the ferromagnetism suggests a defect mechanism. There must be an imbalance between the antiferromagnetic sublattices and this could be produced by vacancies or faults in the crystal structure, or by impurities.

It is interesting in this context that ROTH and SLACK [1960] have invoked non-stoichiometry in antiferromagnetic NiO to explain an anomalous weak ferromagnetism. However, to see if this mechanism is operating here one must measure the stoichiometry to better than 0·01 %.

It was noticed that the more magnetic samples tended to give poorer LAUE X-ray photographs with smeared spots than the practically antiferromagnetic crystals. Some also gave marked fibre patterns. Possibly more significant is the fact that the sample with the largest ferromagnetism was unique in having the form of "a" axis needles as all the other samples were of the common c-axis type. This suggests that the crystal growth conditions which influence the crystal habit [KOSTOV 1966] also play some role in determining the magnetic properties.
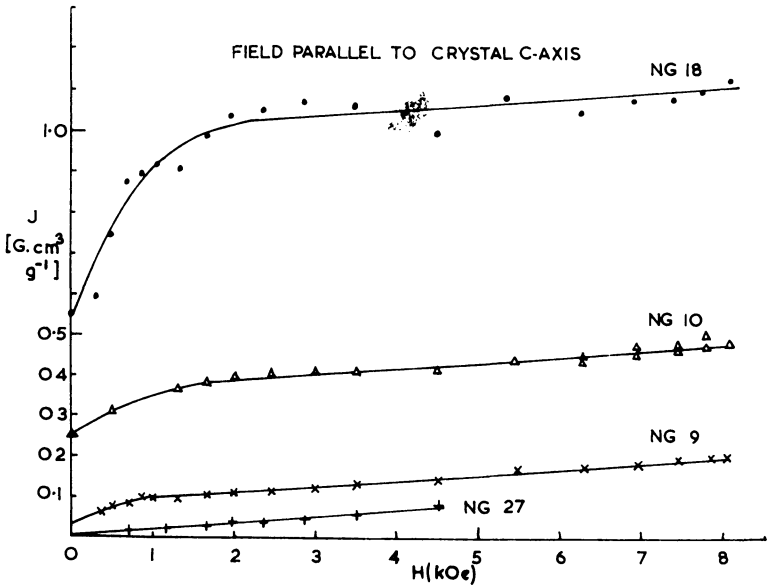
Fig. 7: Magnetization curves of natural goethites.

An experiment was carried out to see if a magnetization could be produced in a practically antiferromagnetic crystal (NG 27) by radiation damage. However, a massive gamma ray dose of 10^7 rad produced only a slight increase in remanence even after heating and cooling in a field. It should be pointed out that in the case of hematite there is conflicting experimental evidence as to the effect of irradiation (with a fast neutron flux) on its magnetic properties [OGILVIE 1963, GALLON 1968].

7. Chemical analysis

STRANGWAY et al. [1968] found no major chemical differences between their samples and few chemical analyses have been published. Chemical analysis is not straightforward as one is not interested in impurity which is present as a second phase but only in that which is incorporated in the crystal lattice. By restricting the investigation to those samples which were either single crystals or well crystallized it was hoped to minimize the possibility of including admixed impurities.

Electron microprobe analysis revealed typical impurity contents of 0.1% Al, Si, and Mg with an apparent correlation between aluminium and the size of the weak ferromagnetism. For example the most magnetic sample (NG 18) with a saturation magnetization of 1 G·cm³·g⁻¹ contained about 0.5% Al whilst the effectively antiferromagnetic goethites with magnetizations of 10^{-2} G·cm³·g⁻¹ had only about 0.03% Al. The other samples fell between these limits.

As such small impurity levels, especially of light elements are on the sensitivity limit of the microprobe an emission spectrographic analysis is being carried out. However, preliminary results confirm the microprobe analyses and will be reported later.

There is also geochemical evidence supporting the presence of aluminium in goethite for not only does it form the isomorphous mineral diaspore (AlOOH) but it is known to substitute for iron in the goethite of oolitic ironstones [SCHELLMAN 1964].

8. Origin of the weak ferromagnetism

A model is proposed in which non-magnetic Al^{3+} by substituting for Fe^{3+} destroys the otherwise perfect compensation between the two antiferromagnetic sublattices. Certainly the aluminium concentrations are of the right order to explain the observed magnetization as 1% Al could give rise to a maximum saturation magnetization at room temperature of 2.8 G·cm³·g⁻¹. Such a model would explain the bulk of the weak ferromagnetism but of course there could also be a small contribution from vacancies or lattice defects.

However, one would expect the aluminium to enter the lattice randomly, and not being preferentially sited in either of the antiferromagnetic sublattices to produce zero moment; certainly in the very large crystallites investigated here. Microprobe examination did not reveal any clustering of impurities, nor is there any experimental

evidence of superparamagnetism which is associated with the defect clusters respon-sible for the weak ferromagnetism in Fe_xO [ROTH 1960].

As the remanence carried by natural samples is most probably a chemical rema-nence (CRM) the geomagnetic field must be sufficient to align a significant fraction of the spin imbalance as the crystallites grow to the stable single domain size. This remanence is generally one or two orders of magnitude smaller than the saturation moment. Although the weak ferromagnetism appears to be produced by aluminium doping the exact mechanism by which this can give the observed magnetization is uncertain.

An interesting consequence of this theory is the possibility that an exchange aniso-tropy exists between the weak ferromagnetism and the antiferromagnetic lattice such that the magnetization shares the high antiferromagnetic anisotropy [MEIKLEJOHN and BEAN 1957]. This means that goethite would have a magnetization with a consi-derable hardness and STRANGWAY, McMAHON and LARSON [1967] report that their TRM was stable in alternating fields up to 1000 oersteds. Magnetic measurements in progress are in favour of the presence of a weak exchange anisotropy.

9. Application to paleomagnetism

Very few paleomagnetic studies have been published which definitely involve goethite. The first was by HOWELL, MARTINEZ and STATHAM [1960] who in their in-vestigation of the Weches formation of Eocene age in Texas, found an interesting example of chemical magnetization associated with limonite. Their unweathered samples were reversely magnetized whereas samples in which the glauconite has weathered to limonite were magnetized close to the present earth's field direction showing that the goethite has acquired a CRM during recent times.

STRANGWAY et al. [1968] found a component of unstable remanence only in the surface layers of the Lyons sandstone of Permian age in Colorado. These surface samples also contain goethite deposited from circulating ground water. The authors consider that the presence of goethite in a rock could also give rise to a secondary magnetization which is a TRM produced by burial, although in the unstable Lyons sandstone this is clearly a CRM.

However, SYMONS [1966] in his study of some late Pre-Cambrian iron ores in Canada found that goethite ore samples showed considerable stability to alternating field demagnetization. Unfortunately, due to the uncertainty in the tectonic correc-tions it was not possible to see if these samples gave a reliable paleomagnetic pole position.

10. Conclusion

Well crystallized mineral samples of goethite have a variable weak ferromagnetism which can be as large as 1 $G \cdot cm^3 \cdot g^{-1}$. A correlation was found between aluminium content and magnetization and a simple model is proposed where the presence of

Al^{3+} in the lattice produces an imbalance between the antiferromagnetic sublattices. The association of a weak ferromagnetism with the basic antiferromagnetism of goethite raises the question of exchange anisotropy which would give the remanence a high stability. However, it has yet to be demonstrated that goethite can carry a remanence which is stable over geological time.

Acknowledgements

References

CHEVALLIER, R.: Propriétés magnétiques de l'oxyde ferrique rhomboédrique (alpha Fe_2O_3). J. Phys. R. 12, 172—188, 1951

CREER, K. M.: On the origin of the magnetization of red beds. J. Geomagn. Geoelectr. 8, 3, 86—100, 1962

FORSYTH, J. B., I. G. HEDLEY, and C. E. JOHNSON: The magnetic structure and hyperfine field of goethite (α-FeOOH). J. Phys. C. (Proc. Phys. Soc. London), ser 2, 1, 179—188, 1968

GALLON, T. E.: The remanent magnetization of hematite single crystals. Proc. Roy. Soc. (London), A 303, 511—524, 1968

GOLDSZTAUB, S.: Structure de la goethite. Soc. Franc. Min. Bull. 25—43, 1935

HOWELL, L., J. D. MARTINEZ, A. FROSCH, and E. H. STATHAM: A note on the chemical magnetization of rocks. Geophysics, 25, 1094—1099, 1960

JAMES, H. L.: Chemistry of the iron-rich sedimentary rocks. Chapt. W, Data of Geochemistry 6th Ed. U. S. G. S. Prof. paper, 440-W, 1966

KOSTOV, I.: Habit types and crystallogenesis of diaspore and goethite. Ann. Univ. Sofia. Fac. Geol. and Geograph. 61 (1), 167—176, 1969

MEIKLEJOHN, W. H., and C. P. BEAN: New magnetic anisotropy. Phys. Rev. 105, 904—913, 1957

OGILVIE, R. E.: Magnetic studies of irradiated hematite crystals. M. I. T. Techn. Report NR 031—686, 1963

ROTH, W. L.: Defects in the crystal and magnetic structures of ferrous oxide. Acta Cryst. 13, 140—149, 1960

ROTH, W. L., and G. A. SLACK: Antiferromagnetic structure and domains in single crystal NiO. J. Appl. Phys. 31, 352—353 S, 1960

SAMPSON, C. F.: The lattice parameters of natural single crystal and synthetically produced goethite (α-FeOOH), Acta Cryst. B25, 1683—1685, 1969

SCHELLMAN, W.: Zur Rolle des Aluminiums in Nadeleisenerz-Ooiden. N. Jahrbuch Min. Monats. 49—56, 1964

STRANGWAY, D. W., R. M. HONEA, B. E. McMAHON, and E. E. LARSON: The magnetic properties of naturally occurring goethite. Geophys. J. 15, 345—359, 1968

STRANGWAY, D. W., B. E. McMAHON, and R. M. HONEA: Stable magnetic remanence in antiferromagnetic goethite. Science, 158, 785—787, 1967

SYMONS, D. T. A.: Paleomagnetic evidence on the origin of the Marquette and Steep Rock hard hematite and goethite deposits. Can. J. Earth Sci., 4, 1—20, 1967

SZYTULA, A., A. BUREWICZ, K. DYREK, A. HRYNKIEWICZ, D. KULGAWCZUK, Z. OBUSZKO, H. RŻANY, and A. WANIC: Susceptibility measurements of antiferromagnetic A-Goethite. Phys. Stat. Sol. 17, K195—197, 1966

VAN DER WOUDE, F., and A. J. DEKKER: MÖSSBAUER effect in α-FeOOH. Phys. Stat. Sol. 13, 181—193, 1966

VAN OOSTERHOUT, G. W.: The structure of goethite. Proc. Int. Conf. Magnetism Nottingham, Institute of Physics, London, 529—532, 1965

VÖLLSTADT, H.: On the determination of rock-magnetic parameters by Thermal Differential Analysis. Geophys. J. 15, 345—359, 1968

WALKER, T. R.: Formation of red beds in modern and ancient deserts. Geol. Soc. Amer. Bull. 78, 363—368, 1967

Magnetization of Fe-Cr Spinels and its Application for the Identification of Such Ferrites in Rocks

E. Schmidbauer, München[1])

Summary: Some magnetic properties of sintered samples of the Fe—Cr spinel system are reported such as Curie temperatures, magnetization vs. temperature curves and magnetic moment data. It is shown how these data in connection with measurements of the lattice parameter can be used to identify compositions of the Fe—Cr spinel series in rocks.

Zusammenfassung: Es wurden an gesinterten Proben des Fe—Cr-Spinell-Systems Messungen der Curie-Temperatur, der thermomagnetischen Kurven und der magnetischen Momente durchgeführt. Es wird gezeigt, wie die Meßresultate in Verbindung mit den Werten der Gitterkonstanten benützt werden können, um Fe—Cr-Spinelle in Gesteinen zu identifizieren.

The magnetic properties of Fe—Cr spinels can be used to identify such spinels in rocks and ore. In nature members of the Fe—Cr spinel system have been found in some basalts mixed with compositions of the titanomagnetite series (Petersen and Nesbitt 1967). Furthermore, in serpentinites they form in part the carrier of the magnetization (Dumsky 1966). In chromium ore Fe—Cr spinels are frequently in solid solution with $MgCr_2O_4$. Finally, mixed crystals of Fe_2TiO_4 (Ulvöspinel) and of members of the Fe—Cr spinel system have been detected in moon rocks.

Fe—Cr spinels are compositions which can be described by the chemical formula $Fe_{3-x}Cr_xO_4$, $0 \leq x \leq 2$ (the end members are Fe_3O_4 and $FeCr_2O_4$). The compositions of the Fe_3O_4 rich part of the system reveal a gradual decrease of the Curie temperatures from 580 °C for Fe_3O_4 to 200 °C for $x = 1.0$ (Francombe 1957, Robbins et al. 1971). This property can in principle be used to establish the exact composition once it is known that the spinels in question belong to the series. This can be checked by microprobe analysis and with the help of x-ray diffraction technique. However, the magnetic data mentioned apply only for crystals which have been produced at 1100 °C. It may be that for natural samples that have been formed at higher temperatures the ion distribution could differ from those prepared at 1100 °C; this would lead to modified Curie temperatures. The Cr ions in the Fe—Cr series are assumed to be located on B-sites only owing to their high stabilization energy for these sites (Miller 1959).

[1]) Dr. E. Schmidbauer, Institut f. Angew. Geophysik d. Universität München, 8 München 2, Richard-Wagner-Straße 10.

Fe_3O_4 is an inverse spinel with Fe^{3+} ions on A-sites whereas the B-sites are populated by equal concentrations of Fe^{3+} and Fe^{2+} ions. With rising Cr content Fe^{2+} ions are forced to A-sites, however, in a non uniform way with increasing x. This has been deduced from lattice parameter data (YEARIAN, KORTRIGHT and LANGENHEIM 1954, FRANCOMBE 1957, SIMONOVA and UGOLNIKOVA 1963). The lattice parameters a_0 do not vary much in the system over the whole range from $x = 0$ to $x = 2$ (a_0 ($x = 0$): 8.395 Å; a_0 ($x = 2$): 8.380 Å) but it is changed in a complicated manner reflecting the variations of the ion distribution. Moreover, there seems to be no percible differ ence in a_0 for specimens sintered at 1300 °C (SIMONOVA et al. 1963) and those fired at 1100 °C (YEARIAN et al. 1954, FRANCOMBE 1957). This fact would be an indication that the CURIE temperatures for the same specimens sintered at different temperatures remain rather constant.

Samples have been prepared at 1100 °C for a number of compositions of $0 \leq x \leq 1.1$, heating pressed pellets of $FeCr_2O_3$ and Fe_2O_3 powders which have been previously mixed in appropriate portions and milled in an agate ball mill under acetone, in evacuated sealed silica tubes up to 50 hrs. For the samples containing higher Cr content this procedure was repeated. Members of the Fe—Cr spinel system of composition $x = 1.2, 1.3, 1.4, 1.5$ have been produced at 1300 °C according to the data of oxygen partial pressure of SEYBOLT 1960 and KATSURA and MUAN 1964. The samples have been checked by x-ray diffraction technique using filtered $Co-K_\alpha$ radiation. They have been found to have pure spinel structure.

For the specimens sintered at 1100 °C the CURIE temperatures of the authors cited above could be confirmed. The samples prepared at 1300 °C show CURIE temperatures which are about $5-10°$ higher.

In order to identify Fe_3O_4 in a specimen one can instead of measuring the CURIE point use the low temperature phase transition of Fe_3O_4 from the cubic to the orthorhombic lattice type at $-150°C$, the so called VERWEY transition. Thus one escapes the problem of heating a sample up to 600 °C which may change the state of the sample. In fields of 1000—2000 Oe this transition leads on cooling to an abrupt decrease in magnetization of 10—20 % for pure stoichiometric Fe_3O_4. An attempt has been made to study how the transition temperature changes on mixing a small portion of Cr to pure Fe_3O_4. However, for compositions of $x = 0.01, 0.02, 0.03$, sintered at 1100 °C, no phase transition could be detected on measuring the magnetization in a field of 500—1000 Oe down to $-185°C$ whereas on pure Fe_3O_4, sintered at 1100 °C, the transition was clearly observable. Usually for Fe_3O_4 containing such small quantities of transition metal ions as Ni^{2+}, Ti^{4+}, Mg^{2+}, Al^{3+} only a shift of the transition temperature of $< 10°C$ to lower temperatures has been observed with the help of measurements of the electrical resistivity. The result for the Cr containing Fe_3O_4 leads to the conclusion that either the transition has been suppressed or shifted to a very low temperature or the magnetic anisotropy which in Fe_3O_4 below the transition is high is lowered remarkably by the addition of Cr ions so that the transition cannot be easily detected by the method mentioned above.

Measurements of the magnetization vs. temperature curves with a magnetic balance in fields of 14 kOe os samples of composition $0 \leq x \leq 1.1$ between $-185\,°C$ and their respective CURIE points yielded curves which change gradually with rising x from the NEEL Q-type shape of Fe_3O_4 to a curve for $x = 1.1$ which is nearly a straight line. The magnetic moments extrapolated from $-185\,°C$ to $0\,°K$ vary almost linearly from about $4\,\mu_B$ (μ_B denotes BOHR's magneton) for $x = 0$ to about $2.5\,\mu_B$ for $x = 1.1$. This result is in good accordance with the values obtained by DERBYSHIRE and YEARIAN 1958 and recently by ROBBINS et al. 1971.

For members of the series $Fe_{3-x}Cr_xO_4$ of $1.3 \leq x \leq 2$, it has been found that the CURIE points lie below room temperature decreasing from about $-30\,°C$ for $x = 1.3$ to $-193\,°C$ for $x = 2$ (FRANCOMBE 1957, ROBBINS et al. 1971). The magnetic moments in this composition range are low.

For the identification of Fe—Cr spinels in rocks using magnetic measurements a difficulty arises from the possibility of oxidation. Measurements of magnetization of synthetically prepared compositions which have been oxidized showed that by the oxidation process at a temperature as high as $500\,°C$ in air it is possible to create cation deficient spinels (SCHMIDBAUER 1969). Such an oxidation process may also occur at lower temperatures in geological times. Thus, for a composition of $x = 0.7$ after oxidation under the condition mentioned a spinel exhibiting reduced lattice parameter and magnetization, however, increased CURIE temperature has been measured. The occurrence of a phase of Fe_2O_3—Cr_2O_3 mixed crystals is apparently somehow impeded.

It seems from the foregoing that measurements of the CURIE temperature alone are not sufficient to determine the composition of an Fe—Cr spinel in a rock sample also if it is confirmed by x-ray diffraction technique that it has a pure spinel phase. The investigation of the CURIE temperatures, the shape of the magnetization vs. temperature curve, the extrapolated values of magnetization to $0\,°K$ and of the lattice parameter of the sample should be sufficient to establish if the spinel in question belongs to the Fe—Cr spinel system and which composition it has. However, it appears that compositions of $x < 1.3$ due to their low CURIE temperatures and low magnetic moments are less suitable to be studied in naturally occurring samples using their magnetic properties than those which are on the Fe rich side of the system. For the former ones low temperature facilities down to liquid helium temperature have to be available.

References

DERBYSHIRE, W. D., and H. J. YEARIAN: X-ray diffraction and magnetic measurements of the Fe—Cr spinels. Phys. Rev. 112, 1603—1607, 1958.

DUMSKY, A.: Das magnetische Störfeld und Magnetisierung der Serpentinite am Südrand des Hohen Bogen. Diplomarbeit, Institut f. Angew. Geophysik d. Univ. München, 1966.

FRANCOMBE, M. H.: Lattice changes in spinel-type iron chromites. J. Phys. Chem. Solids 3, 37—43, 1957.

KATSURA, T., and A. MUAN: Experimental study of the equilibria in the system $FeO—Fe_2O_3—Cr_2O_3$ at 1300°C. Trans. AIME, 230, 77—84, 1964.

MILLER, A.: Distribution of cations in spinels. J. Appl. Phys. 30, 249—270, 1959.

PETERSEN, N., and J. NESBITT: Private communication. School of Physics, University of Newcastle, Newcastle upon Tyne, 1967.

ROBBINS, M., G. K. WERTHEIM, R. C. SHERWOOD and D. N. E. BUCHANAN: Magnetic properties and site distributions in the system $FeCr_2O_4—Fe_3O_4$ ($Fe^{2+}Cr_{2-x}Fe^{3+}_xO_4$). J. Phys. Chem. Solids 32, 717—729, 1971.

SCHMIDBAUER, E.: Magnetic properties of oxidized Fe—Cr spinels. Z. Geophys. 35, 475—484, 1969.

SEYBOLT, A. U.: Observations on the Fe—Cr—O system. J. Electrochem. Soc. 107, 147—156, 1960.

SIMONOVA, M. J., and T. A. UGOLNIKOVA: Concerning the distribution of cations in ferrite and chromite solid solutions. Bull. USSR Acad. Sci. Phys. Ser. 27, 1481—1487, 1963.

YEARIAN, H. J., J. M. KORTRIGHT and R. H. LANGENHEIM: Lattice parameters of the $FeFe_{2-x}Cr_xO_4$ spinel system. J. Chem. Phys. 22, 1196—1198, 1954.

Electrical Resistivity of Fe-Cr Spinels

E. Schmidbauer, München[1])

Summary: The d. c. electrical resistivity of sintered Fe-Cr spinels of composition $Fe_{3-x}Cr_xO_4$, $0.6 \leq x \leq 1.5$, at room temperature lies between $5 \cdot 10^{-1}$ and $6 \cdot 10^4$ ohm cm. From its temperature dependence between -170^0 and $+50^0C$ a semiconducting behaviour of the spinels can be concluded. The activation energy is within the range of 0.12 and 0.29 eV for $x = 0.6$ and 1.5, respectively, and it shows a correlation with the number of Fe^{2+} ions on B-sites of the spinel lattice. For some compositions a break of the resistivity-temperature curves has been found near the ferrimagnetic Curie points.

Zusammenfassung: Der elektrische Widerstand von gesinterten Fe-Cr Spinellen der Zusammensetzung $Fe_{3-x}Cr_xO_4$, $0,6 \leq x \leq 1,5$, liegt bei Raumtemperatur zwischen $5 \cdot 10^{-1}$ und $6 \cdot 10^4$ ohm cm. Die Spinelle sind Halbleiter im untersuchten Temperaturbereich zwischen -170^0 und $+50^0C$. Die Aktivierungsenergie bei Raumtemperatur liegt zwischen 0.12 und 0.29 eV für $x = 0,6$ bzw. $x = 1,5$. Aus dem Verlauf der Aktivierungsenergie mit der Zusammensetzung kann auf einen Zusammenhang mit der Zahl der Fe^{2+}-Ionen auf B-Plätzen des Spinellgitters geschlossen werden. Einige der Ferrite weisen einen Knick der Widerstands-Temperatur-Kurve an ihren ferrimagnetischen Curie-Punkten auf.

1. Introduction

It is known that the low electrical resistivity of Fe_3O_4 is due to electron exchange between Fe^{3+} and Fe^{2+} ions on B-sites of the spinel lattice (electron hopping) [Verwey and de Boer 1936]. In recent years much attention has been paid to electrical conductivity of oxides, however, relatively few investigations deal with spinel systems whose conduction mechanism may be similar to that in Fe_3O_4, i. e., it is determined by high concentrations of B-site Fe^{3+} and Fe^{2+} ions. In this note a study of the resistivity of Fe-Cr spinels is reported.

2. Experiments and results

Measurements of the d. c. electrical resistivity have been performed on sintered specimens of the spinel system $Fe_{3-x}Cr_xO_4$, $0 \leq x \leq 2$, in the temperature range between -170^0 and $+50^0C$. Compositions of $x = 0.6$, 0.9, 1.0, 1.2, 1.3, 1.4, 1.5 have been prepared at 1300^0C firing pressed pellets of mixtures of analytical grade

---

[1]) Dr. E. Schmidbauer, Institut für Angewandte Geophysik der Universität München, 8 München 2, Richard-Wagner-Straße 10.

Fe, Fe_2O_3 and Cr_2O_3 powders, after presintering at 1100^0C, up to 50 hrs in an atmos-phere containing varying O_2 partial pressure between 10^{-6} and 10^{-8} atm. [SEYBOLT 1960, KATSURA and MUAN 1964]. The resulting products have been cooled at a rate of $30^0/min$ from 1300^0 to 800^0C and in about 4 hrs from 800^0C to room temperature. The spinels thus obtained have been checked by X-ray and microscopic techniques. All compositions have been found to be pure spinels with a porosity $<10\%$.

For the measurements pieces of rectangular cross section (about $2 \times 3 \times 5$ mm) have been cut from the sintered samples. A two-probes method was used by clamping the pieces between two metal springs after having rubbed indium amalgam onto the fresh ground surfaces. The measurements for samples exhibiting low resistivity have been carried out with the four-probes technique.

At room temperature the resistivity ϱ (ohm cm) is low for $x = 0.6$ and increases with raising x (Fig. 1). A log ϱ vs. $10^3/T$ plot yields straight lines. Hence the spinels under consideration are semiconductors, the resistivity following the relation $\varrho = \varrho_0$ exp (E_A/kT). Three types of straight lines could be distinguished. The compositions $x = 0.6$, 0.9, 1.0 reveal straight lines over the entire temperature range. Those of $x = 1.2$ and 1.3 yield straight lines with two breakes, whereas for $x = 1.4$ and 1.5 only one break could be detected. For the last mentioned composition the existence of the break is not clearly established as it occurs in the lowest temperature range studied. All breaks are in the vicinity of the CURIE points of the respective spinels.
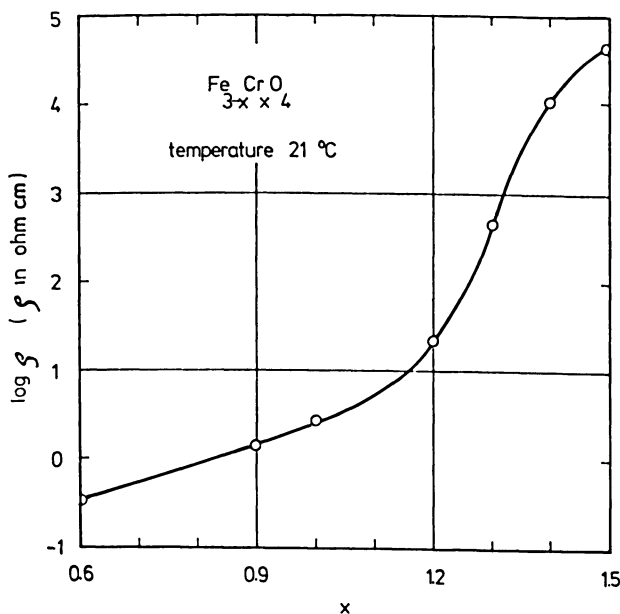
Fig. 1: Electrical resistivity ϱ (ohm cm) as a function of composition x of sintered mixed crystals $Fe_{3-x}Cr_xO_4$; temperature: 21^0C.
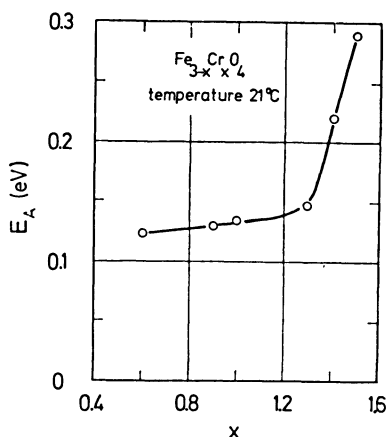
Fig. 2: Activation energy E_A vs. composition x of sintered mixed crystals $Fe_{3-x}Cr_xO_4$; temperature 21 °C.

Therefore either the magnetostriction of the polycristalline material or the exchange interaction may be involved in the change of slope. The influence of ferrimagnetic ordering on the conduction mechanism of several spinels, in the form of a break in the straight lines of log ϱ vs. $1/T$, has been reported by some workers [KOMAR and KLIUSHIN 1954, BELOV, POPOVA and TALALAEVA 1958, ROSENBERG, NICOLAU and BUNGET 1964, REZLESCU 1969].

From the temperature dependence of ϱ no effect of the low temperature crystallographic phase transitions which take place in the Fe-Cr spinel system [FRANCOMBE 1957] could be detected.

In Fig. 2 the activation energy E_A at room temperature is plotted against the composition x. The increase in E_A between $x = 1.3$ and 1.4 is likely to be a consequence of the fact that in this composition range the number of Fe^{2+} ions on B-sites of the spinel lattice becomes very small (whereas the B-site Fe^{3+} ion concentration remains high) [GOODENOUGH 1964]. In terms of a model of electron hopping between B-site Fe^{3+} and Fe^{2+} ions this means that the electron exchange is suppressed to a large extent and a second conduction mechanism may be effective. The origin of the increase in E_A at low Fe^{2+} concentration could also be due to the fact that for a given Fe^{2+} ion an interaction with a neighbored Fe^{2+} ion which may lower the activation energy becomes impossible. An analogous observation of an increase in E_A at room temperature associated with a pronounced drop in the concentration of B-site Fe^{2+} and Fe^{3+} ions had been made on sintered samples as well as single crystals of the Fe-Mg-Cr, Fe-Mn, Fe-Ti and Fe-Mn-Cu spinel systems [VERWEY, HAAYMAN, and ROMEIJN 1947, FUNATOGAWA, MIYATA and USAMI 1959, LOTGERING 1964, BANERJEE and O'REILLY 1966, SIMSA and ANDREJEV 1969]. In a certain range of compositions in these spinel series the conduction can also be assumed to be primarily determined

by the Fe^{2+} and Fe^{3+} ion population on B-sites. For this range the activation energies E_A at room temperature in all systems are <0.15 eV. In a critical range the Fe^{2+} or Fe^{3+} ion concentration on B-sites becomes vanishingly small and the E_A values increase appreciably.

For an analysis of E_A in terms of a detailed conduction model it is important that a plot of E_A vs. composition refers to the same physical state of the compositions, for instance to a ferrimagnetic or paramagnetic state. Therefore eventually the picture presented in Fig. 2 which relates partly to ferrimagnetic samples ($x = 0.6, 0.9, 1.0$) must be altered slightly provided E_A changes at the respective Curie points. However, the increase in E_A is real as the compositions $x = 1.3, 1.4, 1.5$ are non ferrimagnetic at room temperature. It might be that in the various spinel series mentioned above the differences in E_A below and above the Curie points are at least to a certain degree responsible for the changes observed in E_A with composition.

The fact that there is a correlation between the quantity of E_A and the Fe^{2+} ion concentration on B-sites of the lattice in the $Fe_{3-x}Cr_xO_4$ series seems to rule out the possibility that the experimental data for E_A are dominated by grain boundary effects etc., whereas for ϱ_0 increased values must be assumed as compared to single crystals. Preliminary measurements of the dielectric constant ε for $x = 1.4$ and 1.5 at 50 cps and room temperature show that $\varepsilon = 100-200$, thus it deviates from the value of $\varepsilon = 10-20$ which is considered to be normal for single crystals of this type of oxides [Koops 1951, Möltgen 1952, Krötzsch 1964, Dullenkopf and Wijn 1968]. This result indicates some contribution of grain boundaries and barrier layers in the sintered Fe-Cr spinels to the d. c. resistivity as they are the origin for the high dielectric constant.

Acknowledgement

References

Banerjee, S. K., and W. O'Reilly: Coercivity of Fe^{2+} in octahedral sites of Fe-Ti spinels. IEEE Trans. Magnetics Mag-2, 463—467, 1966

Belov, K. P., A. A. Popova, and E. V. Talalaeva: Electrical and magneto-resistance properties of single crystals of manganese ferrite. Soviet Physics—Crystallography 3, 738—743, 1968

Dullenkopf, P., und H. P. Wijn: Kornleitfähigkeitsuntersuchungen an polykristallinen Bariumferriten. Z. angew. Phys. 26, 22—29, 1969

FRANCOMBE, M. H.: Lattice changes in spinel-type iron chromites. J. Phys. Chem. Solids 3, 37—43, 1957

FUNATOGAWA, Z., N. MIYATA, and S. USAMI: Electric resistance and cation distribution of Fe-Mn ferrite system. J. Phys. Soc. Japan 14, 854, 1959

GOODENOUGH, J. B.: Jahn-Teller distortions induced by tetrahedral-site Fe^{2+} ions. J. Phys. Chem. Solids 25, 151—160, 1964

KATSURA, T., and A. MUAN: Experimental study of equilibria in the system FeO—Fe_2O_3—Cr_2O_3 at 1300^0C. Trans. AIME 230, 77—84, 1964

KOMAR, A. P., and V. V. KLIUSHIN: The dependence of the electrical resistivity of ferrites on temperature. Izv. Akad. Nauk USSR Ser. Fiz. 18, 400—402, 1954

KOOPS, C. G.: On the dispersion of resistivity and dielectric constant of some semiconductors at audiofrequencies. Phys. Rev. 83, 121—124, 1951

KRÖTZSCH, M.: Über die Niederfrequenzdispersion der Dielektrizitätskonstanten und der elektrischen Leitfähigkeit polykristalliner Ferrite. Phys. stat. sol. 6, 479—490, 1964

LOTGERING, F. K.: Semiconduction and cation valencies in manganese ferrites. J. Phys. Chem. Solids 25, 95—103, 1964

MÖLTGEN, G.: Dielektrische Untersuchungen an Ferriten. Z. angew. Phys. 4, 216—224, 1953

REZLESCU, N.: Sur le comportement de la résistivité des ferrites de type spinelle dans le domaine du point de CURIE. C. R. Acad. Sc. Paris 268, 136—139, 1969

ROSENBERG, M., P. NICOLAU, and I. BUNGET: On the anomaly of the electrical resistivity in manganese ferrite single crystals near the Curie point. Phys. stat. sol. 4, K125—K128, 1964

SEYBOLT, A. U.: Observations on the Fe-Cr-O system. J. Electrochem. Soc. 107, 147—156, 1960

SIMSA, Z., and N. ANDREJEV: The electrical properties of manganese-copper ferrite. Czech. J. Phys. B 19, 1389—1399, 1969

VERWEY, E. J. W., and J. H. DE BOER: Cation arrangement in a few oxides with crystal structures of the spinel type. Rec. Trav. Chim. Pays-Bas 55, 531—540, 1936

VERWEY, E. J., P. W. HAAYMAN, and F. C. ROMEIJN: Physical properties and cation arrangement of oxides with spinel structures. II. Electronic conductivity. J. Chem. Phys. 15, 181—187, 1947

Rotational Hysteresis Measurements on Oxidized Synthetic and Natural Titanomagnetites

A. J. MANSON, Newcastle[1])

Summary: Rotational hysteresis characteristics were used to study the oxidation of both synthetic and natural titanomagnetites. The hysteresis loss W_R is sensitive to small anisotropy changes in the minerals and can be used as a non-destructive method of determining the oxidation state of titanomagnetites. Results on the low-temperature (200^0C) oxidation of wet-ground synthetic titanomagnetites to cation-deficient spinel show a linear relationship between W_R and the Fe^{2+} ion content. The oxidation of unground synthetics is compared to that of natural basalts when heated at 400^0C in air. The W_R curves of both show a similar type of behaviour, initially decreasing like those of the wet-ground samples, however the activation energy of this initial oxidation was found to be 0.46 ± 0.05 eV per molecule which suggests that titanium migration is occuring. Subsequent heating caused a dramatic increase in anisotropy which is interpreted as the exsolution of lath-like regions of iron-rich spinel and ilmenite.

Zusammenfassung: Die Oxydation von synthetischen und natürlichen Titanomagnetiten wurde mit der Methode der Rotations-Hysterese untersucht. Der Hystereseverlust W_R reagiert empfindlich auf kleine Änderungen der Anisotropie in den Mineralien und kann als zerstörungsfreie Methode zur Bestimmung des Oxydationsgrades von Titanomagnetiten verwendet werden. Die Messungen an in Wasser gemahlenen synthetischen Titanomagnetiten, die bei 200^0C einer Tieftemperatur-Oxydation ausgesetzt worden waren, zeigen einen linearen Zusammenhang zwischen W_R und dem Gehalt an Fe^{2+} Ionen. Die Oxydation von unvermahlenen synthetischen Titanomagnetiten ist vergleichbar mit der von Titanomagnetiten natürlicher Basalte, die in Luft bis 400^0C erhitzt worden waren. Die W_R-Kurven zeigen in diesem Fall einen ähnlichen Verlauf. Sie nehmen zu Beginn ähnlich wie bei den in Wasser gemahlenen Proben ab, jedoch ist die Aktivierungsenergie der anfänglichen Oxydation $0,46 \pm 0,05$ eV je Molekül, was auf eine Wanderung von Titan-Ionen hindeutet. Eine weitere Erwärmung erzeugt einen raschen Anstieg der Anisotropie, die mit der Bildung von Entmischungslamellen von Ilmenit in einer Fe-reichen Spinellphase interpretiert wird.

1. Rotational Hysteresis

The technique of rotational hysteresis measurement has been applied as a non-destructive method of determining the magnetic mineral content of basalts by DAY, O'REILLY and BANERJEE [1970], and to the study of red sandstones by BROOKS and O'REILLY [1970]. Once a set of characteristic W_R curves for magnetic minerals has

---

[1]) A. J. MANSON, School of Physics, University of Newcastle upon Tyne, England.

been compiled it is possible to identify these minerals in natural samples, however it is necessary to compliment these measurements with CURIE temperature determinations.

Rotational hysteresis W_R is defined as the irreversible work done, per unit volume per cycle, against the forces of anisotropy, when a magnetic field is rotated slowly through 360^0 around a sample of magnetic material which is held stationary, and is

$$W_R = - \int_0^{2\pi} L \, d\Phi$$

where L is the torque acting on the sample and Φ is the angle between the magnetization vector and a reference easy axis. When L is constant with azimuthal angle the loss is $2\pi L$.

There are two main sources of anisotropy in titanomagnetites (a) the magnetocrystalline anisotropy of the material itself and (b) the shape anisotropy of the grains. Stress anisotropy is also very important but is proved not to be a contributory factor in the experiments carried out here.

The magnetocrystalline anisotropy energy is defined for a cubic system, such as the titanomagnetites, as

$$E = K_1 \, (\alpha_1^2 \alpha_2^2 + \alpha_2^2 \alpha_3^2 + \alpha_3^2 \alpha_1^2) + K_2 \, (\alpha_1^2 \alpha_2^2 \alpha_3^2)$$

where α_1, α_2, α_3 are the direction cosines and K_1 and K_2 are anisotropy constants.

The general expression for the energy of shape anisotropy of an idealized ellipsoidal grain is

$$E_\Phi = \frac{1}{2} v (N_A \cos^2 \Phi - N_B \sin^2 \Phi) M_S^2$$

where Φ is the angle between the magnetization vector and the easy axis, M_S is the saturation magnetization, N_A and N_B are the demagnetizing factors along the major and minor axes and v is the volume of the grain.

The simplest model which explains the variation of rotational hysteresis W_R with applied field H is one based on the theory of STONER and WOHLFARTH [1948] for the reversal of magnetization in idealized single-domain particles, where only processes of coherent rotation occur. The theory as developed by JACOBS and LUBORSKY [1957] considers single-domain grains in the form of prolate ellipsoids of such an eccentricity that every grain has a uniaxial anisotropy due to the dominance of shape anisotropy, with an easy axis E_A as shown in Fig. 1 (a).

Fig. 1: Theoretical model of rotational hysteresis for a single-domain grain showing the behaviour of the magnetization vector m as the applied field H rotates through 360^0 around the grain in the plane of the diagram, for a) low fields $H \ll H_A$, b) high fields $H \gg H_A$; H and m are shown in several positions, c), d) intermediate fields $\frac{1}{2} H_A \leq H \leq H_A \cdot E_A$ is the easy axis.

ROTATIONAL HYSTERESIS

[a] LOW FIELDS

REVERSIBLE EXCURSIONS OF m ABOUT THE EASY AXIS

[b] HIGH FIELDS

REVERSIBLE EXCURSIONS OF m ABOUT THE APPLIED FIELD

[c] INTERMEDIATE FIELDS

m IN UNSTABLE POSITION

[d]

IRREVERSIBLE FLIP TO A STABLE POSITION
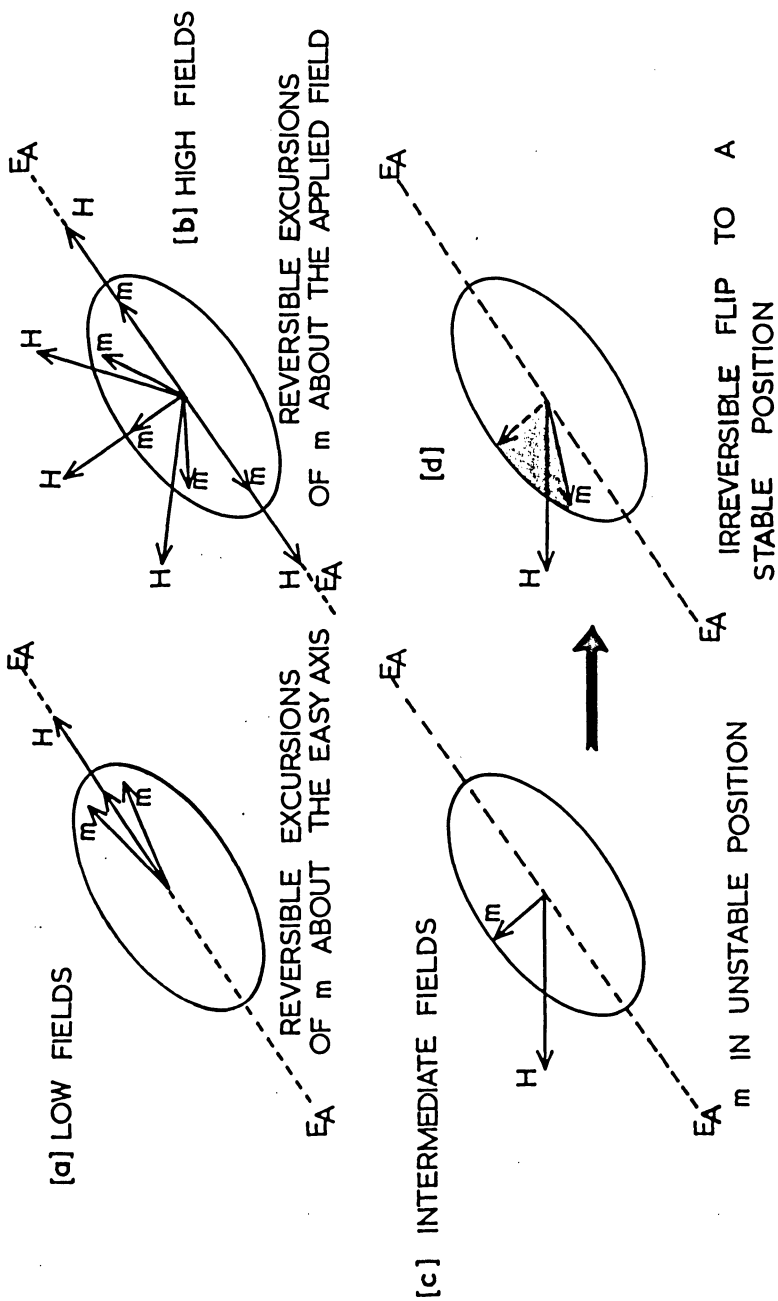
The anisotropy field of a crystal $H_A = 2K/M_S$, is defined as equivalent to the forces of anisotropy holding the magnetization vector m to the easy axis. Now consider the rotation of the applied field H around the stationary particle (Fig. 1(a)) in the plane of the diagram through 360^0 with H initially directed along an easy direction. In case 1(a) where $H \ll H_A$ the magnetization vector will only be pulled away from E_A by small amounts as H rotates and when H is removed at any stage m returns to the easay axis. Thus m performs small reversible excursions about the easy axis and there is no rotational hysteresis loss. At the other extreme 1(b), where $H \gg H_A$, m follows H as it rotates but always lies on the side of H nearest the easy axis. Thus m performs small reversible excursions about H as it rotates and again there is no rotational hysteresis loss. When H is comparable in magnitude to H_A (Fig. 1(c)) a different situation occurs. In the rotation m lags considerably behind H and when m reaches an unstable position, as is shown in Fig. 1(d) it rotates irreversibly or 'flips' from the unstable to the stable position. This is the situation where rotational hysteresis arises and it can be proved that losses only occur between the limits $\frac{1}{2} H_A \leqq$
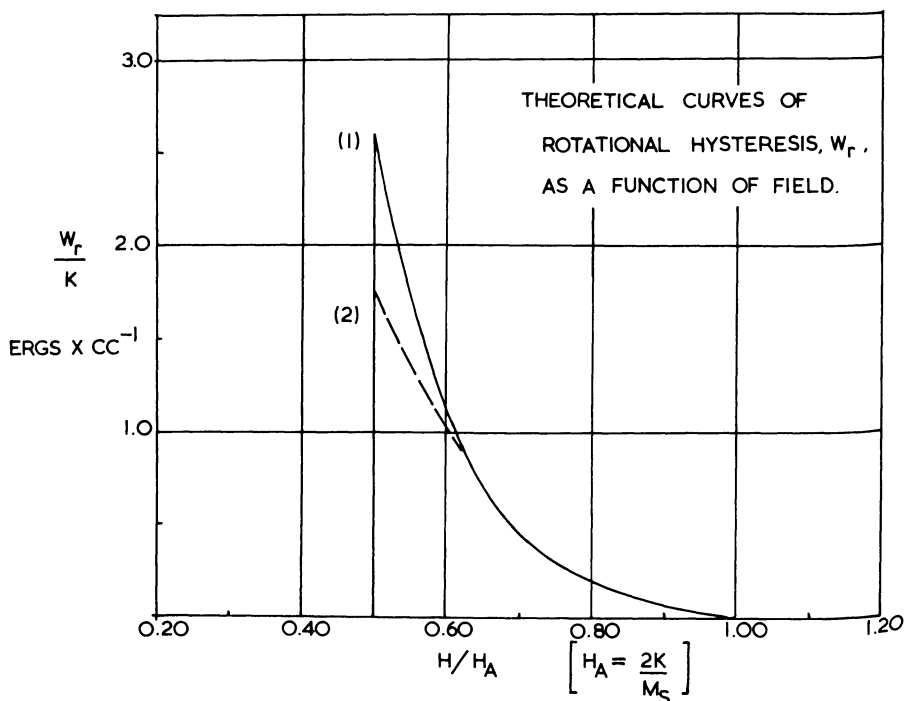
Fig. 2: Theoretical curves of rotational hysteresis plotted as W_R/K, shown as a function of the applied field normalized to H/H_A for an assemblage of single-domain grains of uniaxial anisotropy with (1) the easy axes aligned and (2) the easy axes randomly distributed in space.

$H \leqq H_A$ for a single-domain particle with a uniaxial anisotropy. Theoretical curves are shown in Fig. 2 for the variation of rotational hysteresis (plotted W_R/K) with the normalized applied field for an aggregate of single-domain grains with (1) the easy axes aligned, and (2) the easy axes spherically randomised. It can be shown that the height of the peak is a direct measure of the anisotropy (K) present and that the position of the peak on the field axis is a measure of the anisotropy field ($2K/M_S$). In case (1) $(W_R)_{peak} = 2,6\ K$; in case (2) $(W_R)_{peak} = 1,7\ K$.

All the natural and synthetic titanomagnetite samples measured had random orientations of grain axes, however the above theory is further complicated by the fact that the dominant anisotropy is not uniaxial but has a cubic symmetry (magneto-crystalline). In all samples there was a distribution of size and shape of the grains and some samples consisted mainly of multi-domain particles. These factors tend to give rise to a spread of anisotropy and a less sharp hysteresis peak than the theoretical model. Thus the major obstacle in the attempt to compare the anisotropy of the samples with the simple STONER-WOHLFARTH models is the range of anisotropies impressed on the aggregates by the nature of their size and shape distributions.

The rotational hysteresis is measured on an automatic torque magnetometer. The sample is suspended in a magnetic field from a modified ballistic galvanometer head and the torque experienced by the sample, which is held stationary by automatic compensation, is recorded as the magnetic field is rotated from 0^0 to 360^0 and then back from 360^0 to 0^0. The area of the torque loop thus formed is equal to $2\ W_R$ since two cycles have been completed. All measurements were carried out on the instrument at room temperature.

Titanomagnetites display a range of values of peak position on the field axis from 1 KOe for magnetite to 3 KOe for $x = 0,60$. Maghemite has a peak field of 1 KOe and is difficult to distinguish from magnetite. Hematite is characterized by high-field losses which peak between 10 KOe and 30 KOe depending on the state and purity of the sample.

2. Oxidation of Synthetic Titanomagnetites

Experiments were carried out on wet-ground synthetic titanomagnetites ($< 1\ \mu$ grain diameter) heated in air at 200^0—250^0C to study the behaviour of W_R as oxidation to cation-deficient spinel proceeds; and on unground titanomagnetites ($\approx 10\ \mu$ grain diameter) heated in air at 400^0C to study the behaviour of W_R as the titanomagnetite oxidizes and exsolves to spinel-corundum phases. All of the titanomagnetite samples were dispersed in a matrix of calcium sulphate to avoid effects arising from grain interaction which would occur in the close-packing of grains.

Wet-ground titanomagnetites: A number of wet-ground titanomagnetites with a range of x values from 0,40 to 0,85 were heated at 200^0—250^0C in air for different lengths of time and W_R measured at each stage of heating. A typical example of the type of behaviour of this material is shown in Fig. 3 where W_R is plotted against H for a

Fig. 3: Rotational hysteresis W_R-H characteristics are shown as a function of oxidation at 200°C in air for a wet-ground synthetic titanomagnetite with $x = 0,50$.

titanomagnetite of composition $x = 0,5$. The curves show a systematic decrease of peak height with time of heating and a similar shift of peak position to a lower field value. The percentage of Fe^{2+} ion in each sample was determined by potentiometric chemical analysis, and when the results were plotted against the peak height of the corresponding W_R curves they showed a linear decrease of peak height with decreasing Fe^{2+} ion content (Fig. 4). The magnetocrystalline anisotropy is attributed mainly to Fe^{2+} ions on octahedral sites, which constitutes eighty percent of the total Fe^{2+} content in the sample ($x = 0,50$) the other twenty percent resides on tetrahedral sites. Thus the major reduction in anisotropy is due to the oxidation of Fe^{2+} ions to Fe^{3+} ions on the octahedral and then on the tetrahedral sites in the formation of a cation-deficient spinel. The peak shift on the field axis to the left confirms the reduction in the anisotropy field ($H_A = 2 K/M_S$) however this is slightly complicated by the behaviour of M_S. X-ray analysis of all the samples confirmed the production of only a single phase. Unground titanomagnetites: The second group of experiments involved the heating of unground titanomagnetites at 400°C in air to form an inter-
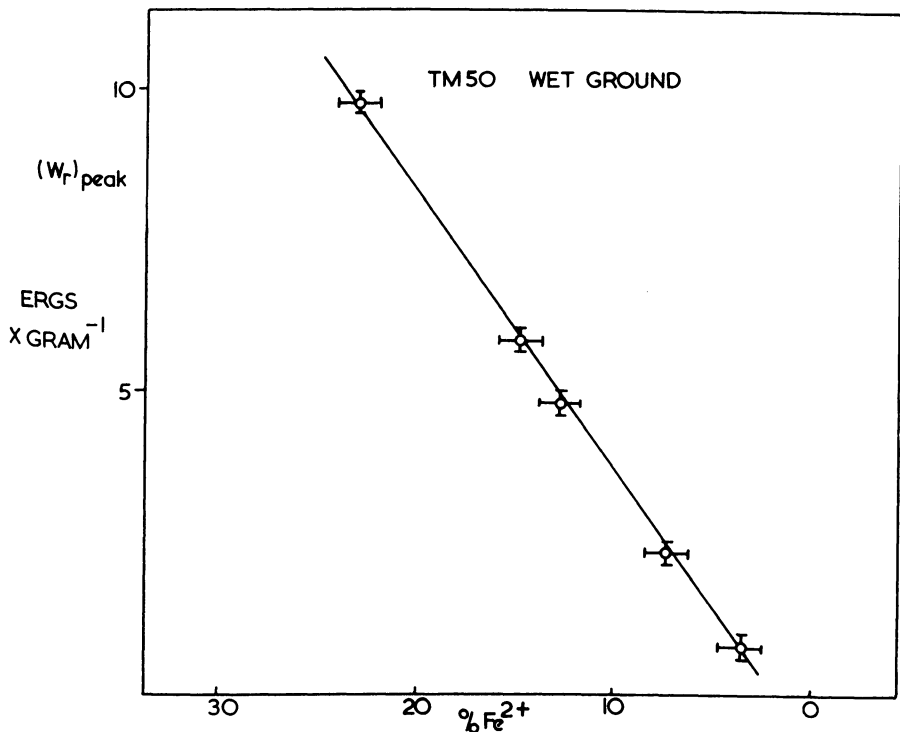
Fig. 4: Rotational hysteresis peak height (W_R) peak is plotted as a function of Fe^{2+} content for the sample shown in Fig. 3.

growth of a rhombohedral phase (ilmenite) and an iron-rich spinel phase as oxidation products. Fig. 5 shows the typical behaviour of titanomagnetite ($x = 0,50$). There is a rapid decrease of anisotropy after only one hour at $400^\circ C$ and an accompanying shift of the peak to the left. This can be interpreted as either the production of cation-deficient spinel or the nucleation of a softer magnetic material such as an iron-rich spinel replacing the original material. Further heating up to twenty hours at $400^\circ C$ produces a dramatic increase in anisotropy which is not observed in the wet-ground materials. The appearance of this very high anisotropy is interpreted as the growth of an iron-rich spinel and its confinement by ilmenite lamellae to elongated grains causing a high shape anisotropy in the iron-rich spinel (magnetite). The reduction in anisotropy, which occurs on further heating up to fifty hours, is thought to be due to either the growth of the iron-rich spinel to more equidimensional regions or the oxidation of the sample to hematite at the grain surfaces; however the latter is less likely to cause such a large reduction in anisotropy as is displayed in the sample, and if there was such a quantity of hematite it would show up in the high field losses.
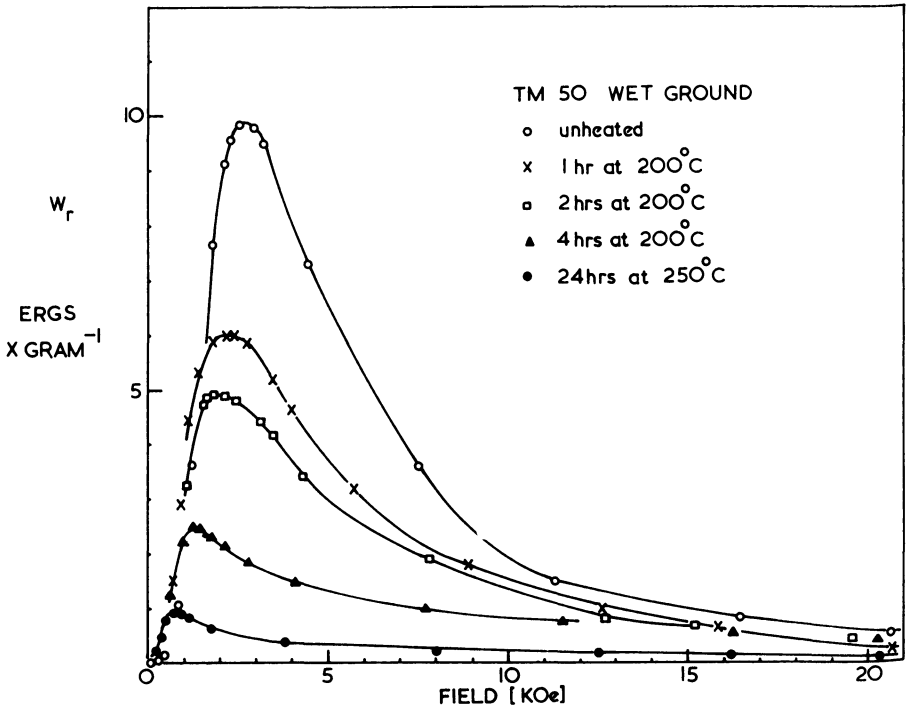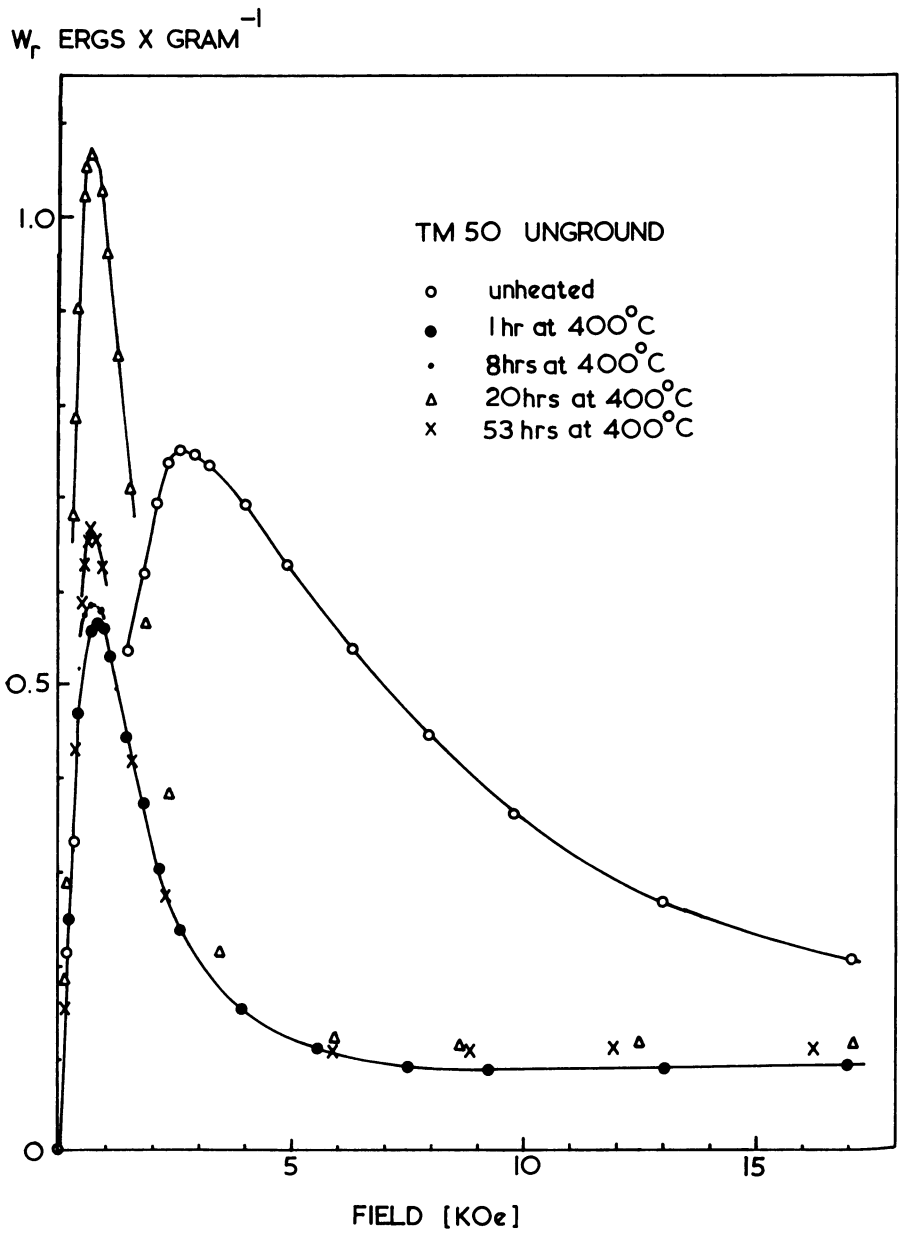
Fig. 5: Rotational hysteresis characteristics W_R-H are shown as a function of oxidation at 400°C in air for a sample of unground synthetic titanomagnetite $x = 0,50$.

3. The Oxidation of Natural Titanomagnetites

A number of basalts containing homogeneous unoxidized titanomagnetite grains were selected, and one in particular from the RAUHER-KULM (RK) was given extensive heat treatments at 400⁰C in air. This sample had titanomagnetite grains with an average diameter of 20 μ of composition $x = 0,50$. The oxidation rate was expected to be much lower in basalts compared to that in synthetics and the time scale of heating at 400⁰C was thus extended to allow for this. The basalt samples were ground to about 50 μ and compressed into cylindrical pellets for measurement. Fig. 6 shows the effect of heating on sample RK up to twenty hours at 400⁰C in air. The anisotropy decreases in RK with heating at it did in the unground synthetic, and this can be interpreted again as either the production of cation-deficient spinel or as the formation of an iron-rich spinel. Fig. 7 shows the effect of heating up to 200 hours at 400⁰C in air together with the twenty hour curve and the original curve for reference. The anisotropy increases markedly after twenty hours of heating, which is what we observed in the synthetic samples, and bears the same interpretation as before. The initial peak shift in RK was measured at three different temperatures (380⁰C, 400⁰C and 420⁰C) and the activation energy of the process or processes causing the shift was found to be $0,46 \pm 0,05$ eV per molecule, which is very close to the value of 0,50 eV obtained by PETERSEN [1969] for the activation energy of titanium diffusion in titanomagnetites. The CURIE temperatures of the oxidation products formed at 400⁰C in both the synthetic and natural titanomagnetites are in the region of 550⁰C which suggests that an iron-rich spinel is formed.

Samples of both natural and synthetic titanomagnetites were sealed in evacuated capsules at a pressure of 10^{-4} torr and heated for two hours in a furnace at 400⁰C and the W_R curves measured before and after. No change in the W_R characteristics were observed, within the experimental error, showing that the samples were completely strain-free, and that the initial reduction in anisotropy was not due to the annealing of strains.

4. Conclusions

Rotational hysteresis measurements in addition to being used as an indicator for the oxidation state can also give us some insight into the processes of oxidation in titanomagnetites. The peak position on the field axis and the peak height are used for both the above investigations. The general shape of the curve and the distribution of losses over the field spectrum can also be used as indicators when compared with standard curves. It is however necessary to compliment the hysteresis measurements with other measurements such as CURIE temperature determinations to give a fuller picture of the samples and their behaviour.
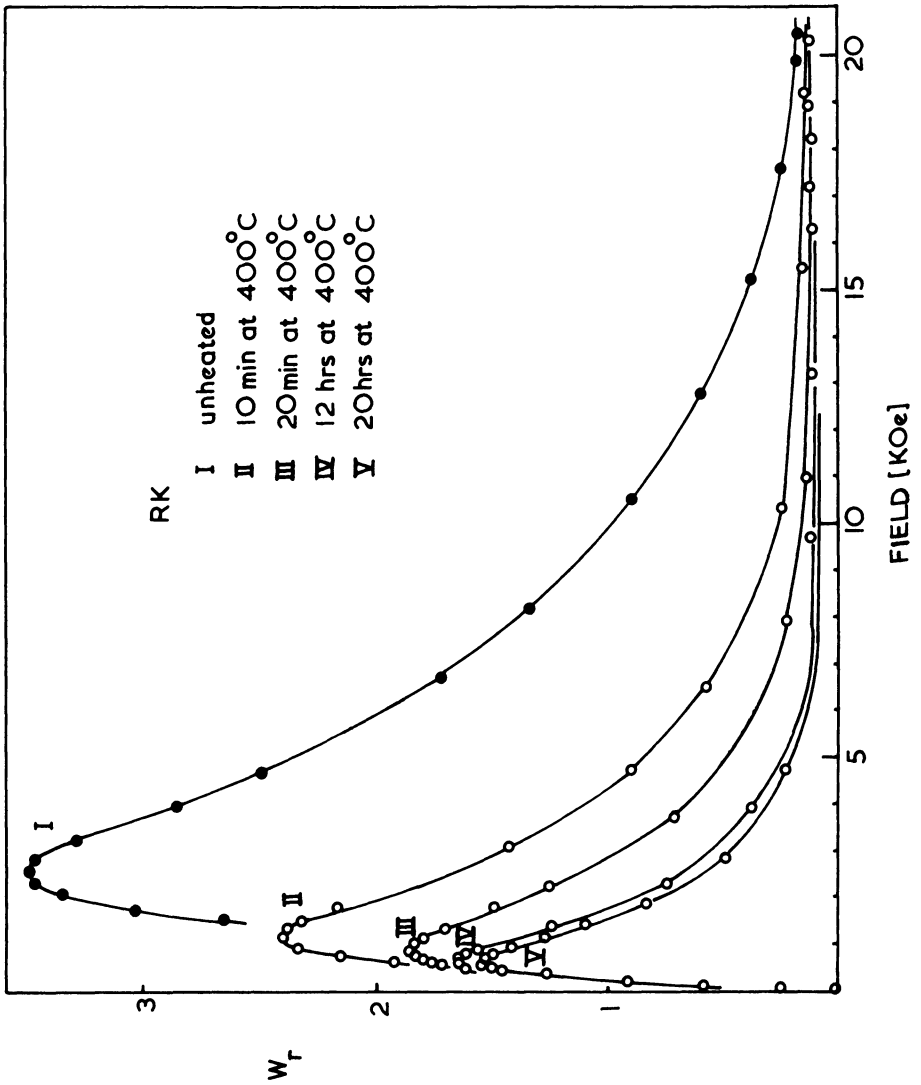
Fig. 6: Rotational hysteresis characteristics W_R-H plotted as a function of oxidation up to 20 hours heating at 400°C in air for a natural basalt from the RAUHER KULM (RK) with titanomagnetite grains of $x = 0,50$. W_R measured in arbitrary units.
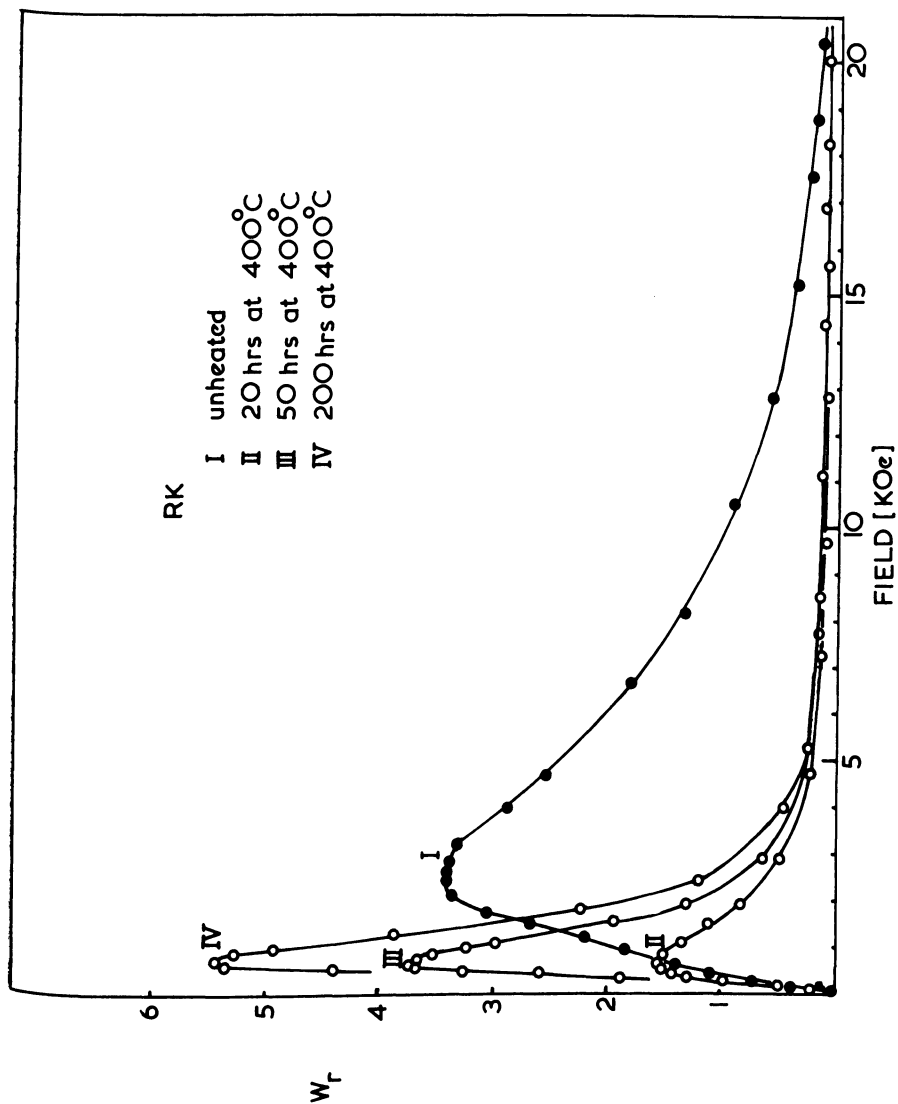
Fig. 7: W_R-H characteristics of natural basalt RK heated up to 200 hours at 400°C in air. W_R measured in arbitrary units.

Acknowledgements

References

BROOKS, P. J., and W. O'REILLY: Magnetic Rotational Hysteresis Characteristics of Red Sandstones, Earth and Planet. Sci. Lett. 9, 71—76, 1970

DAY, R., W. O'REILLY and S. K. BANERJEE: Rotational Hysteresis Study of Oxidized Basalts, J. Geophys. Res., 75, 375—386, 1970

JACOBS, I. S., and F. E. LUBORSKY: Magnetic Anisotropy and Rotational Hysteresis in Elongated Fine-Particle Magnets, J. App. Phys. 28, No. 4, 467—473, 1957

PETERSEN, N.: Calculation of Diffusion Coefficient and Activation Energy of Titanium in Titanomagnetite, Phys. Earth Planet. Interiors 2, 175—178, 1969

STONER, E. C., and E. P. WOHLFARTH: Trans. Roy. Soc. London, A240, 559, 1948

Untersuchung von Gesteinen mit ferrimagnetischen Mineralen mittels der Resonanz der Spin-Präzession der die Erscheinung des Ferromagnetismus bewirkenden Elektronen

Investigation of Rocks Containing Ferrimagnetic Minerals by Means of the Resonance of the Spin-Precession of the Electrons Causing the Phenomenon of Ferromagnetism

W. Anders, München[1])

Zusammenfassung: Befinden sich Elektronen in einem Magnetfeld $\vec{H}$, so präzedieren deren Spins und die mit ihnen gekoppelten magnetischen Momente um die Richtung des Feldes $\vec{H}$. Diese Präzession kann durch ein hochfrequentes Magnetfeld kleiner Amplitude erzwungen werden; dabei wird Energie absorbiert. Die Absorption ist maximal, wenn die Resonanz-Bedingung $\omega = \gamma H$ erfüllt ist ($\omega = 2\pi f$, f = Präzessions-Frequenz, γ = gyromagnetisches Verhältnis). H setzt sich aus verschiedenen Feldern zusammen. Durch Messung von ω und äußerem Magnetfeld können folgende Größen bestimmt werden: γ, Magnetisierung und Form der Probe, mechanische Spannungen, Kristall-Anisotropie-, Magnetostriktions- und Austausch-Konstante. Es wird über erste Messungen an Erzen und Gesteinen mit ferri-magnetischen Mineralen berichtet. Die Proben sind Bruchstücke mit Volumina bis zu einigen Kubik-Millimetern. Die Absorption bei 9,2 GHz wird als Funktion des äußeren Magnetfeldes registriert. Die Auswertung der Kurven ermöglicht eine rasche Abschätzung des relativen Gehaltes an ferrimagnetischen Mineralen. Die Halbwerts-Breite der Absorptions-Kurven nimmt zu in der Reihenfolge Magnetit-Einkristall, Magnetit-Erz, Magnetit-führendes Gestein. Hieraus können Rückschlüsse auf die Struktur der Proben gezogen werden. Die Messungen lassen die Nützlichkeit der Methode zur Untersuchung von Fragen des Gesteins-Magnetismus erkennen.

Summary: When electrons are situated in a magnetic field $\vec{H}$, their spins and the magnetic moments coupled to them precede around the direction of the field $\vec{H}$. This precession can be induced by a high frequency magnetic field of small amplitude; thereby energy is absorbed. The absorption is maximum, when the resonance condition $\omega = \gamma H$ is fulfilled ($\omega = 2\pi f$, f = precession frequency, γ = gyromagnetic ratio). H is composed of different fields. By measuring ω and the external magnetic field the following quantities can be determined: γ, magnetization and shape of the sample, mechanical stress, crystalline anisotropy-, magnetostriction-, and exchange constant.

[1]) Dr. Wilfried Anders, Sektion Physik der Universität München, Lehrstuhl Prof. Rollwagen, 8 München 13, Schellingstraße 2—8.

Preliminary measurements of ores and rocks containing ferrimagnetic minerals are repor-
ted. The samples are pieces of volumes up to a few cubic millimeters. The absorption at
9.2 GHz is recorded as a function of the external magnetic field. The evaluation of the curves
enables a quick estimation of the relative contents of ferrimagnetic minerals. The half-width
of the absorption curves increases in the sequence magnetite monocrystal, magnetite ore,
magnetite containing rock. From this, conclusions on the structure of the samples can be
drawn.
The measurements show the usefulness of this method for the investigation of problems
involved with rock magnetism.

1. Die Resonanz der Spin-Präzession der Elektronen, die die Erscheinung des Ferromagnetismus bewirken („ferromagnetische Resonanz")

Befindet sich ein Teilchen mit dem magnetischen Moment $\vec{\mu}$ in einem Magnetfeld
$\vec{H}$, so erfährt es ein Drehmoment $\vec{\mu} \times \vec{H}$. Besitzt das Teilchen außerdem einen Dreh-
impuls (Spin) $\vec{I}$, so bewirkt das Drehmoment eine zeitliche Änderung dieses Impulses
gemäß $\partial \vec{I}/\partial t = \vec{\mu} \times \vec{H}$. Bei Elementarteilchen sind magnetisches Moment und mecha-
nischer Drehimpuls fest miteinander gekoppelt und parallel oder anti-parallel ge-
richtet. Es gilt daher $\mu = \gamma I$; γ ist das gyromagnetische Verhältnis. Daraus folgt die
Bewegungsgleichung

$$\partial \vec{\mu}/\partial t = \gamma\, \vec{\mu} \times \vec{H} \tag{1},$$

die eine Präzession des magnetischen Momentes um die Richtung des Magnetfeldes $\vec{H}$
mit der Kreisfrequenz

$$\omega = \gamma H \tag{2}$$

beschreibt. Die eben abgeleitete Kreisel-Präzession eines Elementarteilchens, er-
zwungen durch ein Magnetfeld, ist allen Teilchen mit magnetischem Moment und
Spin gemeinsam, also auch den Elektronen. Bei dem hier diskutierten Phänomen
handelt es sich um die Präzession derjenigen Elektronen, die die Erscheinung des
Ferromagnetismus hervorrufen, also beispielsweise der 3-d-Elektronen mit nicht
kompensiertem Spin und damit nicht kompensiertem magnetischem Moment bei
Eisen, Nickel und Kobalt.

An ferro- und ferrimagnetischen Stoffen ist die Beobachtung der freien Präzession
nur selten möglich, da diese meist stark gedämpft ist. Die Relaxationszeiten sind etwa
gleich 10^{-10} sec. Man untersucht daher die erzwungene Bewegung durch Anlegen eines
magnetischen Hochfrequenz-Feldes geringer Stärke senkrecht zum statischen Magnet-
feld. Ist die Frequenz des Wechselfeldes gleich oder etwa gleich der Eigenfrequenz
(2) der Präzession, so wird dem Hochfrequenz-Sender Energie entzogen. Die Ab-
sorption durch die magnetische Probe wird maximal, wenn die Resonanz-Bedingung
(2) erfüllt ist. In der Literatur wird für diese Erscheinung die Bezeichnung „ferro-
magnetische Resonanz" verwendet (bei ferrimagnetischen Stoffen spricht man zu-
weilen auch von „ferrimagnetischer Resonanz").

Eine Besonderheit der ferromagnetischen Resonanz wird durch die Wechselwirkung der Elektronen erzeugt: die einzelnen magnetischen Momente präzedieren nicht unabhängig voneinander, sondern sind durch Austausch-Wechselwirkung stark gekoppelt. Es ist daher üblich, die Bewegungs-Gleichung (1) der magnetischen Momente durch eine Gleichung für die Magnetisierung $\vec{M}$, eine Kontinuums-Größe, in der Form

$$\partial\vec{M}/\partial t = \gamma\,\vec{M} \times \vec{H} \tag{3}$$

zu ersetzen. Gleichung (3) erhält man formal aus Gleichung (1) nach Division durch das zum magnetischen Moment $\vec{\mu}$ gehörige Volumen. In dieser Form — zuzüglich eines Dämpfungs-Gliedes — wurde die Bewegungs-Gleichung von LANDAU und LIFSHITZ im Jahre 1935 abgeleitet. Der experimentelle Nachweis der ferromagnetischen Resonanz gelang allerdings erst 1946 durch GRIFFITHS. Die Erscheinung der ferromagnetischen Resonanz ist zwar immer noch Gegenstand der Grundlagen-Forschung, hat aber schon große Bedeutung vor allem zur Untersuchung der in der Technik genützten Ferrite gewonnen. Eine ausführliche Darstellung hierüber findet man z. B. in dem Buch von LAX und BUTTON [1962]. Über Untersuchungen von Gesteins-Proben mit ferrimagnetischen Mineralen mit dieser Methode ist bisher nichts bekannt geworden.

2. Die physikalische Bedeutung der ferromagnetischen Resonanz

$\vec{H}$ ist das effektive Gleich-Feld am Ort der magnetischen Momente. Es setzt sich im allgemeinen aus mehreren Anteilen zusammen, z. B. äußeres Feld H_0, Entmagnetisierungs-Feld, Kristall-Anisotropie-Feld, magneto-elastisches Feld, Austausch-Feld. Bei geschickter Versuchs-Führung können also durch das Gleich-Feld H_0, bei dem bei fester Frequenz ω maximale Absorption eintritt, die entsprechenden Parameter gemessen werden, nämlich gyromagnetisches Verhältnis, Magnetisierung und Proben-Form, Kristall-Anisotropie-Konstanten, Magnetostriktions-Konstanten und mechanische Spannungen, Austausch-Konstante.

3. Meßprinzip

Um reproduzierbare Verhältnisse zu haben, muß das Gleich-Feld H_0 bei ferromagnetischen Proben gleich einigen kOe sein, damit Bereichs-Strukturen vermieden werden. Nach Gleichung (2) sind daher Frequenzen von einigen GHz notwendig, das heißt, man muß zur experimentellen Untersuchung der ferromagnetischen Resonanz die sogenannte Hohlleiter-Technik anwenden. Der prinzipielle Aufbau der Versuchs-Anordnung ist in Abb. 1a skizziert. Von einem Generator G (z. B. einem Reflex-Klystron) werden elektromagnetische Wellen erzeugt, die sich in einem Hohl-Rohr ausbreiten. In dem Hohlraum-Resonator R werden stehende elektromagnetische Wellen angeregt, die mit einer Halbleiter-Diode D nachgewiesen werden. Bei den in der vorliegenden Arbeit beschriebenen Untersuchungen war die Meß-Frequenz un-

gefähr 9,2 GHz. Für diesen Frequenz-Bereich werden normierte Rohre rechteckigen Querschnitts von etwa 10 mm × 20 mm Kantenlänge benutzt. Der Resonator war ein zylindrisches Rohr von etwa 20 mm Durchmesser und 100 mm Länge. Das Rohr war innen sorgfältig poliert und vergoldet, um eine hohe Güte des Resonators und damit auch eine hohe Nachweis-Empfindlichkeit zu erreichen. Die Abmessungen und die Ankopplungs-Stellen wurden so gewählt, daß ein für das Experiment geeigneter „Schwingungs-Modus" angeregt wird. Ein Moment-Bild des Verlaufs der magneti-schen Feldlinien ist in Abb. 1a gestrichelt angedeutet. Die Probe P befindet sich inner-
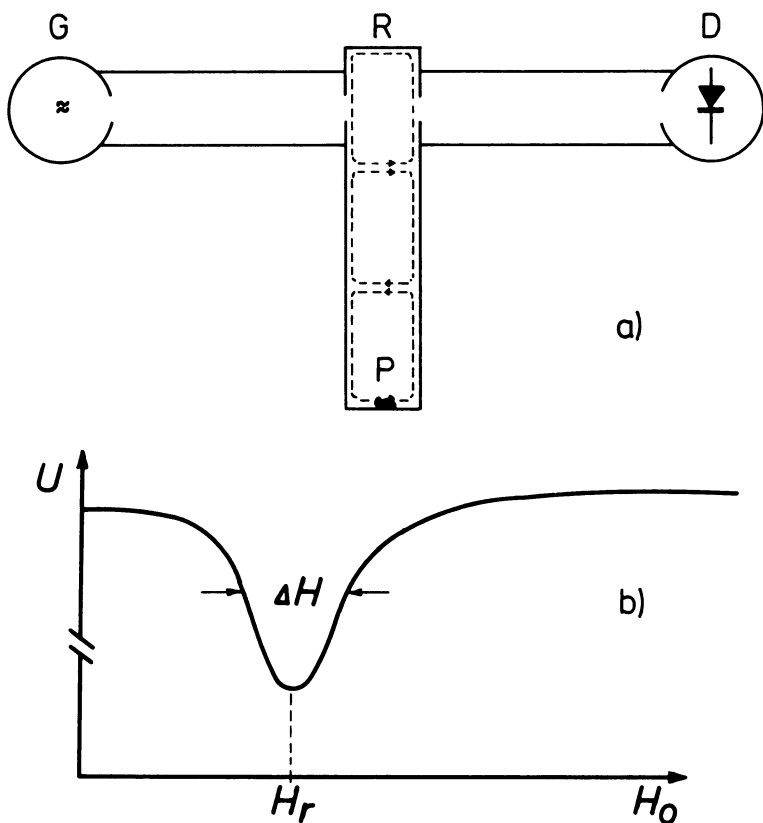
Abb. 1: a) Prinzipieller Meß-Aufbau, G: Mikrowellen-Generator, R: Resonator, D: Halb-leiter-Diode, P: Probe.
b) Gleichspannung an der Diode als Funktion des statischen Magnetfeldes, schema-tisch.

a) Measuring apparatus (schematic view), G: microwave generator, R: resonance cavity, D: crystal rectifier, P: sample.
b) dc-voltage of the rectifier as a function of the steady magnetic field, schematically.
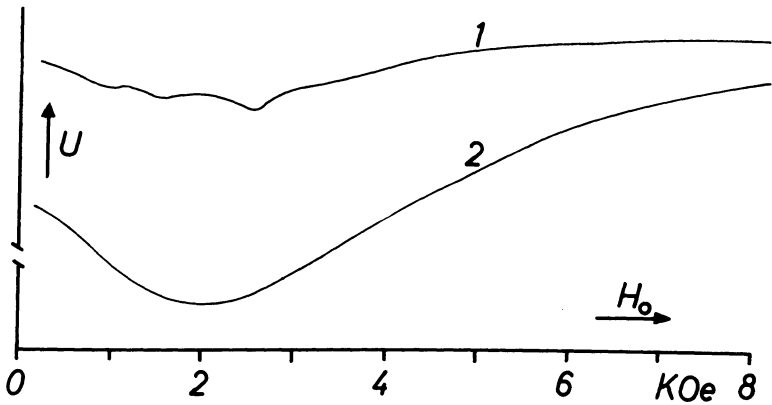
Abb. 2: Beispiele für Meß-Kurven bei 9,2 GHz, aufgezeichnet vom x-y-Schreiber; 1: Magnetit- „Einkristall", 2: Diabas. Spannungs-Empfindlichkeit und Volumen waren bei Probe 2 um den Faktor 4 bzw. 15 größer.

Examples for measuring curves at 9.2 GHz, drawn by the x-y-recorder; 1: Magnetite "single crystal", 2: Diabas. Voltage sensitivity and volume were larger by a factor of 4 and 15, respectively, for sample 2.

halb des Resonators an einer Stelle möglichst homogenen hochfrequenten Magnet-feldes. Das statische Feld H_0 — senkrecht zur Zeichenebene gerichtet — wird von einem Elektromagneten erzeugt, zwischen dessen Polkappen der untere Teil des Mikrowellen-Resonators sich befindet. Die auf die Diode D treffende Leistung hängt von den Verlusten im Resonator R ab, also insbesondere von der Absorption in der Probe P.

Die bei Resonanz-Untersuchungen übliche Änderung der Anregungs-Frequenz ist bei Mikrowellen aus technischen Gründen nicht in ausreichendem Umfang möglich. Statt dessen wird daher das statische Magnetfeld H_0 bei fester Frequenz geändert. Die an der Diode D gemessene Gleichspannung U — ein Maß für die auftreffende Leistung — wird von einem x-y-Schreiber als Funktion von H_0 registriert (vgl. Abb. 1b und 2). Zur Beschreibung der Kurven-Form werden folgende Größen definiert: Resonanz-Feldstärke H_r und Halbwerts-Breite ΔH (vgl. Abb. 1b).

4. Experimentelle Ergebnisse

Es sollte geprüft werden, ob die ferromagnetische Resonanz zur Untersuchung der Eigenschaften magnetischer Gesteine eingesetzt werden kann. Zu diesem Zweck wur-den mehrere Gesteine und Erze untersucht, ohne zunächst auf eine definierte Proben-Form und die spezielle Eignung des Meß-Resonators, der für die Untersuchung von Metallen konstruiert war, zu achten. Als Proben wurden Bruchstücke verwendet — die größten hatten etwa das Volumen eines Erbsen-Korns. Größere Proben konnten

Tabelle 1

Probe	ΔH in kOe	Intensität der Absorption (willkürliche Einheiten)	Bemerkungen
1 Magnetit-Einkristall vom Pfitscher Joch (Österreich)	2,5	500	mehrere Minima
2 Magnesium-Ferrit des Carbonatit vom Kaiserstuhl (Rheingraben)	2,2	250	
3 Magnetit-Erz (Kirunavaara, Schweden)	3,5	200	
4 Titan-Eisen-Erz (Tahawus, New York, USA)	4,5	50	
5 Diabas (Ochsenkopf, Münchberger Gneismasse, Bayern)	5,5	15	
6 Serpentinit (Wurlitz-Woja, Münchberger Gneismasse, Bayern)	6,5	10	starke Absorption bei $H_0 = 0$
7 Diabas (Rock Hill, New Jersey, USA), angereicherte Erzfraktion	4	4	
8 Wie 7, jedoch Erzfraktion mit konz. HCl behandelt	nicht meßbar	1	
9 Basalt (Parkstein bei Weiden, Bayern)	nicht meßbar	1	sehr starke Absorption bei $H_0 = 0$, Kurve stark unsymmetrisch um Minimum
10 Magnet-Kies (Bodenmais, Bayern)	nicht meßbar	1	sehr starke Absorption bei $H_0 = 0$
11 Olivin (Dreiser Weiher, Eifel)			kein Absorptionssignal

nicht untersucht werden, da dielektrische und Wirbelstrom-Verluste die Güte des Resonators so verschlechterten, das die Nachweis-Empfindlichkeit nicht mehr ausreichte. Die Proben wurden auf die Boden-Platte des Resonators geklebt.

In der *Tabelle* sind die untersuchten Gesteine und einige Meßergebnisse zusammengestellt. Zur Charakterisierung der Intensität der Absorption ist der Quotient aus Tiefe des Minimums (bezogen auf das Signal bei sehr hohem Magnetfeld) und Proben-Volumen in willkürlichen Einheiten angegeben. Bei den Proben 8 mit 10 ist eine eindeutige Reihenfolge nicht festzulegen, da die Bestimmung des Volumens nicht genau genug durchgeführt wurde. Abb. 2 zeigt zwei gemessene Kurven. Beim Vergleich ist zu beachten, daß bei Diabas das Volumen und die Schreiber-Empfindlichkeit um den Faktor 15 bzw. 4 größer waren. Für alle Gesteine, insbesondere den Basalt, ist typisch,

daß bereits ohne statisches Magnetfeld eine starke Absorption vorhanden ist. Eine Besonderheit stellt Probe 1 dar. Es existieren mehrere Minima, die darauf hindeuten, daß kein Einkristall vorliegt, sondern möglicherweise drei Kristalle unterschiedlicher kristallographischer Orientierung (Zwillingsbildung). Zur Bestimmung von ΔH wurde die Probe im Feld so gedreht, daß ein Minimum von den anderen deutlich getrennt war.

Auf die Bestimmung der Resonanz-Feldstärken wurde verzichtet, da diese von der Proben-Form abhängen und daher ein Vergleich der verschiedenen Materialien wegen der nicht definierten Formen nicht möglich ist.

Die Halbwerts-Breite ΔH hängt im Idealfall nur von der Dämpfung der Präzession der magnetischen Momente ab. Bei Gesteinen jedoch kommt die Absorptions-Kurve durch Überlagerung der Wirkung vieler Partikel i zustande, deren Resonanz-Feld-stärken H_{ri} unterschiedlich sind (z. B. verschiedene ferrimagnetische Minerale, Ände-rung von Form oder mechanischer Spannung von Korn zu Korn). ΔH charakterisiert dann die Streuung der H_{ri}. Die größte Halbwerts-Breite ist dann zu erwarten, wenn die Erz-Körner als von einander unabhängig betrachtet werden können. Für Magnetit z. B. streuen die H_{ri} bei 9 GHz etwa zwischen 1 und 9 kOe. Diese Grenzwerte sind für eine dünne Scheibe berechnet, die parallel bzw. senkrecht zum statischen Magnet-feld orientiert ist. Bei Gesteinen mit geringem Erzgehalt ist die Voraussetzung unab-hängiger Körner am ehesten erfüllt. Die Richtigkeit dieser Überlegungen wird durch das Experiment bestätigt. Es zeigt sich eine deutliche Zunahme von ΔH in der Reihen-folge Einkristall — Erz — Gestein. Einige Stunden Glühung im Vakuum bei $850\,^0\mathrm{C}$ von Serpentinit und Basalt brachten keine stärkere Veränderung der Kurven, ins-besondere keine Verschmälerung. Daraus ist zu schließen, daß innere Spannungen nicht für die Verbreiterung der Minima verantwortlich sind.

5. Schlußfolgerungen

Eine vollständige Interpretation der Ergebnisse ist wegen der geringen Anzahl der Messungen noch nicht möglich. Jedoch kann gesagt werden, daß die Methode der ferromagnetischen Resonanz geeignet ist, schnell den Gehalt an ferrimagnetischen Mineralen in Gesteinen abzuschätzen. Ein ungefähres Maß hierfür ist das Produkt aus „Intensität der Absorption" und Halbwerts-Breite. Der Aufwand an Geräten zum Aufbau der Apparatur ist zwar relativ groß, jedoch bereiten die Herstellung der Gesteins-Proben (kleine Bruchstücke!) und die Durchführung der Messung keine Schwierigkeiten. Für spezielle Fragen — z. B. nach den inneren Spannungen, der Kristall-Anisotropie und der Form der Erz-Körner — kann die ferromagnetische Resonanz eine wertvolle Ergänzung anderer Untersuchungs-Methoden sein. Unter-suchungen bei verschiedenen Temperaturen sind möglich — bei der hier benutzten Apparatur kontinuierlich zwischen etwa -180 und $+400\,^0\mathrm{C}$. Die Ausbildung des Meß-Resonators als Druck-Kammer ist denkbar.

Für das Interesse an diesen Untersuchungen und zahlreiche Diskussionen habe ich
Herrn Prof. Dr. G. ANGENHEISTER und Herrn Privatdozent Dr. H. SOFFEL vom Insti-
tut für Angewandte Geophysik der Universität München zu danken. Für die Mög-
lichkeit, die Messungen durchzuführen, danke ich Herrn Dr. E. BILLER vom Lehr-
stuhl Prof. Dr. W. ROLLWAGEN der Sektion Physik der Universität München.

Literatur

LAX, B., and K. J. BUTTON: Microwave Ferrites and Ferrimagnetics, McGraw Hill, New York,
   1962

The Single Domain — Multidomain Transition in Natural Intermediate Titanomagnetites

H. Soffel, München[1])

Summary: The domain structures of titanomagnetites of the composition 0,55 Fe_2TiO_4—0,45 Fe_3O_4 of two basalts as dependent on grain size were studied with the BITTER-pattern technique in order to determine (i) the critical radius of the ore grains for the transition from the multidomain to the single domain state, (ii) the type of domain configuration just above the single domain state and (iii) the specific wall energy γ_w. The critical radius for the transition was found to be about 0,7 micron from domain structure observations as well as from theoretical considerations. The specific wall energy was determined experimentally to be $\gamma_{w,180} = 1$ erg/cm² for the investigated titanomagnetites. Above the single domain state a two domain configuration is present and not a four domain configuration as predicted by Stacey [1963].

Zusammenfassung: Die Bereichsstrukturen von Titanomagnetiten der Zusammensetzung 0,55 Fe_2TiO_4—0,45 Fe_3O_4 in zwei Basalten wurden in Abhängigkeit von der Korngröße untersucht, um Informationen zu erhalten über (i) den kritischen Durchmesser der Erzkörner für den Übergang von der Mehrbereichs- zur Einbereichs-Konfiguration, (ii) den Typ der Bereichskonfiguration unmittelbar vor diesem Übergang und (iii) die spezifische Wandenergie γ_w. Für diese Titanomagnetite ergab sich sowohl experimentell als auch theoretisch ein kritischer Durchmesser von 1,4 Mikron. Die spezifische Wandenergie beträgt $\gamma_{w,180} = 1$ erg/cm². Beim Übergang von der Einbereichs- zur Mehrbereichs-Konfiguration bildet sich eine Zwei-Bereichs-Konfiguration aus. Dieses Ergebnis steht im Gegensatz zu Stacey [1963], der auf Grund theoretischer Betrachtungen eine Vier-Bereichs-Konfiguration vorausgesagt hatte.

Introduction

The magnetic properties of an ore grain are altered during crystal growth as the domain configuration changes from the single domain to the multidomain state. The properties principally affected are (i) the intensity of the remanent magnetization which is drastically reduced by the development of one or more domains magnetized in opposite directions, (ii) the stability of the remanent magnetization which is reduced, since the coercive force of multidomain particles is much lower than that

---

of single domain particles. Finally (iii) the magnetic susceptibility which is increased by the production of domain walls, thus increasing the induced magnetization of the rock and its ability to acquire a secondary magnetization.

For paleomagnetic considerations the most important aspects are the time variation of the direction and intensity of the remanent magnetization and its stability against demagnetization procedures. This is dependent on the domain configuration. As will be pointed out later in this paper, the transition from the single domain to the multidomain configuration depends largely on certain bulk properties of the material as well as on the shape and size of the ore grains. Rock specimens generally have a rather wide range of grain sizes so that both single domain and multidomain particles are to be expected. The suitability of a rock for paleomagnetic investigations depends not only on the chemical composition of the ore grains present but also on their size and shape and on whether single or multidomain properties are prevalent.

Domain configuration above the single domain state

The free energy of a ferromagnetic particle is composed of a number of different energy terms of which only those of importance to the magnetic properties will be discussed. According to KITTEL [1965]

$$E_M = 0,5 \cdot N \cdot J_s{}^2 \tag{1}$$

is the magnetic stray field energy, where N is the demagnetization factor of the grain in the direction of the spontaneous magnetization $\bar{J}_s$.

$$E_K = K \cdot (\alpha^2{}_1\alpha^2{}_2 + \alpha^2{}_2\alpha^2{}_3 + \alpha^2{}_3\alpha^2{}_1) \cdot V + \dots \tag{2}$$

is the crystalline anisotropy energy for crystals of cubic symmetry, where K is the crystalline anisotropy constant. V is the volume or that volume fraction of the grain, where the magnetization vectors are not parallel to a direction of easy magnetization. The α_i denote the direction cosines of the magnetization direction with respect to the cubic edges of the crystal.

$$E^+{}_A = I_0 \cdot S^2 \cdot \varphi^2 \tag{3}$$

is the exchange energy between two spins making a small angle φ with each other. I_0 is the exchange integral and S is the spin angular momentum measured in units $h/2\pi$, where h is Planck's constant. $E^+{}_A$ defines the energy which is necessary to distort the parallel or antiparallel orientation of two neighbouring spins. Within a 180^0 wall the magnetization vectors gradually change their direction from one domain to the next by a stepwise rotation through 180^0 so that both crystalline anisotropy energy and exchange energy are involved in the domain wall energy. If this change

occurs in m equal steps, then the angle between neighbouring spins is φ_0/m and the exchange energy between each pair of spins is given by:

$$E^+_A = I_0 \cdot S^2 \cdot (\varphi_0/m)^2. \tag{4}$$

The total exchange energy of a line of $(m + 1)$ spins is thus:

$$E_A = I_0 \cdot S^2 \cdot \varphi^2_0/m. \tag{5}$$

As there are $1/a^2$ such lines per unit area (a being the distance between two neighbouring spins) the exchange anisotropy energy per unit area of a 180^0 wall ($\varphi_0 = \pi$) is given by:

$$E_A = I_0 \cdot S^2 \cdot \pi^2/m \cdot a^2. \tag{6}$$

Within a domain wall the spins deviate from the directions of easy magnetization and the crystal anisotropy energy per unit area in a 180^0 wall of m steps is approximately given by:

$$E_K = K \cdot m \cdot a. \tag{7}$$

The specific energy $\gamma_{w,180}$ of a 180^0 wall (energy per unit area) is given by minimizing $E_W = E_K + E_A$ and setting $\partial E_W/\partial m = 0$ for a domain wall and thus:

$$\gamma_{w,180} = 2 \cdot \delta_w \cdot K \text{ and } \delta_w = \gamma_{w,180}/2 \cdot K, \tag{8}$$

where $\delta_w = m \cdot a$ is the domain wall thickness. Thus the total wall energy of a particle with only 180^0 walls is therefore given by:

$$E_W = \gamma_{w,180} \cdot F \tag{9}$$

where F denotes the total area of domain walls of specific energy $\gamma_{w,180}$. The energy of a particle of volume V due to uniaxial stress σ is given by:

$$E_\sigma = (3/2)\lambda_s \cdot \sigma \cdot V \sin^2\theta, \tag{10}$$

where λ_s is the isotropic magnetostriction constant and θ is the angle between $\vec{\sigma}$ and $\vec{J}_s$. The magnetostatic energy due to an external field $\vec{H}$ is given by:

$$E_H = 0{,}5 \cdot \vec{H} \cdot \vec{J}_s \cdot V. \tag{11}$$

LANDAU and LIFSCHITZ [1935] were the first to point out that by subdivision into a number of magnetic domains the free energy $E = E_M + E_K + E_A + E_W + E_\sigma$

$+ E_H$ of a magnetic particle is reduced. In many cases it is sufficient to consider only a selected number of contributing terms neglecting others such as E_H (when the external field is absent) and E_σ (when no uniaxial stresses are present). If all the exchange anisotropy energy E_A and crystalline anisotropy energy E_K are confined to the volume occupied by the domain walls, then the domain wall energy E_W and the magnetic stray field energy E_M are the most important energy terms. This assumption means that, with the exception of the volume fraction occupied by the domain walls, the magnetization vectors are always parallel or antiparallel to each other and along directions of easy magnetization within the particle.

KITTEL [1949] regarded a simple model of a ferromagnetic particle consisting of a cube of length L divided into n lamellae shaped domains of thickness D with $L = n \cdot D$ (see Fig. 1). The total magnetic stray field energy of a cube without domains (given
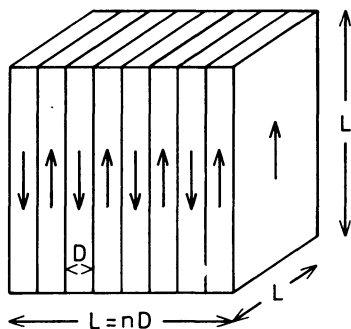
Fig. 1: Cube of edge length L subdivided into n lamellae shaped domains of thickness D with opposite magnetization directions.

by equation (1)) is reduced by the development of magnetic domains. According to KITTEL [1946] the stray field energy per unit area on each of the opposite sides of the cube, where $\vec{J}_s$ is normal to the surface, is given by:

$$E_M = 0{,}8525 \cdot J^2_s \cdot D. \tag{12}$$

The total stray field energy $E_{M,\text{tot.}}$ resulting from the two opposite sides of the cube of area L^2 is thus:

$$E_{M,\text{tot.}} = 2 \cdot 0{,}8525 \cdot J^2_s \cdot D \cdot L^2 = 1{,}75 \cdot J^2_s \cdot D \cdot L^2. \tag{13}$$

The total wall energy $E_{W,\text{tot.}}$ of the cube is given by:

$$E_{W,\text{tot.}} = n \cdot \gamma_{w,180} \cdot L^2 = \gamma_{w,180} L^3/D \tag{14}$$

with $n = L/D$. The domain thickness D is obtained by minimizing $E = E_{M,\text{tot.}} + E_{W,\text{tot.}}$. If we set $\partial E/\partial D = 0$ and solve this equation for D, we get:

$$D = (\gamma_{w,180} \cdot L/1{,}75 \cdot J^2_s)^{1/2} \tag{15}$$

Substituting D by L/n we get:

$$n = (1{,}75\, J^2_s \cdot L/\gamma_{w,180})^{1/2} \tag{16}$$

From equations (15) and (16) we can see that with decreasing diameter L of the particle the number n of domains decreases as well as their thickness D until a single domain configuration represents the state of lowest energy of the particle.

KITTEL [1949] discussed the energy of several types of domain configurations at the transition from the multidomain to the single domain state, which are shown in Fig. 2. Type a) is a typical single domain particle consisting of one domain with
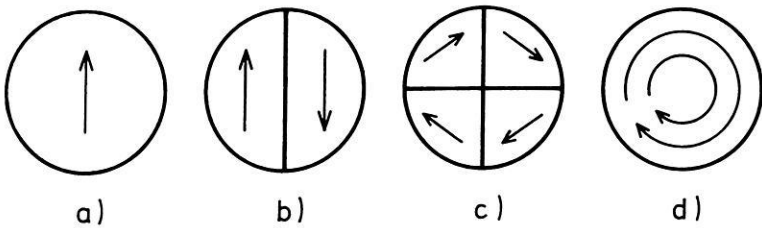
Fig. 2: Possible configurations at the transition from the single (a) to the multidomain state (b—d) according to KITTEL [1949]. a) single domain particle, b) two domain particle, c) four domain particle, d) circular configuration.
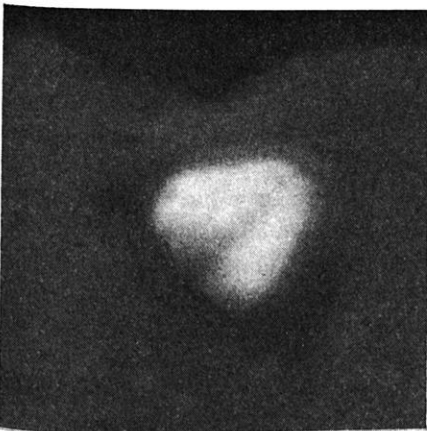
Fig. 3: For caption see 3 pages later.

homogeneous magnetization. The remanent magnetization of this particle equals its saturation magnetization and the coercive force (in cgs units) is (i) $H_c = 0,64 \cdot K/J_s$ in the case of pure crystal anisotropy, (ii) $H_c = 0,48 \cdot (N_a - N_b) J_s$ in the case of pure shape anisotropy and (iii) $H_c = 1,44 \cdot \lambda_s \cdot \sigma/J_s$ in the case of pure stress anisotropy. N_a and N_b denote the smallest and largest demagnetization factor respectively of a rotational elipsoid, λ_s is the isotropic magnetostrictive constant and σ a uniaxial compression.

Following the considerations of KITTEL [1949], the energy of a spherical single domain particle in the absence of an external field H_a and uniaxial stresses σ is exclusively determined by the magnetic stray field energy to be:

$$E_M = 0,5 \cdot N \cdot V \cdot J^2_s = 0,5 \cdot (4\pi/3) \cdot (4\pi/3) R^3 \cdot J^2_s = 0,5 \cdot (4\pi/3)^2 \cdot R^3 \cdot J^2_s, \qquad (17)$$

where $N = 4\pi/3$ is the demagnetization factor of a sphere of radius R and volume V.

Above the single domain state the energy of the particle can be reduced by domain configurations of the type b)—d). Type b) is a two domain particle. Here the stray field energy is reduced to one half by a division of the grain into two equal magnetic domains with opposite magnetization directions in the form of two half spheres. Some energy however is contained in the 180^0 wall separating the two domains, characterized by the domain wall energy $E_W = \gamma_{w,180} \cdot F$, where $F = \pi R^2$ is the area of the wall. With $H_a = 0$ and $\sigma = 0$ the total energy of the particle with such a configuration is given by:

$$E = (1/2) \cdot 0,5 \cdot (4\pi/3^2) \cdot R^3 \cdot J^2_s + \pi \cdot R^2 \gamma_{w,180}. \qquad (18)$$

The critical radius for the transition from the single to the multidomain state is obtained by a comparison of the pure stray field energy of the single domain particle (equ. 17) with the reduced stray field energy plus the wall energy (equ. 18) of the two domain particle by setting (17) = (18). If we solve this for R, we get:

$$R = 9 \cdot \gamma_{w,180}/4 \cdot \pi \cdot J^2_s. \qquad (19)$$

Another possible domain configuration is the four domain state of Fig. 2c. Here the flux is practically closed and the energy is mainly given by the wall energy of the two walls:

$$E = 2 \cdot \pi \cdot R^2 \cdot \bar{\gamma}_w, \qquad (20)$$

where $\bar{\gamma}_w \approx 0,5 \cdot \gamma_{w,180}$ represents a reduced wall energy, as no 180^0 walls are formed for such a configuration. The critical radius for the transition from this configuration to the single domain configuration is obtained in the same way as above by setting (17) = (20) and solving for R:

$$R = 9 \cdot \bar{\gamma}_w/4 \cdot \pi \cdot J^2_s. \qquad (21)$$

A configuration of type d) is only possible, when the crystal anisotropy of the material is extremely low. The magnetization of this particle is then no longer homogeneous but circular with a complete flux closure. The stray field energy is therefore zero and, neglecting any magnetostrictive effects as well as the crystal anisotropy, the energy of this configuration is determined by:

$$E = 4 \cdot \pi \cdot A \cdot R \cdot (\ln (2R/a) - 1), \tag{22}$$

where A is the exchange energy constant, which is related to the exchange integral I_0 by the expression $A = 2 \cdot I_0 \cdot S^2/a$. The critical radius for the transition from the configuration of type d) to the single domain configuration is given by:

$$R = (2,95/J_s) (A/4,2)^{1/2}. \tag{23}$$

The domain structures of small titanomagnetite particles

The rocks investigated are two Tertiary basalts (Rauher Kulm and Parkstein) from the Oberpfalz area, Germany. The rockmagnetic and paleomagnetic properties of these basalts have been extensively studied by several authors [REFAI 1961, PETERSEN 1962, SOFFEL 1968 b, 1969, 1970, PETERSEN and CREER 1969]. Both rocks contain titanomagnetites of the composition 0,55 Fe_2TiO_4—0,45 Fe_3O_4 which are homogeneous in their natural state according to optical and electron microscope studies. The grains are almost spherical (see later Fig. 18) and the sizes range from about 10^{-6} cm to about 10^{-1} cm as determined by SOFFEL [1969]. The saturation magnetization of the ore at room temperature is 100 Gauss and the Curie temperature is 180^0—200^0C. The abundance of the ore is 2—4 percent by volume.

The domain configurations were observed with the BITTER pattern technique on polished sections of the basalt samples. After mechanical polishing the titanomagnetite grains in the basalts were further prepared with an ionic polishing technique after SOFFEL [1968a] in order to produce stress free surfaces. Some representative domain configurations of grains with many domains and grains with very few domains are shown in Fig. 3—15. Most figures are just sketches of the structures and their possible interpretation. This was obtained by studying the motion of the domain walls under the influence of external fields of various strengths and directions and represent a likely distribution of the magnetization within the observed ore grains.

Fig. 3 shows a two domain particle in the Parkstein basalt with a diameter of about 5 microns. The demand for a minimum net magnetization of the ore grain requires the presence of a 180^0 wall separating two oppositely magnetized domains. An external field parallel to the polished surface of the grain in the direction shown in Fig. 3 produces a bending of the domain wall, not a parallel displacement as would be expected from the experiences with large crystals. The net magnetization increases however in the direction parallel to the external field. The strength of the

Fig. 3: Two domain particle in the Parkstein basalt. Photomicrograph and sketch of domain structure. Motion of the domain wall under the influence of an external field parallel to the polished surface.

Fig. 4: Two domain particle in the Rauher Kulm besalt. Sketch of the domain structure and motion of the domain wall under the influence of an external field parallel to the polished surface.

Fig. 5: Sketch of the domain structure of a three domain particle in the Rauher Kulm basalt.

external field, which is in the order of 30 Oe, indicates that the coercive force of the ore grain must be of the same order of magnitude or smaller. The removal of the external field almost restores the initial position of the wall. However, the bending of the domain wall is slightly larger than before the application of the field. (Photomicrograph corresponds to sketch a.)

A two domain particle in the Rauher Kulm basalt is shown in Fig. 4. The diameter is about 5 microns. An external field parallel to the surface and to the 180⁰ wall which separates the two domains again causes a bending of the wall and not a parallel displacement. After a removal of the field the wall moves back into its former position. The coercive force is in the order of 20 Oe.
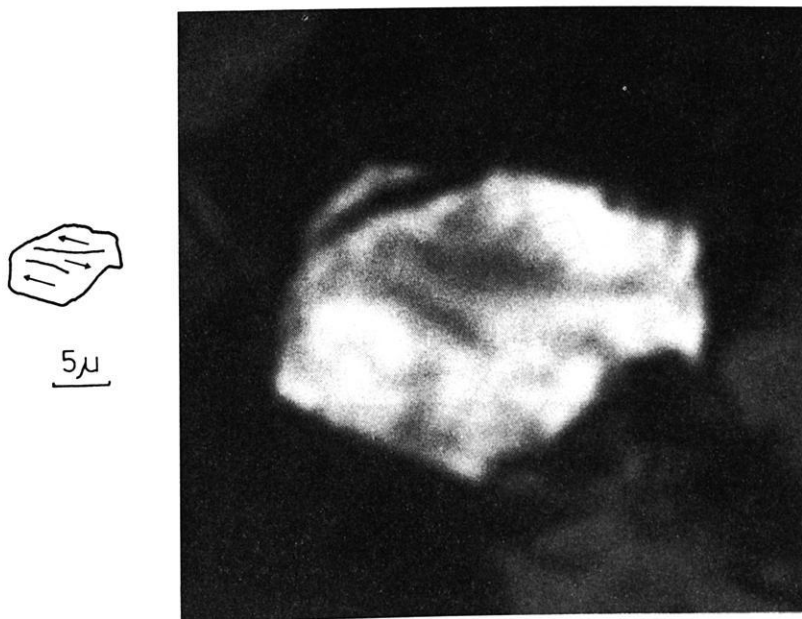
Fig. 6: Three domain particle in the Parkstein basalt. Photomicrograph and sketch of the domain structure.

Examples of grains with a three domain configuration are shown in Fig. 5—7. Fig. 5 showns a grain in the Rauher Kulm basalt with a diameter of about 6 microns. Three domains separated by 180⁰ walls are the most likely domain configuration. A more complicated structure seems to be present in the grain shown in Fig. 6 which is from the Parkstein basalt. Besides the two slightly bent domain walls in the center of the grain (presumably 180⁰ walls) there are other zig-zag-shaped features at the margin of the crystal. These however remained fixed in position when external fields were applied and represent not domain walls but the boundaries between the fresh titanomagnetite in the inside of the ore grain and an oxidized and probably non-magnetic secondary phase at the outside. The sharp decay of the saturation magneti-zation along such borders produces magnetic stray fields which are also decorated by the magnetite colloid used by the BITTER pattern technique.—The ore grain shown in Fig. 7 originates from the Rauher Kulm basalt. Again there are three domains separated by 180⁰ walls. The dots shown in Fig. 6 (sketch) represent etch pits pro-duced by the ionic polishing procedure. They are interpreted as to be dislocation lines intersecting the surface [SOFFEL 1970]. The domain walls seem to have a ten-dency to be ficed to these structures as has already been described by SOFFEL [1970] for large titanomagnetite grains of the same basalts. The variation of the domain
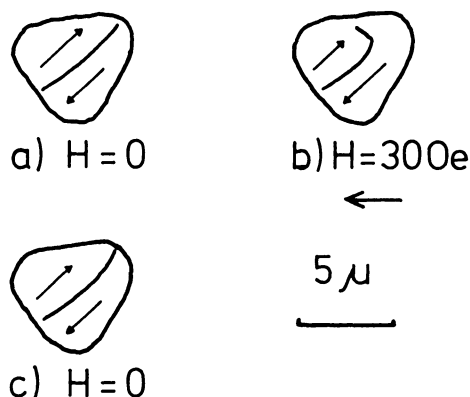
Fig. 7: Three domain particle in the Rauher Kulm basalt. Photomicrograph and sketch of the domain structure. Motion of domain walls under the in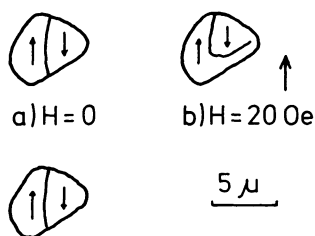fl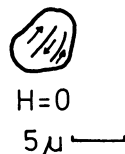uence of external fields parallel to the polished surface. Dots: etch pits due to dislocations intersecting the surface.

structure under the influence of external fields parallel to the polished surface of the ore grain is also shown in Fig. 7.

Some four domain configurations (sketches only) are shown in Fig. 8—13. They are not of type c), which was discussed by KITTEL [1949] and shown in Fig. 2c. The ore grains seem to have more or less lamellae shaped domains separated by 180⁰

a) H = 0   b) H = 50 Oe ↓

c) H = 0   d) H = 50 Oe ↑

e) H = 0   5 μ

Fig. 8: Sketch of the domain structure of a four domain particle in the Parkstein basalt. Motion of domain walls under the influence of external fields parallel to the polished surface. Bold line: crack dividing the grain.

Fig. 9   10 μ   Fig. 10   5 μ   Fig. 11   5 μ
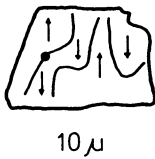
Fig. 9: Sketch of the domain structure of a four domain particle in the Rauher Kulm basalt with bent domain walls. Dot: etch pit due to a dislocation intersecting the surface.

Fig. 10: Sketch of the domain structure of a four domain particle in the Parkstein basalt.

Fig. 11: Sketch of the domain structure of a four domain particle in the Rauher Kulm basalt with bent domain walls due to the interaction with dislocations, which are revealed as etch pits (dots).

walls. Fig. 8 shows a grain from the Parkstein basalt which is cut in two by a crack (dark line). The diameter is about 5 microns. The minimum in the net magnetization of the ore grain requires the presence of 180^0 walls. The variation of the domain configuration under the influence of external fields of various directions parallel to the surface of the grain is also shown in Fig. 8. The domain walls can easily be shifted by fields of the order of 50 Oe and the initial configuration reappears after each magnetizing cycle. In contrast to Fig. 7 the magnetization of the domains is not in the direction of the longest axis of the grain. This point will be discussed later in this paper in connection with Fig. 18.

a) H = 0   b) H = 20 Oe↑   c) H = 0

d) H = 20 Oe↑   e) H = 0   f) H = 20 Oe↓

g) H = 20 Oe   h) H = 0   5 μ
   ←—
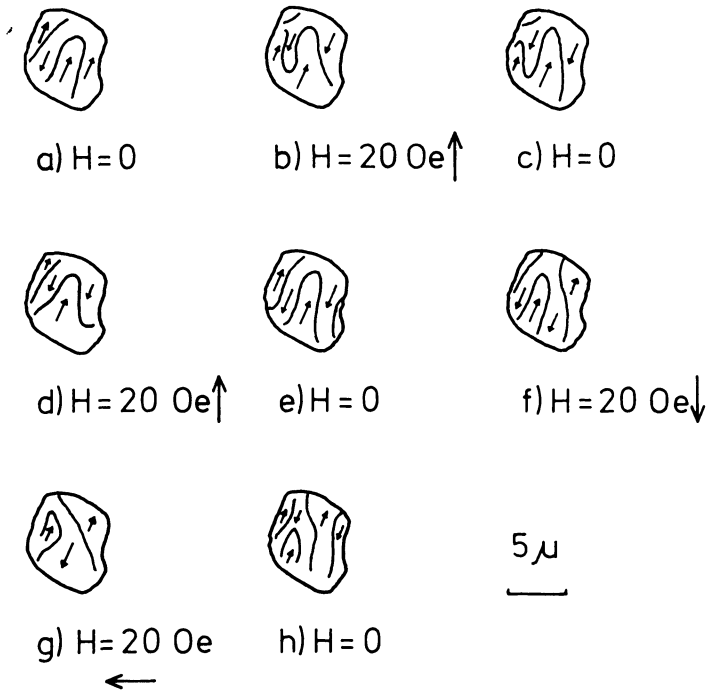
Fig. 12: Sketch of the domain structure of a four domain particle in the Parkstein basalt with bent domain walls. Motion of the domain walls under the influence of external fields parallel to the polished surface.

Fig. 9 shows an ore grain from the Rauher Kulm basalt with a diameter of about ten microns and a four domain configuration. The structure with heavily bent domain walls is quite unusual and has not been observed in materials with large saturation magnetization at room temperature such as Fe ($J_s = 1735$ Gauss), Co ($J_s = 1445$ Gauss) and Ni ($J_s = 509$ Gauss). However it could be possible in a material with a quite small saturation magnetization as for instance the titanomagnetites under consideration ($J_s = 100$ Gauss). The extraordinarily marked decoration by the magnetite colloid of the bent domain walls in the center of the crystal (not shown in Fig. 9) indicates the presence of much larger stray fields along these parts of the domain walls than exist along ordinary 180^0 walls.

The four domain configuration shown in Fig. 10 on the surface of an ore grain in the Parkstein basalt with a diameter of about 6 microns is also connected with slightly bent 180^0 walls.

A more complicated structure is present on the surface of the ore grain in the Rauher Kulm basalt as shown in Fig. 11. The average diameter of the grain is about 8 microns.

a) H = 0   b) H = 10 Oe
                                 →

c) H = 0   d) H = 10 Oe
                                 ←

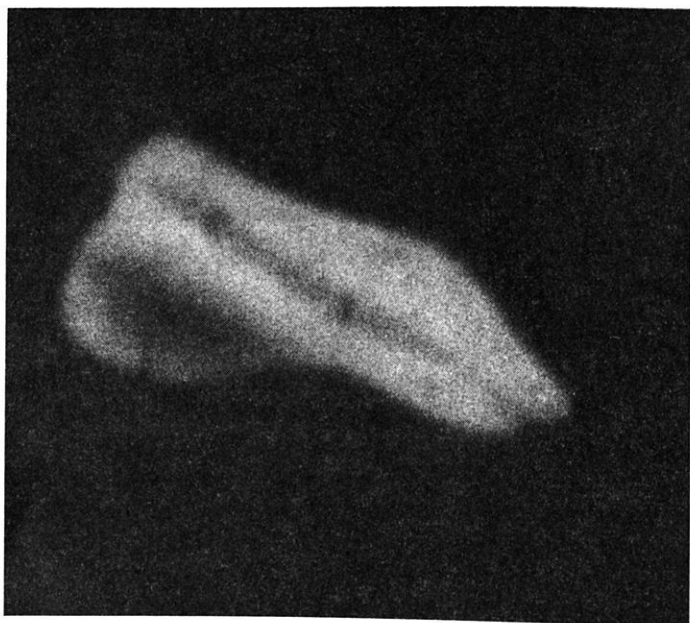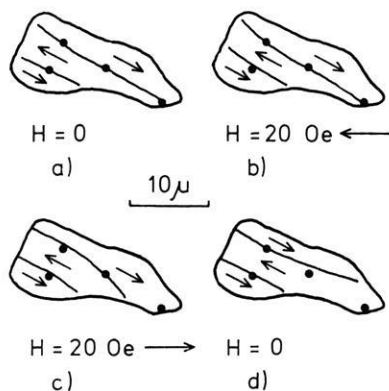   ⌐_____⌐
                                  10 μ

e) H = 0
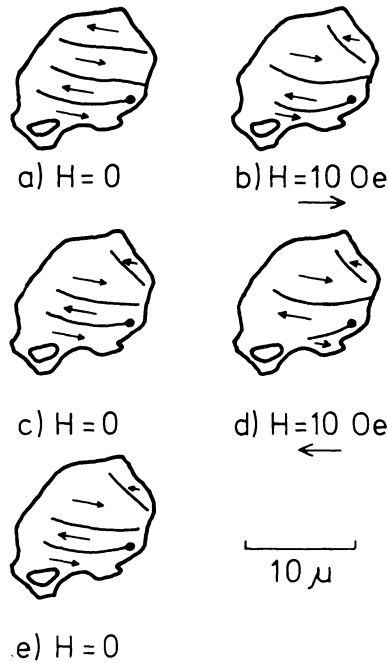
Fig. 13: Four domain particle in the Rauher Kulm basalt. Sketch of the domain structure. Motion of domain walls under the influence of external fields parallel to the polished surface.

The bending of the 180^0 walls in the central part of the crystal is probably due to a series of dislocations which are revealed by etch pits on the surface as previously described in connection with Fig. 7. Only external fields in various directions of the order of about 50 Oe were able to move the domain walls.

The domain structure of an ore grain with about 8 microns in diameter in the Parkstein basalt under the influence of external fields parallel to the surface is shown in Fig. 12. The interpretation of the magnetization directions in the individual domains is the most probable one according to the author's experiences with this material and was derived from domain wall motions. It is by no means unambiguous.

A grain with a diameter of about 12 microns in the Rauher Kulm basalt having a four domain configuration is shown in Fig. 13. There is a nonferromagnetic inclusion in the lower left corner of the grain and a dislocation (revealed as etch pit and marked as a dot) in its lower right corner. The walls can easily be moved by external fields of the order of 10 Oe. One of the walls (the third from the top) remains fixed to the dislocation at one end while the other end can be moved around. No closure domains seem to be present around the inclusion or at the margins of the crystal.

Fig. 14

5μ

a) H = 0   b) H = 20 Oe →

c) H = 0   d) H = 20 Oe ←

10μ
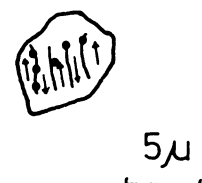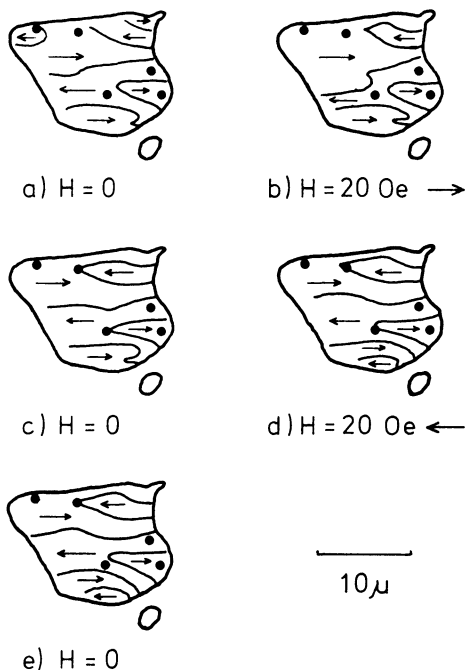
Fig. 15   e) H = 0

Fig. 14: Five domain particle in the Rauher Kulm basalt. Sketch of the domain structure. Dots: etch pits due to dislocations intersecting the surface.
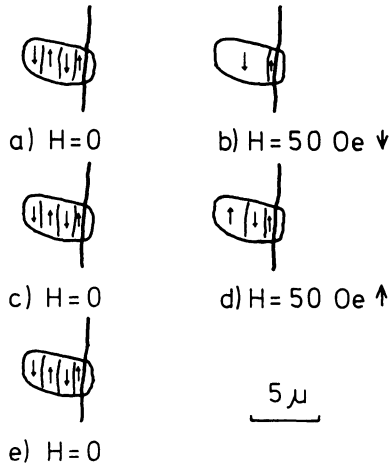
Fig. 15: Sketch of the domain structure of a large multidomain particle in the Rauher Kulm basalt. Motion of domain walls under the influence of external fields parallel to the polished surface. Dots: etch pits due to dislocations intersecting the surface. The multidomain particle is accompanied by a small particle with single domain configuration.

A quite simple five domain configuration on a grain in the Rauher Kulm basalt is shown in Fig. 14. The diameter of the grain is about 8 microns. The 180⁰ walls which seem to be present have a strong tendency to be fixed to the dislocations as already mentioned in connection with Figs. 7, 11 and 13.

A more complicated structure has the grain with a diameter of about 15 microns shown in Fig. 15 (Rauher Kulm basalt). There are a number of dislocations in this grain revealed by etch pits (dots). Some closure domains seem to be present with probably 180⁰ walls. Bent 180⁰ walls are common. The large grain is accompanied by a very small grain with a diameter of about 2 microns with apparently no domain wall. A concentration of the magnetite colloid on two opposite sides of the grain, which is not shown in the sketch, indicates that this grain is probably a large single domain particle.
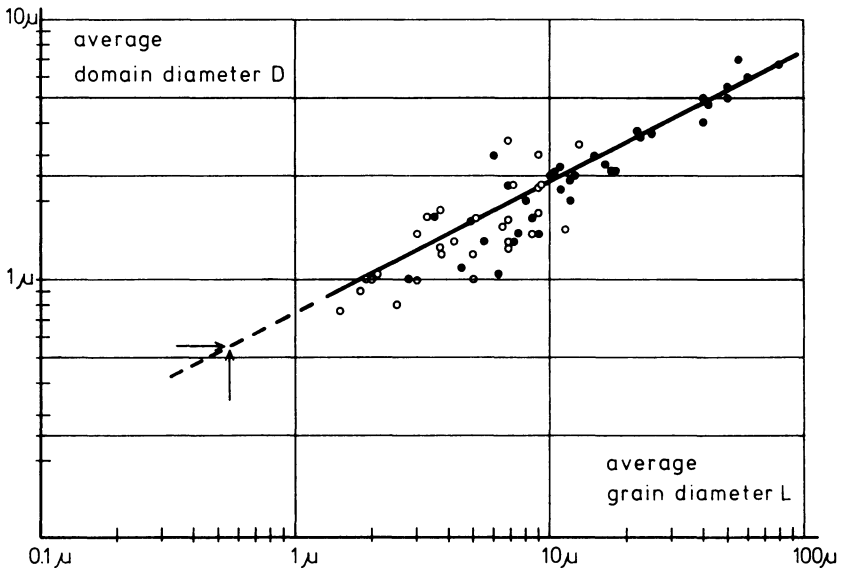
Fig. 16: Plot of the average grain diameter L versus the average domain diameter D in a bilogarithmic scale for particles of various grain sizes in the Parkstein and Rauher Kulm basalt. Open circles: $p > 1$; closed circles: $p < 1$.
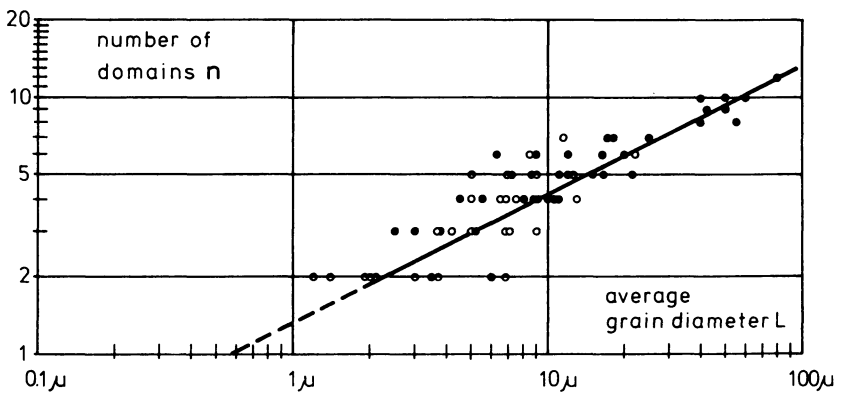
Fig. 17: Plot of the average grain diameter L versus the number n of domains in a bilogarithmic scale for particles of various grain sizes in the Parkstein and Rauher Kulm basalt. Open circles: $p > 1$; closed circles: $p < 1$.

According to the interpretations given in Fig. 3—15 180⁰ walls are the most com-
mon wall type in the very small ore grains. Closure domains associated with 71⁰—or
109⁰ walls occur rarely and only in the very large ore grains.Regarding the titano-
magnetite particles with only two or three domains one may see that of the configu-
ration types above the single domain state as postulated by KITTEL [1949] in Fig. 2
only type b) (the two domain configuration) seems to be realized with these titano-
magnetites. There were no indications for the four domain configuration of type c)
which had been predicted by STACEY [1963] for small ore grains. The presence of
type d) cannot be detected with the BITTER pattern technique. This is only possible
using the KERR technique for the observation of the domains [KRANZ and DRECHSEL
1958]. Experiments to apply the KERR technique to these titanomagnetites failed
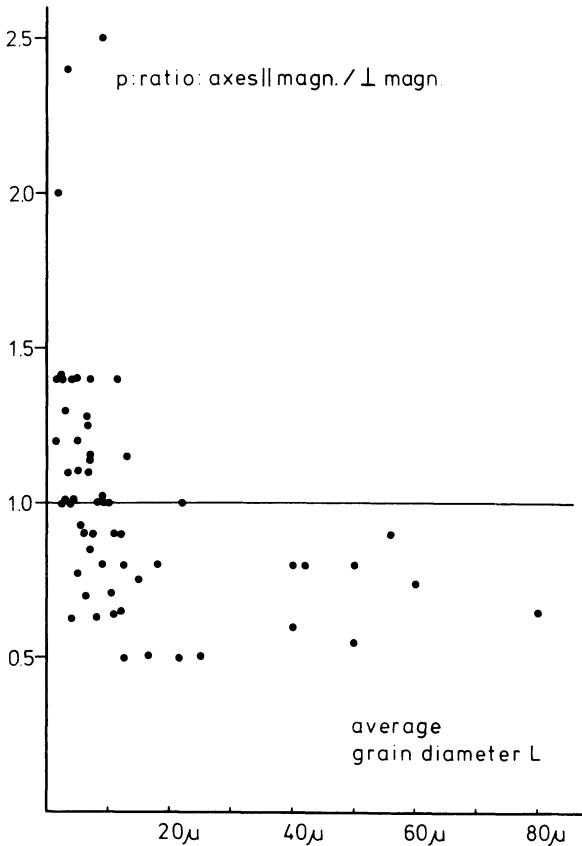
Fig. 18: Plot of the average grain diameter L versus p, the ratio of the diameter of the grains
parallel to that perpendicular to the direction of magnetization of the domains.

however due to uneven surfaces of the ore grains and the too low KERR rotation, which is proportional to the square of the saturation magnetization and therefore two orders of magnitude smaller than in iron.

Nothing can bee said about the third dimension of the domain configuration. The absolute size of the grains and their position within a rock matrix do not permit to observe their domains on different surfaces in order to deduce the domain structure in their interior. As no complicated closure domains occurred at the margins of the crystals, the observed walls seem to continue into the grains indicating the presence of lamellae shaped domains separated by 180^0 wall like those shown in Fig. 1.

In order to examine the relationship between the thickness D of a domain and the diameter L of the ore grain, as given by equation (15) after KITTEL [1949], the mean values of D and L for a large number of grains of different sizes were plotted in a bilogarithmic scale establishing a linear relationship between ln D and ln L (Fig. 16). The slope of the best fitting line equals ½ which is in agreement with the square root relationship of equation (15). Following Equ. (16) and plotting the number of domains (ln n) versus the average grain diameter (ln L) yields Fig. 17. This also shows the expected linear relationship between ln n and ln L with a slope of ½. Equation (15) can be used for the determination of the specific wall energy $\gamma_{w,180}$ in the investigated titanomagnetites. Equating (15) for $\gamma_{w,180}$ we get:

$$\gamma_{w,180} = 1{,}75 \cdot J^2_s \cdot D^2/L. \tag{24}$$

Selecting a corresponding pair of values for D and L from Fig. 16, say $L = 43 \cdot 10^{-4}$ cm and $D = 5 \cdot 10^{-4}$ cm, we get:

$$\gamma_{w,180} = 25 \cdot 10^{-8} \cdot 1{,}75 \cdot 10^{+4}/43 \cdot 10^{-4} \text{ erg/cm}^2 = 1 \text{ erg/cm}^2. \tag{24a}$$

Similar values of around 1 erg/cm^2 for the specific wall energy have also been found for Fe, Co and Ni [see KNELLER 1962]. The approximate thickness δ_w of a domain wall is related to the wall energy by the expression given by equation (8):

$$\delta_w = \gamma_{w,180}/2 \cdot K. \tag{8}$$

With $K = 7 \cdot 10^4$ erg/cm^3 according to SYONO [1965] we get:

$$\delta_{w,180} = 1 \text{ erg/cm}^2/14 \cdot 10^{+4} \text{ erg/cm}^3 = 0{,}07 \cdot 10^{-4} \text{ cm}, \tag{25}$$

which is about 100 times the cell edge dimensions of titanomagnetite (about 8,5 Å).

The so determined value for the specific wall energy $\gamma_{w,180}$ enables us to calculate the critical diameter for the transition from the multidomain to the single domain state in the observed titanomagnetites for types 2b)—2d). The value for the exchange

energy constant A, which appears in equation (23), can be computed from the wall energy and the crystal anisotropy energy constant by the relation [KITTEL 1949]:

$$A = \gamma^2_{w,180}/4 \cdot K = 36 \cdot 10^{-7} \text{ erg/cm,} \tag{26}$$

which is also of the same order of magnitude as the values of A for Fe, Co and Ni [see KNELLER 1962]. Using Equ. (19), (21) and (23) the critical radii for models 2b) to 2d) are:

Type b) (Two domain configuration): $R = 0,72 \cdot 10^{-4}$ cm

Type c) (Four domain configuration): $R = 0,36 \cdot 10^{-4}$ cm

Type d) (Circular configuration): $R = 0,27 \cdot 10^{-4}$ cm.

The type c) configuration, which was actually not observed, requires a critical radius for the grain which is not very different from the expected domain wall thickness (equ. (25)) and is therefore not likely. Type b) yields a critical radius which is by one order of magnitude larger than the domain wall thickness. This is the type which was actually observed and is expected to be the realistic domain configuration above the single domain state. As the crystal anisotropy of this material is quite important ($K = 7 \cdot 10^4$ erg/cm^3) the possibility of type d) must be excluded at least for room temperature.

Fig. 16 and 17 confirm the computed values of the critical radii for the transition from the single to the multidomain state for the investigated titanomagnetites. An extrapolation of the curve of Fig. 16 down to grain sizes smaller than 1 micron shows that the diameter of the ore grain meets the diameter of a domain at a grain size of about 0,6 micron. The critical diameter for the transition has therefore to be about 1 micron. Extrapolation of the curve in Fig. 17 down to $n = 1$ (single domain configuration) points to a critical grain diameter of about 0,6 micron.

Returning to Fig. 17, where ln n is plotted versus ln L, we can see that for a configuration with two to about seven domains there is a considerable scatter for the corresponding diameter L of the ore grain. For instance grains with diameters between 1,2 micron and 6,8 microns were observed to have two domain configuration of type b). The scatter is much smaller for the large ore grains. It seems therefore that ore grains do not always adopt the domain configuration which corresponds to an absolute minimum of the magnetostatic plus the domain wall energy alone. The influence of the other energy terms E_K, E_A, E_H and E_σ, which have been neglected in our model, seems to increase with decreasing diameter of the grain. Furthermore there seem to be difficulties for the nucleation of domains with opposite magnetization directions in the ore grains. All this was not taken into account in the considerations of KITTEL [1949]. For the transition from the single domain to the multidomain configuration we have to consider the same kind of difficulties for the production

of the second reversely magnetized domain as there are in the larger ore grains. If the same amount of scatter of grain sizes for a given number of domains is assumed as for the larger multidomain particles, we can say from Fig. 17 that grains with diameters up to about 2 microns can be single domain particles in these rocks. Observation does confirm this, as a considerable number of small grains of that size were found in the two basalts without any sign of a domain wall (see Fig. 15). This leads to the conclusion that most of the particles with diameters of 1,5 micron or less must be regarded as single domain particles.

The demagnetization factor of the ore grains, which can be expressed in terms of the ratio p between the axis of the grain parallel and perpendicular to the direction of magnetization of the magnetic domains (Fig. 18) seems to have a certain influence on the direction of magnetization of the domains, especially of the very small ore grains. In Fig. 16—17 grains with $p > 1$ are represented by open circles, those with $p < 1$ by closed circles. The distribution of the open and closed circles in Fig. 16 and 17 as well as Fig. 18 show that only the small grains with diameters less than about 12 microns have a strong tendency to be magnetized along the longest axis of the grain, as seen for instance in Fig. 7. Exceptions of this rule occur however, as seen in Fig. 8. Nevertheless it was found that the ore grains tended to be magnetized along their longest axis or along a direction of easy magnetization which forms a small angle with the longest axis of the grains as expected from theory.

The result that the transition from the multidomain to the single domain state for the investigated titanomagnetites in the two basalts takes place at a critical diameter of about 1 micron is in good agreement with the actually observed intensity of the stable component of the thermoremanent magnetization (TRM) of the investigated rocks with coercivities larger than 400 Oe. Within the limits of error it was shown (SOFFEL 1969] that the intensity of the stable component of TRM could quantitatively be explained with the single domain theory of NEEL [1949] when all the ore grains with diameters around or less than 1 micron were assumed to be single domain particles.

Acknowledgement

References

KITTEL, C.: Theory of the Structure of Ferromagnetic Domains in Films and Small Particles. Phys. Rev. 70, 965—971, 1946

—: Physical Theory of Ferromagnetic Domains. Rev. Mod. Phys. 21, 541—583, 1949

—: Introduction to Solid State Physics. J. Wiley and Sons, New York, 2nd Edition, 1965

KNELLER, E.: Ferromagnetismus. Springer-Verlag 1962

KRANZ, J., W. DRECHSEL: Über die Beobachtung von Weiss'schen Bezirken in polykristalli-nem Material durch die vergrößerte magneto-optische KERR-Drehung. Z. Phys. 150, 632—639, 1958

LANDAU, L., E. LIFSCHITZ: On the Theory of the Dispersion of Magnetic Permeability in Ferromagnetic Bodies. Phys. Z. Soviet Un. 8, 153—169, 1935

NEEL, L.: Théorie du Trainage Magnétique des Ferromagnétiques en Grains Fins avec Applications aux Terres Cuites. Ann. Geophys. 5, fasc. 2, 99—136, 1949

PETERSEN, N.: Untersuchungen der magnetischen Eigenschaften von Titanomagnetiten im Basalt des Rauhen Kulm (Oberpfalz) in Verbindung mit elektronenmikroskopischer Beob-achtung. Z. Geophys. 28, 79—84, 1962

PETERSEN, N., K. M. CREER: Thermochemical Magnetization in Basalt. Z. Geophys. 35, 501—516, 1969

REFAI, E.: Magnetic Anomalies and Magnetization of Basalts in the Area Around Kemnath (Oberpfalz). Z. Geophys. 27, 175—182, 1961

SOFFEL, H.: Die Bereichsstrukturen der Titanomagnetite in zwei tertiären Basalten und die Beziehung zu makroskopisch gemessenen magnetischen Eigenschaften dieser Gesteine. Habil. Schrift, Nat. Fak. Univers. München, 1968a

—: Die Beobachtung von Weiss'schen Bezirken auf einem Titanomagnetitkorn mit einem Durchmesser von 10 Mikron in einem Basalt. Z. Geophys. 34, 175—181, 1968b

—: The Origin of Thermoremanent Magnetization of Two Basalts Containing Homogeneous Single Phase Titanomagnetite. Earth Plan. Sc. Letters, 7, 201—208, 1969

—: The Influence of the Dislocation Density and Inclusions on the Coercive Force of Multi-domain Titanomagnetites of the Composition 0,65 Fe_2TiO_4—0,35 Fe_3O_4 in Basalts as Deduced from Domain Structure Observations. Z. Geophys. 36, 113—124, 1970

STACEY, F. D.: The Physical Theory of Rock Magnetism. Adv. Phys. 12, 45—133, 1963

SYONO, Y.: Magnetocrystalline Anisotropy and Magnetostriction of Fe_3O_4—Fe_2TiO_4-Series with Special Application to Rock Magnetism. Jap. J. Geophys. 4, 71—143, 1965

A. F. Demagnetization of Viscous Remanent Magnetization in Rocks

D. Biquand and M. Prévot, Saint-Maur[1])

Summary: We present an attempt of restatement about the question of alternating field (A. F.) demagnetization of weak-field viscous remanent magnetizations (VRM) in rocks. Various examples have been chosen among experimental studies performed on VRM acquired by sedimentary or volcanic rocks, the relevant magnetic mineral being either titanomagnetite or hematite. The hardness with respect to A. F. treatment of a VRM acquired during a given time t varies much from one rock to another even for a given petrological type of rock. For volcanic rocks, in the more extreme case encountered, the VRM acquired during one month is erased by an alternating field of 300 Oe effective value. Similar hardness occurs for titanomagnetite bearing sedimentary rocks. On the contrary, for hematite bearing red sedimentary rocks, not only can the hardness be much stronger than that obtained with titanomagnetite bearing rocks, but also two independent VRM components, a soft one and a hard one, can be present in a given sample. In a red limestone 10% of a VRM of 30 days remains after the action of an alternating field of 1700 Oe effective value.

The decrease of the hardness when reducing t is moderate; for example, the VRM acquired during 15 minutes by the above mentioned red limestone is erased only by a field of 1200 Oe effective value.

A theoretical interpretation is given of all the results, assuming either single domain or multidomain grains. According to the Neel theory, very hard VRM with respect to A. F. treatment are to be expected quite generally with small single domain particles of hematite; in this case the grains carrying the VRM can correspond to a very large range of coercive forces. For the red limestone mentioned above, H_c lies between 2000 and 12000 Oe and the mean diameter of the grains carrying the VRM is about 0.1 μ.

The experimental results obtained with volcanic rocks, in which VRM is probably carried by large grains, does not seem to be in agreement with the Neel theory of multidomain particles. They can be interpreted by assuming, as suggested by Avery' Anov, that the potential barriers which impede the movements of the walls may have the same probability of being overcome by thermal fluctuations, even if their critical fields are different.

Zusammenfassung: Die Frage nach den Möglichkeiten einer Wechselfeld-Entmagnetisierung von Gesteinen mit einer viskosen, in einem schwachen Magnetfeld erworbenen isothermalen remanenten Magnetisierung (VRM) wird diskutiert. Dazu wurden zahlreiche experimentelle Untersuchungen über die VRM von Sedimenten und magnetischen Gesteinen durchgeführt. Träger der Remanenz waren entweder Titanomagnetite oder Hämatit. Gegenüber einer Wechselfeld-Entmagnetisierung war die Stabilität einer VRM, die in einer Zeit t gebildet

---

[1]) Daniel Biquand and Michel Prévot, Laboratoire de Géomagnétisme, 4 avenue de Neptune, 94—Saint-Maur (France).

worden war, sehr unterschiedlich für verschiedene Gesteinstypen und auch für Proben gleicher petrographischer Zusammensetzung. Bei vulkanischen Gesteinen waren in extremen Fällen effektive Wechselfelder von 300 Oe erforderlich, um eine VRM mit $t = 1$ Monat auszulöschen. Ähnliche Stabilitäten konnten auch bei Titanomagnetit führenden Sedimenten gefunden werden. Im Gegensatz dazu ist die Stabilität der VRM von Hämatit führenden roten Sedimentgesteinen erheblich größer, außerdem können hier zwei Arten von VRM, eine instabile und eine stabile, gefunden werden. In einem roten Sandstein waren nach einer Wechselfeld-Entmagnetisierung mit einem effektiven Feld von 1700 Oe noch 10% einer VRM von $t = 30$ Tagen vorhanden. Die Abnahme der Stabilität der VRM bei kleinerem t ist nur mäßig; so waren zum Beispiel bei dem oben genannten roten Kalkstein immerhin noch ein effektives Feld von 1200 Oe erforderlich, um eine VRM mit nur $t = 15$ Minuten auszulöschen.

Zur Interpretation der Messungen werden Modelle mit Einbereichs- und mit Mehrbereichs-teilchen diskutiert. Nach der Theorie von NEEL wird die VRM von großer Stabilität gegenüber Wechselfeld-Entmagnetisierungen auf Einbereichsteilchen von Hämatit zurückgeführt. In einem solchen Fall können sehr große Koerzitivkräfte H_c auftreten. Für den oben erwähnten roten Kalkstein liegt H_c zwischen 2000 und 12000 Oe, und der mittlere Durchmesser der die VRM führenden Erzkörner beträgt etwa 0,1 μ.

Bei der Deutung der VRM von geringer Stabilität, die bei den vulkanischen Gesteinen in den Erzkörnern mit Mehrbereichs-Konfiguration lokalisiert ist, treten Schwierigkeiten mit der NEELschen Theorie auf. Man kann diese überwinden, wenn man wie AVERY' ANOV annimmt, daß die Potentialschwellen, welche die Bewegungen der Blochwände behindern, unabhängig von den mit ihnen verbundenen Koerzitivkräften mit der gleichen Wahrscheinlichkeit durch thermische Fluktuationen überwunden werden können.

1. Introduction

Subjected to a field h during a period t, rocks carry, a period t' after the removal of this field, a remanent magnetization which can be considered, practically (THELLIER 1959, p. 290), as the sum of an isothermal remanent magnetization (IRM) acquired in a short time ($t = 1$ s. for example) plus a viscous remanent magnetization increasing with t and decreasing with t', that we will note VRM (t, h, t'). VRM can have an appreciable intensity only in certain rocks, called "viscous rocks".

This phenomenon of magnetic viscosity, known a long time ago in ferromagnetic substances, is a highly worrying one for paleomagnetists since rocks they study have been subjected in situ to the earth's magnetic field and may have acquired in this field a viscous remanence altering the primary one. THELLIER has shown formerly (1937, 1938) that this VRM could play a significant role in baked clays and volcanic rocks; yet, as a number of these materials are stable in the earth's magnetic field, the easiest way to avoid spurious results in the determination of the mean direction of a group of samples is to eliminate viscous samples, viscosity being easily detected by an adequate test [THELLIER, 1959]. Viscous samples may even often be used; in fact, as their viscosity is often weak, a suitable method of determination of the stable remanent magnetization, for example the THELLIER test, allows one in most cases to eliminate with a good approximation the effect of the VRM acquired in situ [PLESSARD 1967].

This relatively favourable situation has much changed with the wide development of paleomagnetism in the last twenty years, as the study of very many different types

of rocks has been carried on, especially sedimentary rocks. Particularly, it appeared that in the "red rocks", viscosity is not only a rather common phenomenon but also a very strong one [CREER 1957; BIQUAND 1967]: the VRM may be as intense as the stable natural remanent magnetization and sometimes even more intense. Consequently, as people do not want to reject the too numerous viscous rocks, several ways are, in principle, open to them:

—they can try to solve the problem of the separation of the primary remanence from the viscous one by sampling the same geological horizon from different sites where one finds different dips, in order to eliminate the effect of the VRM acquired in situ. But this possibility does not exist in all sedimentary series and besides there remains in any case the disturbing effect of the VRM acquired after sampling;

—they can place the samples for a long time in a field free space before measurements. This procedure erases easily the recent VRM, in particular the one acquired after sampling, but is not adequate to eliminate the geological one; if viscosity is strong, the fraction of this geological VRM which remains after several months may still be intense with respect to the stable natural remanence;

—finally, they can try to "clean" the samples, that is, to remove VRM by a physical treatment. Thermal treatment would be, as a rule, an appropriate method but it is not of common use because it is time consuming and it may alter the magnetic minerals of the rocks. The most frequently used technique is the demagnetization by alternating magnetic fields. It is possible to utilize a very strong field which seems favourable to erase a magnetization acquired in a weak-field. Moreover, magnetic minerals cannot be altered. But two remarks are to be made to the purpose of A. F. treatment:

—first, it is difficult to use, being often the origin of a parasitic magnetization owing to some imperfections of the demagnetization apparatus;

—secondly, the intuitive view, assuming that VRM is, in all cases, rather soft with respect to A. F. treatment, is not experimentally supported.

The present paper summarizes the experimental work which has been performed on this last subject and gives a theoretical interpretation of it.

2. Experimental Studies of A. F. Demagnetization of the VRM

2.1 Historical restatement

F. RIMBERT was the first author to undertake systematic experiments about the effect of alternating fields upon the different types of remanent magnetization of rocks, VRM among others [RIMBERT, 1956, 1958]. From the experiments she made with four samples of basalt and tephrite, she deduced that the effective intensity H_d of the alternating field erasing, to the approximation of some percent, a weak-field VRM, is small, even if the time t is large. From her formula for H_d as a function of h and t, she inferred that in the earth's magnetic field $H_d = 20$ Oe for $t = 7$ years. Using the same formula we see that $H_d = 100$ Oe for a VRM acquired since the

beginning of the Brunhes epoch of geomagnetic polarity. The second RIMBERT's assertion was that H_d does not depend on the nature of the rock. These results, combined with a somewhat intuitive conception of the nature of the phenomenon of magnetic viscosity, have led a number of people to suppose that, in paleomagnetic studies, the VRM acquired in situ is in all cases easily erased by alternating magnetic fields, although the demagnetization experiments were not extensive and did not concern, particularly, sedimentary rocks. Consequently, a few people, Russian and French authors [SHOLPO and SHOLPO, 1965; TRUKHIN, 1966; AVCHYAN and FAUSTOV, 1966; BIQUAND and PRÉVOT, 1970; PRÉVOT and BIQUAND, 1970; BIQUAND, PRÉVOT and DUNLOP, 1971], have developed experiments about A. F. demagnetization of the VRM. These works refer particularly to the fact that the hardness of the VRM is much variable from one rock to another and can be extremely high.

2.2 Some preliminary remarks

We will present some results taken from Russian authors or extracted from our own work. These results are chosen among the experiments made on volcanic or sedimentary rocks, the carrier of remanence being either titanomagnetite or hematite. But let us present first a few remarks:

1. Most of the Russian authors worked on massive rock samples whereas our experiments have been performed with rocks previously reduced to powder. Let us notice that the initial demagnetization state is obtained by A. F. treatment in the first case and by mixing the powder in the second one. Besides, we have performed a particular method to analyse the effect of alternating fields upon VRM which allows to study the hardness of VRM acquired during very short periods of time. We refer for the description of this method to a previously published paper [BIQUAND and PRÉVOT, 1970].

2. In the present paper we are not concerned with the problem of the eventual "hardening" of an ancient VRM under the influence of some physical or chemical modification taking place during the geological times. In fact, the term "hardening" does not make here reference to a behaviour with respect to A. F. demagnetization but to the fact that this magnetization would be no more viscous at the present time.

3. We will refer only to experiments carried out with weak-field VRM, especially VRM due to the earth's magnetic field which are the most interesting ones for paleomagnetism. Some experiments in higher fields have been reported elsewhere [BIQUAND et al., 1971].

4. When we affirm that the VRM may have varying hardness with respect to A. F. treatment, this does not mean that we refer especially to VRM acquired during long periods, geological times for example. If the influence of t on the hardness is sure, it is not the most important parameter [BIQUAND and PRÉVOT, 1970; PRÉVOT and BIQUAND, 1970; BIQUAND et al., 1971]; a VRM acquired during a long time in one rock may be softer than a VRM acquired during a short time in another rock. We

have chosen for this paper, except for some experiments described at the end of section II, the experiments performed with a constant time t equal approximately to one month.

2.3 Results with volcanic rocks

Figure 1 shows A. F. demagnetization curves of VRM acquired during one month in the earth's magnetic field by various volcanic rocks. As usually observed in igneous rocks, the carrier of remanence is titanomagnetite. This assertion is confirmed by the shape of the curves giving the isothermal remanent magnetization (IRM) as a function of the field which generates it: the IRM saturates below 2000 Oe.

The hardness of the VRM acquired during a given time t is very much varying from one rock to another, but in general it appears much larger than in RIMBERT'S experiments. In the more extreme case encountered the VRM acquired during one month is only erased by an alternating field whose effective (r.m.s.) intensity is about 300 Oe. For such volcanic rocks it may be difficult, if viscosity is important, to determine the direction and even the polarity of the primary remanent magnetization. A few lavas from the Velay area, which still have, after cleaning, a normal direction of magnetization, are nevertheless characterized by a reversed TRM, as it can be shown by studying the underlying baked contact.
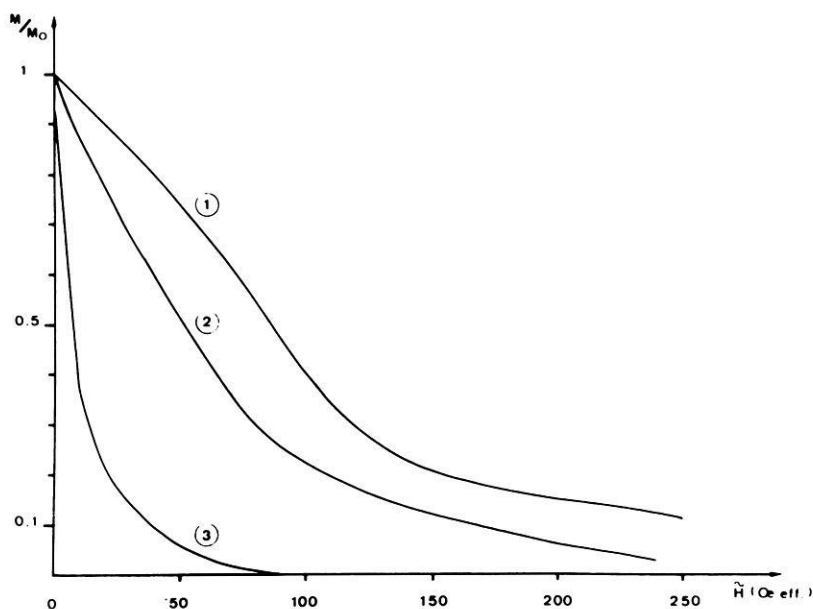
Fig. 1: Normalized A. F. demagnetization curves of VRM acquired during one month in the earth's magnetic field ($h = 0,46$ Oe) by basalt samples collected from three different lava flows from Velay and Aubrac (Massif Central, France).
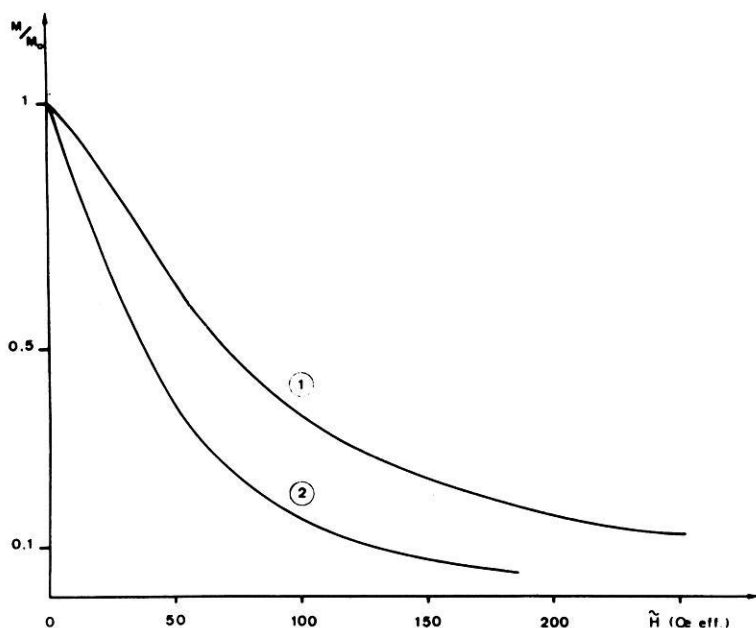
Fig. 2: Normalized A. F. demagnetization curves of VRM corresponding to $t = 1$ month and $h = 0,46$ Oe for two titanomagnetite bearing clays from the Massif Central (France). Curve (1): Senèze deposit; curve (2): Aubepin deposit.

2.4 Results with titanomagnetite-bearing sedimentary rocks

Figure 2 shows A. F. demagnetization curves of VRM acquired during one month in the earth's magnetic field by two sedimentary samples taken from two argillaceous formations, the Aubépin and the Senèze series, situated in the Velay area (Massif Central, France). Owing to the large intensity of magnetization, the carrier of remanence is thought to be titanomagnetite. The fact that IRM saturates for a relatively low field (about 2000 Oe) supports this proposal which has been confirmed for the sample 1 by X-ray-analysis. The size of grains of these titanomagnetites is probably smaller than in most volcanic rocks.

The hardness of VRM acquired by the sedimentary rocks studied is of the same order as that found for volcanic rocks in 2.3 and differs equally from one sample to another. But the relative viscosity being often much more strong in sedimentary rocks than in volcanic ones, the part of the VRM acquired in situ which remains after treatment by alternating fields of 100 or 200 Oe effective field can be still important with respect to the primary magnetization. In the worse case, the residual VRM may conceal the actual negative polarity of this last one. This case has been encountered in some layers from the Aubépin (BIQUAND 1969) or from the Senèze

[PRÉVOT and DALRYMPLE 1970) formations. Now, when they are studying oceanic sedimentary cores, most people do not clean the samples with an alternating field higher than 100 or 200 Oe peak. Consequently, one viscous effect is perhaps to the origin of the surnumerous "direct" levels, recognized in some oceanic cores, which do not seem to correspond to direct geomagnetic polarity events [KENNETT and WAT-KINS 1970).

2.5 Results with hematite-bearing rocks

Many paleomagnetic investigations are based upon "red rocks" the carrier of remanence of which seems to be in most cases hematite. In such rocks, viscosity is often very large.

The hardness with respect to A. F. treatment of VRM acquired by these rocks has been studied by Russian and French authors. Some of their results are shown in figure 3. The hardness is much variable but in general much stronger than that obtained with titanomagnetite-bearing rocks. Curves (2), (3) and (4) show that two
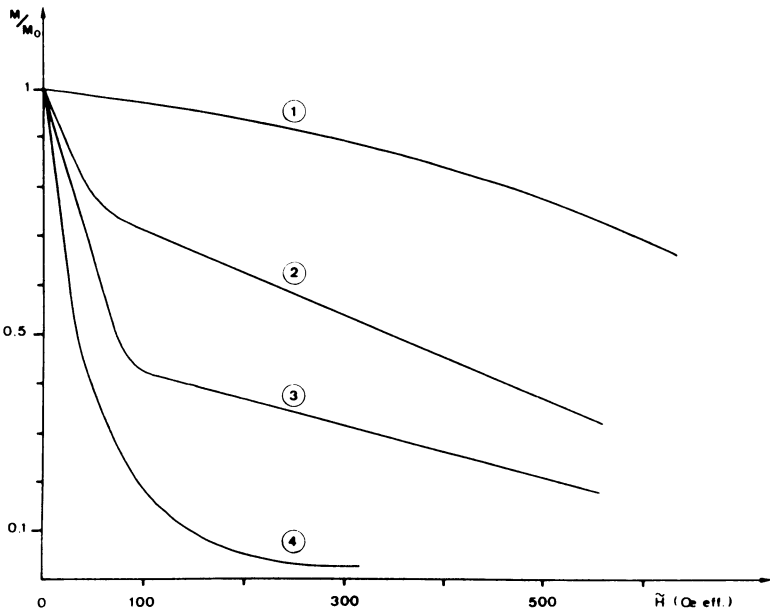
Fig. 3: Normalized A. F. demagnetization curves of VRM acquired during about one month in the earth's magnetic field by hematite bearing sedimentary samples. Curve (1): red limestone from Aix-en-Provence-Basin; Curves (2), (3), (4), drawn from AVCHYAN and FAUSTOV [1966], are obtained with red-earth clays of the Kazan stratum and of the Tatanic stratum: curve (2) corresponds to sample no 1010, curve (3) to sample no 1034 and curve (4) to sample no. 1112.

independent components of VRM, the hardnesses of which are not related, may be present in each sample, the soft component being the origin of the rapid initial decrease of the curves. The case of sample 1 is more simple: the hard component is the only one present.
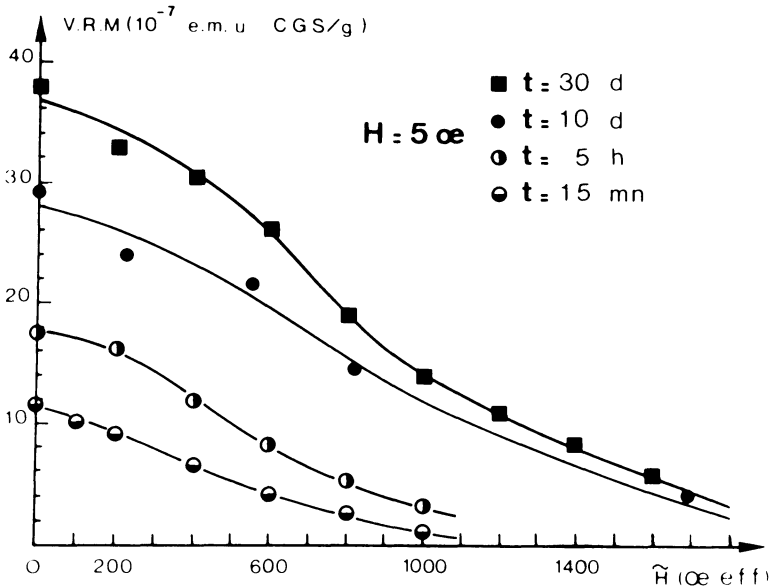
Fig. 4: A. F. demagnetization curves of VRM acquired by the red limestone corresponding to curve (1) in figure 3.

Figure 4 shows, for this last sample, demagnetization curves for VRM acquired during varying times t under the influence of a field of 5 Oe. A field of such an intensity allows to study easily the influence on the hardness of time t even when this last one has very low values. The hardness of a VRM acquired in 5 Oe is the same, for the same value of t, as the one acquired in the earth's magnetic field; ten percent of a VRM acquired during 30 days subsist after the action of an alternating field the effective intensity of which is 1700 Oe. In other words, in such a case, the A. F. treatment does not allow, undoubtedly, to distinguish the primary remanence from the viscous one acquired in situ. Moreover, we see that if the hardness decreases when reducing t, this decrease is weak: a field with an effective intensity of 1200 Oe is required to erase a VRM acquired during 15 minutes.

A number of authors have been confronted when studying red rocks with a puzzling secondary magnetization resistant to A. F. treatment and directed along the present geomagnetic field. This magnetization, supposed recent owing to its direction,

was thought to be either a cristalline one or a "hardened" viscous one. Our results show that it can be a VRM, recent indeed, but nevertheless very resistant with respect to alternating fields.

3. Theoretical Interpretation

Two cases are to be distinguished according to the single domain or multidomain structure of magnetic grains. The theoretical approach in the two cases is somewhat different and we will discuss them seperately.

3.1 Single-domain grains

The results obtained in section 2.5 for some red rocks can be interpreted by the single domain theory of viscosity developed by NÉEL [1949] if we assume that the VRM is carried by the fine-grained hematite responsible of the red colour of the rock.

Let us consider (fig. 5) the NÉEL diagram (v, H_c) in which each particle in a remanent ensemble is specified by a point, the coordinates for which are its volume v and its coercive force H_c. Let us consider in this diagram the "blocking-curves", $\mathcal{H}(T, h, t)$
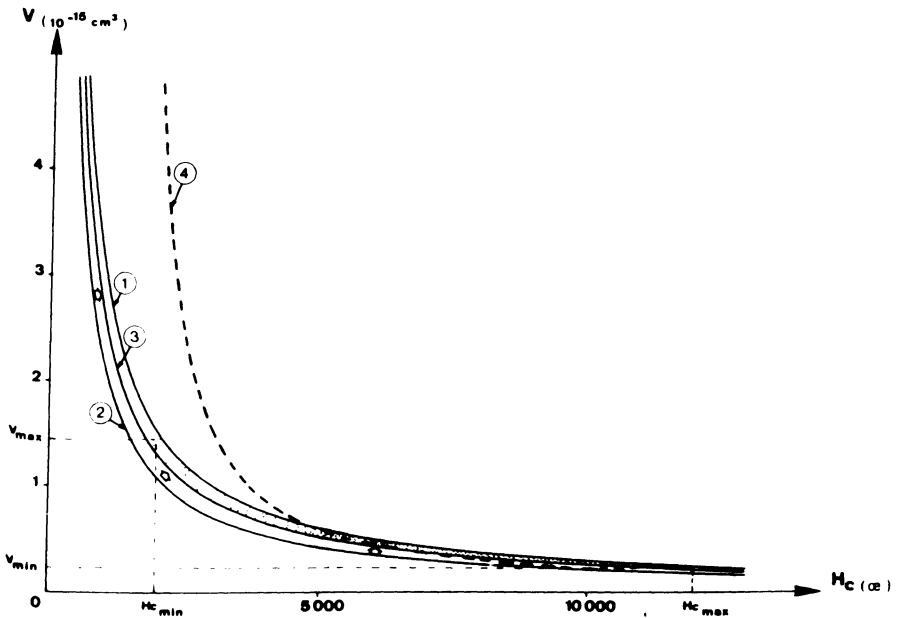
Fig. 5: Diagram giving, according to the NÉEL single domain theory, an estimate of the volume-coercive force distribution for the grains carrying the VRM (30 days, 5 Oe, 5 hours) corresponding to the upper curve of figure 4. The area in grey contains 80% of the magnetization. For further explanations see text.

in Néel's notation, separating stable particles from superparamagnetic ones under the conditions (T, h, t), T being the absolute temperature, which is constant and equal to room temperature in the experiences reported here. When h is weak or equal to zero, the equation of curve $\mathscr{H}$ is:

$$v \cdot H_c = \frac{2kT}{I_s}(Q + \ln t) \tag{1}$$

in which k is Boltzmann's constant, I_s the spontaneous magnetization of the grains (having a value of 1 emu/cm³ for hematite) and Q a factor essentially constant having a value of 22.7.

The different curves $\mathscr{H}$ represented in figure 5 correspond to the following respective values for t:

curve (1) $t = 30$ days
curve (2) $t = 3$ minutes
curve (3) $t = 5$ hours

The grains carrying the viscous remanence acquired in thirty days in a low field (5 Oe for example) are situated between the two curves (1) and (2) if the time t' is equal to 3 minutes or between the two curves (1) and (3) if the time t' is equal to 5 hours. It can be seen that the grains carrying the VRM (t, h, t') may correspond to a large range both for H_c and v, whatever t and t' are. In particular, VRM can affect grains with a very high coercivity even for a short time t, provided that the volumes are sufficiently small.

The grains which are unblocked by the alternating field H are those which are on the left side of a curve of the type (4) and which equation is:

$$v \frac{(H_c - H)^2}{H_c} = \frac{2kT}{I_s}(Q' + \ln t) \tag{2}$$

Q' being essentially constant having a value of 22.0. This curve has the vertical asymptote $H_c = H$, and, when H increases, shifts to the right with an almost horizontal translation. We see that the hardness of a VRM with respect to A. F. treatment can be extremely variable according to the distribution of grains in the VRM area. In particular, the occurence of a hard VRM can be explained by the presence of viscous grains with high coercivities and correlatively very small volumes. Moreover, a given rock can carry at the same time a soft and a hard VRM (figure 3, curves (2), (3) and (4)) if two distinct populations of magnetic grains, having very distinct average values of H_c and v, are present in the VRM area.

The coercive force and the diameter of the grains carrying the VRM can be calculated [Biquand, Prévot and Dunlop, 1971] by using the method applied by Dunlop and West [1969] to partial TRM. Let us particularly study the case of hard VRM, for example the case of the VRM, corresponding to the curves of figure 4. The partic-

ular curve (4) represented in figure 5 corresponds to the alternating field $H_{1/2}$, equal to 1130 Oe, which erases half of the VRM acquired in thirty days. The coercive force of the grains just concerned by this alternating field is $H_{c_{\frac{1}{2}}} = 5450$ Oe and their diameter is $d_{1/2} = 0.1$ μ. Using the experimental demagnetizing curve of figure 4 we find that 80% of the VRM (30 d, 5 Oe, 5 h) is carried by grains whose coercive forces are comprised between 1960 and 12100 Oe (H_c min. and H_c max. in figure 5), the corresponding diameters being 0.14 μ and 0.08 μ. The figure 5 allows also to understand why the hardness does not depend critically on parameters t and t'. All curves defining different VRM are very near one of each other. On such a small scale the density of grains in the proximity of these curves is constant. Consequently the VRM (30 d, 5 Oe, 5 h) and the VRM (15 mn, 5 Oe, 1 mn) are carried by grains whose characteristics are closely related. For the second VRM we still have $H_{c1/2} = 4500$ Oe and $d_{1/2} = 0.09$ μ.

The extreme coercivities which are involved to explain such hard VRM encountered in red rocks are plausible only with hematite grains. In this mineral large coercivities cannot be due to an anisotropy of form owing to the weak intensity of the spontaneous magnetization and are probably due to magnetocristalline anisotropy.

In magnetite grains, H_c, which seems to be due to an anisotropy of form, is much more weak. A large value of the macroscopic coercive force (2000 Oe) may be found in igneous rocks bearing silicates with exsolved magnetite particles [EVANS and MC ELHINNY, 1969], but it is not common. The moderate hardness of the VRM acquired by the titanomagnetite-bearing sedimentary rocks could be explained, consequently with the monodomain theory.

3.2 Multidomain grains

The first theoretical interpretation of viscous magnetization in rocks bearing dispersed multidomain magnetic grains was given by NÉEL [1955], using the model he had previously proposed for ferromagnetic substances [NÉEL, 1950, 1951]. He arrived at the conclusion that the effect of t is equivalent to the effect of a supplementary fictive field $\pm H_i(t)$ of which the maximum value is given by:

$$H_i(t) = S_v(Q + \ln t)_{\rfloor} \tag{3}$$

where S_v and Q do not depend on t.

The effect of thermal fluctuations being reduced to the effect of a magnetic field, it is obvious that, in the PREISACH-NÉEL diagram, the curves of equal relaxation time and of equal magnetic field will be parallel. As can be seen in figure (6a), these curves are straight lines parallel to the b axis. The VRM acquired when t increases from t to $t + \Delta t$ corresponds to a well-defined and quite narrow range of critical fields a, which varies from a_m to $a_m + \Delta a_m$. In other words, there is an univocal relationship between t and a. The alternating magnetic field H_d which erases a VRM

(t, h, t') is equal to the maximum value a_m of the critical field and increases with t and S_v. So, it can be expected that, for multidomain grains, a hard VRM (t, h, t') is correlated with a higher S_v value than a soft VRM (t, h, t'). On the other hand, it can be deduced from equation (3) that the slope of the curve VRM $= f(t)$ is determined by the value of S_v and increases with it. Thus a hard VRM should be also characterized by a more rapid increase with t than a soft one.

VRM in volcanic rocks being usually carried by multidomain grains, the NÉEL theory should be valid for these rocks, in particular for the samples corresponding to figure 1. Let us consider, for example, the samples 1 and 3. The hardness of the VRM acquired by these two samples being very different, the slopes of the curves VRM $= f(t)$ should not be, consequently, the same. On the contrary we find that the slope of these curves is essentially the same for the two samples. Thus our experimental results cannot be explained by the NÉEL theory.

A possible explanation of these results is that the movements of domain walls which results in, respectively, magnetization due to thermal fluctuations and magnetization by an isothermal "instantaneous" process are not necessarily related with the same type of potential barriers. AVER'YANOV [1967] has shown that barriers with different critical fields may have the same probability of being overcome by
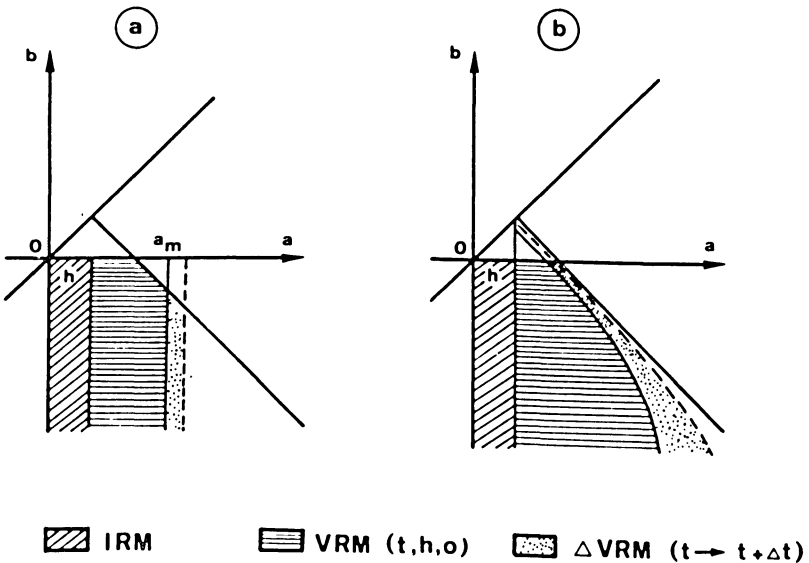

Fig. 6: PREISACH diagram for multidomain grains showing the distribution of the two critical fields a and b for a VRM acquired in a field h (the initial demagnetized state is obtained by mixing the powder):

    a distribution involved by the NÉEL theory;
    b distribution according to BELOKON' and al.

thermal fluctuations. In particular, VRM can be created by overcoming potential barriers with relatively high critical fields. So, in the PREISACH diagram, curves of equal magnetic field and of equal relaxation time are different (BELOKON' et al., 1969). When t increases from t to $t + \Delta t$, the growing of the VRM corresponds to a large range of critical fields (fig. 6b). The results presented above for the volcanic rock samples 1 and 3 can now be explained easily if we assume that the increase of the VRM, though being the same in the two cases, is due to overcoming of potential barriers with quite different critical fields: less than to 10 Oe for sample 3 and equal approximatly to 90 Oe for sample 1.

Let us notice that this qualitative interpretation is analogous to the explanation given above for single domain grains. But critical fields of multidomain grains being usually less than to 100 Oe for magnetite [PARRY, 1965], it is obvious that VRM with very high coercivities cannot be expected with large particles.

4. Conclusion

The fact that the VRM acquired in the earth's magnetic field by rocks, especially by hematite bearing sedimentary rocks, can be quite difficult to erase by the widely used A. F. demagnetization technique, is a rather worrying phenomenon in paleo-magnetism. But let us notice that a thermal treatment is probably more efficient to erase the VRM, because this magnetization is due to thermal fluctuations. The identity between the effects of time and temperature is obvious when the NÉEL theory of monodomain grains is considered: the temperature θ_d needed to erase thermally a weak field VRM is not related with the coercivities of the grains carrying this magnetization.

The upper limit of the temperature θ_d for a VRM acquired by a rock during the present geomagnetic polarity epoch should be near $300 \,^{0}C$ according to WILSON and SMITH [1969] or near $200 \,^{0}C$ according to DUNLOP [1969]. A heating at moderate temperatures should be thus sufficient to destroy any weak field VRM, hard or not.

References

AVCHYAN, G. M. and S. S. FAUSTOV: On the stability of viscous magnetization in variable magnetic fields. Izv. ,Earth Physics, no. 5, 96—104, 1966

AVER'YANOV, V. S.: Theory of the thermally activated magnetic viscosity in multidomain particles of a ferromagnetic substance, I and II. Izv., Earth Physics, no. 8, p. 74—82 and no. 9, 45—50, 1967

BELOKON', V. I., V. V. KOCHEGURA and L. E. SHOLPO: The model of the viscous magnetization process in a small field as obtained from the Preisach-Néel scheme. Izv., Earth Physics, no. 1, 63—68, 1969

BIQUAND, D.: Sur les directions de l'aimantation rémanente des couches rouges du Trias supérieur du Bassin de Carentan (Normandie). C. R. Ac. Sc., Paris, 264, sér. D, 1597—1600, 1967

BIQUAND, D.: Incertitudes de la détermination des époques de polarité géomagnétique directe et inverse dans certaines formations sédimentaires. VIIIe Congrès INQUA, 1969, Résumé des communications, p. 343.

BIQUAND, D. and M. PRÉVOT: Sur la surprenante résistance à la destruction par champs magnétiques alternatifs de l'aimantation rémanente visqueuse acquise par certaines roches sédimentaires au cours d'un séjour, même bref, dans le champ magnétique terrestre. C. R. Ac. Sc., Paris, 270, sér. B, 362—365, 1970

BIQUAND, D., M. PRÉVOT and D. J. DUNLOP: Une aimantation rémanente visqueuse très résistante envers les champs alternatifs dans une roche sédimentaire contenant de fines particules d'hématite. J. Phys., 32, C_1^- 1043 à C_1^- 1044, 1971

CREER, K. M.: Paleomagnetic investigations in Great-Britain 5, the remanent magnetization of unstable Keuper marls. Phil. Trans. Roy. Soc., London, A, 250, 130—143, 1957

DUNLOP, D. J.: Comments on a paper by R. L. WILSON and P. J. SMITH "The nature of secondary natural magnetization in some igneous and baked rocks". J. of Geomagn. and Geoelec., 21, 4, 797—799, 1969

DUNLOP, D. J. and G. F. WEST: An experimental evaluation of single domain theories. Rev. Geophys., vol. 7, 4, 709—757, 1969

EVANS, M. E. and M. W. McELHINNY: An investigation of the origin of stable remanence in magnetite bearing igneous rocks. J. of Geomagn. and Geoelec., 21, 4, 757—773, 1969

KENNET, J. P. and N. D. WATKINS: Geomagnetic polarity change, volcanic maxima and faunal extinction in the south Pacific. Nature, vol. 227, 5261, 930—934, 1970

NÉEL, L.: Théorie du trainage magnétique des ferromagnétiques en grains fins avec applications aux terres cuites. Ann. Geophys., 5, 2, 99—136, 1949

NÉEL, L.: Théorie du traînage magnétique des substances massives dans le domaine de Rayleigh. J. Phys. Rad., 11, 2, 49—61, 1950

NÉEL, L.: Le traînage magnétique. J. Phys. Rad., 12, p. 339—351, 1951

PARRY, L. G.: Magnetic properties of dispersed magnetite powders. Philos. Mag., 11, 110, 303—312, 1965

PLESSARD, C.: Vérification expérimentale du test de E. Thellier concernant l'élimination approchée de l'effet d'aimantation visqueuse dans les roches. IAGA Bull., 24, 1967

PRÉVOT, M. et D. BIQUAND: Sur la plus ou moins grande résistance de l'aimantation rémanente visqueuse portée par des roches sédimentaires ou volcaniques au traitement par des champs magnétiques alternatifs. C. R. Ac. Sc., Paris, 270, sér. B, 1365—1368, 1970

PRÉVOT, M. and G. B. DALRYMPLE: Un bref épisode de polarité géomagnétique normale au cours de l'époque inverse Matuyama. C. R. Ac. Sc., Paris, 271, 2221—2224, 1970

RIMBERT, F.: Sur l'action de champs alternatifs sur des roches portant une aimantation rémanente isotherme de viscosité. C. R. Ac. Sc., Paris, 242, 2536—2538, 1956

RIMBERT, F.: Contribution à l'étude de l'action des champs alternatifs sur les aimantations rémanentes des roches. Applications géophysiques. Rev. Inst. franç. Pétrole, XIV no. 1 et 2, 1—123, 1959

SHOLPO, G. P. and L. E. SHOLPO: A study of the processes of stabilization of the remanent magnetism of rocks. Izv. Earth Phys., 5, 108—116, 1965

THELLIER, E.: Sur l'aimantation dite permanente des basaltes. C. R. Ac. Sc., Paris, 204, 876—879, 1937

THELLIER, E.: Sur l'aimantation des terres cuites et ses applications géophysiques. Ann. Inst. Phys. Globe, Paris, 16, 157—302, 1938

THELLIER, E. and O. THELLIER: Sur l'intensité du champ magnétique terrestre dans le passé historique et géologique. Ann. Géophys., 15, 3, 285—376, 1959

TRUKHIN, V. I.: An experimental investigation of magnetic viscosity. Izv., Earth Phys., 5, 105—111, 1966

WILSON, R. L. and P. J. SMITH: The nature of secondary natural magnetization in some igneous and baked rocks. J. Geomagn. Geoelec., 20, 4, 367—380, 1968

Some Palaeomagnetic Problems
of Strongly Oxidized Rocks

K. M. STORETVEDT, Bergen[1])

Summary: Based on some recent palaeomagnetic data a brief outline of the most important paleomagnetic problems caused by low temperature oxidation is presented.

Zusammenfassung: Der Einfluß der Oxydation von Erzmineralen bei tiefen Temperaturen auf Ergebnisse des Paläomagnetismus wird unter Berücksichtigung neuerer Untersuchungen kritisch diskutiert.

Directions of remanent magnetization of rocks only have palaeomagnetic applicability when it can be inferred that they were acquired essentially parallel to a geomagnetic field existing at a given time in the geological past. Only magnetizations associated with relatively high magnetic stability will have a reasonable chance of persisting throughout geological times. Therefore, the magnetizations deduced after erasing the low stability components have generally been considered as representative estimates of past geomagnetic fields. For instance, the high magnetic stability of many lavas has been related to grain-size effects and to a high degree of high temperature oxidation [LARSON, OZIMA, OZIMA, NAGATA, STRANGWAY 1969a]. Recently, however, the role of low temperature oxidation processes, for instance in lavas, has been better documented indicating that the build-up of the palaeomagnetic record may be far more complex than generally assumed [STORETVEDT 1970a]. Thus, recent studies of Permian lava flows of Southern Norway [STORETVEDT and PETERSEN 1970] and of Devonian volcanics of the Orkney islands [STORETVEDT and PETERSEN 1971] have revealed low temperature magnetization processes covering a considerable span of geological time. Up to three different magnetization directions of high thermal stability (blocking temperature around 650°C) have been observed in a single lava specimen. The conclusions reached from the analysis of remanent magnetization are strongly supported by magnetomineralogical evidence. After having observed such complex structures and anticipated their importance in nature by noting a large number of potential examples in the literature one feels strongly that many of the traditional procedures in palaeomagnetism may result in serious misinterpretations.

---

[1]) Dr. K. M. STORETVEDT, Department of Geophysics, University of Bergen, Bergen, Norway.

It is the opinion of the present author that a new attitude or approach to palaeo-magnetic problems is highly needed. The following discussion of two recent papers may serve as a brief outline of some of the most important aspects of this matter.

The first study to be considered is one dealing with three Palaeocene basaltic lava flows from Colorado [LARSON, MUTSCHLER, BRINKWORTH 1969b]. The primary opaques have been variably affected by high-temperature oxidation, i. e. mainly the development of ilmenite lamellae in titanomagnetites and the progressive alteration into phases as metailmenite, haematite and pseudobrookite. In samples of no or little high temperature alteration maghemitization (a low temperature oxidation process) has taken place in varying degrees. Haematite occurs both as deuteric and as supergene alteration products. Although these observations suggest that secondary magnetization components of high magnetic stability may exist in these lava flows, LARSON and coworkers apparently suggest that the stable magnetic components deduced (except for four samples) are entirely of deuteric origin. However, a closer inspection of the distribution of the directional data presented reveals remanence properties which are not in accord with this assumption.

The sample directions cleaned for low stability magnetization by application of AC fields up to 250 Oe are shown in fig. 1. An observation of exceedingly great importance is the tendency of smeared distributions. This is clearly recognized by flow 1 data (solid arrow) but there is also evidence that an overall meridional distribution (broken arrow) exists.
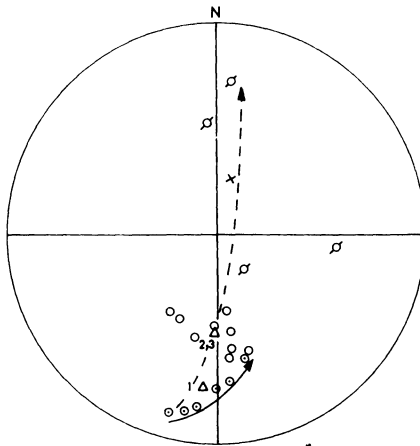
Fig. 1: Magnetization directions (cleaned in 250 Oe) of samples from three Palaeocene lava flows from Colorado as given by LARSON et al. [1969b]. All directions are on upper hemisphere. Samples from flow 1 are marked with a dot in centre. Triangles are flow mean directions. Sample directions with ticks have been excluded from statistical analysis by the authors. The cross is the present inclined dipole. The arrows indicating directional trends have been added by the present author.

It seems likely that the dominating component (reversed) reflect the original geomagnetic field, but in addition there are good reasons for adopting a second component of normal polarity. This latter component is probably associated with the observed low temperature ore mineral transformations in which maghemite and haematite may be the important magnetic phases. The slow reaction rate at low temperatures has probably enabled secondary magnetizations to be formed over a longer time interval; the processes appear at least to have proceeded into the subsequent normal polarity epoch. The two principal magnetization components suggested (a reversed one of partly deuteric and partly secondary origin and a normal one of entirely secondary origin) cannot be expected to be exactly antiparallel and consequently intermediate directions are likely to occur. Thus, a rock formation which is variably affected by remagnetization in the opposite field may exhibit apparently stable magnetization directions distributed to a greater or lesser extent along a great circle through the two field directions involved. Therefore, if high bulk stability is uncritically associated with originality of magnetization false information, for instance about the geomagnetic field behaviour in the act of polarity inversion, may be provided.

Four samples with deviating remanence directions (marked with ticks in fig. 1) were excluded from statistical treatment. Because of a relatively strong intensity of magnetization in these samples LARSON and coworkers suggest remagnetization by lightning. In view of the available information, however, this latter assumption appears entirely at question. Thus, such an increase of the remanence intensity (which is commonly recorded in the weathering zone of igneous rocks) may be directly connected with a strongly developed maghemitization, and the anomalous samples concerned may well contain a strong low temperature magnetization of normal polarity. The high coercive forces of the magnetic oxidation products render the AC method (at least in its present state of development) rather irrelevant. For achieving a splitting-up of any composite magnetization of oxidized rocks the high stability region of the remanence has to be carefully analysed down to very low intensities [STORETVEDT 1970a, STORETVEDT and PETERSEN 1970, 1971]. At present, this can only be achieved by application of thermal demagnetization carried out in a nearly ideal field-free space. Furthermore, it appears wrong to deal rigorously with sample mean directions in the analysis of palaeomagnetic data because an averaging of specimen directions of each sample would have a tendency to obscure existing directional trends which may be of decisive importance for a proper interpretation of the formational results.

The unavoidable conclusion of the above discussion is that LARSON and coworkers have apparently not been aware of the remagnetization problems indicated by their data. Consequently, the mean directions estimated are unlikely to represent true estimates of the palaeofields in question. In fact, it does not seem unlikely that the palaeoinclination of two of the lava flows (flows 2 and 3) has been overestimated by as much as 40 degrees.
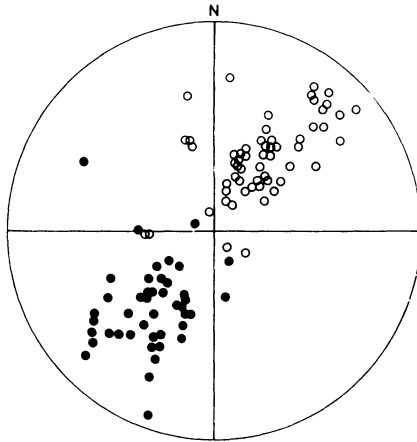
Fig. 2: Palaeomagnetic results (sample directions) of Lower Devonian lavas from Southern Scotland as given by McMurry [1970]. The directions are corrected for tectonic movements. Open circles are directions in upper hemisphere and full circles directions in lower hemisphere.

Another example strongly anticipating remagnetization problems is given by a recent paper by McMurry [1970] on Lower Devonian lavas of Southern Scotland. Again, the data presented involve routine AC analysis only but no information about the ore minerals is given. However, a recent study of some other Lower Devonian lavas of Southern Scotland has revealed haematite as a very important remanence carrier [Storetvedt and Halvorsen 1968]. The predominance of haematite strongly indicates the presence of an extensive low temperature oxidation. That such low temperature processes also must have affected the lavas studied by McMurry [1970] is strongly indicated by the results of fig. 2. Though tilt correction gives a three-fold increase in Fisher's [1953] dispersion parameter K there is a clear directional trend in the data. Thus, the variation in inclination in the normal as well as in the reversed group is about 90 degrees while the corresponding variation in declination is roughly 25 degrees in both cases. Nevertheless, McMurry [1970] considers the tilt-corrected data as representing true palaeomagnetic directions of pre-folding (pre-Upper Devonian) origin. Concerning the possibility of remagnetization [Storetvedt 1970b] he states: "If partial remagnetization were important, one would not expect to find antiparallel normal and reversed directions. On the other hand, if it is assumed that the lavas have been almost completely remagnetized (and this would have to produce normal and reversed directions as well) then the fold test indicates that this happened in Devonian times which is the period of interest anyway".

These arguments implicitly state that the remagnetization problems have not been fully understood. Of great importance in this context is the evidence of a simple geomagnetic polarity sequence in Old Red Sandstone time, i. e. the polarity changed

from normal to reverse in late Lower-early Middle Devonian [STORETVEDT 1970b, STORETVEDT and PETERSEN 1971]. As the development of low temperature magnetizations may be extremely slow (thus more than 50 m. y. appear to have been necessary for a complete ore mineral oxidation in some Permian lava flows of Southern Norway) these processes may have been important in the considered rocks far beyond the time of postulated field inversion. Thus, lavas which underwent a relatively high ore mineral oxidation in the Lower Devonian would have greater possibilities of maintaining the original polarity (normal) than those being relatively unoxidized at the time of field inversion. These latter flows would more easily change their polarity during the further chemical alterations. For both polarity groups, however, a certain "contamination" of the oppositely directed magnetization may be expected. On present information this seems to be a reasonable explanation of the data of fig. 2.

Because of the significant increase in the dispersion parameter after applying tilt correction McMURRY [1970] appears to be rather over-confident about his results. It must be strongly stressed, however, that such an improvement of the grouping of remanence directions does not necessarily imply that a single magnetization component is at hand, but merely that a pre-folding magnetization contributes the larger magnetic fraction of the remanence studied. Consequently, a "positive fold test" does not make further laboratory tests superfluous.

For reasons given above it seems reasonable to conclude that most likely the data of McMURRY [1970] do not reflect a true Devonian geomagnetic field for Europe. A splitting-up of the supposed composite magnetization would (after correction for tectonism) probably give magnetization directions of quite shallow inclination.

Remagnetization problems as discussed above are likely to be very common in surface formations having originated at low-intermediate palaeolatitudes. For instance, they appear to be fundamental problems in European Palaeozoic lavas [STORETVEDT 1970a]. On the other hand, composite magnetizations giving deviating resultant directions are far less pronounced in the Palaeozoic red beds. This difference is most likely due to the fact that low temperature oxidation will advance rather slowly in compact rocks like lavas while in the sediments an ultimate oxidation state of the ore minerals may have been achieved relatively soon after deposition.

In the experience of the present author the following points are relevant when dealing with palaeomagnetism of strongly oxidized rocks:

1. After removal of unstable components of magnetization a close inspection of all the data at the specimen level of observation is necessary. "Strung-out" tendencies of stable bulk magnetization should be carefully looked for. A straightforward calculation of sample means, site means etc. and exclusion of apparently anomalous results may easily spoil essential information about the magnetization build up.

2. A careful analysis of the high stability region of the remanence (down to low intensity levels) is always necessary. Even in cases of clustered groupings and of nearly exact antiparallelism between normal and reversed groups such an analysis has proved worth while. At present, thermal demagnetization seems to be the only

relevant demagnetization technique. However, as the blocking temperature spectrum of the various components involved may be nearly identical the experimental problems are generally severe.

3. If it has been shown that the magnetization consists of one single component or if one or more sub-components has been sucessfully separated the estimation of relevant mean values can proceed. It should be stressed, however, that at least in some cases (for reasons given above) only indications of the various remanence directions can be achieved. Therefore, lava flows of high bulk magnetic stability may well be unsuitable for many palaeogeophysical studies.

References

FISHER, R. A.: Dispersion on a sphere, Proc. Roy. Soc. London, Ser. A, 217, 295—305, 1953

LARSON, E. E., Mituko OZIMA, Minuro OZIMA, T. NAGATA and D. STRANGWAY: Stability of remanent magnetization of igneous rocks, Geophys. J., 17, 263—292, 1969a

LARSON, E. E., F. E. MUTSCHLER and G. L. BRINKWORTH: Paleocene virtual geomagnetic poles determined from volcanic rocks near Golden, Colorado, Earth and Planet. Sci. Letters, 7, 29—32, 1969b

McMURRY, E. W.: Palaeomagnetic results from Scottish lavas of Lower Devonian age, In Palaeogeophysics (Academic Press, London), 253—262, 1970

STORETVEDT, K. M.: On remagnetization problems in palaeomagnetism; further considerations, Earth and Planet. Sci. Letters, 9, 407—415, 1970a

STORETVEDT, K. M.: The Devonian palaeomagnetic field for Europe, In Palaeogeophysics (Academic Press, London), 247—252, 1970b

STORETVEDT, K. M., and E. HALVORSEN: On the palaeomagnetic reliability of the Scottish Devonian lavas, Tectonophysics, 5, 447—457, 1968

STORETVEDT, K. M., and N. PETERSEN: On chemical magnetization in some Permian lava flows of Southern Norway, Z. Geophys., 36, 569—588, 1970

STORETVEDT, K. M., and N. PETERSEN: Palaeomagnetic properties of the Middle-Upper Devonian volcanics of the Orkney islands, 1971, submitted to Earth and Planet. Sci. Letters.

An Advanced Device for Chemical Demagnetization
of Red Beds[1])

P. J. Burek, Karlsruhe[2])

Summary: It is possible to separate in red beds secondary, chemically grown magnetic components (CRM) from the originally acquired depositional remanence (DRM) by means of HCl-bleaching under pressure. A device useful for the chemical demagnetization technique is described. The chemically derived palaeomagnetic results are supported by palaeoclimatic evidence.

Zusammenfassung: Durch HCl-Bleichung unter Druck können in Rotsedimenten sekundäre, chemische Magnetisierungskomponenten (CRM) von der ursprünglichen, depositionellen Remanenz (DRM) getrennt werden. Eine für die chemische Entmagnetisierung nützliche Druckzelle wird beschrieben. Die auf diese Art erarbeiteten paläomagnetischen Resultate werden paläoklimatisch gestützt.

The chemical demagnetization method proves to be an effective way to remove secondary chemically grown magnetic components (CRM) within the red staining of clastic sediments from the originally acquired depositional remanence (DRM). Earlier a simple device for chemical demagnetization of red beds by means of high pressure HCl was described [Burek 1969]. However, that pressure cell turned out to be useful only for coarse to medium grained sandstones, but had serious disadvantages for more compact materials. Sealing problems did not allow to force acids through the inner parts of fine grained and well cemented sediments.

Fig. 1 shows details of a more sophisticated device. It is basically the "Hassler cell", used by the oil industries to test permeability and porosity of castic materials. The device described below is very similar to one I have on loan from Mobil Research and Development Inc., Dallas, Texas.

The pressure cell (Fig. 1) essentially consists of a steel cylinder with an inlet for oil and an inner rubber hose. The ends of the hose are bent over both rims of the cylinder and are clamped with two sealing-plates around the end of the cylinder. By means of a hydraulic press oil is forced between the walls of the cylinder and the clamped

---

ACID-INLET

UPPER SEALING-PLATE

$\emptyset$

RUBBER HOSE

OIL-INLET

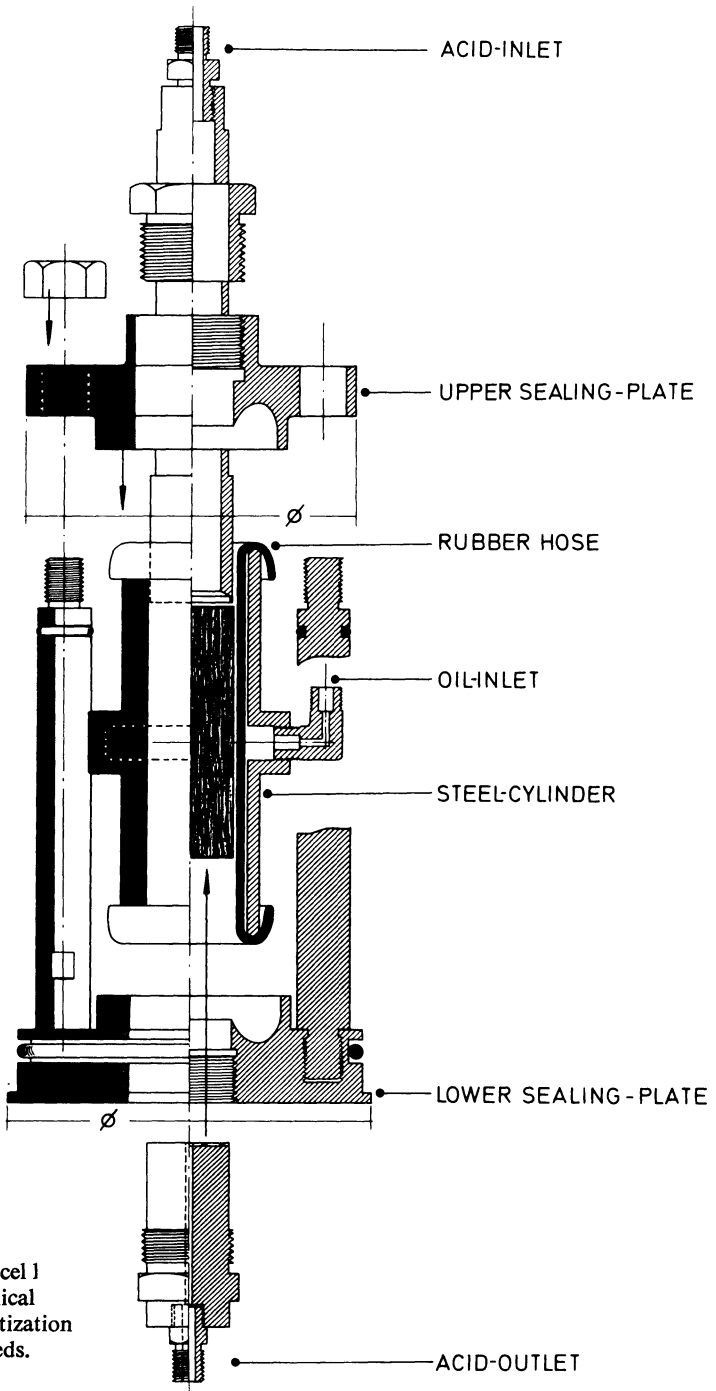STEEL-CYLINDER

LOWER SEALING-PLATE

$\emptyset$

Fig. 1:
Pressure cel l
for chemical
demagnetization
of red beds.

ACID-OUTLET

off rubber hose. This provides an excellent seal around sediment discs within the pressure unit, which allows to apply pressures > 50 kg cm^{-2} on the sediment samples.

HCl with 3 N dilution is introduced through a tubing system into the pressure device. The bottom part of the acid inlet has the same diameter ($\varnothing = 2.5$ cm) as the sediment discs. This allows to enclose the acid-tubing system within the pressure unit. Several samples rest on the acid outlet, which too is enclosed by the sealing device.

By means of regulated compressed air HCl is forced through the sediment discs (maximum pressure ≈ 50 kg cm^{-2}). The acid penetrates the sediment and bleaches the originally red colored samples. To facilitate the penetration of well cemented, fine grained material, it might be dehydrated first in a vacuum or it can be useful to attach a vacuum pump to the bottom part of the pressure cell. The magnetic grains of the heavy mineral fraction are usually not dissolved; they are only slightly attacked at the outer parts and edges. This is a desirable effect which removes secondary chemical alteration of the magnetic grain fraction, too.

After the bleaching process distilled water is forced through the samples to clean them from remaining HCl. Finally the specimens are dried by forcing compressed air through them. Stepwise bleached specimens subsequently can be treated by standard demagnetization techniques to remove secondary magnetic components within the remaining magnetic heavy mineral fraction.

Fig. 2 shows directions of the natural remanent magnetization (NRM) of Cambro-Ordovician red beds from Wadi Ram and Petra (29.7 N, 35.3 E) in the Southern Jordanian Desert. The normally magnetized group quite accurately reflects the present geomagnetic field. It was not possible to remove this secondary magnetization with the alternating field or thermal demagnetization technique.

High coercitive forces (> 2800 Oe) and high CURIE temperatures ($> 630\,°$C) indicate that hematite is the carrier of the chemically grown, very stable secondary magnetization (CRM), which almost completely dominates the remanence (NRM) of these desert red beds. There were very few samples that to a certain extent showed a memory of the original detrital magnetization (DRM). It therefore was concluded that groundwater percolating through the sandstone series continuously transports iron to the surface where Fe-hydroxides are precipitated, accounting for the red staining. The cement is quartz. Due to the arid conditions of the sampling area the Fe-hydroxides are dehydrated to hematite, producing the stable secondary chemical magnetization.

Fig. 3 shows directions of the NRM before and after chemical demagnetization. The changes are consistent and can be subdivided into two groups of opposite polarity, which are different from the present geomagnetic field. The NRM intensities were first in the order of 10^{-3} to 10^{-4} emu cm^{-3}, but decreased after bleaching to 10^{-6} to 0.5×10^{-7} emu cm^{-3}.

The Cambro-Ordovician pole of the Arabian shield derived from these chemically demagnetized rocks is found to be close to the Azores (36.7 N, 36.6 W, $n = 20$, $K = 20$, $\alpha_{95} = 7.5°$). This result is consistent with other palaeomagnetic data from
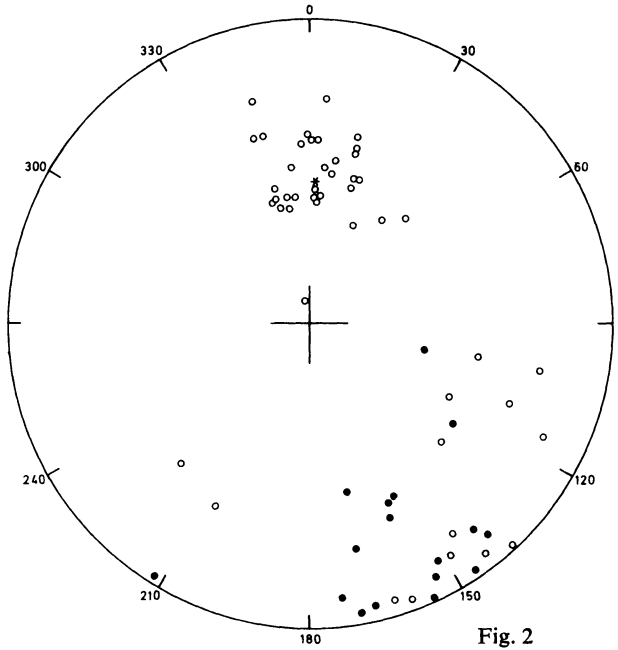
Fig. 2
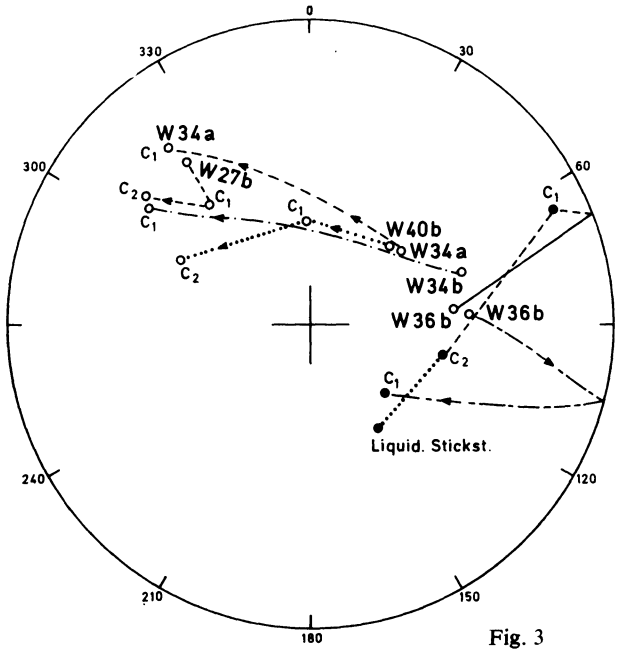
Fig. 3

Africa [BRIDEN 1968, BROCK 1968, GRAHAM and HALES 1961, McELHINNY, BRIDEN, JONES and BROCK 1968]. Extensive Ordovician glaciation traces in the Western Sahara are now well established [BEUF, BIGU-DUVAL, STEVAUX and KULPICKI 1966, FAIRBRIDGE, pers. commun.] and support the Lower Palaeozoic, palaeomagnetic poles. Furthermore, the sampling localities have a distance of about 70° Latitude from the Lower Palaeozoic magnetic poles; it is probably more than mere coincidence that the lower part of the Jordanian Ram Series is of aeolian, i. e. arid origin. Somewhat further to the east, in the Persian Gulf area extensive evaporite sequences (Lower Hormuz Series of the Eastern Zagros fold belt) have been deposited in Lower Cambrian times. This again is evidence for an arid environment of the area.

The Lower Palaeozoic palaeoclimatic profile (from polar glaciation to equator near aridity) clearly supports the Lower Palaeozoic magnetic poles, their dipole-character and their close relation to the rotational axis of the earth.

Acknowledgements

References

BEUF, S., B. BIGU-DUVAL, J. STEVAUX, and G. KULPICKI: Ampleur des glaciations Siluriennes au Sahara. Rev. Inst. Franc. Petrole Ann. Combust. Liquides, 21, 263—381, 1966.

BRIDEN, J. C.: Palaeomagnetism of the Ntonya ring structure, Malawi. J. Geophys. Res., 73, 725—733, 1968.

Fig. 2: NRM-grouping of Lower Palaeozoic Ram Sandstones (Jordan) before chemical demagnetization.

Fig. 3: Changes of NRM-directions after chemical bleaching of Lower Palaeozoic Ram Sandstones (Jordan).

BROCK, A.: Palaeomagnetic results from the Hook intrusives, Zambia. Nature, 216, 359—360, 1967.

BUREK, P. J.: Device for Chemical Demagnetization of Red Beds. J. Geophys. Res., 74, 27, 6710—6712, 1969.

GRAHAM, K. W. T. and A. L. HALES: Preliminary palaeomagnetic measurements on Silurian sediments from South Africa. Geophys. J., 5, 318—325, 1961.

McELHINNY, M. W., J. C. BRIDEN, D. L. JONES and A. BROCK: Geological and geophysical implications of palaeomagnetic results from Africa. Rev. Geophys., 6, 2, 201—238, 1968.

On the Size Distribution of Submicroscopic Magnetite and Titanomagnetite Fine Particles in Basalt

H. Markert[1]) and N. Steigenberger[2]), München

Summary: An attempt was made in order to investigate the size distribution spectrum of sub-microscopic ferrimagnetic particles in a basalt sample from the Rauher Kulm (Germany). On the basis of Neel's (1949) single-domain theory and its extensions summarized by Kneller (1966), the decrease of saturation remanent magnetic moment (produced at any fixed measuring temperature in a magnetic field of 5000 Oe) with increasing temperature (from 4°K up to room temperature) was attributed to an increasing fraction of particles becoming superparamagnetic above their respective volume-dependent critical temperatures. The implicit suppositions necessary to calculate the size distribution spectrum of that fraction of particles that become superparamagnetic within a temperature range of 4°K to 300°K are discussed together with the procedure of evaluating this spectrum from the measuring curve. Pure magnetite as well as pure titanomagnetite fine particles had been found to contribute commonly to the fration of superparamagnetic particles. In the case of magnetite the abundance of particles ranging between 600 Å and 1000 Å in diameter is about 0,94% by volume of the total ore content of the rock, while in the case of titanomagnetite the contribution of particles having diameters of 50 Å to 200 Å amounts to about 37% by volume of the total ore content of the rock.

Zusammenfassung: Ausgehend von Neel's (1949) Einbereichstheorie und ihrer bei Kneller (1966) zusammengestellten Erweiterungen wurde versucht, das Größenverteilungsspektrum des Anteils der submikroskopisch kleinen unter den ferrimagnetischen Ausscheidungen in einer Basaltprobe des Rauhen Kulm (Deutschland) zu bestimmen. Der angewandten Untersuchungsmethode liegt die Interpretation der mit wachsender Temperatur abnehmenden Sättigungsremanenz als Indiz für eine entsprechende Zunahme des superparamagnetischen Anteils der kleinen ferrimagnetischen Teilchen zugrunde. Die Sättigungsfeldstärke betrug 5000 Oe, die Temperatur konnte von 4°K bis Zimmertemperatur variiert werden. Die Erläuterung des gewählten Untersuchungs- und Auswertungsverfahrens wurde zum Anlaß genommen, auch seine wichtigsten impliziten Voraussetzungen kurz zu diskutieren. Es konnten sowohl reine Magnetit-Teilchen der Größe 600 Å—1000 Å mit einer Häufigkeit von etwa 0,94 Volumenprozent des gesamten Erzgehaltes, als auch Titanomagnetit-Teilchen von etwa 50 Å bis 200 Å Durchmesser und der Häufigkeit von rund 37 Volumenprozent des Erzgehaltes nachgewiesen werden.

[1]) Dr. H. Markert, Physikalisches Institut der Phil.-Theol. Hochschule Bamberg, 86 Bamberg, Jesuitenstraße 2.

[2]) N. Steigenberger, Sektion Physik der Universität München, Lehrstuhl Prof. Dr. Rollwagen, Abteilung Prof. Dr. Stierstadt.

§ 1: Introduction

According to NEEL (1949, 1955), there are two different mechanisms for the production of total thermoremanent magnetization in ferro- and ferrimagnetic materials: one, based on the temperature-dependent mobility and on the relaxation time of the domain walls of large crystals and of multidomain particles, the other working only on single-domain particles.

While initially the model of domain walls frozen in between potential barriers at temperatures lower than their individual "blocking temperatures" was thought to be the dominant process for the production of thermoremanence, during the last years an increasing number of authors (EVERITT 1961, YOUNG and HARGRAVES 1967, HARGRAVES and YOUNG 1969, EVANS, MCELHINNY and GIFFORD 1968, SOFFEL 1968, DUNLOP 1968, SOFFEL 1969, DUNLOP 1969a, 1969b) emphasized the importance of the second mechanism. Indeed the magnetic properties of fine ferrimagnetic particles
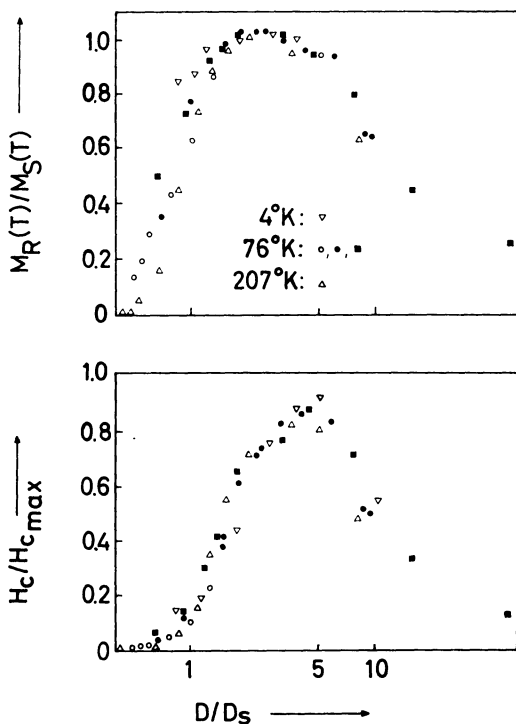

Fig. 1: Normalized saturation remanent magnetic moment and normalized coercivity of 40 Co 60 Fe fine particles as a function of their normalized diameters D/D_s, redrawn from KNELLER and LUBORSKY (1963). For the meaning of D_s see the legend of Fig. 2.

of submicroscopic dimensions are very suitable to explain the origin of stable total thermoremanent magnetization because of the following reasons:

1. With regard to ferro- and ferrimagnetic single-domain particles there exists a relationship that assigns to any pair of values of fixed relaxation time τ_0 (of magnetic reversal of the particle in zero magnetic field) and of given particle volume V a critical temperature T_B above which the particle will behave superparamagnetically, i.e. above which the energy of thermal agitation $k \cdot T$ is at least as high as the crystalline anisotropy energy $|K_1| \cdot V$ and thus sufficient to reverse the magnetic moment of the particle at zero magnetic field within τ_0.

2. The critical temperature T_B increases with increasing volume V if τ_0 is fixed at an arbitrary chosen value, while at fixed V T_B decreases with increasing τ_0 (see § 3, eq. (14)). Thus, if a single-domain particle in a low magnetic field, starting from a temperature T_1 higher than the CURIE temperature T_C, is cooled below T_C, it first will behave superparamagnetically, i.e. show a thermoremanent magnetic moment that will not be stable but go to zero within very small values of τ_0 as soon as the magnetic field vanishes. When, however, the particle temperature continues to decrease, its relaxation time τ_0 will increase exponentially and will, as well as its coercivity H_c and its thermoremanent magnetization, reach very high values within a small critical temperature range, i.e. the particle will then show very stable thermoremanence.

To illustrate this behavior more in detail, let us plot the normalized saturation remanent magnetic moment M_R/M_S as well as the normalized coercivity $H_c/H_{c\max}$ of fine particles versus their normalized diameters D/D_s as shown in Fig. 1 for fine particles of 40 Co 60 Fe studied by KNELLER and LUBORSKY (1963).

Both curves have a marked maximum ($H_{c\max} \approx 2000$ Oe) at particle diameters of about 5 times the critical value D_s below which the particles behave superparamagnetically. For magnetite and 0,56-titanomagnetite at room temperature D_s amounts to about 600 Å and 700 Å, respectively[1]).

The theoretical maximum value $H_{c\max}$ of the coercive force H_c is, according to KNELLER (1966), given by

$$H_{c\max} \approx 2 \cdot |K|/J_s \tag{1}$$

—with K and J_s denoting the crystalline anisotropy constant and the saturation magnetization, respectively—and corresponds to magnetization reversal of each particle by spin rotation in unison. Generally $H_{c\max}$ cannot be measured since some fraction of the small grains still behave superparamagnetically while, the more the normalized particle diameter D/D_s increases, the curling and buckling mechanisms and later the formation of antiparallel magnetized domain nuclei also become ener-

---

[1]) As is shown in § 3 of this paper.

getically more favourable. Thus three ranges of normalized particle diameters D/D_s may be distinguished: the first one is characterized by

$$\partial(H_c/H_{c\,max})/\partial(D/D_s) > 0, \tag{2}$$

the last one subsuming all kinds of multidomain particles, and, finally, the transition region where the buckling and curling processes are thought to take place. All particle assemblages falling into the first category have, according to NEEL (1949), relaxation times given by[1]

$$1/\tau_0 = (2e|K|/J_s m_e) \cdot |3G\lambda + NJ_s^2| \cdot (2v/\pi \cdot GkT)^{1/2} \cdot \exp(-|K| \cdot v/kT) \tag{3}$$

where e denotes the electron charge, m_e its mass, $|K|$ the crystalline anisotropy constant, J_s the saturation magnetization of the particles, λ their saturation magnetostriction, G the shear modulus, N the demagnetizing factor and v the particle volume.

In multidomain particles and in large crystals, according to MARKERT (1970), the domain walls are digged in between networks of repulsive dislocations which subdivide the domain walls into sections corresponding to those of the networks. If therefore in this case, as proposed by EVERITT (1962), the relaxation time is formulated by

$$1/\tau_0 = (1/t_0) \cdot \exp(-\Phi/kT), \tag{4}$$

then, according to MARKERT (1970), in the simplest case of saturation remanence of a nickel single crystal the activation energy Φ needed to initiate a BARKHAUSEN jump of a domain wall, is given by

$$\Phi = 2J_s \cdot (H_c - NJ_R) \cdot F \cdot R_{eff}. \tag{5}$$

Here J_s again denotes the saturation magnetization, N the demagnetizing factor of the sample, H_c and J_R its coercivity and saturation remanence, respectively, R_{eff} the half width of the repulsive interaction force between the $(\bar{1}01)$-$180°$-domain walls and the primary dislocation arrangements, and F the mean area[2] of one of those sections that are built up in the domain walls by the interacting primary dislocation configurations and hence are projections of the respective areas of the network of primary dislations itself. With respect to nickel and approximately also with respect to magnetite at room temperature R_{eff} and F amount to $0,25 \cdot 10^{-4}$ cm and to about 10^{-7} cm^2,

---

[1] For extended calculations see AHARONI (1969).

[2] F depends in a rather complicated manner on the structure of the primary dislocations. Quantitative estimations with regard to different rates of workhardening are given by MARKERT (1970), eq. (7.28), (7.107) and (7.177).

respectively. Therefore, at least in cases where $(H_c - N \cdot J_R) \leq 1$ Oe, i.e. if the shifted hysteresis loop is rectangular, we get at $T = 270\,°\text{K}$:

$$\Phi_{\text{Fe}_3\text{O}_4} \leq 1{,}25 \cdot 10^{-9} \ [\text{erg}] \,. \tag{6}$$

At the upper end of our first range of normalized particle diameters D/D_s, i.e. just before $d\,(H_c/H_{c\,\text{max}})/d\,(D/D_s)$ changes its sign from plus to minus, the ratio D/D_s is given by

$$(D/D_s)_0 \approx 5 \tag{7}$$

and thus we get with respect to magnetite critical particle volume v_0:

$$v_0 = (4/3) \cdot \pi \cdot (5 \cdot D_s/2)^3 \approx 1{,}4 \cdot 10^{-14}\,\text{cm}^3 \,. \tag{8}$$

Since at room temperature K_1 of magnetite amounts to $1{,}2 \cdot 10^5$ erg/cm³, we get

$$|K_1| \cdot v_0 \approx 1{,}6 \cdot 10^{-9} \ [\text{erg}] \,. \tag{9}$$

That means: $\Phi_{\text{Fe}_3\text{O}_4}$ given by eq. (6) is smaller than $|K_1| \cdot v_0$ is at the upper end of our diameter range I. But this upper end of range I coincides with the upper end of the validity range of equation (3) which cannot hold true in our transition range as with regard to buckling and curling mechanisms the volume v of eq. (3) no longer
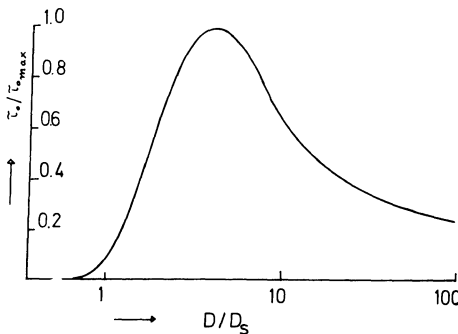
Fig. 2: Schematic sketch of a hypothetical relationship between the normalized relaxation times $\tau_0/\tau_{0\,\text{max}}$ (of magnetic reversal of single-domain particles in zero magnetic field according to eq. (3)) and the normalized particle diameters D/D_s. D_s means the critical particle diameter that, according to eq. (14) and with regard to given temperature T_0 and fixed time of measurement t', subdivides the particles into two categories, the first one containing only particles having diameters $D \geq D_s$ and behaving as ferrimagnet, the second one subsuming all particles characterized by $D < D_s$ and behaving superparamagnetically at $T \geq T_0$ and within times $t \geq t'$. $\tau_{0\,\text{max}}$ denotes the maximum relaxation time occurring at the upper end of the validity range of eq. (3).

means the volume of the whole particle but an activation volume of those spins that initiate the respective processes of buckling or curling.

Because of eqs. (3) and (4) even the relaxation time τ_0 is very much higher at $(D/D_s)_0$ $= 5$ than in the multidomain range and thus we may expect that $(\tau_0/\tau_{0\max})$, if plotted versus (D/D_s), like $(H_c/H_{c\max})$ and (J_R/J_s) also passes through a maximum at (D/D_s) ≈ 5 as schematically shown in fig. 2.

If we now measure the stability of remanent magnetization either by their time constant τ_0 or by the minimum initial amplitude of the alternating magnetic field necessary to demagnetize that remanence, in both cases fig. 1 and 2 will illustrate that these criteria are best fulfilled by particles having diameters of about $(D/D_s) \approx 5$. Thus it seemed to be of interest to look for the presence and concentration of such submicroscopic particles in samples of natural basalt.

§ 2: Measuring Method

At first it was thought that electron microscopy might be the best method of measuring the size distribution of fine particles but there are many problems of preparation of the samples that give rise to remarkable uncertainty with regard to whether all of the very fine particles are really observable. Besides electron microscopy there are still two other methods, one using electron microprobe analysis, the other, as proposed by GONSER, WIEDERSICH and GRANT (1968), MÖSSBAUER spectroscopy. But the first one only has a maximum resolving power of about 10^3 Å, while the second one must be calibrated by use of results got from another one. So we decided to measure the temperature dependence of the saturation remanence and from this to calculate the size distribution spectrum. Since the evaluation in this case till now is problematic, we tend to interpret the results also as a test of this magnetic method.

The experimental device as well as the experimental procedure used were rather simple: a system of two concentrical DEWAR vessels, the inner one containing the sample and liquid helium—if measurements should be done also at very low temperatures—, the outer one liquid nitrogen or other cooling fluids, had been put into a field coil (capable to produce magnetic fields of about 5000 Oe) outside of which the stray field of the sample had been measured by two probes of a fluxgate magnetometer. Of course at low temperatures where the crystalline anisotropy constant increases to very high values, an external magnetic field of 5000 Oe is not sufficient to saturate magnetite or titanomagnetite fine particles. But, fortunately, this is not necessary with regard to our method since all we need are field magnitudes high enough to guarantee at least an approximation to saturation remanence. To be certain that our fields are satisfying these requirements we measured the influence of external magnetic fields on the saturation remanence and found the latter remaining constant when the field amplitude was increased from $1,6 \cdot 10^3$ Oe at the first measurement to $5 \cdot 10^3$ Oe at the last one. This result holds even at nitrogen temperature. Thus we think 5 kOe to be sufficiently high.

Because of the simplicity of the apparatus the main problems of our magnetic method did not arise from the experimental technique but from numerous premises that are necessary if one, starting from the temperature-dependent saturation remanence, tries to calculate the size distribution spectrum of the submicroscopic ferrimagnetic particles in natural basalt from the Rauher Kulm. This situation will be discussed in some detail in the following section.

§ 3: Method of Calculation of Size Distribution Spectra

Since the aim of these paper is not only to estimate the size distribution spectra of fine particles in samples of the Rauher Kulm, but also to test our magnetic measuring method, we thought it might be of some interest to point out the main steps of calculation and by this way to review the (most important) premises necessary for doing these steps.

Provided we have already measured the temperature dependence of the saturation remanent magnetic moment $M_R(T)$, we start from the $[M_R(T)/M_S(T)]$-T curve[1]) by differentiating it and thus get the ratio

$$\Delta(M_R/M_S)/\Delta T = f(T) \tag{10}$$

as a function of T, as is shown in fig. 4. Now we may interpret the quantity

$$|\Delta(M_R/M_S)/\Delta T| \tag{11}$$

as measuring, due to increasing temperature, the rate of increase of the fraction of superparamagnetic fine particles among all ore grains of the sample. But to succeed in doing this we have to postulate:

[1]) A typical curve of this kind is shown schematically in fig. 3.
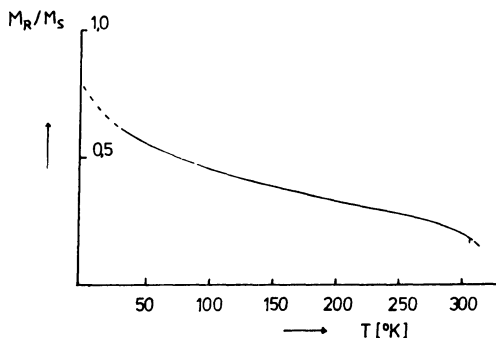
Fig. 3: Schematic sketch of a $[M_R(T)/M_s(T)] - T$ curve.
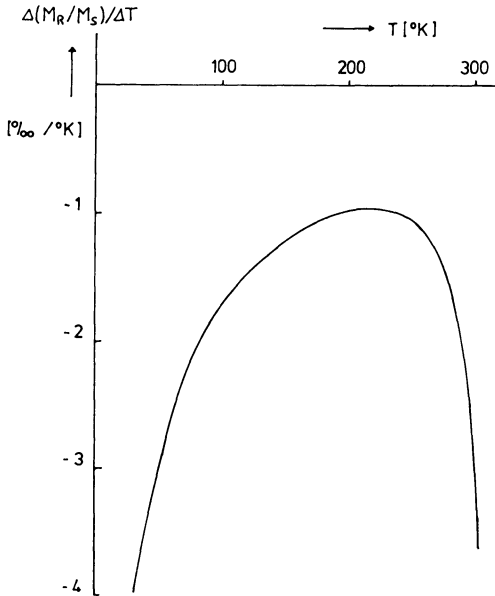
Fig. 4: Sketch of the $(\Delta\,[M_R(T)/M_S(T)]/\Delta T) - T$ curve obtained from Fig. 3 by differentiating with respect to T.

1. The titanium concentration of the particles does not depend on their diameter D. This has been established by microprobe analysis for ore grains larger than 1 micron.
2. Those contributions to the total ratio (M_R/M_S) that result from the multidomain particles of the sample, does not change with temperature at least within the accuracy of a first order approximation[1]).
3. Interactions between single particles are negligible, i.e. the packing density of the fine particles is sufficiently small.

Since our strategy of evaluation is to transform expression (11) into the ratio

$$\Delta\,(M_R/M_S)/\Delta D \tag{12}$$

and to plot (12) versus particle diameter D, we at first must try to calculate the ratio

$$\Delta T/\Delta D \tag{13}$$

as a function of temperature and thus we need to establish a relationship between the

---

[1]) Experimental investigations concerning the dependence of (M_R/M_S) of large multidomain particles on temperature T and on particle diameter (D/D_s) are on work and will be published elsewhere.

critical diameter D_s and the temperature T. According to NEEL (1949) and KNELLER (1966), this dependence of D_s on temperature T is given by

$$D_s = \begin{cases} (9/\pi)^{1/3} \cdot [(8 \cdot k \cdot T/|K_1|) \cdot \ln(2 \cdot t' \cdot \lambda_0)]^{1/3}, & \text{if } K_1 < 0 \\ (3/\pi)^{1/3} \cdot [(8 \cdot k \cdot T/|K_1|) \cdot \ln(2 \cdot t' \cdot \lambda_0)]^{1/3}, & \text{if } K_1 > 0, \end{cases} \quad (14)$$

where t' means the time of measurement and where the LARMOR frequency λ_0 due to NEEL (1949) can be expressed by

$$\lambda_0 = (2 e |K_1|/J_s m_e) \cdot |3 G \cdot \lambda + N J_s^2| \cdot (2 v/\pi \cdot G k T)^{1/2} \quad (15)$$

with all symbols denoting the same quantities as in eq. (3). In fig. 5a and 5b eq. (14) is illustrated with respect to magnetite and to titanomagnetite ($x = 0.54$), respectively. From these curves obviously there arises a new problem: the whole temperature range must be subdivided by two critical temperatures T_1 and T_2 into three different zones defined by

$$\lim_{T \to T_1} (dT/dD) = 0 \quad (16)$$

and by

$$\lim_{T \to T_2} (1/(dT/dD)) = 0, \quad (17)$$

respectively. These zones of possible evaluation are given by

I: $0 < T < T_1$,
II: $T_1 < T < T_2$,
III: $T_2 < T$.   (18)

But there are still two other points of interest:

1. The frequency factor λ_0 occurring in eq. (14) had been interpreted by NEEL (1949) to be the LARMOR frequency of the system of all coupled spins of a fine particle, i.e. to be the frequency of homogenous spin precession taking place around one of the axis of crystalline anisotropy and determined by an effective magnetic field corresponding to the crystalline anisotropy constant K_1. Thus eq. (15) had been calculated with respect to ferromagnetic particles only and at best it may approximately be applied with respect to them. Even an improved and more generalized solution deduced by BROWN (1959; 1963) from GILBERT's (1955) equation of motion   .

$$\partial M/\partial t = \gamma \cdot Mx [H + H' - \eta \cdot (\partial M/\partial t) + H_{random}] \quad (19)$$

—where M denotes the total magnetic moment of the particle, H the applied field,
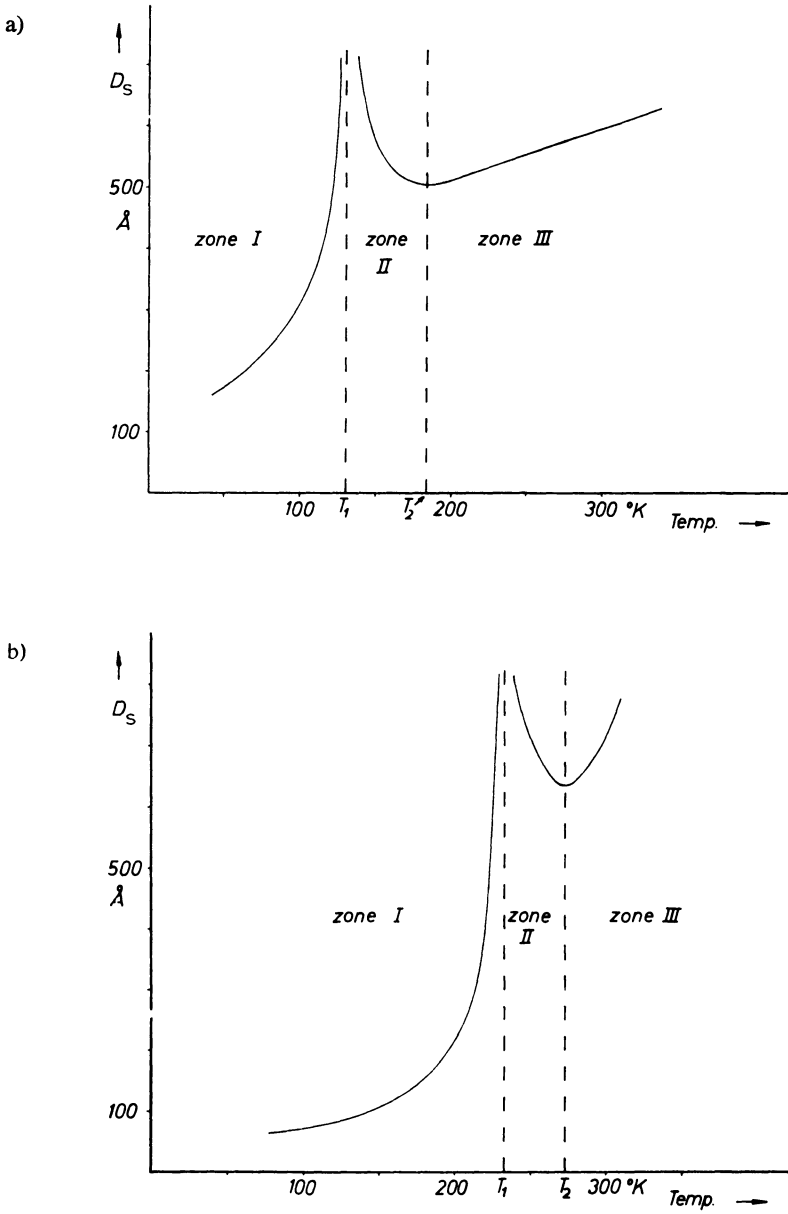
a)

b)

Fig. 5: Temperature dependence of the critical particle diameter D_s according to eq. (14) and
with regard to a measuring time $t' = 10$ sec.
a) magnetite   b) titanomagnetite ($x = 0,56$).

H' the demagnetizing field, H_{random} the random part of an fluctuating torque expressed in terms of an effective field, η a damping term and γ the gyromagnetic ratio—holds only with respect to ferromagnetic fine particles.

But we want to apply eq. (14) with regard to ferrimagnetic particles! Thus even in the simplest case we have to start not from eq. (19) but more probably from a system of equations of motion for two sublattices given by

$$\partial M_1/\partial t = \gamma_1 \cdot [M_1 x (H_0 + H_{1A} - \lambda \cdot M_2 + H_{\text{random}})] \tag{20}$$

$$\partial M_2/\partial t = \gamma_2 \cdot [M_2 x (H_0 + H_{2A} - \lambda \cdot M_1 + H_{\text{random}})], \tag{21}$$

where M_i denotes the total magnetic moment of the i-th sublattice, γ_i its gyromagnetic ratio, H_{iA} its effective anisotropy field ,H_0 the applied field, λ the intersublattice exchange constant and H_{random} again the random part of a fluctuating torque expressed in terms of an effective magnetic field.

If in a first order approximation for simplicity H_{random} is replaced by a radio-frequency field

$$H_{\text{random}} \approx H_{rf} \cdot \sin \omega t \tag{22}$$

with H_{rf} being parallel to the resultant field

$$H_0 + H_{\text{eff}\,A} = H_0 + (H_{1A} \cdot M_1 + H_{2A} \cdot M_2)/(M_1 + M_2) \tag{23}$$

and with ω representing the mean frequency of fluctuation, and if

$$|\lambda \cdot (M_1 - M_2)| \gg \text{Max}(H_0, H_{1A}, H_{2A}), \tag{24}$$

i.e. at temperatures far from compensation region, then, according to FONER (1963), there are two well-defined solutions of eq. (20) and (21), given by the frequencies

$$\omega_1 = -\gamma_{\text{eff}} \cdot (H_0 + H_{\text{eff}}), \tag{25}$$

where

$$\gamma_{\text{eff}} = -(M_1 - M_2)/(S_1 - S_2) \tag{26}$$

and

$$H_{\text{eff}} = (H_{1A} \cdot M_1 + H_{2A} \cdot M_2)/(M_1 - M_2), \tag{27}$$

and by

$$\omega_2 = \lambda \cdot (\gamma_2 \cdot M_1 - \gamma_1 \cdot M_2) + \dots, \tag{28}$$

where

$$\gamma_1 = M_1/S_1, \quad \gamma_2 = M_2/S_2 \tag{29}$$

and where S_i denotes the total angular momentum of the i-th sublattice.

The low-frequency mode of eq. (25) is expected to occur in the microwave region. It corresponds to the ferromagnetic resonance mode and is thus called "ferrimagnetic resonance". The high-frequency mode of eq. (26) has no ferromagnetic analogy. It is called "ferrimagnetic exchange resonance" and its frequency for ordinary ferrites is in the infrared or optical region.

The existence of two solutions of the system of equations of motion (20), (21) gives rise at least to a twofold problem:

a) It is not clear whether the frequency constant λ_0 in eq. (14) must be replaced by ω_1 from eq. (25) or by ω_2 due to eq. (28) or by none of them.

b) The solutions (25) and (28) are valid only far from the compensation region where, at the respective compensation points, the resultant magnetic moment $M = (M_1 + M_2)$ as well as the resultant angular momentum $S = (S_1 + S_2)$ becomes zero. That means: even if either ω_1 or ω_2 is thought to be the correct frequency constant with regard to eq. (14), it must be expected to change to extreme values if temperature reaches one of that compensation points.

Now let us remember the second point of interest announced above in connection with equations (14) to (18).

2. Eq. (14) had been deduced from the NEEL formula (3) using the premise of magnetic reversal of each particle by spin rotation in unison. But at least within the transition region of particle diameters D/D_s, delineated in § 1 by the two requirements

$$\partial(H_c/H_{c\,\max})/\partial(D/D_s)<0 \tag{30}$$

$$5 \lesssim D/D_s < c \tag{31}$$

(with the critical ratio c denoting the transition to multidomain behavior), the buckling and (or) the curling process may become energetically more favourable than magnetization reversal by homogenous rotation of all spins[1]). If this would be true, then, according to KNELLER (1966), the crystalline energy constant K_1 of eq. (14) should be replaced within that transition region by

$$|K_1| - \pi \cdot k \cdot J_s^2/S^2 , \tag{32}$$

with J_s denoting the saturation magnetization, k varying from $k = 1,08$ (if the particles are approximately infinite cylinders) to $k \approx 1,39$ (if the particles are spheres) and with S being defined by

$$S = b/b_0 \tag{33}$$

---

[1]) According to calculations of FREI, SHTRIKMAN and TREVES (1957), in magnetite the curling mechanism should dominate even at particle diameters $D \gtrsim 200$ Å, i. e. at values $(D/D_s) \gtrsim 0,5$. Till now however, these predictions seem not to be proved rigorously by experiment.

$$b_0 = A^{1/2}/J_s, \qquad (34)$$

where A should designate the exchange constant and b the smaller radius of a particle having the shape of a spheroid.

Since neither the first problem concerning the frequency factor λ_0 of eq. (14) nor the second one dealing with the replacement of K_1 by expression (32), seems to be resolvable at present, in order to get at least a zero-approximation of the size distribution spectrum of fine ferrimagnetic particles in basalt, for the time being we have no option than to postulate the validity of equations (14) and (15) within the whole diameter range of single-domain particles, i.e. within

$$0 \le (D/D_s) < c, \qquad (35)$$

where c again denotes the critical ratio of transition to multidomain behavior.

On these premises we now get the ratio $(\Delta T/\Delta D)$ as a function of T by differentiating the curves of fig. 5a and 5b, as is shown in figs. 6a and 6b, respectively.
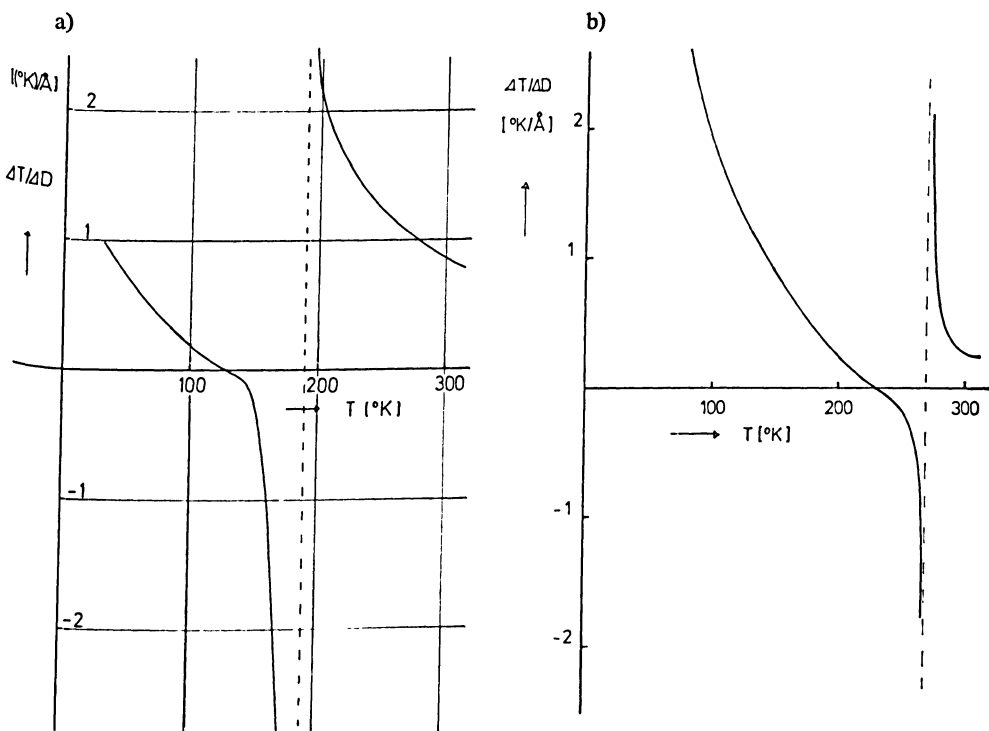

Fig. 6: $(\Delta T/\Delta D)$ — T curve obtained from Fig. 5 by differentiating D_s with respect to T and plotting the inverse values versus T.
a) magnetite   b) titanomagnetite ($x = 0{,}56$).

The last steps of evaluation then are to calculate with regard to each of the three zones defined in eq. (18), the ratio $\Delta (M_R/M_S)/\Delta D$ by multiplying $\Delta (M_R/M_S)/\Delta T$ with $(\Delta T/\Delta D)$, then to add these ratios $\Delta (M_R/M_S)/\Delta D$ calculated with respect to zones I to III of eq. (18), and to plot the result versus D.

§ 4: Experimental Result and its Evaluation Due to § 3

Our experimental result is illustrated in fig. 7, where the full line shows the remanent magnetic moment $M_R (T)$ of a sample of the Rauher Kulm basalt plotted versus the measuring temperature which had been varied between 4°K and room temperature. Evaluation due to the method outlined in § 3, requires the use of normalized values M_R/M_S instead of the remanent magnetic moment M_R itself. Since we did not measure the temperature dependence of the saturation magnetic moment $M_s (T)$, we have to refer to respective measurements done by CREER and PETERSEN (1969) on samples of the RK-basalt. If we extrapolate their curve down to lower temperatures till 4°K, we can calculate the normalized $M_R (T)/M_S (T)$-T-curve shown in fig. 8 (full line). The
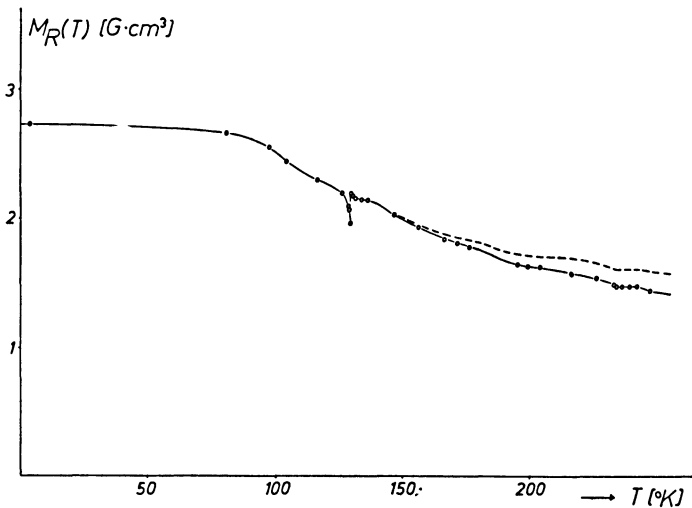
Fig. 7: Experimental result: the temperature dependence of the saturation total remanent magnetic moment of a basalt sample of the Rauher Kulm (Germany) measured between 4°K and room temperature. Each measuring point had been produced by magnetizing the sample at the respective temperature in a magnetic field of 5000 Oe (see § 2), removing the external field and reading the value of time-dependent total magnetic moment belonging to a measuring time of $t' = 10$ sec. The minimum at $T = 130$°K—where the crystalline anisotropy constant of pure magnetite becomes zero—is due to pure magnetite fine particles of 600 Å to 1000 Å in diameter (see Fig. 11) which contribute about 0,94% by volume of the total ore content. The dashed line shows a curve that should be observed instead of the measured one if no magnetite fine particles were precipitated at all.
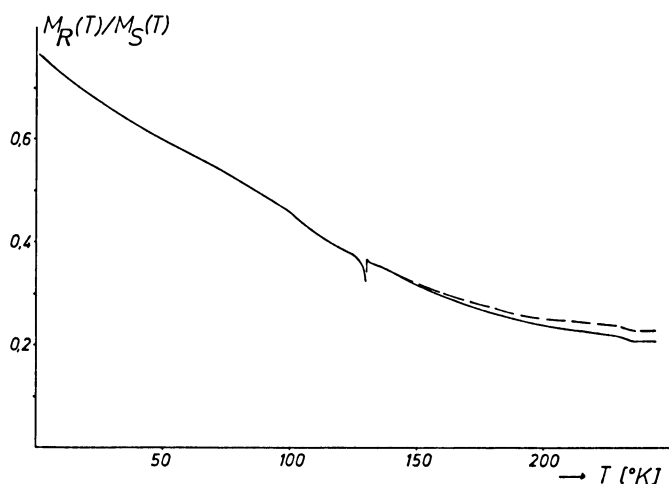
Fig. 8: Temperature dependence of the normalized saturation remanent magnetic moment of the same basalt sample as mentioned in Fig. 7. The $M_S(T)$-values had been extrapolated (at low temperatures) and taken over from respective curves measured by CREER and PETERSEN (1969).

difference between the curves in figs. 7 and 8 results from the fact that, due to CREER and PETERSEN (1969), below $-50\,°$C the saturation moment $M_S(T)$ decreases with decreasing T. But since these measurements had been done at maximum magnetic fields of about $14 \cdot 10^3$ Oe, possibly that decrease of magnetic moment might be only simulated by the crystalline anisotropy which, at low temperatures, rapidly increases with decreasing T. As we do not know what the truth is and also cannot decide it by experiment, we shall calculate during our further evaluation for both cases:

1. $M_R(T)/M_S(T)$ decreases with T as is shown in fig. 8[1]).
2. $M_R(T)/M_S(T)$ depends on T in the same manner as $M_R(T)$ does, i.e. between $4\,°$K and room temperature $M_S(T)$ is assumed to be constant.

Let us now attend to the minimum that we had found at $130\,°$K, as is shown in figs. 7 and 8. According to eq. (14) and to figs. 5a and 5b, we should expect an extreme value of the critical particle diameter D_s at that temperature where the respective crystalline anisotropy constant passes through zero. At this very temperature even single domain particles of large diameter will behave superparamagnetically, i.e. will not contribute to the total remanent magnetic moment of the sample. Thus at this critical temperature T_{crit} both $M_R(T)$ and $M_R(T)/M_S(T)$ should have a minimum. From the critical temperature $T_{\text{crit}} = 130\,°$K it follows that the minimum shown in

---

[1]) New measurements by CREER (see paper by K.M.CREER in this issue) have shown, that the titanomagnetites in the RK-basalt are of the Q-type after NEEL.

Fig. 9: Size distribution of titanomagnetite ($x = 0,56$) fine particles in the basalt sample of the Rauher Kulm (Germany) calculated from Fig. 7 due to the evaluation method described in § 3. The abundance of fine particles having diameters of 50 Å to 200 Å amounts to about 36,7% by volume of the total ore content.

Fig. 10: Size distribution of titanomagnetite ($x = 0,56$) fine particles in the basalt sample of the Rauher Kulm (Germany) if calculated from Fig. 8 due to the evaluation method described in § 3 and thus implicitly based also on the $M_S(T) - T$ curves of CREER and PETERSEN (1969) which we, however, suppose to be not quite correct at low temperatures because of the unsufficiently low saturation magnetic fields of 14 kOe used by these authors.

figs. 7 and 8 must be caused by *magnetite* fine particles, since, according to SYONO (1965), the crystalline anisotropy constant of magnetite becomes zero just at the same temperature $T_0 = 130°K$. Hence, if our RK-basalt contains magnetite fine particles, it must be possible to indicate them also by other methods. Indeed, according to PETERSEN (1965), in RK-basalt a magnetite content of about 2 volume percent of the total ore content can be concluded from $M_S(T)$-T measurements as well as from those concerning the high frequency effective resistance method described by FRAUNBERGER (1963) and PETERSEN (1965).

If we, starting from the relative depth of the minimum shown in fig. 7, and taking into account the difference between the saturation magnetic moments of magnetite and titanomagnetite ($x = 0,56$), try to estimate the vol. percentage of magnetite fine particles becoming superparamagnetic between 127°K and 130°K (the minimum has a maximum width of 3°K), we find again a value of 2 vol. percent magnetite.

As, immediately above 130°K, $M_R(T)$ abruptly grows to its former magnitude, it follows from fig. 5a that all the magnetite fine particles that had been superparamagnetic at $T_c = 130°K$ must have minimum dimensions of about 500 Å in diameter! With increasing temperature these magnetite fine particles will, due to fig. 5a, again gradually become superparamagnetic and thus again lower the remanent magnetic moment $M_R(T)$. If we correct the $M_R(T)$-T curve by this contribution, we get the curve represented in fig. 7 by the dashed line and the corresponding one in fig. 8.

Let us now deal with these corrected curves. Due to our interpretation of the decrease of $M_R(T)/M_S(T)$ with increasing T, as pointed out in § 3, we deduce from figs. 7 and 8 that there should also exist a lot of titanomagnetite fine particles in our RK-basalt sample. But if this is so, why do we not find a second minimum at $T = 235°K$, where, according to fig. 5b and to eq. (14), the crystalline anisotropy constant K_1 of titanomagnetite ($x = 0,56$) goes to zero? We suppose: we cannot find this minimum since, due to SYONO (1965), the zero point of K_1 of titanomagnetite depends very sensitively on the titanium oxide concentration. Thus, even if the latter varies only within, say, 5 percent, the respective zero points of K_1 will spread over an intervall of at least 20°K and therefore the postulated minimum should be extremely flat, as indeed is observed in fig. 7.

If we now, due to the method outlined in § 3, calculate the size distribution curves of the titanomagnetite ($x = 0,56$) fine particles of our RK-basalt sample, we get the spectrum shown in fig. 9 if we start from fig. 7 and that of fig. 10 if we start from fig. 8. Obviously the former is the more probable one.

Let us finally apply our method of evaluation also on the magnetite-minimum at 130°K. Then we can additionally estimate the size distribution of the magnetite fine particles. The result is illustrated in fig. 11. It shows the onset of the spectrum till its maximum contributions at particle diameters of about 900 Å. The percent scale on the ordinate refers to the magnetite content of the total ore fraction i.e.: for instance 6% particles of 600 Å—700 Å in diameter means: 0,12 vol. percent of the total basalt sample.
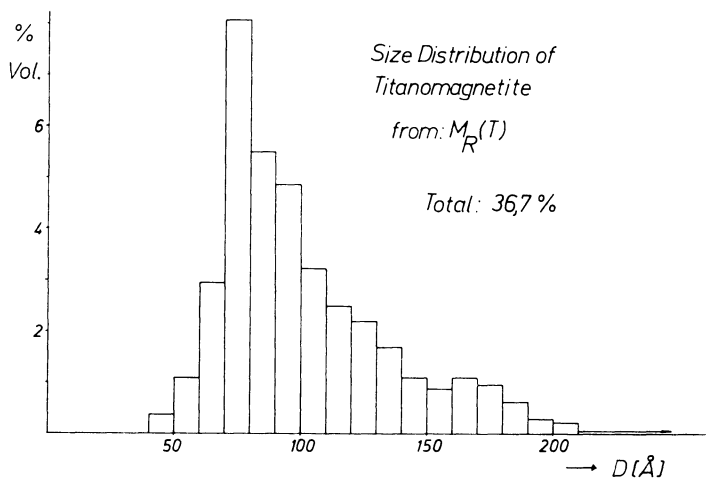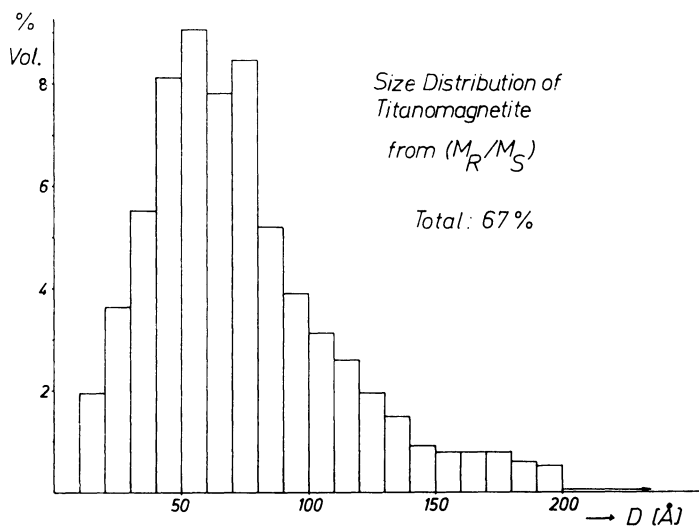
Size Distribution of Magnetite
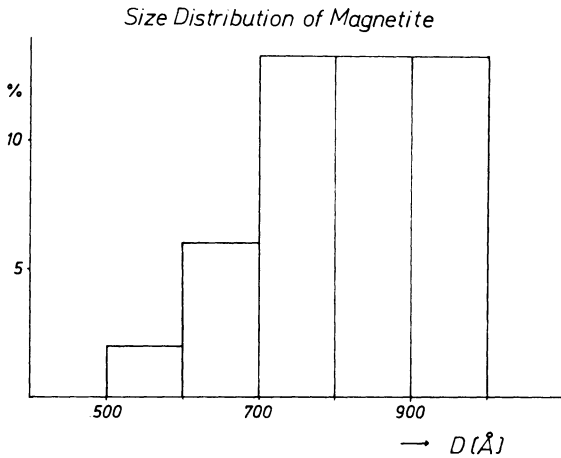
Fig. 11: Size distribution of pure magnetite fine particles in the basalt sample of the Rauher Kulm (Germany) calculated from the shape of the minimum shown in Fig. 7. The ordinate values refer to the magnetite content (2% by volume) of the total ore fraction of the sample. The calculation had not been continued to diameters larger than 1000 Å since the respective particles probably will exceed the validity range of our method of calculation.

§ 5: Final Remarks

From our first results as well as from the analysis of our method there arise new problems that should be studied to perfect this method to a very sensitive instrument of investigation of ore bearing rocks:

1. Our size distribution spectrum should be compared with others obtained from electron microscopy (first attemps concerning such studies had already been made by the rock magnetism group at the "Institut für Angewandte Geophysik" in Munich) and by the Mössbauer effect.
2. From the chemical viewpoint of possible precipitation, growth and oxidation mechanisms of titanomagnetite fine particles it should be investigated whether the equilibrium titanium concentration might depend on the particle diameter.
3. The temperature dependence of the ratio M_R/M_S of synthetic samples containing only multidomain particles of given diameter should be studied.
4. The temperature dependence of M_R/M_S of synthetic samples containing only single-domain particles of given diameter should also be studied.
5. The temperature dependence of the gyromagnetic ratio γ should be investigated.
6. Precise studies of temperature dependence of M_R/M_S, of the coercivity H_c and of the magnetic aftereffect should be done near and exactly at the zero point of the crystalline anisotropy constant K_1 and around possible compensation points.

Acknowledgements

References

AHARONI, A.: Effect of a magnetic field on the superparamagnetic relaxation time. Phys. Rev. 177, 793—796, 1969.

BROWN, JR., W. F.: Relaxation behavior of fine magnetic particles. J. Appl. Phys. 30 Suppl., 130—133, 1959.

—: Thermal fluctuations of a single-domain particle. J. Appl. Phys. 34, 1319—1320, 1963.

CREER, K. M., N. PETERSEN: Thermochemical magnetization in basalts. Z. Geophys. 35, 501—516, 1969.

DUNLOP, D. J.: Monodomain theory: experimental verification. Science 162, 256—258, 1968.

—: Preisach diagrams and remanent properties of interacting monodomain grains. Phil. Mag. 19, 369—378, 1969a.

—: Hysteretic properties of synthetic and natural monodomain grains. Phil. Mag. 19, 329 to 338, 1969b.

EVANS, M. E., M. W. McELHINNY, A. C. GIFFORD: Single domain magnetite and high coercivities in a gabbroic intrusion. Earth Plant. Sc. Letters 4, 142—146, 1968.

EVERITT, C. W. E.: Thermoremanent magnetization: I. Experiments on single domain grains. Phil. Mag. 6, 713—726, 1961.

—: Thermoremanent magnetization: III. Theory of multidomain grains. Phil. Mag. 7, 599—616, 1962

FONER, S.: Antiferromagnetic and ferrimagnetic resonance. In: "Magnetism", ed. by RADO, G. T., and H. SUHL, Academic Press, New York/London 1963.

FRAUNBERGER, F.: Die Wechselfeldpermeabilität bei höheren Frequenzen als Mittel zur Lösung magnetischer und metallkundlicher Probleme. Z. Angew. Phys. 17, 266—269, 1964.

FREI, E. H., S. SHTRIKMAN, D. TREVES: Critical size and nucleation field of ideal ferromagnetic particles. Phys. Rev. 106, 446—455, 1957.

GILBERT, T. L.: A Lagrangian formulation of the gyromagnetic equation of the magnetization field. Phys. Rev. 100, 1243, 1955.

GONSER, U., H. WIEDERSICH, R. W. GRANT: MÖSSBAUER studies on the superparamagnetic behavior of magnesioferrite precipitates. J. Appl. Phys. 39, 1004—1005, 1968.

Hargraves, R. B., W. M. Young: Source of stable remanent magnetism in Lambertville diabase. Amer. Journ. Sc. 267, 1161—1177, 1969.

Kneller, E.: Theorie der Magnetisierungskurve kleiner Kristalle. In: ,,Handbuch der Physik", vol. XVIII/2, ed. by Flügge, S., Springer, Berlin/Heidelberg/New York 1966.

— : F. E. Luborsky: Particle size dependence of coercivity and remanence of single-domain particles. J. Appl. Phys. 34, 656—658, 1963.

Markert, H.: Über den Ultraschalleinfluß auf den Barkhauseneffekt sowie über die Notwendigkeit und den Entwurf einer neuen Modellvorstellung zum Magnetisierungsablauf in verformtem Nickel — basierend auf der Wechselwirkung der segmentweise gewölbten 180°-Blochwände mit relaxationsartig-irreversibel verschiebbaren Versetzungsanordnungen. Diss., Nat. Fak. Univers. München, 1970.

Neel, L.: Théorie du trainage magnétique des ferromagnétiques en grains fins avec applications aux terres cuites. Ann. Geophys. 5, 99—136, 1949.

— : Some theoretical aspects of rock magnetism. Adv. Phys. 4, 191—243, 1955.

Petersen, N.: Beobachtung einiger mineralogischer und magnetischer Eigenschaften dreier Basaltproben nach unterschiedlicher thermischer Behandlung. Diss., Nat. Fak. Univers. München, 1965.

Soffel, H.: Die Bereichsstruktur der Titanomagnetite in zwei tertiären Basalten und die Beziehung zu makroskopisch gemessenen magnetischen Eigenschaften dieser Gesteine. Habil.-Schrift, Nat. Fak. Univers. München, 1968.

— : The origin of thermoremanent magnetization of two basalts containing homogenous single phase titanomagnetite. Earth Plant. Sc. Letters 7, 201—208, 1969.

Syono, Y.: Magnetocrystalline Anisotropy and Magnetostriction of Fe_3O_4—Fe_2TiO_4-Series —with Special Application to Rock Magnetism. Jap. J. Geophys. 4, 71—143, 1965.

Young, W. M., R. B. Hargraves: A procedure for investigating the natural remanence of minerals in rocks. Vortrag Nr. 110, Generalversammlung der IAGA, St. Gallen, 1967.

The Effect of Radiation with Fast Neutrons
on the Saturation Remanence of a Basalt

H. Soffel, München[1])

Summary: The saturation remanence $J_{sat.rm.}$ of a basalt sample from Rauher Kulm (Germany) containing homogeneous and mostly multidomain titanomagnetites and its decrease with a. c. demagnetization up to 700 Oe effective field was measured before and after radiation with fast neutrons (1—10 MeV) with a flux density of $2 \cdot 10^{12}$ neutrons per cm^2. With the exception of the a. c. demagnetization range from 0—10 Oe, where $J_{sat.rm}$ after radiation was about 1% larger than before radiation, no change of the demagnetization curves could be detected. This suggests that essentially higher flux rates of fast neutrons or other particles are necessary to produce an appreciable increase of the coercive force of titanomagnetites in basalts and to contribute to a "hardening" of viscous remanent magnetization.

Zusammenfassung: Es wurde die Sättigungsremanenz $J_{sat.rm.}$ einer Basaltprobe vom Rauhen Kulm (Oberpfalz) und ihre Abnahme mit fortschreitender Wechselfeld-Entmagnetisierung bis 700 Oe effektiver Feldstärke vor und nach der Bestrahlung der Probe mit schnellen Neutronen (1—10 MeV) mit einer Flußdichte von $2 \cdot 10^{12}$ Neutronen pro cm^2 gemessen. Der Basalt enthält homogene Titanomagnetite und vorwiegend Mehrbereichs-Teilchen. Außer in dem Entmagnetisierungs-Bereich von 0—10 Oe, wo $J_{sat.rm.}$ nach der Bestrahlung um etwa 1% größer war als zuvor, wurden keine Veränderungen der Entmagnetisierungs-Kurven beobachtet. Daraus wird geschlossen, daß wesentlich höhere Flußdichten von schnellen Neutronen oder entsprechende Strahlungsschäden durch andere Teilchen notwendig sind, um die Koerzitivkraft der Titanomagnetite in Basalten erheblich zu vergrößern und zum „Aushärten" von viskosen Remanenzen beizutragen.

Introduction

Most rocks are able to acquire viscous remanent magnetization (VRM) in a small magnetic field such as (i) the earth magnetic field, (ii) interplanetary fields and (iii) fields on the surface of celestial bodies. VRM can further be produced by uniaxial stresses, i. e. by (i) tectonic effects, (ii) shock wave effects, (iii) thermal expansion and (iiii) the sampling procedure. A characteristic property of VRM is its more or less rapid decay with time and its instability against a. c. and/or thermal demagnetization.

The stability of a remanent magnetization is influenced by the real structure of ferrimagnetic minerals in rocks. Lattice imperfections (dislocations, inclusions, inter-

---

[1]) Universitätsdozent Dr. Heinrich Soffel, Institut für Angewandte Geophysik der Universität München, 8 München 2, Richard-Wagner-Straße 10.

sticial atoms, vacancies) are able to impede domain wall motions and rotation pro-
cesses in multidomain and single domain particles respectively. The production of
secondary lattice imperfections can therefore result in an increase of coercive force
and in a "hardening" of previously unstable VRM and decrease or even stop its
decay with time.

Lattice imperfections can be produced artificially by radiation with particles of
high kinetic energy, i. e. by fast neutrons of several MeV. Typical lattice damages are
then displacement spikes and depleted zones [see SEEGER 1965] with a diameter of
some 10^{-7} cm and dislocations. From the small size of the lattice imperfections pro-
duced by radiation it can be expected that only very high rates of the particle flux
can have measurable effects with regard to the coercive force i. e. magnetic stability
of ferrimagnetic particles in rocks.

In the following we describe the results of preliminary measurements on a basalt
sample which had been subjected to radiation with high energy neutrons.

Experimental results

The material under study was a small cylinder (8 mm high, 8 mm in diameter) of
a basalt from Rauher Kulm (Oberpfalz, Germany). The magnetic properties of this
basalt have been studied extensively by several authors [i. e. PETERSEN 1962, SOFFEL
1968]. The rock contains homogeneous titanomagnetites (0,45 ulvöspinel, 0,55 magne-
tite) with an abundance of 4 percent by volume. The grains are almost spherical and
multidomain particles are predominant.

The sample was subjected to a radiation with fast neutrons (1—10 MeV) with a
total flux of about $2 \cdot 10^{12}$ neutrons per cm^2. A cadmium capsule around the sample
shielded it from thermal neutrons in order to reduce the induced γ ray activity. The
sample temperature was kept at $35\,^0C$ during the radiation experiment. The magnetic
measurements were made 10 days later when the γ ray activity of the sample had
decayed below a critical value.

A sensitive parameter with regard to changes of the coercive force of a rock sample
is its saturation remanence $J_{sat.rm.}$ and its decrease as a. c. demagnetization proceeds.
$J_{sat.rm.}$ is also studied to detect changes of the magnetic properties of ferrimagnetic
particles due to heating in paleomagnetic intensity work [McELHINNY and EVANS
1968]. An increase of coercive force due to a production of lattice imperfections is
expected to change the curve of $J_{sat.rm.}$ versus proceeding a. c. demagnetization in
the way as shown in Fig. 1. $J_{sat.rm.}$ should be larger after radiation and should be
more stable with respect to a. c. demagnetization, at least in the low field range.

Before and after radiation the sample had been saturated in a 10000 Oe d. c. field
and measured with a spinner magnetometer. The a. c. demagnetization was carried
out in a field free space with effective a. c. fields up to 700 Oe. The sample was saturat-
ed and demagnetized three times before and after radiation in order to avoid spurious
effects. Each time $J_{sat.rm.}$ and the demagnetization curves could be reproduced
within $<0,5\%$.
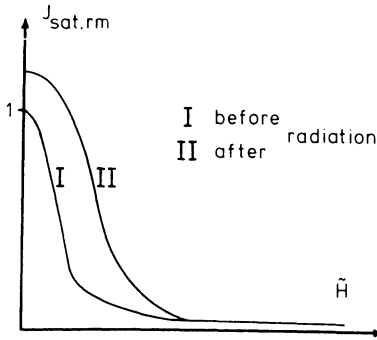
Fig. 1: Expected influence of radiation on the a. c. demagnetization curve of the saturation remanence $J_{sat.rm.}$ of a rock with mostly multidomain particles.
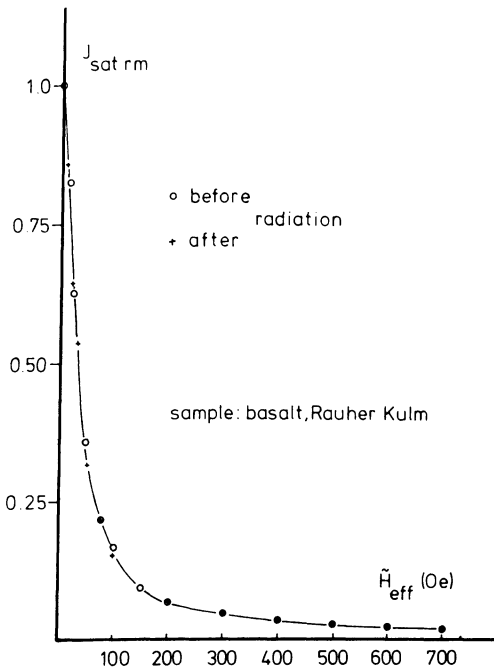
Fig. 2: Saturation remanence $J_{sat.rm.}$ of a basalt from Rauher Kulm (Oberpfalz, Germany) during a. c. demagnetization up to 700 Oe effective field. Circles: before radiation, crosses: after radiation with fast neutrons.

Fig. 2 shows the decrease of the $J_{sat.rm.}$ with proceeding a. c. demagnetization before (circles) and after (crosses) radiation. The values of the saturation remanence were normalized with respect to $J_{sat.rm.}$ before radiation. Within the limits of accuracy of this representation no changes could be found in this curve. Fig. 3 however shows the decrease of $J_{sat.rm.}$ before (circles) and after (crosses) radiation in the range of demagnetizing fields up to 50 Oe. In this enlarged representation a minute effect in the sense of Fig. 1 can be observed. In the range of demagnetizing fields from 0—10 Oe the values of $J_{sat.rm.}$ after radiation (crosses) are slightly larger (about 1 %) than $J_{sat.rm.}$ before radiation (circles). The effect is so small however that it can also be due to small variations of the intensity of the standard sample used for calibration of the spinner magnetometer.
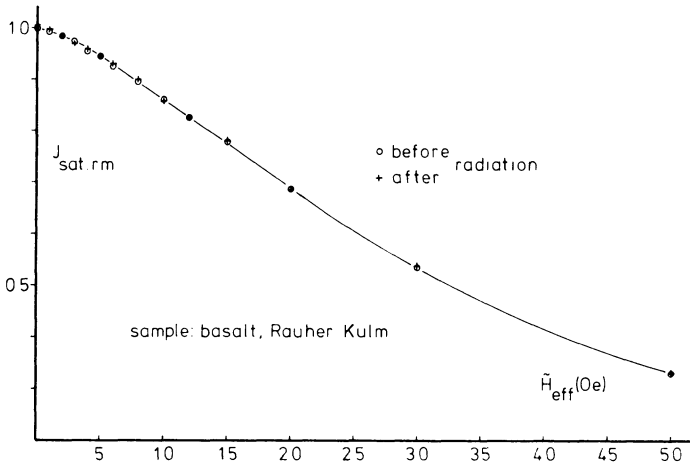
Fig. 3: Enlarged representation of the curve shown in Fig. 2 for the demagnetization range from 0—50 Oe.

Conclusion

Radiation with fast neutrons with a flux density of $2 \cdot 10^{12}$ neutrons per cm^2 or a radiation with other particles producing an equivalent rate of lattice damage can be excluded as a possible source for the "hardening" of VRM. The number of lattice imperfections due to such a radiation seems to be too low and their size too small to have any appreciable effect on the coercive force of titanomagnetites. It is therefore planned to repeat the measurements with the same material but with a considerable higher flux rate of fast neutrons (up to 10^{18} neutrons per cm^2).

Acknowledgement

References

McELHINNY, M. W., and M. E. EVANS: An Investigation of the Strength of the Geomagnetic Field in the Early Precambrian. Phys. Earth Planet. Interiors, 1, 485—497, 1968

PETERSEN, N.: Untersuchungen magnetischer Eigenschaften von Titanomagnetiten im Basalt des Rauhen Kulm (Oberpfalz) in Verbindung mit elektronenmikroskopischer Beobachtung. Z. Geophys. 28, 79—84, 1962

SEEGER, A.: Moderne Probleme der Metallphysik, Vol. I, Springer, Berlin, Heidelberg, New York, 1965

SOFFEL, H.: Die Bereichsstrukturen der Titanomagnetite in zwei tertiären Basalten und die Beziehung zu makroskopisch gemessenen magnetischen Eigenschaften dieser Gesteine. Habil. Schrift, Nat. Fak. Universität München, 1968

On Some Magnetic and Magneto-Optic Properties
to be Studied on Fine Precipitations in Glasses

H. MARKERT, Bamberg[1])

Summary: Two open questions are discussed concerning the process and the dynamics of magnetic spin reversal of ferro- and ferrimagnetic fine particles; and correspondingly two experiments are propagated that promise to give us new informations about these problems. The first experiment deals with a method of measuring the frequency factors occuring in the respective alternative formula suggested by NEEL [1949] and by BROWN [1959, 1963] and AHARONI [1969] in order to describe the relaxation time of viscous remanent magnetization (of the magnetic aftereffect). The second experiment is a magneto-optical one and is thought to be suitable for studies of the dynamics of magnetic spin reversal taking place in ferro- and ferrimagnetic fine particles at their coercive forces. The theoretical background of this latter experiment, i.e. the description of temperature-dependent and of field-dependent changes of the resultant magnetic moment of a ferromagnetic fine particle in terms of spin wave theory and of magnon-magnon and magnon-phonon interactions, are discussed in some detail in order to predict, based on two hypotheses, a probable experimental result and to explain at least qualitatively the already known phenomena accompanying the process of magnetic spin reversal.

Zusammenfassung: Fragen der Ummagnetisierungsprozesse in kleinen ferro- und ferrimagnetischen Einbereichsteilchen und der Dynamik solcher Vorgänge werden erörtert und zwei Experimente vorgeschlagen, die hierüber neue Informationen zu liefern versprechen: Einmal ein Verfahren zur Messung des Frequenzfaktors, der in dem von NEEL [1949] vorgeschlagenen Ausdruck für die Relaxationszeit der magnetischen Nachwirkung sowie in den von BROWN [1959, 1963] und von AHARONI [1969] aufgrund allgemeiner Überlegungen hergeleiteten Formeln auftritt und ihre Verifikation erlaubt, und zum anderen ein magneto-optisches Experiment, das geeignet erscheint, die Dynamik der Ummagnetisierung zu studieren. Der theoretische Hintergrund dieses zweiten Experiments, nämlich die Beschreibung der Feld- und der Temperaturabhängigkeit der Magnetisierung kleiner ferromagnetischer Einbereichsteilchen im Rahmen der Spinwellentheorie und der Magnon-Magnon und Magnon-Phonon Wechselwirkungen, wird etwas ausführlicher diskutiert, so daß es schließlich möglich ist, eine qualitative Voraussage über das mutmaßliche Versuchsergebnis zu machen und zu begründen.

1. Introduction

This paper does not deal with measurements already done but its aim is to propagate a new experimental project recently started here together with the 'Institut für Ange-

---

[1]) Dr. H. MARKERT, Physikalisches Institut der Phil.-Theol. Hochschule Bamberg, 86 Bamberg, Jesuitenstraße 2.

wandte Geophysik', University of Munich: the investigation of physical, particularly magnetic and magneto-optic properties of ferrimagnetic and antiferromagnetic fine particles in glass matrices, i.e. of ferrimagnetic and antiferromagnetic glass samples. Studies of magnetic properties of fine particles are evidently of great interest with regard to paleomagnetism and to various technical applications. But in spite of numerous papers published during the last ten years and concerning the magnetic properties of fine particles, there are a great lot of open questions mainly resulting from — or leading to — the same two central unsolved problems:

1. What is, on a quantum-mechanical scale, the mechanism that governs the magnetic spin reversal of fine ferromagnetic particles and how does it depend on particle size, on particle shape and on temperature.

2. How must this mechanism be modified and generalized to be applicable to ferrimagnetic and antiferromagnetic fine particles.

Contrary to the common methods used by most of the former authors who tried to answer these questions by studying the magnetic properties of ferromagnetic precipitations in a metallic matrix, as for instance of cobalt in copper, it seems to be more promising to attack these questions by investigating at the same time not only the magnetic but also the magneto-optic properties of fine ferrimagnetic precipitations in a glass matrix, i.e. of ferrimagnetic glass samples. To illustrate the advantage of this procedure, two experiments recently started here, shall be discussed.

2. Magnetic Aftereffect in Ferrimagnetic Glasses

One of the very important geophysical applications of rock magnetism is to estimate the paleointensity of thermo-remanent magnetization of old rocks. To succeed in doing this, one must take into account the magnetic aftereffect of these rocks, i.e. one has to start from an equation

$$J_R(0) = J_R(t) \cdot \exp(\lambda \cdot t),   \tag{2.1}$$

where $J_R(t)$ denotes the thermo-remanent magnetization at the present time and $J_R(0)$ the original intensity of TRM of the sample and $\lambda = 1/\tau$ the time constant of the magnetic aftereffect. As had been pointed out in more detail by MARKERT [1971] in another paper of this colloquium, the time constant λ depends sensitively on the temperature T and on the activation energy E necessary to initiate the magnetic aftereffect, i.e. there holds a relationship given by

$$\lambda(T) = \lambda_0 \cdot \exp(-E/k_B \cdot T),   \tag{2.2}$$

with k_B designating the BOLTZMANN constant, and λ_0 being a frequency factor of the same order of magnitude as the LARMOR frequency of a spin system precessing

around an effective crystalline field H_k, given by

$$H_k = 2 \cdot |K_1| / J_s,$$ (2.3)

which is parallel to the easy axis of crystalline anisotropy and is determined by the crystalline anisotropy constant $|K_1|$ and by the saturation magnetization J_s.

According to NEEL [1949], in the simplest case of ferromagnetic single-domain fine particles of uniaxial anisotropy, λ_0 is given by:

$$\lambda_0 = (2 \cdot e \cdot |K_1| / J_s \cdot m_e) \cdot |3 \cdot G \cdot \lambda_s + N \cdot J_s^2| \cdot (2 \cdot v / \pi \cdot G \cdot k_B \cdot T)^{1/2}$$ (2.4)

— with e denoting the charge of an electron, m_e its mass, G the shear modulus, λ_s the saturation magnetostriction, N the demagnetizing factor of a particle of volume v — while in zero field the activation energy of such particles, provided they are spheroidal, mainly depends on the crystalline energy constant $|K_1|$:

$$E = |K_1| \cdot v.$$ (2.5)

If an external magnetic field H_e is applied, according to KNELLER [1966] and to BROWN [1959, 1963], the field-dependent activation energy $E(H_e)$ can be written as

$$E(H_e) = (v \cdot J_s / 2) \cdot H_k \cdot (1 \pm H_e / H_k)^2,$$ (2.6)

where H_k is defined by eq. (2.3) and where the negative sign corresponds to antiparallel alignment of the external magnetic field H_e relative to the magnetization J_s of the particle.

NEEL's [1949] estimation of λ_0, as given by eq. (2.4), had been improved subsequently by BROWN [1959, 1963] and also by AHARONI [1969], but all of these calculations had been started from the premise of one system of aligned spins building up the resultant magnetization of each particle, i.e. from the supposition of ferromagnetic single-domain particles.

Thus, as had been discussed by MARKERT [1971] in another paper of this colloquium, it seems to be still an open question what will happen if there are two antiparallel spin-sublattices, i.e. if one tries to apply the above mentioned calculations also on ferri- and on antiferromagnetic fine particles.

If NEEL [1949] is right, then even in ferrimagnetic fine particles λ_0 should be given by the LARMOR frequency

$$\lambda_0 = (\gamma / 2 \cdot \pi) \cdot H_{eff},$$ (2.7)

with

$$H_{eff} = H_e + H_k$$ (2.8)

and γ denoting the gyromagnetic ratio given by

$$\gamma = -(J_1 - J_2)/(S_1 - S_2) = -J/S,   \tag{2.9}$$

where J_1, J_2, S_1, and S_2 designate the resultant magnetization and angular momenta of the two sublattices, respectively.

If, on the other hand, it would be acceptable to generalize and to use the calculations of BROWN [1959, 1963] and of FONER [1963] with regard to the ferrimagnetic case too, then, one would get two different resonance frequencies

$$\omega_1 = -\gamma_{\text{eff}} \cdot (H_e + H_{\text{eff}})   \tag{2.10}$$

and

$$\omega_2 = \lambda \cdot (\gamma_2 \cdot J_1 - \gamma_1 \cdot J_2) + \dots,   \tag{2.11}$$

with

$$\gamma_{\text{eff}} = -(J_1 - J_2)/(S_1 - S_2),   \tag{2.12}$$

$$H_{\text{eff}} = (H_{1A} \cdot J_1 + H_{2A} \cdot J_2)/(J_1 - J_2)   \tag{2.13}$$

$$\gamma_1 = J_1/S_1 \quad \text{and} \quad \gamma_2 = J_2/S_2,   \tag{2.14}$$

where H_{iA} denotes the effective anisotropy field of the i-th sublattice, λ designates the intersublattice exchange constant. All other symbols maintain their former meaning.

But as well if eq. (2.7) holds true as if eqs. (2.10) or (2.11) are right, anyway the frequency λ_0 goes to extreme values at the so called compensation points where either $(J_1 - J_2)$ or $(S_1 - S_2)$ becomes zero. Because of the magnetic aftereffect which, due to the following expression

$$J_R(0) = J_R(t) \cdot \exp \{\lambda_0 \cdot t \cdot \exp [(v \cdot J_s/2) \cdot H_k \cdot (1 \pm H_e/H_k)^2/k_B \cdot T]\}   \tag{2.15}$$

and due to eq. (2.3), depends sensitively on λ_0 and on $|K_1|$, it is of great interest even with respect to paleomagnetism to clarify the problems concerning λ_0 and the zero point of $|K_1|$ as well. To succeed in doing this, obviously samples will be needed containing fine ferrimagnetic particles of given size and concentration in a matrix which should be nonmetallic in order to avoid eddy current damping of the magnetic spin reversal to be studied at the critical compensation temperatures of that fine particles.

According to SHIRK and BUESSEM [1970], at least in barium ferrite glasses precipitations of barium ferrite $BaFe_{12}O_{19}$ of variable given size can be produced by varying the tempering temperature. By a similar procedure, magnetite fine particles should be precipitable from a glass containing stoichiometric solid solution of iron oxide ions. Thus we think it to be possible to get ferrimagnetic glass samples that are suitable with regard to measurements of the magnetic aftereffect of the saturation remanence at various low temperatures. Having such samples we hope to decide the above outlined problems experimentally by the following way:

1. By measuring the saturation remanence $J_R(t)$ as a function of time t at various temperatures between, say, $-200\ °C$ and room temperature we will get the ratio $\ln(J_R(0)/J_R(t))$, plot it versus t, as is schematically shown in fig. 1, and will find the time constant $\lambda(T)$.

2. Then we will plot $\ln(\lambda(T))$ versus $1/k_B \cdot T$, as is illustrated in fig. 2, and by this way we will find the frequency λ_0 as well as the activation energy E.

The apparatus suitable to do these measurements, is the same one that we had already used for measuring the size distribution of fine particles in basalt of the Rauher Kulm, as had been reported by MARKERT [1971] in another paper of this colloquium.
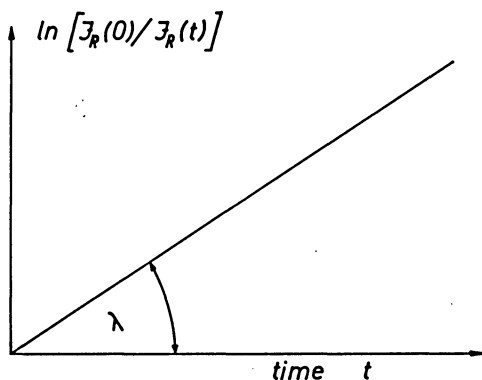
Fig. 1: Schematic sketch of linear relationship between $\ln[J_R(0)/J_R(t)]$ and time t at given temperature T, illustrating the method of calculating the time constant $\lambda(T)$ defined by eq. (2.1), from measurements of viscous remanent magnetization J_R.
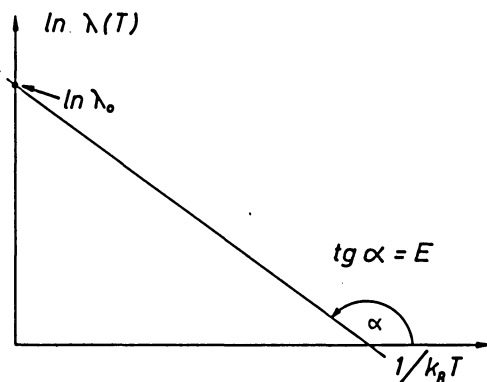
Fig. 2: Schematic sketch of linear relationship between $\ln[\lambda(T)]$ and $1/k_B \cdot T$ as described by eq. (2.2). This kind of representation of the $\lambda(T)$-values calculated due to Fig. 2.1., allows the determination of NEEL's [1949] frequency factor λ_0 (given by eq. (2.4)) as well as the calculation of the activation energy E occurring in eq. (2.2).

3. Magneto-optical Properties of Fine Particles:
A New Experimental Project and its Theoretical Background, the Process of
Magnetic Spin Reversal

The usual models of magnetic spin reversal of ferro- and ferrimagnetic fine particles are that of homogenous rotation of all spins (in each particle), the buckling and the curling mechanism[1]). These models are based on the well known half-classical micromagnetic methods of energy minimization which, at best, enable us to estimate the critical starting fields of magnetic spin reversal but say nothing about possible mechanisms which might take place during this process and could bring it about.

If we would try to study the dynamics of magnetic spin reversal processes and would do it under an atomic viewpoint — which still is a largely unsolved problem of magnetism — obviously we would have to start from an investigation of the excited states of these fine particles in order to calculate their energy levels, and also we should take into consideration the role played by a variable external magnetic field. That means: we would have to study the magneto-optical properties of ferro- and ferrimagnetic fine particles. In doing this we would need a lucid matrix, i.e. the most suitable samples again are ferrimagnetic glasses.

Let us now briefly discuss a second new experiment which will illustrate the problems concerning the dynamics of magnetic reversal and which we, common with the rock-magnetism group of Prof. Dr. G. ANGENHEISTER's "Institut für Angewandte Geophysik", recently had started here, hoping to get new information on such quantities as relaxation times and activation energies of the dominating processes of magnetic spin reversal.

Suppose we would have a ferrimagnetic glass sample containing uniformly oriented fine particles of given size, say, magnetite fine particles of about 600 Å in diameter. Then there exists a critical temperature T_s above which these particles will behave superparamagnetically. We will do our experiment at a slightly lower temperature $T_0 = T_s - \Delta T$, with $\Delta T \ll T_s$. Under this condition the coercivity as well as the normalized remanence of our magnetite glass sample will be very high, i.e. the hysteresis loop must be nearly rectangular. Let H_c be the coercivity at T_0. Now we magnetize our sample up to saturation and after this go back along the descending branch of its hysteresis loop to a point given by $H_0 = -H_c + \Delta H$, with $|H_c| \gg \Delta H$, i.e. we try to make the state of magnetization as unstable as possible, as is illustrated in fig. 3a.

From these conditions it seems to be evident that even fluctuations in temperature or in magnetic field that are only slightly higher than the mean values resulting from thermal agitation at T_0, will initiate the reversal of the magnetic moments of the particles from point 1 towards point 2 of their hysteresis loop shown in fig. 3b. Thus it should also be possible to activate this magnetic reversal by incidenting light, i. e. by photon interactions.

[1]) See for instance E. KNELLER [1966].

H_0
=
$-H_c + \Delta H$

M

$\approx 10^3 Å$
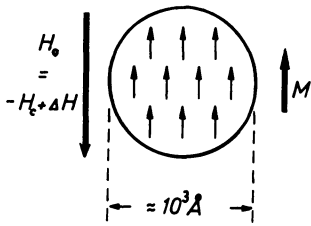
Fig. 3a: Schematic representation of anti-parallel alignment of total magnetic moment M of a ferromagnetic single-domain fine particle of about 600 Å in diameter in an external magnetic field $H_0 = -H_c + \Delta H$, $|\Delta H| \ll |H_c|$, where the state of magnetization of the particle corresponds to that illustrated by point 1 in Fig. 3b.

3

1

$-H_c$ H_0 $H^{(e)}$

2
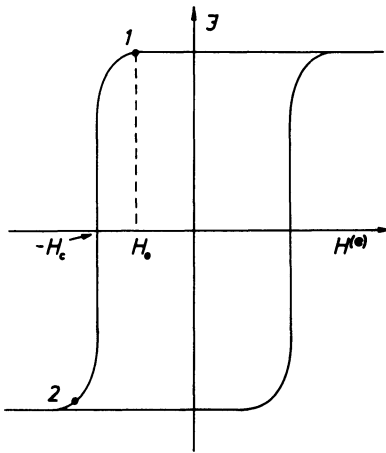
Fig. 3b: Schematic representation of the hysteresis loop and the magnetization state of a ferromagnetic single-domain fine particle at a temperature slightly below the critical temperature of changing into superparamagnetic behavior and just before starting of magnetic spin reversal (from point 1 to point 2 of the descending branch of the hysteresis loop).

$\hbar\omega_1$ $\hbar\omega_2$

$\hbar\omega_1 \gtrless \hbar\omega_2$ Stokes
Anti-Stokes
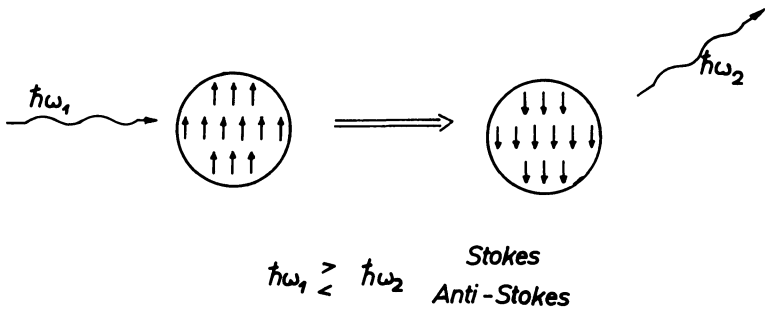
Fig. 3c: Schematic illustration of the process of magnetic spin reversal taking place in a ferromagnetic fine particle of magnetization state characterized by point 1 in Fig. 3b, if initiated and activated by means of photon-magnon interaction which, for its part, is expected to lead to a RAMAN effect of STOKES or Anti-STOKES type.

To search more deeply into the problems of those interactions between photons and single domain particles, let us now try to explain at least to some extent the theoretical background concerning the dynamics of magnetic reversal of fine particles as they are offering themselves from an atomic viewpoint. Since most of these questions are open till now, we will confine our considerations on two relatively simple limiting cases and try to develop, as a first attempt, two approximative models of magnetic reversal that will enable us to understand qualitatively the occurrence of hysteresis in these cases.

To begin with, imagine a ferromagnetic particle consisting of only three equidistant atoms, each having spin $h/4\pi$ and being linked with the others by exchange interactions. If only the ZEEMAN energy and the exchange energy are taken into account, the spin Hamiltonian can be written as

$$H = -\mu_0 \cdot g \cdot \hbar^{-1} \cdot H \cdot \sum_i S_i - J \cdot \hbar^{-2} \cdot \sum_{i<j} S_i \cdot S_j, \qquad (3.1)$$

where J is the exchange integral, S_i and S_j the spin operators that act upon the ith and jth spin, respectively, g is the spectroscopic splitting factor, μ_0 the BOHR magneton, $\hbar$ the PLANCK constant divided by $2 \cdot \pi$, and H is the operator of the external field. Since our three-spin particle per definitionem shall have no resultant orbital momentum, its total angular momentum is given by its resulting spin momentum $\vec{S}$ the magnitude of which amounts to $|\vec{S}| = \hbar\sqrt{S(S+1)}$, with $S = 1/2, 3/2$. Thus, if we would compare to selection rules governing the transitions of single atoms, we should expect the energy level diagram to consist of a quartet system due to $S = 3/2$ and with the magnetic quantum number m varying from $-3/2$ over $-1/2$ and $+1/2$ to $+3/2$, and of a doublet system characterized by $S = 1/2$, $m = \pm 1/2$. Just this kind of term system had been found by BEAN and LIVINGSTON [1959] who calculated the eigenfunctions and relative eigenvalues of a SCHRÖDINGER equation built up by the Hamiltonian of eq. (3.1). The respective results are illustrated in fig. 4 where H_e denotes the external magnetic field while the spin wave functions are symbolized by triplets of arrows; the upper levels are both degenerated. In this connection perhaps it may be of interest to realize the orders of magnitude of ZEEMAN and of exchange energy. While the ZEEMAN energy amounts to

$$g \cdot \mu_0 \cdot H \approx 1{,}85 \cdot 10^{-20} \cdot H \ [\text{emu}], \qquad (3.2)$$

if $g = 2$ and H is taken in [Oe], we find, for instance with regard to Ni, the exchange energy I to become:

$$I_{Ni} = 3{,}43 \cdot 10^{-14} \ [\text{emu}] = 2{,}14 \cdot 10^{-2} \ [\text{eV}]. \qquad (3.3)$$

(To compare to the energy of thermal agitation, remember that $k_B \cdot T = 1{,}38 \cdot 10^{-16} \cdot T$ [emu]).

Let us now try to develop a model of the magnetization process that would relate the energy level diagram of fig. 4 at least qualitatively to the magnetization curve of our three-spin system. If we first confine our considerations to states of thermal equilibrium, according to their respective energies all levels have stationary exitation probabilities depending only on the magnitudes of H and T, respectively, and thus an application of statistical mechanics yields, due to BEAN and LIVINGSTON [1959], to the magnetization

$$J = \varkappa \cdot H_e = \frac{N \cdot g^2 \cdot \mu_0^2}{3 \cdot k_B \cdot T} \cdot H \cdot \frac{\sum\limits_n S \cdot (S+1) \cdot \exp(-E_n/k_B \cdot T)}{\sum\limits_n \exp(-E_n/k_B \cdot T)}, \qquad (3.4)$$

where $N = 6$ denotes the total number of energy levels, while the eigenvalues E_n are given by

$$\begin{cases} E_n = E_0 + (n-1) \cdot g \cdot \mu_0 \cdot H, & \text{with } n = 1, \ldots, 4 \text{ and } S = 3, \\ E_n = E_0 + (n-4) \cdot g \cdot \mu_0 \cdot H + 3 \cdot J, & \text{with } n = 5, 6, \text{ and } S = 1, \end{cases} \qquad (3.5)$$

and with E_0 designating the energy of the ground state.
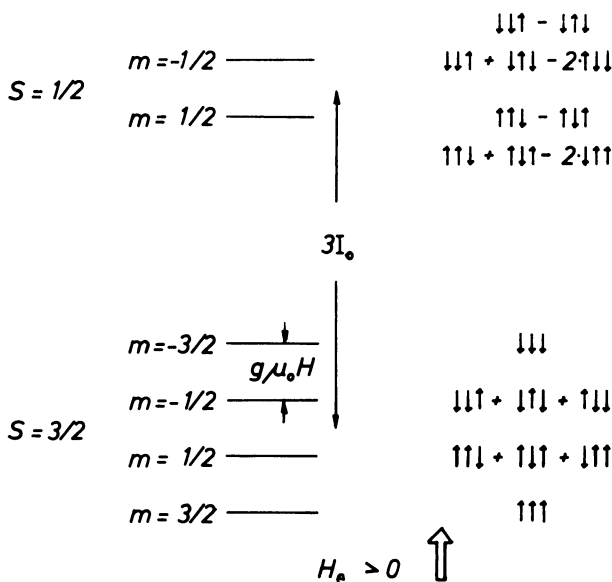
Fig. 4: Schematic representation of the energy level diagram of a system of three equidistant atoms, each having spin $\hbar/2$ and being linked with the others by exchange interaction [due to BEAN and LIVINGSTON 1959]. The spin wave functions belonging to the relative eigenvalues of eq. (3.1) are symbolized by triplets of arrows. m means the magnetic quantum number, $g \cdot \mu_0 \cdot H$ the ZEEMAN energy and I_0 the exchange energy. The upper levels are both degenerated.

If we now look at the states of non-equilibrium caused for instance by an alternating magnetic field

$$H(t) = H_0 \cdot \cos(\omega \cdot t), \tag{3.6}$$

we will find more or less remarkable deviations from eq. (3.4) depending on whether the relaxation time τ_R necessary at a given temperature T to establish thermal equilibrium, is less than the period of field change $\tau_H = 2 \cdot \pi/\omega$ or not. In the former case of

$$\tau_R(T) \ll \tau_H \tag{3.7}$$

the spin system will behave superparamagnetically whereas it should show hysteresis if

$$\tau_R(T) > \tau_H. \tag{3.8}$$

To illustrate this latter case some more in detail, in fig. 5 a schematic representation is given of the equilibrium excitation probability $\omega_e(T)$ corresponding to point 1 of the
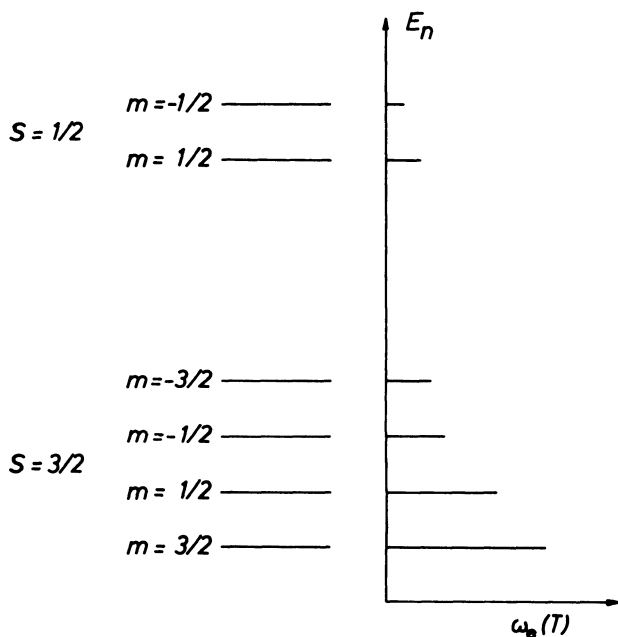
Fig. 5: Schematic representation of the equilibrium excitation probabilities $\omega_e(T)$ belonging to the eigenstates of the three-atom system, if its magnetization state corresponds to point 1 of the hysteresis loop sketched in Fig. 6.
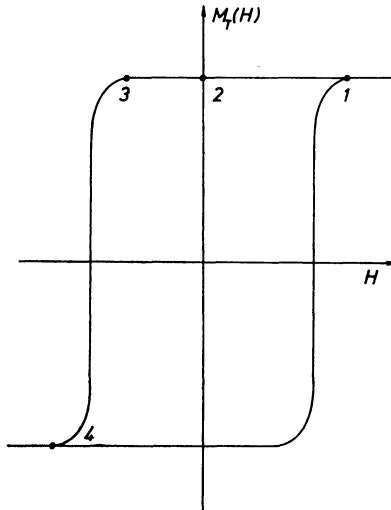
Fig. 6: Schematic sketch of the hysteresis loop of the three-atom system described in Fig. 4 and belonging to a temperature slightly below the critical one above which super-paramagnetic behavior will take place.
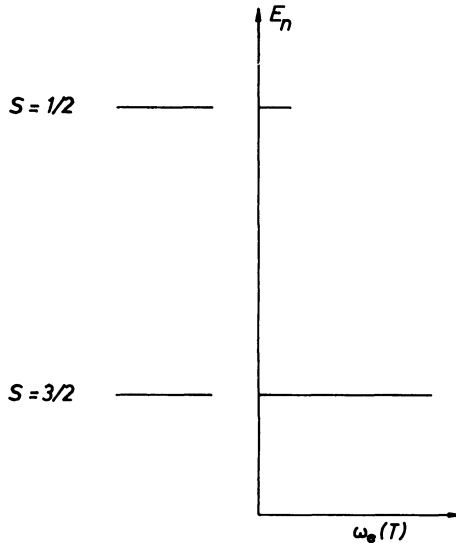
Fig. 7: Schematic representation of the degeneration taking place in the energy level diagram of Fig. 5 at zero external field, i.e. in the state of remanent magnetization corresponding to point 2 of the descending hysteresis branch in Fig. 6. ω_e (T) again denotes the respective equilibrium excitation probability.

magnetization curve sketched in fig. 6. If the magnetic field H, according to eq. (3.6), decreases towards zero, the ZEEMAN-splitted energy levels corresponding to $S = 3/2$ and $1/2$, respectively, will move together and at $H = 0$ they will degenerate to the two-term system shown in fig. 7. But, since within each ZEEMAN subset of levels the transition probability is very low[1]), the respective relaxation times $\tau_R^{(3/2)}$ (T) are satisfying condition (3.8) and thus the resulting magnetic moment $\mathfrak{M}$ (T) of the spin system will nearly remain stable even when H passes through zero. Further decrease of the magnetic field again leads to ZEEMAN splitting but now, according to eq. (3.8), the excitation probability, for instance at point 3 of the descending branch in fig. 6, will be distributed over the energy levels as schematically is shown in fig. 8. If we assume that the probability ω_{tr} $(T) = 1/\tau_R$ (T) of transitions between suitable energy levels of the two different subsets, i.e. between levels with $\Delta S = \pm 1$, $\Delta m = 0, \pm 1$, at least in a rough estimation may be described by

$$(1/\tau_R(T))_s = 2 \cdot v_0 \cdot \exp(-|E_m - E_n|/k_B \cdot T), \qquad (3.9)$$

where v_0 denotes the LARMOR frequency and E_m and E_n are suitable levels given by eqs. (3.5), then at any given temperature T, there exists a critical magnetic field $-H_c$ (T) at which

$$2 \cdot v_0 \cdot \exp(-|E_m - E_n|/k_B \cdot T) = \tau_H. \qquad (3.10)$$

Thus, when H decreases below $-H_c$, i.e. when

$$H < -H_c < 0, \qquad (3.11)$$

allowed transitions from the quartet to the doublet term subsystem and back again will become probable and by this way, the spin system will indirectly reverse its magnetization, i.e. go from point 3 to point 4 in fig. 6.

If the above outlined model of magnetic reversal of very small particles is true, its main concept, namely the necessity of indirect transitions composed by a first transition from the quartet subsystem to the intermediate state of excited doublet levels and by a second one leading back to a new equilibrium excitation distribution of both the doublet and the quartet sublevels, should be capable of being verified just by means of the same experiment that had been supposed in the beginning of this paragraph. Indeed, the transitions from the quartet to the doublet sublevels as well as the reverse ones should be observable by means of RAMAN scattering, the first giving raise to the STOKES-type RAMAN effect, the second leading to Anti-STOKES scattering. With regard

[1]) If transitions take place within same ZEEMAN multiplet, especially at $S = 3/2$, then it follows that at least one of the three atoms must make a forbidden transition of type S_{atom} = constant.
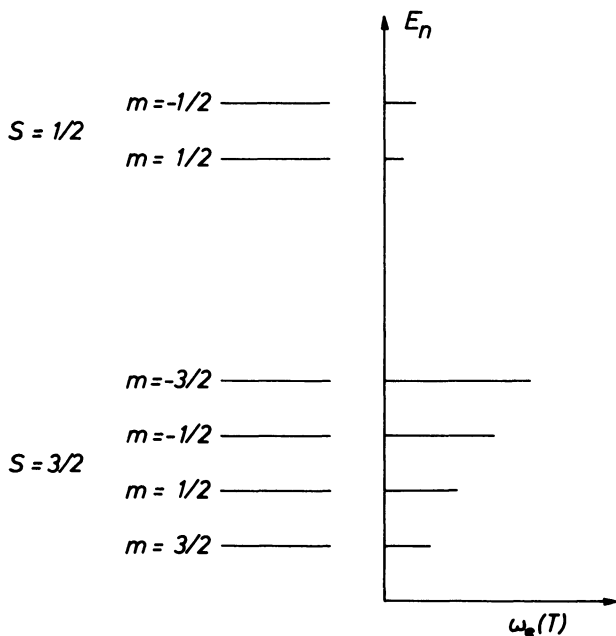
Fig. 8: Schematic sketch of energy levels and relative quasi-equilibrium excitation proba-
bilities $\omega_e\,(T)$ corresponding to the magnetization state of a ferromagnetic single-
domain particle illustrated by point 3 of the descending hysteresis branch shown in
Fig. 6.

to nickel atoms having the exchange energy noted above, in both cases of Stokes as
well as of Anti-Stokes scattering the magnitude of line shift should be expected to
amount to about

$$\Delta\,(1/\lambda)\approx\pm516\,\left[\text{cm}^{-1}\right].\tag{3.12}$$

Additionally we should obviously observe an absorption peak at a wave length
corresponding to the energy gap of $3\cdot J$ between the quartet and doublet sublevels,
i.e. in the infrared region at about

$$\lambda\approx19{,}3\cdot10^{-4}\,\left[\text{cm}\right].\tag{3.13}$$

Let us now attend to an assemble of a large number of spins coupled by exchange
interaction and regularly ordered in a spin lattice built up by a corresponding crystal
lattice. If we try to consider the dynamics of magnetic spin reversal taking place in
such a system, we have to confine to demonstrate at least the principally unsolved

problems arising till now even from the simplest case of magnetic spin reversal of fine particles: the magnetic spin reversal of ferromagnetic maximum single-domain particles, i.e. of single crystal particles as large in diameter as to maintain just single-domain behavior.

According to AKHIEZER [1968], the Hamiltonian of such a particle can be formulated by

$$
\begin{aligned}
H = &-\frac{1}{2} \cdot \sum_{l \neq l'} J(R_{ll}) \cdot S_l \cdot S_{l'} + 2 \cdot \mu_0 \cdot H_0^{(e)} \cdot \sum_l S_l^{(z)} + \\
&+ 2 \cdot \mu_0^2 \cdot \sum_{l \neq l'} \frac{1}{R_{ll'}^5} \cdot (R_{ll'}^2 \cdot S_l \cdot S_{l'} - 3 \cdot (R_{ll'} \cdot S_{l'}) \cdot (R_{ll'} \cdot S_l)) - \\
&- 2 \cdot \beta \cdot \frac{\mu_0^2}{a^3} \cdot \sum_l (S_l^{(z)})^2,
\end{aligned}
\tag{3.14}
$$

where the first term represents the exchange interaction, the second one the interaction between the spins and the external magnetic field while the third term describes the magnetic dipole interaction and the last one the magnetic anisotropy (with β denoting the anisotropy constant and a the lattice parameter). But even if we take into account only the first two terms on the right hand side of eq. (3.14), it can be verified that now wave functions as those corresponding to the constant-energy levels of our above discussed three-atom system, do not describe eigenstates of the Hamiltonian (3.14). To get really an eigenfunction that represents the first excited state one has to built up the superposition of single wave functions $S_l^+ \mid 0 >$:

$$
|1_k> = \sum_l \exp(i \cdot k \cdot R_l) \cdot S_l^+ |0>,
\tag{3.15}
$$

where k denotes a wave vector, $\mid 0 >$ the ground state vector, and where the atomic spin operators S_l^+, S_l^-, $S_l^{(z)}$ are defined by

$$
S_l^\pm = S_l^{(x)} \pm i \cdot S_l^{(y)}
\tag{3.16a}
$$

$$
[S_l^{(z)}, S_{l'}^\pm] = \pm S_l^\pm \cdot \delta_{ll'}
\tag{3.16b}
$$

$$
\sum_l S_l^{(z)} |0> = -N \cdot S \cdot |0>
\tag{3.16c}
$$

$$
S_l^- |0> = 0,
\tag{3.16d}
$$

with N designating the number of spins and S the spin quantum number. Eq. (3.15) means: the first excited state is that of one excited spin wave of wave vector k, i.e. of one excited magnon which lowers the resultant spin by $\hbar$ and the resultant magnetic moment by $g \cdot \mu_0$ (if g denotes the spectroscopic splitting factor and μ_0 the BOHR magneton). From eq. (3.15) together with the first two terms on the right hand side

of eq. (3.14), it follows that the ground state energy of our particle is given by

$$E_0 = -2 \cdot \mu_0 \cdot N \cdot S \cdot H_0^{(e)} - S^2 \cdot N \cdot \sum_l I(R_{lm}), \tag{3.17}$$

while the energy of the excited magnon amounts to

$$\hbar \cdot \omega(k) = 2 \cdot \mu_0 \cdot H_0^{(e)} + S \cdot \sum_l I(R_{lm}) \cdot (1 - e^{i \cdot k \cdot R_{lm}}) \tag{3.18}$$

and may be approximated in the case of

$$k \cdot R_{lm} \ll 1 \tag{3.19}$$

with regard to a cubic lattice of lattice constant a, by

$$\hbar \cdot \omega(k) = 2 \cdot \mu_0 \cdot H_0^{(e)} + 2 \cdot S \cdot I_0 \cdot a^2 \cdot k^2, \tag{3.20}$$

where I_0 is the exchange integral between nearest neighbours. Thus, with respect to the first excited state, the energy of our maximum single domain particle can be written in the form

$$E_1(k) = E_0 + \hbar \cdot \omega(k). \tag{3.21}$$

For simplicity let us now first confine our attention to particles the excited states of which are built up only by one, two or n independently excited magnons, i.e. by a "gas" of noninteracting "free" magnons. The energy of such a particle is then given by

$$E_n(k_1, \ldots k_l) = E_0 + \sum_j^l n_j \cdot \hbar \cdot \omega(k_j), \text{ with } \sum_j^l n_j = n, \tag{3.22}$$

its resultant angular momentum amounts to

$$\sum_l^N S_l^{(z)} = -\hbar \cdot (N \cdot S - n) \tag{3.23}$$

and its total magnetic moment decreases to

$$M_t(n) = g \cdot \mu_0 \cdot (N \cdot S - n). \tag{3.24}$$

Unfortunately the energy states $E_n(k_1, \ldots k_l)$ cannot be illustrated in a diagram as clearly as in our first example dealing with the three-atom limiting case, since now we

have no simple energy levels but either, in the relatively simple case of $E_1(k_1)$, the well known dispersion law of eq. (3.20) of a spin wave, or, in the case of $E_n(k_1 \ldots k_l)$, its generalization to a function depending on $l \leq n$ parameters k_1 to k_l. Thus we prefer to renounce on a graphical illustration.

If we now would develop at least a first-order approximative model of magnetic spin reversal and hysteresis on the basis of transitions taking place between the above defined energy states $E_n(k_1, \ldots, k_l)$, we should know solutions of the following problems:

1. How does the equilibrium total magnetic moment $M_t(n)$ of our ferromagnetic maximum single-domain particle depend on the magnetic field.

2. What kinds of magnon-magnon and magnon-phonon interaction processes must take place in order to establish the different states of equilibrium belonging to given temperatures and magnetic fields.

3. What are the orders of magnitude of the relaxation times characterizing the processes mentioned above in point 2.

To begin with point 1. we realize that on the basis of our concept of changes in total magnetic moment belonging exclusively to corresponding transitions between different magnon excitation states, the equilibrium number $\bar{n}$ of excited magnons must depend on temperature T and on the internal magnetic field $H_0{}^{(i)}$. Thus, according to eq. (3.24), and if we take into account only the potential energy, the exchange energy and the stray field energy at given T, the equilibrium number $\bar{n}(H_0{}^{(i)})$ should follow from minimization of the total energy

$$E_t = H_0^{(i)} \cdot M_t(n) + 2 \cdot S \cdot I_0 \cdot \sum_i^l n_i \cdot (a \cdot k_i)^2 + N_D \cdot g^2 \cdot \mu_0^2 \cdot \frac{(N \cdot S - n)^2}{V},$$

(3.25)

where

$$0 \leq H_0^{(i)} \quad \text{and} \quad \sum_i^l n_i = n,$$

and with N_D denoting the demagnetizing factor of the particle, V its volume, and all other symbols maintaining their former meaning. By minimization of eq. (3.25) with respect to n we find

$$\bar{n}(H_0^{(i)}) = N \cdot S - \frac{V}{2 \cdot N_D \cdot g^2 \cdot \mu_0^2} \cdot \left[g \cdot \mu_0 \cdot H_0^{(i)} + 2 \cdot S \cdot I_0 \cdot \sum_i^l (a \cdot k_i)^2 \right]$$

(3.26)

and, due to eq. (3.24),

$$\overline{M}_t(\bar{n}(H_0^{(i)})) = \frac{V}{2 \cdot N_D \cdot g \cdot \mu_0} \cdot \left[g \cdot \mu_0 \cdot H_0^{(i)} + 2 \cdot S \cdot I_0 \cdot \sum_i^l (a \cdot k_i)^2 \right].$$

(3.27)

Particularly, if $H_0^{(i)} = 0$, we find from eq. (3.27) the equilibrium remanent magnetic moment

$$\overline{M}_R = \frac{S \cdot I_0 \cdot V}{N_D \cdot g \cdot \mu_0} \cdot \sum_i^l (a \cdot k_i)^2 . \tag{3.28}$$

To illustrate eq. (3.28) with regard to a nickel fine particle of, say, 10^3 Å in diameter, we put $N_D = 4 \cdot \pi$, $g \cdot \mu_0 = 1.85 \cdot 10^{-20}$ (emu), $S = 1/2$, $I_0 = 3.4 \cdot 10^{-14}$ (emu), $\max (k_i) = 2 \cdot \pi \cdot 10^6$ cm^{-1}, $a \approx 1 \cdot 10^{-8}$ cm and get

$$\overline{M}_R / V = 290 \text{ Gauss} . \tag{3.29}$$

From a rather formal point of view, neglecting that eqs. (3.17) to (3.24) had been deduced by the premise of $N \gg n$, we might even estimate the coercivity from eq. (3.26) by requiring

$$\bar{n} (H_{0_c}^{(i)}) = N/2 . \tag{3.30}$$

Doing this we would find

$$H_{0_c}^{(i)} = 2 \cdot \frac{S \cdot I_0}{g \cdot \mu_0} \cdot \sum_i^l (a \cdot k_i)^2 \tag{3.31}$$

and with regard to our above used example of a nickel fine particle

$$H_{0_c \text{ Ni}}^{(i)} = 7.3 \cdot 10^3 \, [\text{Oe}] . \tag{3.32}$$

But in spite of this surprisingly good value, eq. (3.31) cannot be considered to be a satisfying estimation of the coercive force at least because of the following reason: eq. (3.31) had been deduced from extrapolating eq (3.27) to magnetic fields $H_0^{(i)} < 0$, but in this case the real equilibrium values of the magnetic moment will depend upon the magnetic field as is shown in fig. 9, i.e. by a relationship

$$\overline{M}_t (\bar{n} (H_0^{(i)})) = \frac{V}{2 \cdot N_D \cdot g \cdot \mu_0} \cdot \left[g \cdot \mu_0 \cdot H_0^{(i)} + 2 \cdot S \cdot I_0 \cdot \sum_i^l (a \cdot k_i)^2 \right] - 2 \cdot \overline{M}_R \tag{3.27 a}$$

with

$$H_0^{(i)} < 0 ,$$

while the extrapolation of eq. (3.27) only leads to a quasi-equilibrium condition illustrated in fig. 9 by the dashed lines. These quasi-equilibrium states take place
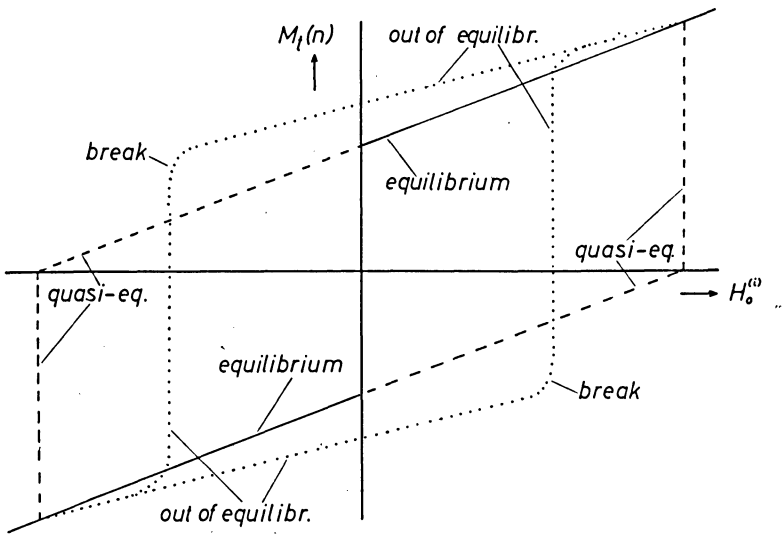
Fig. 9: Possible types of magnetization curves of maximum single-domain particles. The full lines show the curve of minimum energy estimated on the basis of eq. (3.27) if $H_0^{(t)} > 0$, and on eq. (3.27a) if $H_0^{(t)} < 0$. The dashed lines represent the state of quasi-equilibrium again estimated by eqs. (3.27) and (3.27a) whereby eq. (3.27) is thaught to be valid with respect to the descending hysteresis branch even at magnetic fields $-H_{0_c}^{(t)} \leq H_0^{(t)} < 0$ (where $\mp H_{0_c}^{(t)}$ is given by eq. (3.31)), and if, with regard to the ascending branch, eq. (3.27a) is extrapolated even to fields $H_{0_c}^{(t)} \geq H_0^{(t)} > 0$. The dotted curve represents a some more realistic non-equilibrium type of hysteresis loop that must be expected if relaxation processes and magnetic aftereffect also are taken into account.

below zero magnetic field if the spin lattice maintains its former arrangement when $H_0^{(t)}$ passes through zero.

Thus, even if we would use a less simple approximation of the exchange energy as we did in eq. (3.25), i.e. if we would start from an exchange energy given, due to AKHIEZER [1968], by

$$E_{ex} = \sum_k \varepsilon(k) \cdot \bar{n}(k), \qquad (3.33)$$

with the PLANCK magnon distribution

$$\bar{n}(k) = \frac{1}{\exp(\varepsilon(k)/k_B \cdot T) - 1} \qquad (3.34)$$

and

$$\varepsilon(k) = \left[k_B \cdot \theta_C \cdot (a \cdot k)^2 + \mu_0 \cdot (H_0^{(i)} + \beta \cdot M_0) \right]^{1/2} \cdot$$
$$\cdot \left[k_B \cdot \theta_C \cdot (a \cdot k)^2 + \mu_0 \cdot (H_0^{(i)} + \beta \cdot M_0) + 4 \cdot \pi \cdot \mu_0 \cdot M_0 \cdot \sin^2 \vartheta_k \right]^{1/2} \qquad (3.35)$$

denoting the magnon energy (where k designates the wave vector of the magnon, k_B the BOLTZMANN constant, θ_C the CURIE temperature, β the crystalline anisotropy constant, M_0 the saturation magnetization at zero temperature and δ_k the angle between k and the anisotropy axis), we would not come to a satisfying description of the descending hysteresis branch and its critical break at $H_{0_c}^{(i)}$ (also indicated schematically in fig. 9 by the dotted curves) because of the following reason that we wish to formulate as a hypothesis:

We think the process of magnetic spin reversal of fine particles should be understood to be a phase transition of first order leading to a breaking up of the spin lattice at a critical magnetic field $-H_{0_c}^{(i)}$ in order to enable a new antiparallel alignment of the spins at fields $H_0^{(i)} < -H_{0_c}^{(i)} < 0$. Indeed, if we try to consider the dynamics of magnetic spin reversal from our model of a "gas" of "free" magnons travelling through a spin lattice of antiparallel magnetic moment, we have to describe the phenomenon taking place in our spin system at $-H_{0_c}^{(i)}$ and $\overline{M}_t = 0$ by unstable fluctuations of all spins similar to those occurring at the CURIE point, and formally resulting from the requirement that at $-H_{0_c}^{(i)}$ we should have as much magnons as remaining lattice spins.

Before pointing out this hypothesis to some more extent, let us attend to points 2. and 3. of the above listed open problems of magnetic spin reversal. To be capable to explain hysteretic behavior by transitions between energy states belonging to different numbers of excited magnons, we would need the following kinds of magnon-magnon and magnon-phonon interaction processes of suitable lifetimes:

1.   Field-independent processes that should affect the thermal excitation of magnons as well as their thermal equilibrium distribution. To perform thermal excitation we would need:

1.1. Magnon-phonon interactions of the following types:

1.1.1. The transformation of two phonons into a magnon in order to be capable to excite additional magnons and to reduce by this way the total magnetic moment.

1.1.2. The transformation of a magnon into two phonons in order to be capable to reduce the number of excited magnons and to increase the total magnetic moment.

1.1.3. The absorption of a phonon by a magnon in order to be capable to increase the magnon energy without changing the total magnetic moment.

1.1.4. The emission of a phonon by a magnon in order to be capable to lower the magnon energy without changing the total magnetic moment.

1.2. Magnon-magnon interactions of the following kind:

1.2.1. Magnon-magnon scattering in order to be capable to change the magnon distribution with respect to their wave vectors k and without changing by this way the total magnetic moment.

2. Field-dependent processes that should render it possible to change the total magnetic moment by means of varying external magnetic fields. To be capable to affect this we would need:

2.1. Magnon-magnon interactions of the following kind:

2.1.1. The process of absorption of a magnon by a second magnon, i.e. the two magnon coalescence in order to be capable to increase the total magnetic moment without changing the total magnon energy.

2.1.2. The process of splitting of a magnon into two magnons, i.e. the magnon decay process in order to be capable to lower the total magnetic moment without changing the total magnon energy.

2.2. Magnon-phonon interactions of the following type:

2.2.1. The decay of a travelling phonon into two magnons above a critical external threshold field H_0 in order to be capable to decrease the total magnetic moment and to increase at the same time the magnon temperature at the expense of the external magnetic field as well as of the thermal energy of the crystal lattice.

If we now would have a look at the literature in order to find out which of the above enumerated interactions already had been investigated theoretically, we would see that indeed all these processes already had been studied to more or less extent and particularly with respect to their individual reciprocal lifetimes, i.e. their probabilities. Since, apart from interaction 2.2.1., the hitherto theoretical treatments of all others had been reviewed quite clearly by KEFFER [1966] and by AKHIEZER [1968] who also had listed their reciprocal lifetimes and mean probabilities, and since the process of number 2.2.1. already had been studied theoretically as well as experimentally by MATTHEWS and MORGENTHALER [1964], we renounce to repeat here the respective results. Instead of this we would confine to the following remarks:

1. If we designate the mean probabilities of the above listed interaction processes, i.e. their mean reciprocal lifetimes τ, by ω and indicate the individuell process by an index corresponding to its above enumeration, then it may easily be proved that, according to AKHIEZER [1968], at temperatures $T \ll \theta_C$ (with θ_C denoting the CURIE temperature) and in thermal equilibrium there holds a relationship of the following kind:

$$\omega_{1.2.1.} \gg \omega_{2.1.2.} = \omega_{2.1.1.} > \omega_{1.1.3.} = \omega_{1.1.4.} \gg \omega_{1.1.1.} = \omega_{1.1.2.} . \tag{3.36}$$

From this it follows, due to AKHIEZER [1968], that the dominating magnon-magnon scattering process leads to the appearance of a quasi-equilibrium BOSE magnon distribution the temperature of which, i.e. the spin temperature, may differ from

the phonon temperature, i.e. the temperature of the crystal lattice. Consequently the corresponding magnetic moment then may differ from the equilibrium magnetic moment given, due to our above first order approximation, by eqs. (3.27) and (3.27a). Thermal equilibrium, i.e. the equalization of spin and lattice temperature, and equilibrium magnetic moment will occur only slowly in comparison with $\omega_{1.2.1.}$, i.e. within a relaxation time given by $\tau_{eq} \approx 1/\omega_{1.1.1.} = \omega_{1.1.2.}$.

Thus, if we wish to avoid remarkable magnetic aftereffect, we might not exceed sufficiently low rates of field acceleration determined by

$$(\partial H_0^{(i)}/\partial t)_{max} \ll M_0 \cdot \omega_{1.1.1.}/\chi(H_0^{(i)}),\tag{3.37}$$

with M_0 designating the saturation magnetization and $\chi(H_0^{(i)})$ the susceptibility of the equilibrium magnetization curve given in our estimation by eqs. (3.27), (3.27a).

2. All investigations of magnon-magnon and magnon-phonon interactions that had been carried out till now refer, as far as we know, only to the case of $H_0^{(i)} \geq 0$. Thus it is still an open question how the above reviewed results of these investigations must be modified at $H_0^{(i)} < 0$, and to continue in our consideration we have to introduce a second hypothesis:

we assume that there is no marked change in physical behavior of our maximum single-domain particle when $H_0^{(i)}$ passes through zero, since we cannot find any plausible reason for it. If discussed on the basis of our model, all what may happen is that either the coalescence mechanism might be favoured at the expense of the splitting process, or that the reverse case would take place. But the first alternative would imply a break down of the total magnetic moment immediately below zero magnetic field, i.e. a very small coercive force contrary to our supposition of marked rectangular hysteresis, while the second case would entail an increase of total magnetic moment at $H_0^{(i)} < 0$ which again disagrees with our supposition as well as with all experimental experience. Thus we believe that at $H_0^{(i)} < 0$ our spin system has no chance to come to its real equilibrium state given by eq. (3.27a) but at best will follow the quasi-equilibrium curve shown in fig. 9.

3. A process that would really be suitable to explain rectangular hysteresis should be characterized at least by the following properties:

a) it should set in markedly just below a critical threshold field $-H_{0_c}^{(i)}$;

b) it should produce additional magnons or pairs of magnons;

c) it should raise the spin temperature up to a critical value sufficient to break the spin lattice open in order to enable a subsequent new but antiparallel alignment of the spins.

Among all interactions we had listed above, the only one that might possibly effect this break down of magnetic moment at a critical field $-H_{0_c}^{(i)}$ seems to be the last one numerated in our terminology by 2.2.1.

If the above outlined considerations were true, they should lead at least to three predictions capable to be verified by experiment:

1. If the magnetic spin reversal taking place at the coercivity $H_{0_c}{}^{(i)}$, is caused as well as accompanied by a breaking up of the spin lattice and by its subsequent antiparallel alignment, the whole process should be capable of being described in terms of phase transition which, due to EHRENFEST [1933], should be of first order since, because of the rectangular hysteresis loop, the magnetization of each particle, i. e. the first derivative of the free enthalpy G with respect to the magnetic field H, shows a break at $(\mp)H_{0_c}{}^{(i)}$ while the susceptibility χ, i. e. the second derivative of G with respect to H, has discontinuities at these points $(\mp)H_{0_c}{}^{(i)}$.

But if the magnetic spin reversal of fine particles indeed can be understood as phase transition of first order, then their magnetocaloric effect Q as well as their volume magnetostriction ω should also show discontinuities at $(\mp)H_{0_c}{}^{(i)}$ since, due to STIERSTADT [1971], there exist two other field-dependent second derivatives of G, namly

$$\partial^2 G/\partial T\, \partial H = -(1/H\cdot T)\cdot Q_P \qquad\qquad (3.38\,\text{a})$$

and

$$\partial^2 G/\partial P\, \partial H = (V/H)\cdot \omega_T, \qquad\qquad (3.38\,\text{b})$$

with T denoting the temperature, V the particle volume and with the indices "P" and "T" indicating the conditions of constant pressure and of constant temperature, respectively.

Thus, it should be of interest to look for field-dependent discontinuities of Q_P and of ω_T of ferro- and ferrimagnetic single-domain fine particles.

2. It should be possible to force the heating of the spin lattice and thus to lower the coercivity of the maximum single-domain particles by exerting suitable external influences on them. Such influences should be:

   a) Ultrasonic irradiation at magnetic fields $-H_{0_c}{}^{(i)} < H_0{}^{(i)} \ll 0$, i. e. application of the experiment of MATTHEWS and MORGENTHALER [1964] on our problem.

   b) Irradiation by infrared and by visible light, i.e. magnon creation by means of photon-magnon interactions and particularly by application of transverse and parallel pumping experiments described for instance by SPARKS [1964] and by KEFFER [1966]. Since, due to KEFFER [1966], these pumping experiments work in the way that an incidenting photon first creates a $(k=0)$-magnon which then splits into two magnons of equal and opposite wave vectors k_1 and k_2, and since the photon energy $\hbar\cdot\omega$ is allowed to be much higher than that of the $(k=0)$-magnon, the whole process also may be capable of being described in terms of RAMAN scattering.

Although in our second limiting case of maximum single-domain particles the above outlined model of magnetic reversal by means of magnon-magnon and magnon-phonon interactions leads to considerable hysteresis, it is no realistic approximation of the

magnetization processes taking place in ferromagnetic single-domain particles at least because of the following reason:

the magnons excited in a fine particle of about 10^{-5} cm in diameter by thermal agitation or by external magnetic fields, cannot be considered to be *traveling* spin waves, as we however did above, but can, on the contrary, exist only as *standing* spin waves, i. e. as pairs of magnons with equal and opposite wave vectors k and $-k$.

Just this fact, however, seems to be not only the source of most of the unsolved problems concerning the process of magnetic reversal in fine particles, but also an object of high interest from a theoretical viewpoint as well as from an experimental one. We cannot explain this here in detail but shall confine to some final remarks:

1. Most of the above discussed magnon-magnon and magnon-phonon interactions would violate the theorem of conservation of momentum if taking place between pairs of magnons of opposite wave vectors, i. e. they are forbidden processes with respect to standing spin waves.

2. In fine particles instead of a continuum we have only discrete possible values of k.

3. To explain hysteresis and hysteresis losses in fine particles, we need interactions between pairs of magnons with opposite wave vectors k and pairs of phonons again with opposite wave vectors q. But, as far as we know, the probabilities of such processes seem not to be calculated till now.

4. As already outlined above, the most important and interesting ferro- and ferrimagnetic resonance experiments are those concerning transverse and parallel pumping, see for instance KEFFER [1966] and SPARKS [1964], i. e. those which deal with transitions between photons or phonons on the one hand and pairs of magnons of opposite wave vectors k on the other. Obviously such kinds of interactions are of great interest also with regard to the processes of magnetic spin reversal of fine particles and with respect to our above mentioned experimental project of activation of magnetic reversal of fine particles by means of photon interactions. And, although we do not know enough facts to describe the process of magnetic reversal of fine particles already in detail, we can predict that by means of parallel and transverse pumping experiments, i. e. by suitably incidenting visible or infrared light, we should be able to reduce the coercivity of our particles remarkably, since by this way we would produce pairs of magnons of opposite k which would lower the total magnetic moment and thus initiate the above discussed process of breaking up of the spin lattice and of magnetic reversal. As also already mentioned above, due to KEFFER [1966], we should additionally be capable to observe RAMAN scattering of the STOKES type, as is indicated in our fig. 3c.

Acknowledgements

Munich), Prof. Dr. K. STIERSTADT (Sektion Physik, University of Munich), Priv.-Doz. Dr. H. SOFFEL (Institut für Angewandte Geophysik, University of Munich), Dr. K. BINDER (Reaktorstation Garching, Munich), and Dr. N. PETERSEN (Institut für Angewandte Geophysik, University of Munich) for their interest in these problems and for many helpful discussions.

References

AHARONI, A.: Effect of a magnetic field on the superparamagnetic relaxation time. Phys. Rev. 177, 793—796, 1969.

AKHIEZER, A. I., V. G. BAR'YAKHTAR and S. V. PELETMINSKII: "Spin Waves", North-Holland Publishing Company, Amsterdam 1968.

BEAN, C. P. and J. D. LIVINGSTON: Superparamagnetism. J. appl. Phys. 30S, 120—129, 1959.

BROWN, W. F.: Relaxation behavior of fine magnetic particles. J. appl. Phys. 30S, 130—133, 1959.

— : Thermal fluctuations of a single-domain particle. J. appl. Phys. 34, 1319—1320, 1963.

EHRENFEST, P.: Proc. Acad. Sci. Amsterdam 36, 153, 1933.

FONER, S.: Antiferromagnetic and ferrimagnetic resonance. In: "Magnetism", ed. by RADO, G. T. and H. SUHL, Academic Press, New York/London 1963.

KEFFER, F.: "Spin Waves", in: Handbuch der Physik, Band XVIII/2, ed. by FLUEGGE, S., and H. P. J. WIJN, Springer-Verlag, Berlin/Heidelberg/New York, 1966.

KNELLER, E.: Theorie der Magnetisierungskurve kleiner Kristalle. In: Handbuch der Physik, Band XVIII/2, ed. by FLUEGGE, S., and H. P. J. WIJN, Springer-Verlag, Berlin/Heidelberg/ New York, 1966.

MARKERT, H.: On the size distribution of submicroscopic magnetite and titano-magnetite fine particles in basalt. Z. Geophys., 1971, this issue.

MATTHEWS, H., and F. R. MORGENTHALER: Phonon-pumped spin wave instabilities. Phys. Rev. Lett. 13, 614—616, 1964.

NEEL, L.: Théorie du trainage magnétique des ferromagnétiques en grains fins avec applications aux terres cuites. Ann. Geophys. 5, 99—136, 1949.

SHIRK, B. T., and W. R. BUESSEM: Magnetic properties of barium ferrite formed by crystallization of a glas. J. Amer. Cer. Soc. 53, 192—196, 1970.

SPARKS, M.: "Ferromagnetic relaxation theory". McGraw-Hill, New York/San Francisco/ Toronto/London, 1964.

STIERSTADT, K.: Private communication, 1971.

On the Origin of the Magnetization of Impact Breccias on Earth

J. POHL, München[1])

Summary: Measurements of the magnetization of impact breccias with glassy components (Ries Crater, Rochechouart Structure, Lake Mien, Lake Dellen) have shown that these breccias have a sometimes quite intense and stable remanent magnetization, which can be used for paleomagnetic investigations. The magnetic mineral fraction is determined by the content of ferromagnetic minerals in the original rocks from which the breccia was made, then by changes and formation of new minerals by impact metamorphism and during cooling of the breccia after sedimentation on the earth's surface. Many of these processes lead to the formation of magnetite, at least as an intermediate product before further oxidation. In the hot glass containing breccias the remanent magnetization is mainly a thermoremanent magnetization, but may be partly also a chemical or a thermochemical remanent magnetization.

Zusammenfassung: Messungen der Magnetisierung von Einschlagbreccien, die glasige Anteile enthalten (Ries Krater, Rochechouart Struktur, Lake Mien, Lake Dellen), haben gezeigt, daß diese Breccien eine manchmal sehr starke und stabile remanente Magnetisierung haben, die für paläomagnetische Untersuchungen verwendet werden kann. Die Träger der Magnetisierung sind bedingt durch den Gehalt an ferromagnetischen Mineralien in den ursprünglichen Gesteinen, aus denen die Breccie gebildet wurde, und durch die Veränderungen und Neubildung von ferromagnetischen Mineralien durch die Stoßwellenmetamorphose und bei der Abkühlung der Breccie nach der Sedimentation an der Erdoberfläche. Viele dieser Prozesse führen zur Bildung von Magnetit, zumindest als Zwischenstufe vor weiterer Oxydation. Die remanente Magnetisierung, die in den heißen Breccien gebildet wurde, ist hauptsächlich eine thermoremanente Magnetisierung, kann jedoch zum Teil auch eine chemische oder thermochemische remanente Magnetisierung sein.

In this article a short qualitative description is given of the main processes, as far as they are known today, which contribute to the origin of the magnetic mineral phases and the magnetization of some impact breccias in meteorite craters on earth. Most observations and deductions have been obtained from investigations on the suevite breccia of the Ries Crater (Germany), but it can be expected that the general features are also valid for impact breccias in many other meteorite craters on earth, especially since the breccia in the Ries seems to be quite typical and has not suffered much alteration since its formation.—A study of the magnetic properties of impact breccias

---

[1]) J. POHL, Institut für Angewandte Geophysik, 8 München 2, Richard-Wagner-Str. 10.

on earth is of interest in order to compare them with the magnetic properties of similar breccias on the moon. The pressure and temperature conditions of the impact by which these breccias are formed on the moon, are comparable to those on earth, but the absence of an oxidizing atmosphere leads to magnetic minerals and magnetic properties which are characteristically different from those on earth.

The breccias which are formed by the impact of a meteorite (or a comet) on the earth surface are found inside the crater as crater filling and outside the crater as ejected material (see e. g. FRENCH and SHORT 1968, Bayer. Geolog. Landesamt 1969). The most interesting breccias for magnetic investigations contain glassy components, often in form of lumps or in pancake form (Fladen). The glass has been formed by shock melting (and perhaps partly volatilization and recondensation) of the rocks in the impact area, which for the investigated breccias consisted mostly of igneous and metamorphic rocks. The glass formation is restricted to the central impact area, with a diameter of about 1/10 to 1/5 of the final crater diameter. The necessary pressures and residual (after decompression) temperatures for the glass formation are of the order of 500 kbar and 1200 °C respectively (e. g. stage III after ENGELHARDT, STÖFFLER and SCHNEIDER 1969). During the ejection the glass is generally mixed with only brecciated material with a lower degree of shock metamorphism to form the impact breccia.

In the Ries Crater the glass containing breccia (Suevite) apparently forms mainly the upper layer of the crater filling and of the throwout outside the crater. This can be deduced from geological observations (ENGELHARDT et al. 1969) and from measurements of the magnetic anomalies associated with these layers (POHL and ANGENHEISTER 1969). In several Canadian craters glass containing breccias have also been found by drilling in deeper parts of the crater filling (e. g. DENCE 1964) and it seems that in some craters more or less homogeneous impact melts containing only few brecciated inclusions have been produced. The magnetization of a possible impact melt of this kind has been investigated by ROBERTSON (1967).

The duration of the whole impact process, including crater formation and ejection of material, is very short, even for craters having several tens of km in diameter. A few minutes after the impact most of the sedimentation is finished and generally no further movements, except perhaps some sliding or similar phenomena, occur, if no magmatic processes have been induced by the impact. In very big craters ($<$ 50 km) isostatic movements can however take place later. The tuff like appearence of the glass containing breccias indicates that in the short time intervall between the impact and the sedimentation the strongly heated material could not cool down to room temperature and that the breccias still had temperatures of several hundred degrees centigrade at the moment of their formation on the earth's surface. Detailed investigations for the suevite breccia have been made by HÖRZ (1965).

The measurements of the magnetization of the glass containing impact breccias from several impact structures (Ries Crater, Germany, POHL 1965, POHL and ANGENHEISTER 1969; Rochechouart Structure, France, POHL and SOFFEL 1971, to be published elsewhere; Lake Mien, Lake Dellen, Sweden, POHL, unpublished data) have shown

that these breccias have a stable, sometimes quite intense magnetization, which can be used for paleomagnetic investigations (Ries Crater, Rochechouart Structure). The intensity of the magnetization of the investigated samples is very variable (about 20 mG to 0.001 mG), but the direction of the remanent magnetization shows very small scattering ($\alpha_{95} < 2-3°$). Ac-demagnetization gave no appreciable change of the directions ($1-2°$ for the mean values). Most samples still have 50% of their original natural remanent intensity at peak ac-fields of 200 to 300 Oe. Repeated measurements of the NRM after 6 month storing in the earth field yielded the same results within 1 or 2°. Viscous components therefore seem to be not important. KÖNIGSBERGER ratios generally range between 5 and 10.

The results of thermomagnetic analysis of suevite samples show that a magnetic phase with a CURIE-point near 580 °C is the main magnetic phase. Thus magnetite or magnetite with a possible small titanium content is the main carrier of the magnetization. The contribution of other magnetic phases with lower CURIE-points is almost insignificant. No indications for CURIE-points above 580 °C have been found, as could perhaps be expected for nickel-iron particles coming from the meteorite itself or for hematite.

Descriptions of the ore minerals in the suevite and especially in the glasses have been published by CHAO 1963, SCHÜLLER and OTTEMANN 1963, EL GORESY 1964, 1968 and KLEINMANN 1969. Small Ni—Fe spherules and Fe spherules have been found sometimes, but their occurence is too rare to contribute to the magnetic properties of the suevite. Pyrrhotite has also been described, but there is no indication for this phase in the thermomagnetic curves of magnetic concentrates from the suevite. Magnetite is found in all polished sections and occurs mainly in the two following forms: Primary magnetite, generally with small Ti-content, which was already present in the original basement rocks. The grains which have diameters up to several hundred microns are often broken, partially molten and recrystallised in small aggregates. Many grains show partial martitization; secondary magnetite, generally no visible association with original magnetite grains, mainly in skelettal or droplet form, occuring mainly in glasses. The grains are often very small, up to the limit of resolution of the light microscope. Magnetite has further been mentioned as a decomposition product of mafic minerals (biotite, amphibole) which become thus more or less opaque in thin sections (CHAO 1969, ENGELHARDT et al. 1969).

Until now a remanence with a constant direction of magnetization could be measured only in breccias containing glassy parts. In breccias containing only fragmented rocks without glass the formation of a remanent magnetization with a constant direction is not probable. The rocks have certainly been remagnetized in the earth field at the passage of the shock wave (SHAPIRO and IVANOW 1966, HARGRAVES and PERKINS 1969 and own experiments), but the sedimentation of the fragments yields a statistical distribution of the directions. No thermoremanent magnetization can be expected, since the temperature in these breccias is in most cases not much above room temperature at their formation on the earth surface. The lithic breccia of Rochechouart (KRAUT

1969) may be an example for this kind of breccia. The remanence was to weak to be measured with the available instruments ($< 10^{-6}$ G, POHL and SOFFEL 1971).

Measurements of the magnetization of a representative selection of weakly shocked thrownout specimens from the crystalline basement rocks in the Ries Crater area show that their magnetization is generally small (mean value 0.05 mG), except for some granodiorite and amphibolite specimens. The magnetization of the suevite however, which was made from the same rocks is 20 to 30 times larger and in some localities even much more. This increase of the magnetization must clearly be associated with the impact metamorphism and subsequent changes in the breccia during cooling on the earth's surface. As magnetite is the dominating ferrimagnetic mineral the production of magnetite, at least as an intermediate phase before further oxidation, must be characteristic of several of these processes.

In the central impact area, where the highest pressures occur, the temperatures may attain many thousands of degrees. In suevite glasses numerous indications for temperatures up to at least 2000 °C can be found. Molten quartz grains, the decomposition of zircon into baddeleyite and quartz and the occurence of many ore minerals in droplet form have been mentioned in this respect (EL GORESY 1968, ENGELHARDT et al. 1969). If the temperatures are high enough all minerals are completely molten and glasses similar to the mainly paramagnetic ($\chi < 10^{-5}$) tektite glasses can be produced (SENFTLE and THORPE 1959, THORPE, SENFTLE and CUTTITA 1963, OSTERTAG, ERICKSON and WILLIAMS 1969, SENFTLE, THORPE and SULLIVAN 1969). In most suevite glasses the degree of melting and mixing is however very variable and incomplete. The susceptibilities in weak fields generally range between 10^{-4} and 10^{-5}. In the thermomagnetic curves of the glasses a ferrimagnetic component with a CURIE-point near that of magnetite can always be seen. The magnetite, mainly in the secondary form as described above, can have been formed from primary iron oxydes or other iron ores or in regions with a high iron concentration resulting from uncompletely dissolved iron rich mafic minerals. As magnetite is the stable phase at atmospheric O_2-pressure above 1400 °C, the high temperatures which occured in the glasses favoured the oxydation of iron to magnetite rather than to hematite, which seems to be absent in many glasses (EL GORESY 1964).

In the area around the central impact area, where the shock waves are no longer intense enough to produce real melting ($p < 500$ to 600 kbar) the decomposition (oxidation) of biotite and amphibole by shock-metamorphism can produce iron oxides, apparently magnetite, as has been described by CHAO (1968) and ENGELHARDT et al. (1969). —Magnetite itself is quite stable up to shock-wave pressures of about 0.7 Mbar (ANDERSON and KANAMORI 1968, AHRENS, ANDERSON and RINGWOOD 1969), where a high pressure modification is produced. At pressures below 500 to 600 kbar no major changes for existing magnetite must be expected. Calculations of the HUGONIOT-temperature of magnetite with the shock-wave data of ANDERSON and KANAMORI (1968) show that at these pressures magnetite is only moderately heated up to tempera-

tures of several hundred degrees centigrade.—Nothing is known until now about the influence of the shock-waves on titanomagnetites.

After the formation of the breccia on the earth's surface by sedimentation from the air its temperature is determined by the temperatures of the hot glassy components, which had not much time for cooling, and of the less heated brecciated rock fragments. Thermal changes then occur in the oxidizing atmosphere during cooling. Again several processes tend to produce magnetite. Titanomagnetites present in igneous rocks decompose by thermal treatment in air with production of a Ti-poor spinel phase having a high CURIE-point (500 to 580 °C, e. g. NAGATA 1966, CREER and PETERSEN 1969, PETERSEN 1970). Iron sulfides in igneous rocks and metamorphic rocks are oxidized with production of magnetite which dominates then their magnetic behaviour (FRÖLICH 1968). Biotite also decomposes with production of magnetite when heated in air (WONES and EUGSTER 1965). Some of these changes may however already be produced by the immediately preceding shock metamorphism and it is not yet possible to separate these effects from the effects of temperature alone during cooling.

The remanent magnetization with a constant direction in outcrops up to 30 km apart can evidently only have been formed after the sedimentation of the breccia and at the same time when the changes described in the last section took place. In the case of the hot suevite breccias the remanence is mainly a thermoremanent magnetization, but a chemical or thermochemical origin for part of the remanent magnetization must also be taken into consideration.

The magnetite produced by most of the processes described above occurs mainly in form of very small and to a great extent as single domain grains. The good stability of the remanent magnetization in these breccias can be explained in this way (SOFFEL 1968). For paleomagnetic applications we have however to bear in mind that the remanent magnetization in the impact breccias is an almost instantaneous record of the earth's magnetic field, as in the short time intervall during which the remanent magnetization is formed, the secular variation can have no averaging effect for the dipole field.

Acknowledgement

References

Ahrens, T. J., D. L. Anderson, and A. E. Ringwood: Equations of state and crystal structures of high-pressure phases of shocked silicates and oxides. Rev. Geophysiscs, 7, 667—707, 1969

Anderson, D. L., and H. Kanamori: Shock-wave equations of state for rocks and minerals. J. Geophys. Res., 73, 6477—6502, 1968

Bayer. Geolog. Landesamt: Das Ries. Geologica Bavarica, 61, 478 S., München 1969

Beals, C. S., M. J. S. Innes, and J. A. Rittenberg: Fossil Meteorite Craters. The Solar System, ed. by Middlehurst and Kuiper, Vol. IV, 235—284, Chicago 1963

Chao, E. C. T.: The petrographic and chemical characteristics of tektites. Tektites, ed. by J. A. O'Keefe, 51—94, University of Chicago Press 1963

Chao, E. C. T.: Impact metamorphism. Research in Geochemistry, ed. by P. A. Abelson, Vol. 2, 204—233, J. Wiley & Sons, Inc., New York 1967

Chao, E. C. T.: Pressure and temperature histories of impact metamorphosed rocks—based on petrographic observations. Shock metamorphism of natural materials, ed. by B. M. French and N. M. Short, 135—158, Mono Book Corp., Baltimore 1968

Creer, K. M., and N. Petersen: Thermochemical magnetization in basalts. Z. Geophys., 35, 501—516, 1969

Dence, M. R.: A comparative structural and petrographic study of probable canadian meteorite craters. Meteoritics, 2, 249—270, 1964

Engelhardt, W. v.: Chemical composition of Ries glass bombs. Geochim. et Cosmochim. Acta, 31, 1677—1689, 1967

Engelhardt, W. v., and D. Stöffler: Stages of shock metamorphism in crystalline rocks of the Ries Basin, Germany. Shock Metamorphism of Natural Materials, ed. by B. M. French and N. M. Short, 159—168, Mono Book Corp., Baltimore 1968

Engelhardt, W. v., D. Stöffler, and W. Schneider: Petrologische Untersuchungen im Ries. Geologica Bavarica, 61, 229—295, 1969

El Goresy, A.: Die Erzmineralien in den Ries- und Bosumtwi-Krater-Gläsern und ihre genetische Deutung. Geochim. et Cosmochim. Acta, 28, 1881—1891, 1964

El Goresy, A.: The opaque minerals in impactite glasses. Shock Metamorphism of Natural Materials, ed. by B. M. French and N. M. Short, 531—553, Mono Book Corp., Baltimore 1968

French, B. M., and N. M. Short, eds.: Shock metamorphism of natural materials. Mono Book Corp., Baltimore 1968

Frölich, F.: Beiträge zum Erkundungsprogramm Materieparameter im Bereich der Erdkruste, Teil I: Verfahrensgrundlagen, Erprobungsergebnisse, Testtechnik. Abh. Geomagn. Inst. Potsdam, Nr. 41, 5—55, Berlin 1969

Hargraves, R. B., and W. E. Perkins: Investigations of the effect of shock on natural remanent magnetism. J. Geophys. Res., 74, 2576—2589, 1969

HÖRZ, F.: Untersuchungen an Riesgläsern. Beitr. z. Mineral. u. Petrogr., 11, 621—661, 1965

KLEINMANN, B.: Magnetite bearing spherules in tektites. Geochim. et Cosmochim. Acta, 33, 1113—1120, 1969

KRAUT, F.: Über ein neues Impaktit-Vorkommen im Gebiete von Rochechouart-Chassenon. Geologica Bavarica, 61, 428—450, 1969

OSTERTAG, W., A. A. ERICKSON, and J. P. WILLIAMS: Magnetic susceptibility of some synthetic and natural tektites. J. Geophys. Res., 74, 6805—6810, 1969

PETERSEN, N.: The diffusion coefficient of titanium in magnetite. Phys. Earth Planet. Interiors, 2, 175—178, 1970

POHL, J.: Die Magnetisierung der Suevite des Rieses. Neues Jb. Mineral. Monatshefte, Heft 9—11, 268—276, 1965

POHL, J., and G. ANGENHEISTER: Anomalien des Erdmagnetfeldes und Magnetisierung der Gesteine im Nördlinger Ries. Geologica Bavarica, 61, 327—336, 1969

SCHÜLLER, A., and J. OTTEMANN: Vergleichende Geochemie und Petrographie meteoritischer und vulkanischer Gläser. Neues Jb. Mineral. Abhandl., 100, 1—26, 1963

SENFTLE, F. E., and A. N. THORPE: Magnetic susceptibility of tektites and some other glasses. Geochim. Cosmochim. Acta, 17, 234—247, 1959.

SENFTLE, F. E., A. N. THORPE, and S. SULLIVAN: Magnetic properties of microtektites. J. Geophys. Res., 74, 6825—6833, 1969

SHAPIRO, V. A., and N. A. IVANOV: The stability parameters of dynamic magnetization compared with other types of remanent magnetization. Akad. Nauk SSSR Izv. Fizika Zemli, No. 10, 97—104, 1966

SOFFEL, H.: Die Bereichsstrukturen der Titanomagnetite in zwei tertiären Basalten und die Beziehung zu makroskopisch gemessenen magnetischen Eigenschaften dieser Gesteine. Habilitationsschrift, Universität München, München 1968.

THORPE, A. N., F. E., SENFTLE, and F. CUTTITA: Magnetic and chemical investigations of iron in tektites. Nature, 197, 836—840, 1963

WONES, D. R., and H. P. EUGSTER: Stability of biotite: experiment. theory and application. Am. Mineralogist, 50, 1228—1272, 1965

Remanent Magnetization of the Bergell Granite

F. HELLER, Zürich[1])

Summary: The rockmagnetic properties of granites of the northern Bergell massif (Switzerland) are due to their content of magnetite and ilmenohematite. Whereas the magnetite only possesses unstable components of remanent magnetization, the ilmenohematite displays a very stable magnetization of different polarity. In the north of the sampling area the ilmenohematite is magnetized reversely, in the south normally, i. e. parallel to the present geomagnetic field direction. The change in polarity is based on a self-reversal mechanism probably caused by the oxidation and exsolution process of ilmenohematite during cooling of the granite.

Zusammenfassung: Die Granite des nördlichen Bergeller Massivs (Schweiz) führen Magnetit und Ilmenohämatit als Träger ihrer gesteinsmagnetischen Eigenschaften. Während der Magnetit nur instabile Komponenten der remanenten Magnetisierung besitzt, weist der Ilmenohämatit eine sehr stabile Magnetisierung verschiedener Polarität auf. Im Norden des Untersuchungsgebietes ist der Ilmenohämatit invers magnetisiert, im Süden normal, d. h. parallel zur Richtung des heutigen erdmagnetischen Feldes. Der Polaritätswechsel beruht auf einem Selbstumkehrmechanismus, der wahrscheinlich durch die Oxidation und Entmischung des Ilmenohämatits während der Abkühlung des Granits bedingt ist.

1. Introduction

The palaeo- and rockmagnetic investigations of recent years are mostly concerned with research on basic volcanic rocks. Not much research has been done up to now on intrusive rocks, because they were often subjected to various geological processes, which can make an interpretation of a magnetic study difficult. In this paper the analysis of the remanent magnetization of a tertiary intrusive body, the Bergell massif, has been attempted. As the massif was only formed towards the end of the Alpine orogeny, the magnetic character of the rocks ought to be of a comparatively simple nature.

The Bergell massif is situated on the Swiss-Italian frontier between the valleys of Maira (Val Bregaglia) and Adda (Val Tellina), and covers an area of about 250 km² (Fig. 1). Tonalites are the oldest rocks; they form the south and south-eastern part of the batholith. In the northern part younger granodiorites and granites are predominant. Their biotite age has been dated radiometrically to about 25 m. y. [ARM-

---

[1]) Friedrich HELLER, Institut für Geophysik, ETH Außenstation Hönggerberg, CH-8049 Zürich.
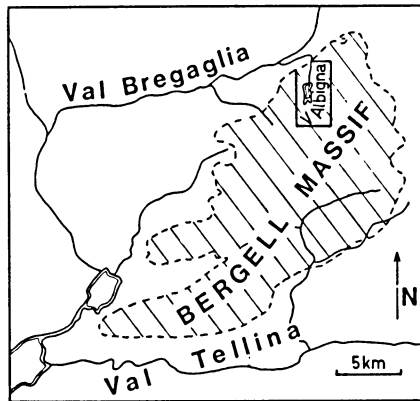
Fig. 1: Sketch map of the Bergell massif with sampling area (V. Albigna).

STRONG, JÄGER and EBERHARDT, 1966]. The last intrusive phase consists of granite-aplites, pegmatites and quartz veins. We have investigated the coarse-grained por-phyritic granites and the fine-grained granite-aplite dikes of the central northern part around the Albigna reservoir.

2. Magnetic mineralogy

According to the microscopic observations magnetite and ilmenohematite*) are responsible for the magnetic character of both types of rocks. The ratio between the two ore minerals varies considerably as well as the gross content. At the most about 1 % of ore was found (Fig. 4b).

The magnetite is mostly idiomorphic and octahedral. The size of the grains reaches an average diameter of about 1 mm, but varies considerably from about 0,01 to about 5 mm. The x-ray fluorescence and the microprobe analyses have shown that the rocks contain homogeneous and almost pure magnetite, having small admixtures of Ti (0.1 weight %) and Mn (0.2 weight %) and traces of Cr, Co and V. These chemical results coincide well with the CURIE temperature of 560—580°C we have meas-ured.

The ilmenohematite unlike magnetite has an extremely irregular form, as feldspars and quartz have rubbed away the edges of the grains. The distribution of grain sizes is like that of magnetite. Ilmenohematite displays three mineral phases: ferromagnetic titanohematite, paramagnetic ferroilmenite and rutile (Fig. 2). In a matrix of titano-hematite there are ferroilmenite lamellas in various sizes and quantities arranged like a string of pearls. One can find two exsolution generations of both Fe-Ti minerals.

*) nomenclature by BALSLEY and BUDDINGTON [1958]

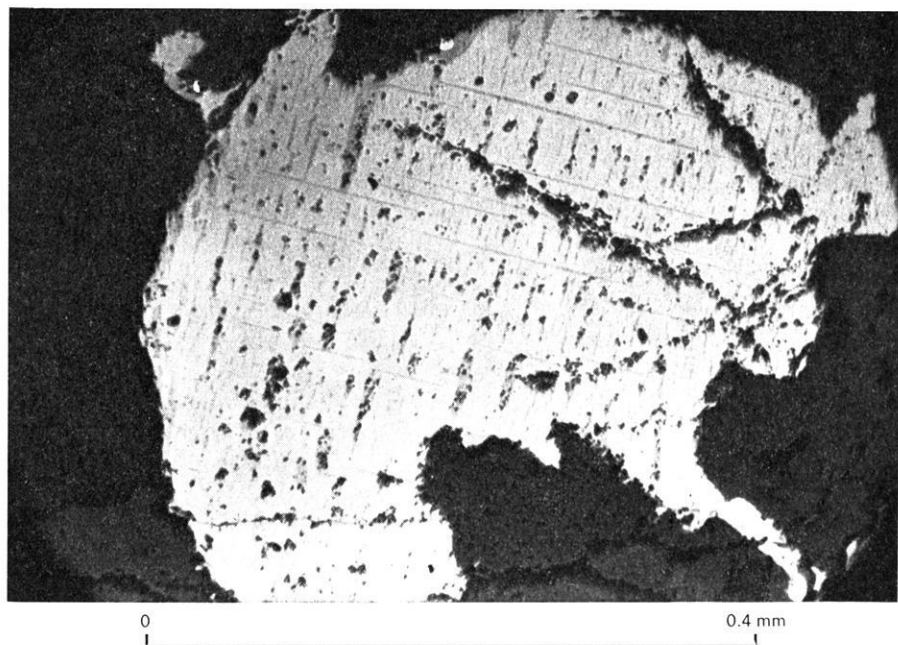0   0.4 mm

Fig. 2: Photomicrograph showing ferroilmenite exsolution lamellae of different sizes and long, thin rutile needles in the light titanohematite matrix.

The second generation of titanohematite is visible in microscope especially in the southern part of the sampling area.

1. generation:
   a) broad, partly elongated oval ferroilmenite lamellae in fair quantity
   b) titanohematite matrix

2. generation:
   a) numerous and smaller (down to submicroscopic size) ferroilmenite lamellae
   b) titanohematite exsolutions in ferroilmenite lamellae of the first generation

The youngest exsolutions are long and thin rutile needles. These are of particularly frequent occurrence in the southern part of the sampling area.

In ilmenohematite the same trace elements apart from Cr have been found by x-ray fluorescence spectroscopy as in magnetite: Fe, Ti, Mn and traces of Co and V. In consequence of the submicroscopic ferroilmenite exsolutions the titanium content of titanohematite could not be established quantitatively by means of the microprobe. The CURIE temperature of titanohematite was determined by thermomagnetic and thermal demagnetization experiments. The measured temperature of about $600\,^{0}C$ is
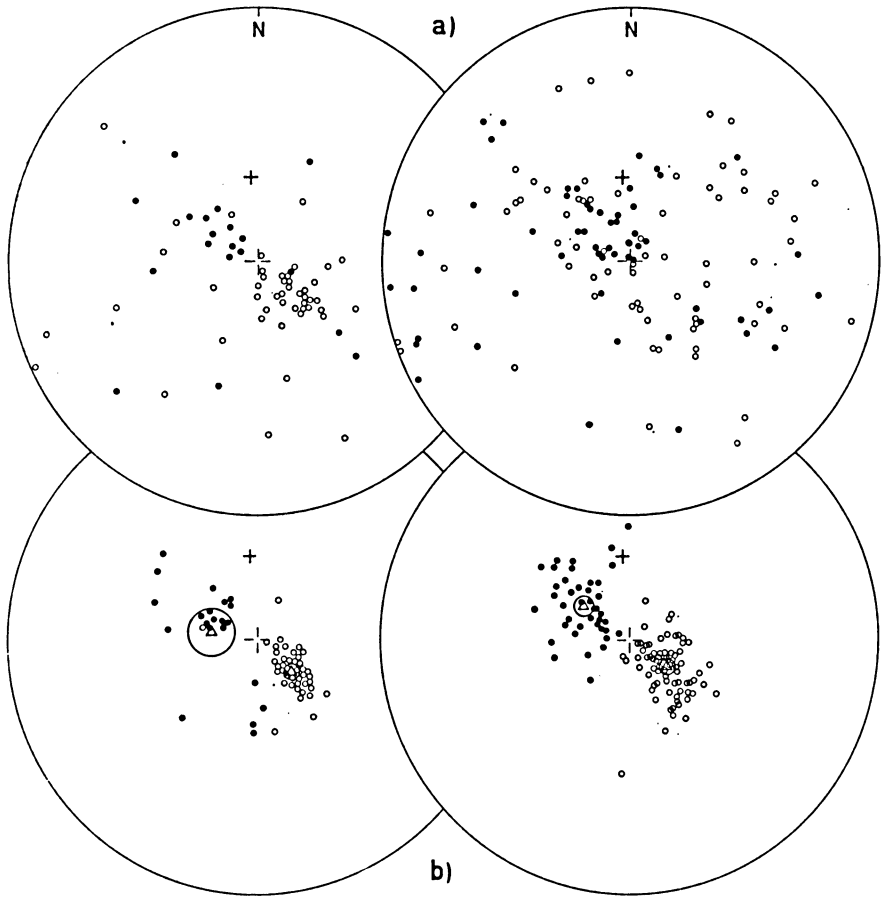
Fig. 3: Equal-area projection of a) NRM directions and b) ChRM directions. Granite-aplites are on left side, porphyritic granites are on right side. Dots are on lower hemisphere, open circles are on upper hemisphere. Crosses indicate the direction of present geomagnetic field. Triangles and surrounding circles give the mean directions of the antiparallel ChRM and the 95% confidence intervals of these means respectively.

Fig. 4: a) AC-demagnetization curves of NRM intensities.
   b) Ilmenohematite and magnetite content of nine rock specimens.
   c) AC-demagnetization curves of NRM directions. Dots are on lower hemisphere, open circles on upper hemisphere. Cross indicates the direction of present geomagnetic field.
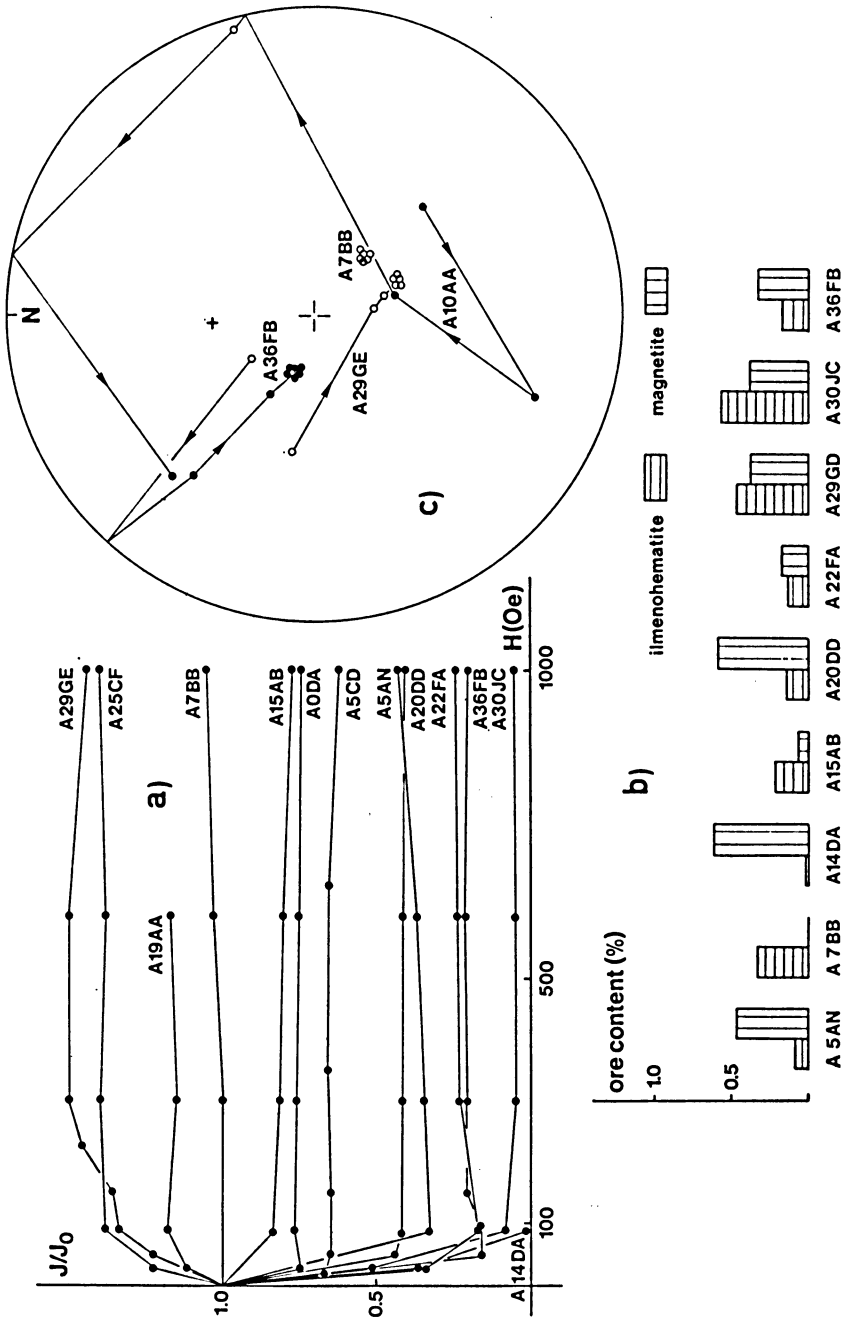
equivalent to an ilmenite content of about 10 mol % [NAGATA and AKIMOTO 1956]. The ferroilmenite contains about 90 mol % ilmenite in solid solution with hematite. The ilmenite content of ilmenohematite is about 40 mol %.

If we agree magnetite was primarily formed as pure magnetite and that the gross ilmenite content of ilmenohematite did not change at all after crystallization, we can deduce (according to BUDDINGTON and LINDSLEY [1964]) that the granite rocks had a crystallization temperature of about 800^{0}C.

3. Remanent magnetization

The direction and the intensity of natural remanent magnetization (NRM) vary considerably in both types of rocks examined. The porphyritic granites display no preferred directions of NRM vectors at all (Fig. 3a), whereas in the granite-aplites two antiparallel directions are faintly marked. The intensity of NRM ranges between $1\,\gamma$ and $100\,\gamma$ in porphyritic granites and between $1\,\gamma$ and $20\,\gamma$ in granite-aplites. The smaller intensity and scatter of NRM in granite-aplites is the result of a reduced magnetite content in these rocks.

The stability of NRM has been tested by various methods. In this section the results of AC-field demagnetization are outlined. Three stability groups can be distinguished (Fig. 4a, c):

1. unstable group $H_c <$ 100 Oe

By application of AC-fields with peak values up to 100 Oe the intensity of remanent magnetization decreases to $<5\%$ of NRM (e. g. Fig. 4a, A14DA). The direction of the remanent magnetization varies arbitrarily at each stage of demagnetization (e. g. Fig. 4c, A10AA). Specimens of this stability type come from the northern most part of the sampling area.

2. metastable group $H_c <$ 100 Oe and $>$ 1500 Oe

A stable level of remanent magnetization is reached after demagnetization in peak fields up to 100 Oe (e. g. Fig. 4a, A20DD and Fig. 4c, A36FB). This level is maintained even when applying higher AC-fields (up to 1500 Oe). We call this stable magnetization a characteristic remanent magnetization (ChRM). Most specimens from the Albigna district belong to this stability group.

3. stable group $H_c >$ 1500 Oe

The vector of NRM does not change in demagnetizing fields up to 1500 Oe peak value. NRM = ChRM. Members of this group mostly are granite-aplite specimens.

The connection between ore petrology and stability of remanent magnetization is clearly illustrated in Fig. 4. Unstable specimens contain only magnetite, stable ones possess only ilmenohematite. Metastable specimens have different portions of both minerals.

The ChRM of both rock types shows two well marked, antiparallel directions (Fig. 3b). The mean values of declination and inclination are:

Porphyritic granites $D = 307^0$ $I = 71^0$ $\alpha_{95} = 3.5^0$

$D = 126^0$ $I = -75^0$ $\alpha_{95} = 2.1^0$

Equivalent data are valid for granite-aplites.

From the above mentioned data of normal and reverse ChRM of porphyritic granites we have calculated the virtual geomagnetic palaeopole positions as shown in Fig. 5. They are quite different from the other middle European pole positions
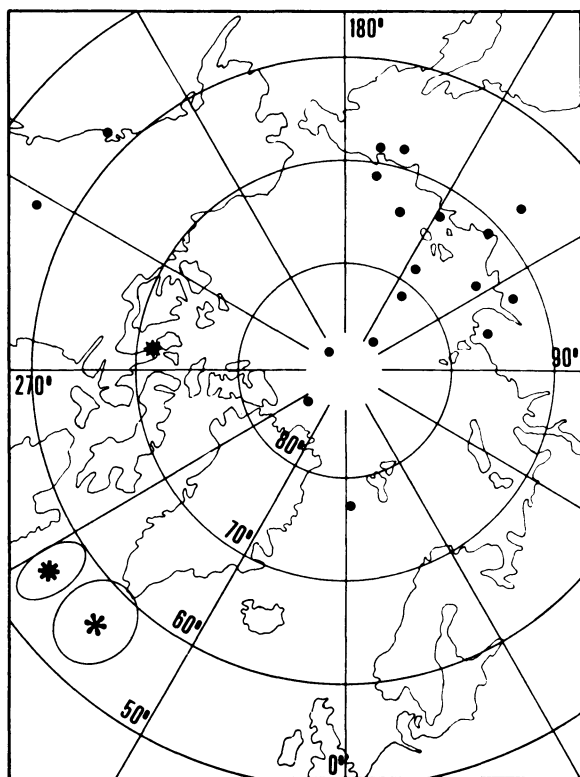

Fig. 5: Paleomagnetic pole positions given by the mean directions of ChRM of porphyritic granite.

✳ normal group ⎫
⎬ with 95% confidence ovals.
✱ reverse group ⎭

✶ after anisotropy correction (calculated from all specimens).

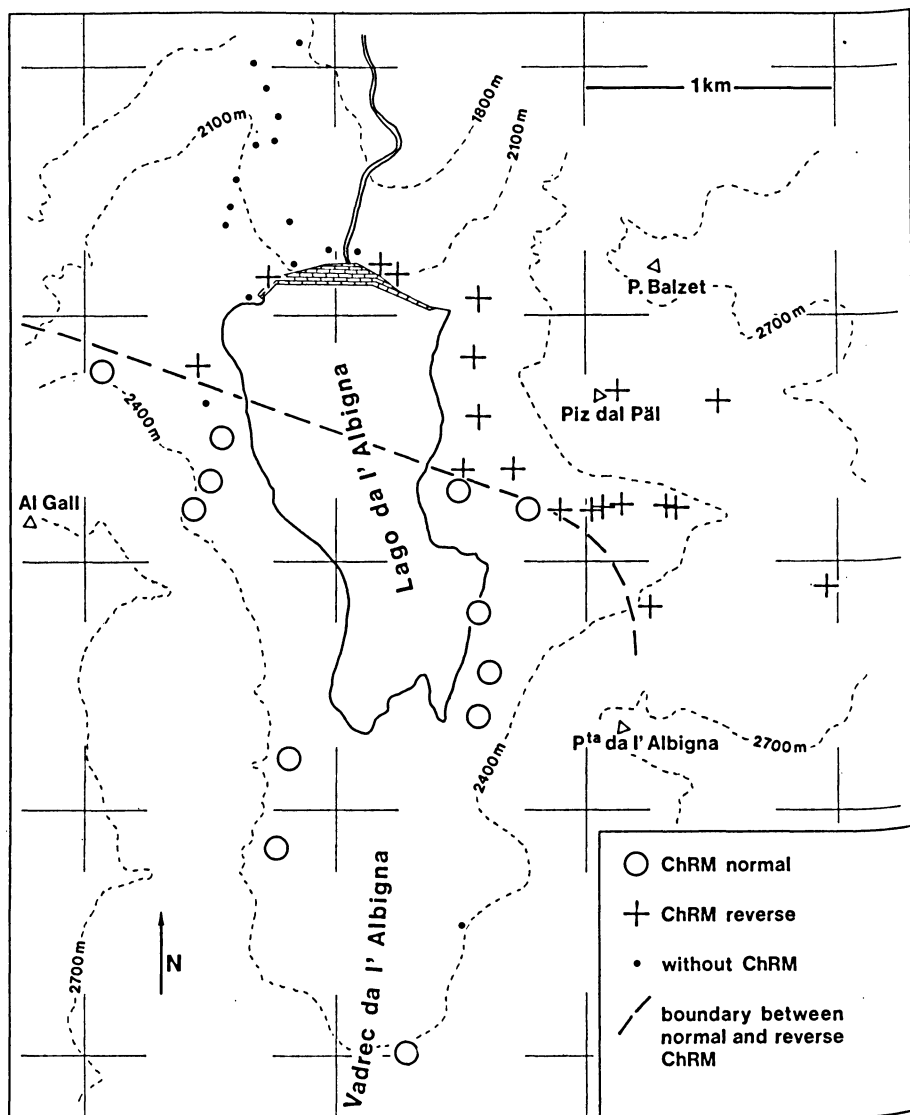● other middle European pole positions of Oligocene-Miocene age found by various researchers.

Fig. 6: Regional development of characteristic remanent magnetization.

of Oligocene to Miocene age. We have found a strong anisotropy of susceptibility in the Bergell rocks. As this anisotropy influences the direction of ChRM, we have corrected the ChRM directions according to the method suggested by HARGRAVES [1959]. The resulting palaeopole position (long. E: 263.5⁰; lat. N: 71.5⁰) fits into the palaeopoles given by some other research workers.

In the porphyritic granites of the region examined we can distinguish from N to S three zones with different development of ChRM (Fig. 6):

1. A zone without ChRM from the northern contact of the massif almost to the height of the dam. There is no ilmenohematite present in the rocks of this area.

2. A zone with reverse polarity of ChRM.

3. A zone with normally polarized characteristic remanent magnetization.

The ChRM directions display an extraordinarily low scatter on each sampling site and over each polarity zone. "Falsely" polarized specimens were not detected in the two regions of different ChRM polarity.

In view of the sharp regional separation of ChRM polarities the course and development of the polarity boundary is of increased importance when dealing with the reversal phenomenon. The steeply dipping boundary plane strikes E—W in the Albigna valley and bends into a N—S direction in the eastern part of the valley. It runs parallel to the internal structure of the granite (cf. DRESCHER and STORZ [1926]). Studying this in detail (m—10 m range) we see the boundary is very tortuously and very sharply developed (Fig. 7) without any relation to texture and structure of the rocks. No transition zone with flat inclinations has been established in cm—m range. Measurements made on single grains of ilmenohematite taken from the immediate boundary confirm the sudden change of ChRM polarity.

The polarity of ChRM in granite-aplites examined was generally equal to that of neighbouring porphyritic granites. However, there are exceptions in both polarity zones. Thus, for instance, we have found some reversely polarized dikes of granite-aplite crossing the polarity boundary of porphyritic granites (Fig. 7) without influencing the polarity of porphyritic granites or without being influenced by the change in polarity of these rocks.

4. Discussion

What is the mechanism controlling the reversal of ChRM polarity in porphyritic granites? Field-reversal or self-reversal are the two possible answers to this question. At present self-reversal seems the only possible answer. This is suggested by the following reasons.

First the course of the polarity boundary in detail. If ChRM is caused by thermal processes only, the development of the polarity boundary should depend on the cooling history of the granite. In such a large batholith as the Bergell massif the planes of equal temperature during cooling are bent evenly. Fairly large temperature differ-
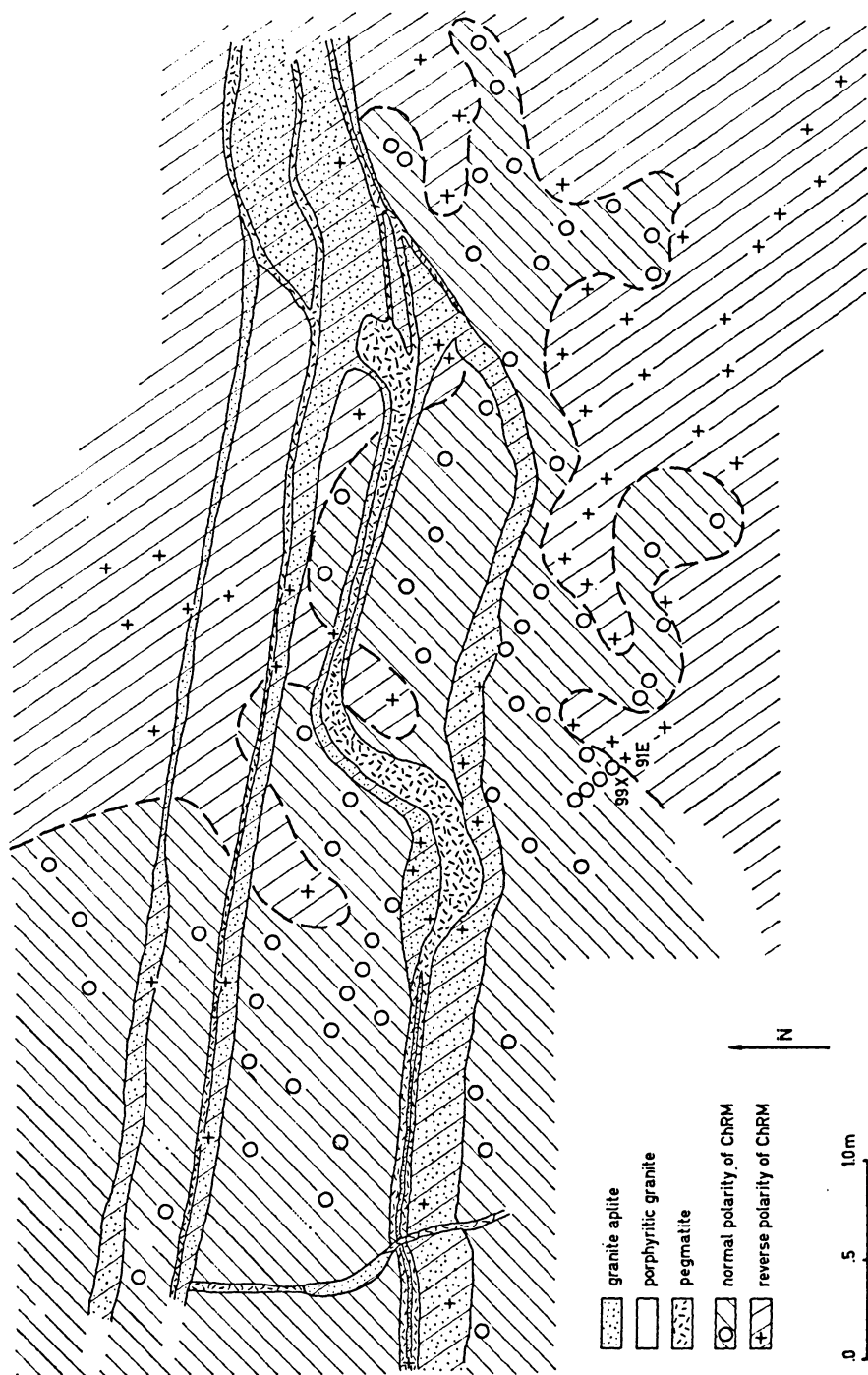
granite aplite

porphyritic granite

pegmatite

normal polarity of ChRM

reverse polarity of ChRM

0 .5 10m

Fig. 7: Detail of the boundary between the normally and the reversely polarized ChRM zone
of porphyritic granites.

___

ences over short distances, which would cause the complicated and sharp reversion
boundary mentioned above, are not conceivable. Therefore we cannot explain this
polarity change by field-reversal.

A second reason is given by the magnetic behaviour of granite-aplites in Fig. 7.
These granite-aplites and the neighbouring porphyritic granites have no influence on
each other with regard to the magnetic properties. The ilmenohematites of both rocks
are exsolved to the same mineralogical composition. The thermal demagnetization
curves of both rock types coincide. Because of the small thickness of the dikes both
rocks must have cooled at approximately the same time. Therefore, if we accept
field-reversal to be the cause for the given polarity change, we should find no differ-
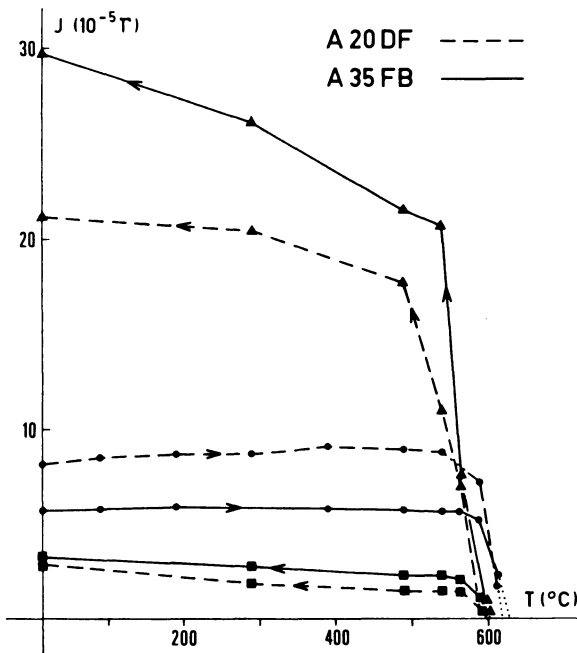ence in the behaviour of ChRM polarity in both rock types of Fig. 7.

Fig. 8: Thermal treatment of prophyritic granite.
● thermal demagnetization of ChRM (in zero field)
▲ total artificial PTRM
■ AC-stable artificial PTRM (peak fields up to 600 Oe).
Originally specimen A20DF was polarized reversely, specimen A35FB normally.

The thermal demagnetization experiments carried out according to the progressive method [HELLER, SCRIBA and WEBER 1970] have shown no direct proof of self-reversal. The demagnetization curves of ChRM of normally and reversely magnetized specimens are identical (Fig. 8). Artificial total PTRM (partial thermoremanent magnetization) and AC-stable PTRM of all specimens investigated are polarized normally. It is interesting to note that the intensity of AC-stable PTRM (= ChTRM) reaches only about half the intensity of original ChRM. The magnitude of the quotient of ChTRM/ChRM depends on the original polarity of stable magnetization (Fig. 9). Originally reversely polarized specimens have a quotient 0.3—0.6, originally normally polarized specimens have a quotient of 0.5—0.9.

If the magnetic properties of ilmenohematite have not changed during thermal treatment—the NÉEL temperature decreases slightly by homogenization of titano-hematite—the process of the original thermal magnetization in both polarity zones therefore must have undergone a second magnetization process. Both together formed ChRM. The observed exsolutions in ilmenohematite suggest that chemothermorema-nent magnetization (CTRM) is the secondary magnetization.

There is also a mineralogical petrological clue to self-reversal. The ilmenite-hem-atite series—x FeTiO$_3$ $(1-x)$ Fe$_2$O$_3$—has been known to display self-reversal. UYEDA [1958] and CARMICHAEL [1961] experimentally could establish self-reversal in certain Fe-Ti ratios of this series (perfect self-reversal for $x = 0.45—0.6$ and "imperfect" self-reversal for $x = 0.18—0.25$). A nonreproducible self-reversal in this series ($x = 0.05—0.1$) recently was found by MERRIL and GROMMÉ [1969].

We think that self-reversal in the Bergell ilmenohematites has taken place as a consequence of magnetostatic interaction [NÉEL 1951]. For the reversal, the oxidation state of granite plays the decisive role. In the area examined it increases from north to south: At the contact in the north, biotite is the predominant mineral containing Fe.
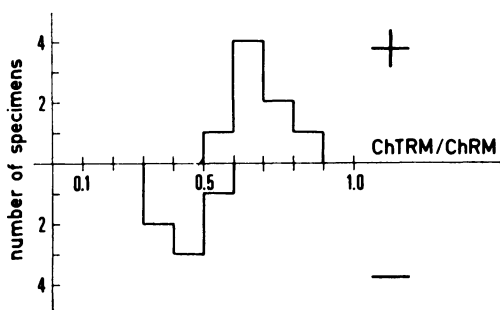

Fig. 9: The quotient ChTRM/ChRM is dependent on the original polarity of ChRM. The sign '+' incidates an originally normal ChRM direction, the sign '—' an origi-nally reverse ChRM direction.
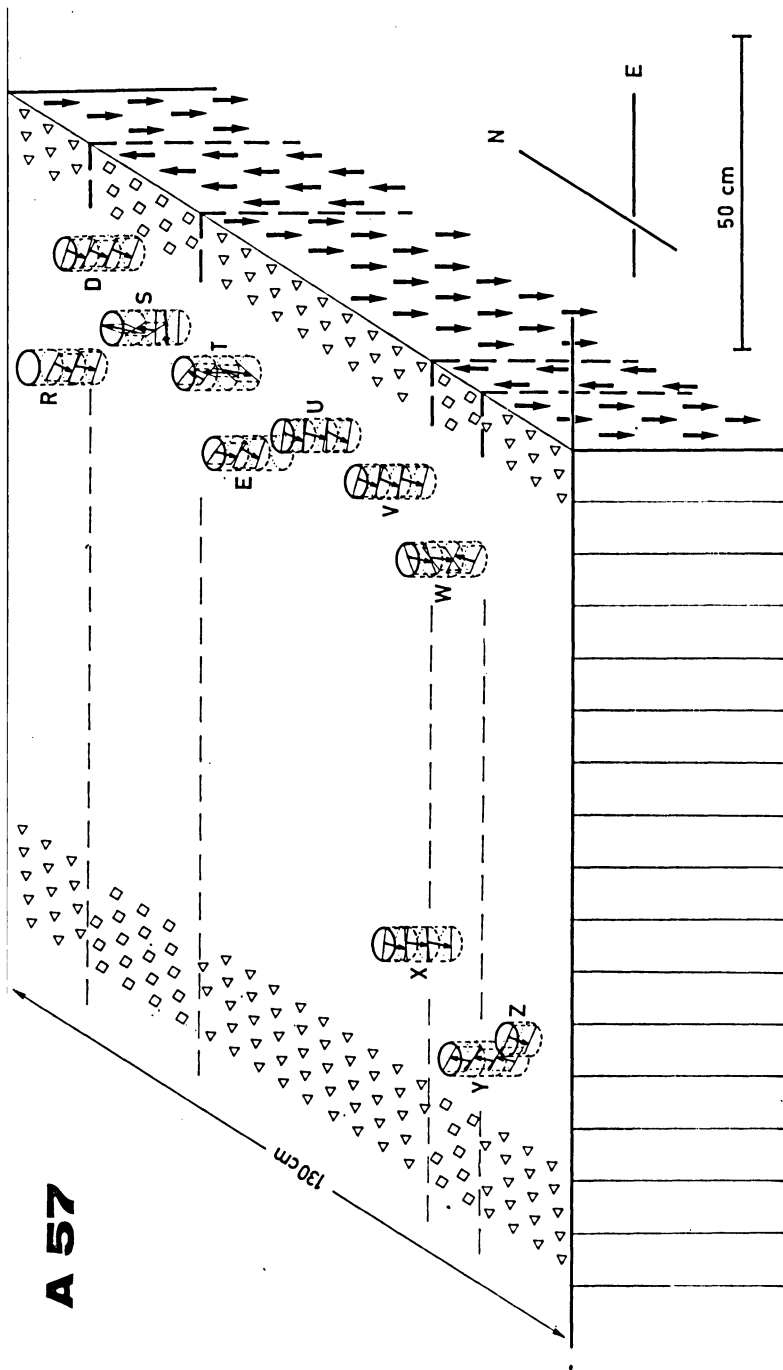
Fig. 10: Example of a granite-aplite dike zoned by some strips of antiparallel ChRM polarity. The dike strikes E−W and dips very steelpy to N. The ChRM directions of the specimens are indicated by little arrows.

Towards the south the rocks contain more magnetite at the expense of biotite. This is indicated by an increasing intensity of the initial susceptibility too. At the height of the dam ilmenohematite is added; the intensity of susceptibility slightly decreases. The ilmenohematite is more strongly oxidized in a southerly direction, i. e. it becomes richer in rutile, and the secondary titanohematite exsolutions grow larger. We therefore assume that in the northern zone of reverse polarity the secondary titanohematite exsolutions are not large enough to be more than superparamagnetic. On the polarity boundary the critical grain size for a long relaxation time is reached and the remanent magnetization is reversed by magnetostatic interaction. If this conception is correct, the geomagnetic palaeofield at the time of magnetization must have been opposite to the present geomagnetic field.

The above mentioned quotient of ChTRM/ChRM supports the conception. The CTRM was obtained in one or two stages of magnetization on the basis of one or two generations of titanohematite respectively. Thus in the reverse zone TRM and CTRM of the first stage add up (ChTRM/ChRM = 0.3—0.6). In the normal zone the oppositely directed CTRM of the second stage superimposes the sum of magnetizations of the first stage (ChTRM/ChRM = 0.5—0.9). Because of this opposite alignment of magnetizations the magnitude of the quotient is larger in the normal zone.

Finally a last phenomenological evidence for the postulated self-reversal. The granite-aplite dike of Fig. 10 displays several oppositely polarized ChRM zones arranged parallel to its borders. The transitions between these polarity zones are again sharply defined. Flat inclination of ChRM observed in one specimen is caused by antiparallel arrangement of ChRM, i. e. this specimen contains both: normal and reverse ChRM. The normal magnetization strips are magnetized about ten times less than the reverse zones. This intensity reduction of normal specimens can be explained by the same mechanism causing the reversal in porphyritic granites. Here again two opposite magnetization stages in normally magnetized ilmenohematite are present. Although research work on this dike—e. g. magnetic-petrological correlation—has not yet been completed, in this case too we can explain the polarity change only by self-reversal caused by oxidation and exsolution of ilmenohematite during cooling.

References

ARMSTRONG, R. L., E. JÄGER, and P. EBERHARDT: A comparison of K-Ar and Rb-Sr ages on Alpine biotites. Earth Plan. Sci. Letters, 1, 13—19, 1956

BALSLEY, J. R., and A. F. BUDDINGTON: Iron-titanium oxide minerals, rocks, and aeromagnetic anomalies of the Adirondack area, New York. Econ. Geol., 53, 777—805, 1958

BUDDINGTON, A. F., and D. H. LINDSLEY: Iron-titanium oxide minerals and synthetic equivalents. J. Petr., 54, 310—357, 1964

CARMICHAEL, C. M.: The magnetic properties of ilmenite-haematite crystalls. Proc. Roy. Soc. London, 263, Ser. A, 508—530, 1961

DRESCHER, F. K., and M. STORZ: Ergebnisse petrographisch-tektonischer Untersuchungen im Bergeller Granit. N. Jb. Min., B. B. 54, Abt. A, 284—291, 1926

HARGRAVES, R. B.: Magnetic anisotropy and remanent magnetism in hemoilmenite from ore desposits at Allard Lake, Quebec. J. Geoph. Res., 64, 1565—1578, 1959

HELLER, F.: Magnetische und petrographische Eigenschaften der granitischen Gesteine des Albignagebietes (Nördliches Bergeller Massiv). Dissertation ETH Zürich, 1971

HELLER, F., H. SCRIBA, and M. WEBER: A furnace for magnetic investigations of rocks. Geophys. J. R. astr. Soc., 21, 531—534, 1970

MERILL, R. T., and C. S. GROMMÉ: Nonreproducible self-reversal of magnetization in diorite. J. Geoph. Res., 74, 2014—2024, 1969

NAGATA, T., and S. AKIMOTO: Magnetic properties of ferromagnetic ilmenites. Geofis. Pura Appl., 34, 36—50, 1956

NÉEL, L.: L'inversion de l'aimantation permanente des roches. Ann. Geophys., 7, 90—102, 1951

UYEDA, S.: Thermo-remanent magnetism as a medium of palaeomagnetism, with special reference to reverse thermo-remanent magnetism, Jap. J. Geoph., 2, 1—123, 1958

Anomalien des erdmagnetischen Feldes im Gebiet der jungen Vulkane Südwestdeutschlands

Magnetic Anomalies in the Areas of Young Volcanism in Southwestern Germany

O. Mäussnest, Stuttgart[1])

Zusammenfassung: In Südwestdeutschland können drei vulkanische Epochen unterschieden werden: eine alte Phase im Zusammenhang mit der variszischen Gebirgsbildung und zwei junge Phasen, von denen die eine spätkretazisch, die andere gegen Ende des Tertiärs zu datieren ist. Die magnetischen Felduntersuchungen des spätkretazischen Vulkanismus im Kraichgau sowie des obermiocänen Vulkanismus der Schwäbischen Alb sind abgeschlossen; zur Zeit werden Feldmessungen in den tertiären Vulkangebieten des Hegaus und des Rheintalgrabens durchgeführt. Bei den magnetischen Feldmessungen wurde eine große Zahl bisher unbekannter vulkanischer Vorkommen neu gefunden.

Summary: In southwestern Germany we have three volcanic periods. An old phase is in connection with the folding-up of the Variscan. Both the other phases are relatively young, one at the end of the Cretaceous the other in the Miocene. The magnetic field research in the late-Cretaceous volcanic Kraichgau area and in the upper-Miocene volcanic area of the Swabian Jurassic has been completed. Magnetic field research is carried out at this moment in the Tertiary volcanic areas of the Hegau and the Rhinetalgraben. In connection with magnetic field research a great number of yet unknown volcanic pipes were discovered.

In Südwestdeutschland ist eine erste vulkanische Epoche sichtbar im Schwarzwald und im Odenwald. Sie steht im Zusammenhang mit der variszischen Gebirgsbildung. Es kam damals insbesondere zur Bildung von Graniten und Porphyren. Diese erste vulkanische Epoche dürfte vor etwa 200 Millionen Jahren zu Ende gegangen sein. Die Vermessung der Anomalien des erdmagnetischen Feldes in diesem Vulkan-Gebiet ist erst für einen späteren Zeitpunkt vorgesehen.

Diesem paläozoischen Vulkanismus folgte eine lange Zeit der Ruhe, die etwa 130 Millionen Jahre gedauert haben dürfte. Die vulkanischen Kräfte wurden zum zweiten Mal in Südwestdeutschland aktiv gegen Ende der Kreidezeit vor etwa 70 Millionen Jahren. Sie waren aktiv auf der Ostseite des Rheintalgrabens in der Kraichgau-

---

[1]) Dr. O. Mäussnest, Institut für Geophysik der Universität Stuttgart, 7 Stuttgart 1, Richard-Wagner-Straße 44.
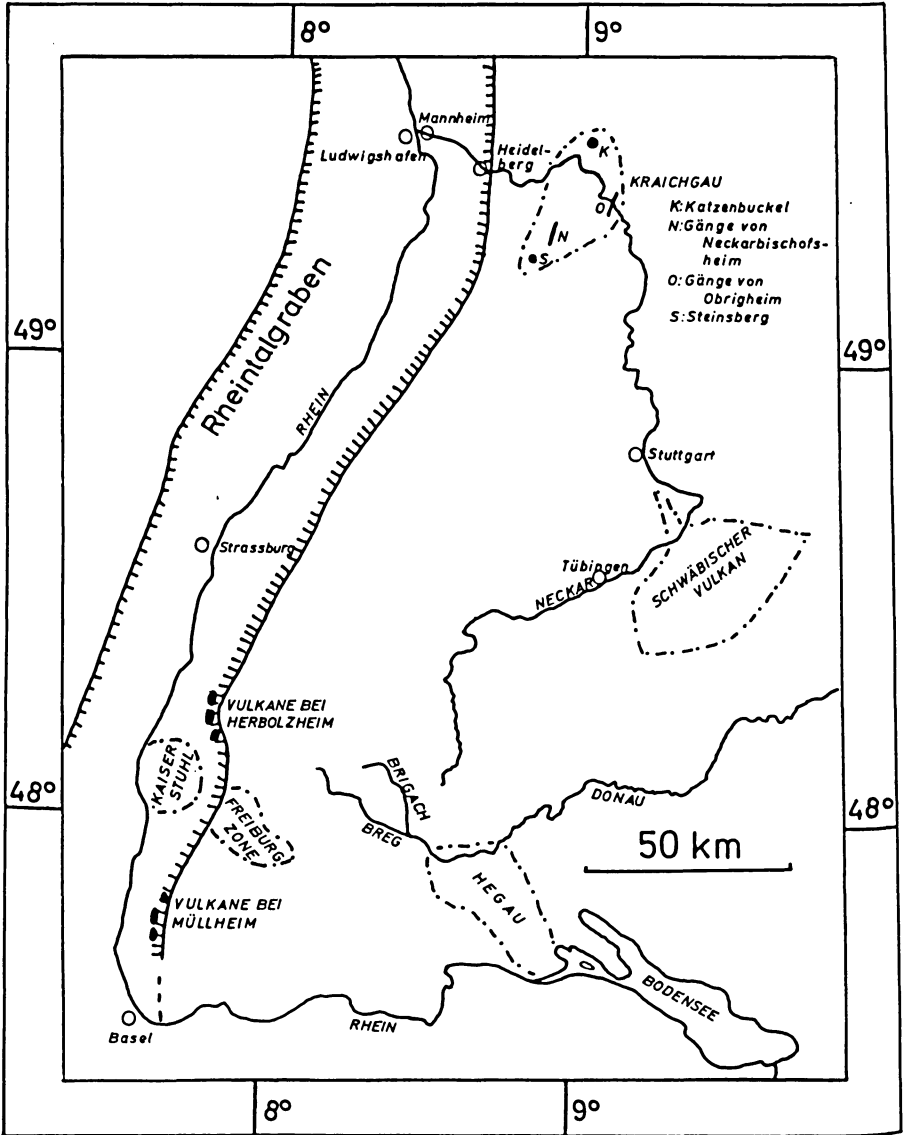
Übersichtskarte des jungen südwestdeutschen Vulkanismus

Tertiary volcanism in southwestern Germany

Depression zwischen den Erhebungen des Schwarzwaldes im Süden und des Oden-
waldes im Norden. Die Gesteine dieser Vulkanprovinz sind basisch. Alle Anomalien
der hier bekannt gewordenen vulkanischen Vorkommen wurden vermessen. Soweit
geeignete Aufschlüsse vorhanden waren, wurden auch Proben entnommen und ihre
Magnetisierung vermessen. Im Schrifttum sind Basaltgänge bei Obrigheim-Neckarelz
und Neckarbischofsheim beschrieben; ferner werden zwei basaltische Schlote er-
wähnt (Steinsberg bei Weiler/Kreis Sinsheim und Katzenbuckel bei Waldkatzenbach,
schon im südlichsten Teil des Odenwaldes gelegen).

Alle vulkanischen Vorkommen dieser Provinz haben normale Magnetisierung. Bei
den Feldmessungen wurden mehrere bisher unbekannte Basaltgänge bei Obrigheim-
Neckarelz und südwestlich von Neckarbischofsheim ein neuer langer Basaltgang
gefunden. Alle Basaltgänge haben ein typisches rheinisches Streichen; die bereits
bekannt gewesenen Basaltgänge sind alle sehr viel länger als bisher angenommen
wurde. Allerdings handelt es sich um keine über Kilometer anhaltenden Gänge,
sondern jeweils um kurze Gangstücke, die mit seitlicher Versetzung aneinanderreihen.
Im Gebiet der zerstörten Obrigheimer Eisenbahnbrücke über den Neckar liegt ein
von Neckarschottern verdeckter Schlot. — Über die Vermessung der ΔZ-Anomalien
dieser Vulkanprovinz wird in Kürze zusammen mit E. BECKSMANN/Freiburg i. Br.
berichtet werden.

Nach dem Erlöschen des Vulkanismus in der Kraichgau-Depression schlummerten
die vulkanischen Kräfte in Südwestdeutschland wieder für etwa 50 Millionen Jahre,
bis sie im Laufe des Miocäns erneut und mit großer Heftigkeit in drei Gebieten
wieder erwachten: Schwäbische Alb, Hegau und Rheintalgraben.

Aufgrund der bis jetzt bekannt gewordenen Altersbestimmungen kann man an-
nehmen, daß der Vulkanismus zuerst im Gebiet der Schwäbischen Alb etwa südöst-
lich von Stuttgart aktiv wurde. Ausführliche geologische Untersuchungen dieser
Vulkanprovinz erfolgten durch BRANCO [1894, 1895], REICH [1915] und CLOOS [1941],
der für diese Vulkanprovinz die Bezeichnung „Schwäbischer Vulkan" einführte. Es
handelt sich um einen ausschließlich basaltischen Vulkanismus, der bereits im An-
fangszustand endete; BRANCO [1894, 1895] führte für einen derartigen Vulkanismus
die Bezeichnung „embryonaler Vulkanismus" ein.

In dieser Vulkanprovinz wurden die Anomalien im Gelände und die Magnetisie-
rung von Proben in jahrelanger Arbeit ausführlich untersucht. Zu Beginn der Feld-
messungen waren im geologischen Schrifttum und in den geologischen Karten etwa
185 Schlote insgesamt aufgeführt. Bei etwa 20 dieser Vorkommen wurden keine
magnetischen Anomalien gefunden. Die nichtbestätigten Vulkane waren solche, bei
denen die Funde nur sehr vage oder gar nicht beschrieben worden waren. Neu ge-
funden wurden bei den Feldmessungen, die sich über die Jahre 1953—1968 erstreck-
ten, rund 160 bisher unbekannte Eruptionspunkte des Schwäbischen Vulkans; wäh-
rend dieser Zeitspanne wurden bei geologischen Untersuchungen und bei der forst-
lichen Standortkartierung rund 10 Schlote neu gefunden. Man kennt daher heute im
Gebiet des Schwäbischen Vulkans rund 335 Eruptionspunkte, von denen knapp die

Hälfte durch die Vermessung der ΔZ- und ΔH-Anomalien des erdmagnetischen Feldes in dieser Vulkanprovinz gefunden wurde. Diese annähernde Verdoppelung der bekannten Eruptionsstellen war dadurch möglich, daß es eine ganze Reihe von Hinweisen auf noch unentdeckte Schlote gibt, die zum ersten Mal systematisch bei der Vermessung der Anomalien des erdmagnetischen Feldes ausgewertet, teilweise auch erst bei den Feldmessungen erkannt wurden.

Im Normalfall zeigen in obermiocänen Vulkanprovinzen rund $1/3$ aller Vorkommen eine inverse Magnetisierung. Im Gebiet des Schwäbischen Vulkans dagegen haben nur 15% aller Schlote eine ganze oder teilweise inverse Magnetisierung.

Zwei Schlote des Schwäbischen Vulkans haben Blitzschlagmagnetisierung; es sind dies die Tuffvorkommen Calver Bühl und Konradfels, beide im Gebiet des Meßtischblattes Dettingen/Erms Nr. 7422 gelegen. Die Blitzschlagmagnetisierung tritt jeweils im Gipfelbereich auf, wo nackter Basalttuff ansteht. Genauere Untersuchungen wurden am Calver Bühl durchgeführt, der außerhalb der Gipfelzone ΔZ-Anomalien bis $+1000\,\gamma$ hat. Im Gipfelbereich dagegen treten ΔZ-Anomalien des Erdfeldes auf mit einer absoluten Störamplitude bis $33000\,\gamma$, wobei die beiden Meßpunkte mit den extremsten Werten knapp 6 m voneinander entfernt sind. Deklinationsmessungen in diesem Gebiet ergaben Werte zwischen 45^0W und 120^0E. Die hier für gesteinsmagnetische Messungen entnommenen Proben ergaben für die Inklination der Remanenz Werte zwischen -21^0 und $+56^0$; die Deklination der Remanenz nimmt jeden nur möglichen Wert an. Die maximale Remanenz im Gebiet der Blitzschlagmagnetisierung beträgt $10120\,\gamma$. Während bei basaltischen Gesteinen Q-Faktoren (Q-Faktor $= J_{rem,\,nat}/J_{ind}$) bis 5 die Regel sind, wurde hier ein maximaler Q-Faktor von 124 erhalten.

Da die Basalttuffe der Alb keine geeigneten Bau- oder Schottersteine abgeben, liegen nur sehr mangelhafte Aufschlußverhältnisse vor. Aus diesem Grunde konnten nur an wenigen Schloten Proben für paläomagnetische Messungen entnommen werden. Als mittlere Richtung der Remanenz des Schwäbischen Vulkans ergab sich nach einer Entmagnetisierung der Proben im Wechselfeld die Deklination $D = 4^010'$ und die Inklination $I = 72^0$, woraus sich die Pollage $81^010'$N, $24^030'$E ergibt. Der magnetische Pol der Nordhalbkugel lag damit zur Zeit der Tätigkeit des Schwäbischen Vulkans im Gebiet von Nordostland (Spitzbergengruppe).

Ausführlichere Angaben über die Vermessung der ΔZ-Anomalien des erdmagnetischen Feldes im Gebiet des Schwäbischen Vulkans und die gesteinsmagnetischen Messungen können den Arbeiten von MÄUSSNEST [1969a, 1969b, 1970] entnommen werden.

Soweit man heute weiß, wurden vor etwa 18 Millionen Jahren die vulkanischen Kräfte im Rheintalgraben aktiv. Neben dem Vulkangebirge des Kaiserstuhls, das sich mitten im Rheintalgraben 350 m hoch erhebt, entstand eine ganze Reihe kleinerer Vulkane, die wohl mit Vorliebe an den Randverwerfungen des Rheintalgrabens aufsitzen. Die vulkanische Tätigkeit des Kaiserstuhls soll etwa 2 Millionen Jahre angedauert haben. Eine detaillierte Vermessung der Anomalien des erdmagnetischen

Feldes im Gebiet des Kaiserstuhl-Vulkangebirges wurde noch nicht veröffentlicht;
es liegen bis jetzt nur Übersichtsmessungen von MEYER [1902] und REICH, CLOSS und
SCHOENE [1940] vor.

Die magnetischen Feldmessungen des Autors in ΔZ beschränken sich bis jetzt in
der Rheintalgraben-Vulkanprovinz auf Einzeleruptionspunkte, die den Kaiserstuhl
als Aureole umgeben. Bis jetzt wurden Schlote in den Gebieten Emmendingen—Her-
bolzheim und Kandern—Müllheim in ΔZ vermessen; eine ganze Reihe dieser Schlote
hat eine inverse Magnetisierung.

Besonders interessant waren die Messungen an einem Schlot zwischen Herbolzheim
und Ringsheim, der im Hauptrogenstein-Steinbruch am Rande der Vorbergzone
zwischen diesen beiden Orten aufgeschlossen ist. In diesem Steinbruch sind zwei Tuff-
aufschlüsse vorhanden, die auf ein gangförmiges Vulkanvorkommen hinweisen. Die
ausführliche Vermessung der ΔZ-Anomalien des erdmagnetischen Feldes im Gebiet
dieses vulkanischen Vorkommens, die auf Anregung von Herrn Prof. Dr. W. WIM-
MENAUER/Freiburg i. Br. erfolgte, ergab im Gegensatz zu den bisherigen Angaben
im Schrifttum, daß hier kein vulkanischer Gang vorliegt, sondern ein überraschend
großer Schlot. Den Ostrand des Schlotes bilden die kleinen Tuffvorkommen im
Hauptrogenstein-Steinbruch; nach Westen reicht der Schlot bis zur Bahnlinie Offen-
burg—Freiburg i. Br. Durch die Rheintalgrabentektonik bedingt ist dieser Schlot
bis auf einige ganz kümmerliche Reste in der Tiefe verschwunden, verdeckt durch
junge und jüngste Ablagerungen und damit dem Auge des kartierenden Geologen
entzogen.

Über die Vermessung der ΔZ-Anomalie des Erdfeldes im Gebiet dieses Schlotes
und der anderen bereits vermessenen Schlote bei Emmendingen-Herbolzheim und
Kandern-Müllheim wird demnächst ausführlich berichtet werden.

Das dritte Gebiet tertiären Vulkanismus in Südwestdeutschland ist der Hegau,
gelegen zwischen der jungen Donau im Norden zwischen Donaueschingen und Tutt-
lingen und dem Untersee bzw. Rhein zwischen Schaffhausen und Steckborn. Nach
den bis jetzt bekannt gewordenen radiometrischen Altersbestimmungen begann die
vulkanische Tätigkeit in dieser Vulkanprovinz vor 15,5 Millionen Jahren und soll
über 8 Millionen Jahre angedauert haben. Demnach dürfte der Vulkanismus hier
erst begonnen haben, nachdem der Kaiserstuhl erloschen war. Man nimmt an, daß
die vulkanische Tätigkeit im Süden dieser Vulkanprovinz begonnen hat und langsam
nach Norden gewandert ist.

Eine ausführliche geologische Untersuchung des ziemlich komplexen Hegauvulka-
nismus steht immer noch aus. Zur geologischen Orientierung muß auf die unvoll-
ständige Beschreibung von RECK [1923] verwiesen werden.

Wie im Kaiserstuhl hat man auch im Hegau — im Gegensatz zum Schwäbischen
Vulkan — eine ganze Reihe von Förderprodukten zu unterscheiden. Die Haupt-
gruppen im Hegau sind Basalte mit ihren Schlottuffen, Phonolithe, Hornblendentuffe
und Deckentuffe. Vermessungen der ΔZ-Anomalien des erdmagnetischen Feldes er-
folgten an allen aufgeführten Arten von Förderprodukten. Entsprechend ihrem Che-

mismus bzw. ihrer mineralogischen Zusammensetzung zeigen die Basalte und ihre Tuffe die größten ΔZ-Anomalien.

Alle bis jetzt in ΔZ vermessenen Basalt- und Basalttuffvorkommen der Hegau-Vulkanprovinz sind normal magnetisiert, abgesehen von zwei Schloten, die jeweils eine invers magnetisierte Partie zeigen. Die bis jetzt vorliegenden gesteinsmagnetischen Messungen an Hegaubasalten und Basalttuffen wurden zu einer Berechnung der Lage des magnetischen Poles der N-Halbkugel zur Zeit des basaltischen Hegauvulkanismus herangezogen; die Proben wurden im Wechselfeld entmagnetisiert. Es ergab sich die Pollage 79^0N, 89^0E; damit kommt der magnetische Pol in das Gebiet zwischen der Wiese-Insel und Nordland zu liegen [MÄUSSNEST 1971]. Verglichen mit dem Ergebnis der Pollagenberechnung für den Schwäbischen Vulkan zeigt sich kein wesentlicher Unterschied in der Breite, jedoch in der Länge.

Blitzschlagmagnetisierungen wurden im Gipfelbereich zweier Basaltschlote gefunden. Es sind dies der Hohenstoffel (Meßtischblatt Nr. 8218) und der Grießlen (Meßtischblatt Nr. 8118).

Alle bis jetzt in ΔZ vermessenen Phonolithvorkommen zeigen nur normale Magnetisierung. Obwohl sie bereits zu den leicht sauren Gesteinen gehören (es wird ein SiO_2-Gehalt von 55% angegeben) und damit eine Verarmung an Ferromagnetica vorliegt, heben sie sich deutlich durch Anomalien des erdmagnetischen Feldes von ihrer Umgebung ab.

Auch alle Hornblendentuffvorkommen zeigen, soweit sie bis jetzt in ΔZ vermessen sind, nur eine normale Magnetisierung. Auch die Hornblendentuffe verursachen deutliche Anomalien des magnetischen Feldes der Erde.

Soweit bis jetzt bekannt ist, sind die Deckentuffe des Hegaus — wurzellose Tuffmassen, die teilweise sehr mächtig werden (in der Mineralwasserbohrung Singen/Htw. wurde eine Mächtigkeit von 222 m angetroffen) — aufgrund ihrer Zusammensetzung zwischen den Basalten und den Phonolithen einzuordnen. Die bei den Feldmessungen gefundenen ΔZ-Anomalien des Erdfeldes haben Werte, die im Normalfall zwischen denen basaltischer und phonolithischer Hegaugesteine liegen. Alle bis jetzt in ΔZ vermessenen Hegaudeckentuffe sind normal magnetisiert; eine inverse Magnetisierung ist in der ganzen Hegauvulkanprovinz also eine große Ausnahme.

Die Hegauvulkanprovinz ist, von ihrem nördlichsten Teil abgesehen, sehr stark eiszeitlich überprägt worden. Zahlreiche Vulkanitvorkommen wurden ganz oder teilweise mit glazialen Ablagerungen zugedeckt. Emporragende Basaltvorkommen sind mit mächtigen Basaltblockmeeren umgeben, die ihre Entstehung zu einem großen Teil der eiszeitlichen Solifluktion verdanken. Gletscher haben Basaltvorkommen abgehobelt und zum Teil sehr mächtige Basaltblöcke mitgenommen, die dann wieder — oft in großer Massierung — an anderer Stelle zur Ablagerung kamen.

Der kartierende Geologe hat dadurch sehr große Schwierigkeiten, in seine Kartenaufnahmen zutreffende Angaben über die vulkanischen Bildungen einzutragen, da er nicht weiß, ob vulkanische Gesteine unter glazialen Ablagerungen verborgen sind, ob Ausbisse von Vulkaniten Einzelvorkommen zuzuschreiben sind oder Teile eines

großen Vorkommens, ob ein massiertes Vorkommen großer Basaltblöcke einen Schlot anzeigt oder diese durch Solifluktion oder Gletschertransport zusammengetragen wurden und einen Schlot vortäuschen.

In solchen Fällen gibt eine Vermessung der Anomalien des erdmagnetischen Feldes, wie sie vom Autor seit vielen Jahren in der Hegau-Vulkanprovinz durchgeführt wird, raschen und zuverlässigen Aufschluß. Die Feldmessungen ergaben zahlreiche Berichtigungen der Angaben in den geologischen Karten und im geologischen Schrifttum hinsichtlich des Hegauvulkanismus. Zahlreiche Deckentuffvorkommen, die unter glazialen Ablagerungen verborgen waren, konnten aufgefunden werden. Ferner konnte Form und Ausdehnung zahlreicher schon bekannter Deckentuffvorkommen näher festgelegt werden; insbesondere ergab sich dabei, daß die vielen kleinen isolierten Deckentuffvorkommen zwischen den Dörfern Duchtlingen—Hilzingen—Weiterdingen (Meßtischblatt Gottmadingen Nr. 8218) tatsächlich e i n e große Deckentuffmasse darstellen; es dürfte sich hier wahrscheinlich um das zweitgrößte Deckentuffvorkommen dieser Vulkanprovinz handeln.

Bei einer Reihe von Basaltvulkanen, die in den geologischen Karten enthalten waren, wurde keine ΔZ-Anomalie des erdmagnetischen Feldes erhalten, die von einem Schlot verursacht sein konnte. Diese Schlote verdanken ihre unberechtigte Eintragung in die geologischen Karten einem massierten Auftreten von Basaltlesesteinen, die an ihrem Fundort durch Solifluktion oder Gletschertransport gebracht worden waren. Andererseits machten ΔZ-Anomalien des erdmagnetischen Feldes auch auf eine ganze Reihe von Schloten aufmerksam, die noch nicht bekannt waren. Im nördlichen Teil der Hegauvulkanprovinz treten zahlreiche Basaltgänge auf, deren Eintragungen in den geologischen Karten aufgrund der ΔZ-Anomalien besonders häufig berichtigt werden müssen, insbesondere hinsichtlich ihrer Erstreckung.

Während es keine verbindenden vulkanischen Durchbrüche zwischen der Hegauvulkanprovinz und dem Schwäbischen Vulkan gibt, existieren solche zwischen den Vulkanprovinzen des Hegaus und des Kaiserstuhls, die vorzugsweise im Gebiet um Freiburg i. Br. liegen. Von diesen Vorkommen wurde bis jetzt nur dasjenige von Alpersbach in ΔZ vermessen. Nach Abschluß der Hegauarbeiten soll bevorzugt dieses Übergangsgebiet zwischen zwei Vulkanprovinzen untersucht werden.

Die ausführliche magnetische Untersuchung der jungen südwestdeutschen Vulkangebiete ist nur dank der Unterstützung der Deutschen Forschungsgemeinschaft möglich.

Literatur

BRANCO, W.: Schwabens 125 Vulkanembryonen und deren tufferfüllte Ausbruchsröhren; das größte Maargebiet der Erde. Jh. Ver. vaterl. Naturkde Württ., 50, 505—997 und 51, 1—337, 1894 und 1895

CLOOS, H.: Bau und Tätigkeit von Tuffschloten; Untersuchungen am Schwäbischen Vulkan. Geol. Rdsch. 21 (6—8), 709—800, 1941

Mäussnest, O.: Magnetische Untersuchungen im Gebiet des Schwäbischen Vulkans. Geol.
    Rdsch., 58, 512—520, 1969a

—: Die Ergebnisse der magnetischen Bearbeitung des Schwäbischen Vulkans. Jber. u. Mitt.
    oberrh. geol. Ver., N. F., 51, 159—167, 1969b

—: Regionalmagnetische Vermessung Mittelwürttembergs. Geol. Jb., 88, 1970

—: Magnetische Untersuchungen an einigen Förderschloten und Deckentuffen der Hegau-
    Vulkanprovinz. Oberrh. Geol. Abh., 20, 1971 (im Druck)

Meyer, G.: Erdmagnetische Untersuchungen im Kaiserstuhl. Ber. Naturf. Ges. Freiburg/Br.,
    12, 134—173, 1902

Reck, H.: Die Hegauvulkane. Berlin (Bornträger), 1923

Reich, H.: Stratigraphische und tektonische Studien im Uracher Vulkangebiet. Freiburg i. Br.
    (Speyer u. Kaerner), 1915

Reich, H., H. Closs und H. Schoene: Über magnetische und gravimetrische Untersuchungen
    am Kaiserstuhl. Beitr. Angew. Geophysik, 8, 45—77, 1940

Paleomagnetic Investigations on Igneous Rocks from the Rhön, Germany[1])

G. Bock and H. Soffel, München[2])

Summary: In the Rhön area (Germany, geographical coordinates: 50,5 °N, 10 °E) 130 samples were collected from 13 Tertiary basalt and 3 Tertiary phonolite sites for paleomagnetic measurements. The mean site direction of the natural remanent magnetization (NRM) is $I = 78^0$, $D = 30^0E$, $k = 4$, $\alpha_{95} = 21^0$. The unstable components of NRM were removed by a. c. demagnetization up to 200 Oe. Unlike the basalts, the remanence of the phonolites was completely unstable. After a. c. demagnetization the following data for the 13 basalt sites were obtained: $I = 62^0$, $D = 359^0E$, $k = 8$, $\alpha_{95} = 16^0$. A relation between rock type and direction of remanent magnetization was observed. The mean site direction of the stable component of remanent magnetization yields a virtual geomagnetic pole (VGP) with $\lambda' = 83^0N, \Phi' = 163^0W$. The semiaxes of the oval of confidence are $\delta p = 20^0$, $\delta m = 25^0$. The position of the VGP on the polar wandering curve for Europe indicates that the Rhön basalts were formed in late Tertiary which is in agreement with geological observations.

Zusammenfassung: An 13 tertiären Basalten und 3 tertiären Phonoliten der Rhön (geographische Koordinaten: 50,5° N, 10° Ost) wurde an 272 Proben aus 130 Handstücken paläomagnetische Messungen durchgeführt. Die mittlere Richtung der natürlichen remanenten Magnetisierung (NRM) aller Aufschlüsse beträgt: $I = 78^0$, $D = 30^0$ E, $k = 4$, $\alpha_{95} = 21^0$. Wechselfeld-Entmagnetisierung bis zu 200 Oe beseitigte bei den Basalten die unstabilen Anteile der NRM, wohingegen bei den Phonoliten auch mit stärkeren entmagnetisierenden Feldern keine stabile Richtung der Remanenz erhalten werden konnte. Nach der Wechselfeld-Entmagnetisierung ergab sich für die 13 Basalte folgender Mittelwert für die Richtung der Remanenz: $I = 62^0$, $D = 359^0$, $k = 8$, $\alpha_{95} = 16^0$. Zwischen Gesteinstyp und Richtung der stabilen Remanenz konnte eine Abhängigkeit gefunden werden. Der zur Richtung der stabilen Remanenz gehörende virtuelle geomagnetische Pol (VGP) hat die Koordinaten: $\lambda' = 83^0$ N, $\Phi' = 163^0$ W. Die Halbachsen der Fehlerellipse sind $\delta p = 20^0$ und $\delta m = 25^0$. Die Lage des VGP auf der Polwanderungs-Kurve für Europa deutet darauf hin, daß die Rhön-basalte im oberen Tertiär gefördert wurden. Dies steht mit geologischen Untersuchungen im Einklang.

General geological and petrological description

The Rhön is situated in the eastern part of the "Hessische Senke" which is the north eastern continuation of the Rhine Graben. The geographical coordinates are

---

50,5⁰ North, 10⁰ East. Together with the Vogelsberg area it is the most extended region of tertiary volcanic rocks in central Europe. The igneous rocks of the Rhön area are dated at the end of the Miocene and the beginning of the Pliocene [BÜCKING 1916].

With regard to the age of the Rhön volcanic rocks they can be devided into three groups according to FICKE [1961]:

1) The feldspar basalts that originated during the first eruptions.
2) Hornblende basalt, basanite, limburgite and basaltic tephrite which are members of the main eruptions.
3) Phonolites were produced at all times, but mainly during the later eruption periods.

Titanomagnetites are the dominant carriers of the remanence. The average ore grain diameter is about 40 μ. In a few ore grains exsolution lamellae of ilmenite could be detected. The measured CURIE temperatures correspond to that of titanomagnetites with $x = 0,5—0,6$.

Sampling sites and measurement of the remanent magnetization

From 16 sites situated in an area of nearly 500 km² 130 samples were collected yielding 272 specimens. With respect to the above classification of the volcanic rocks in the Rhön area the number of sites, samples and specimens are given in table 1.

The remanent magnetization of all specimens was measured with a Princeton spinner magnetometer. This instrument has been described by PHILLIPS and KUCKES [1967]. Table 2a shows the mean data of the natural remanent magnetization (NRM) obtained for all sites. (NRM, inclination i, declination d of the NRM, precision parameter k according to FISHER [1953], circle of confidence α_{95}, number N of the speci-

Table 1: Number of sites, samples and specimens in relation to the rock type

Name and number of sites	Rock type	Number of specimens: N	Number of samples: N′
4 sites: B 6—9 (Holzberg), Ko (Köpfchen), Leu (Leubach), Sch (Schwarzenacker)	feldsparbasalt	88	42
1 site: Zi (Ziegenberg)	hornblendebasalt	14	10
8 sites: B 1—5, B 10—12, B 13—16, (all Holzberg), Bi (Billstein), K (Kreuzberg), L (Leimbach), Ro (Roth), Th (Thüringer Hütte)	basanite	134	54
3 sites: P (Poppenhausen), R (Rupsroth), SW (Steinwand)	phonolite	36	24

Table 2a: Remanent magnetization before a. c. demagnetization

site	Min	NRM	Max	i	d	k	α_{95}	N	N'
B 1—5	155	458	767	+83	100	34	6,5	14	5
B 6—9	193	508	699	−28	164	2	23	17	7
B 10—12	307	453	738	+79	358	13	11	13	5
B 13—16	587	826	1268	+77	359	28	9,5	12	5
Bi	114	300	466	+68	21	63	4,5	18	5
Ko	76	192	367	0	243	2	22	18	10
K	145	317	526	+66	355	25	6	23	9
L	385	1176	2120	+62	34	40	6	14	8
Leu	85	300	724	+55	181	2	28	24	10
P	14	60	153	+75	14	2	20	21	12
Ro	50	175	298	+12	125	4	21	13	6
R	2	32	92	+83	277	17	11	11	8
Sch	53	426	2842	−27	159	1	22	29	15
SW	1	3	6	+41	244	2	46	4	4
Th	180	348	494	+66	11	17	7	27	10
Zi	55	282	455	+41	162	14	10	14	10
mean:		366		+78	30	4	21		

Table 2b: Remanent magnetization after a. c. demagnetization

site	Min	RM	Max	i	d	k	α_{95}	N	N'	H_{eff}
B 1—5	32	89	147	+82	135	146	3	14	5	150
B 6—9	227	641	876	−40	162	13	10	14	5	100
B 10—12	151	206	319	+83	12	120	4	13	5	150
B 13—16	134	427	626	+85	19	161	3	12	5	150
Bi	12	16	20	+53	42	22	8	18	5	200
Ko	106	166	224	−62	212	77	4	12	10	150
K	37	67	84	+53	339	40	5	23	9	200
L	107	393	895	+57	29	30	7	14	8	150
Leu	28	52	125	−55	143	11	9	24	10	150
P	unstable									
Ro	40	83	143	−46	123	77	4	13	6	150
R	unstable									
Sch	70	207	616	−68	171	31	5	25	13	200
SW	unstable									
Th	23	68	144	+48	43	8	10	27	10	150
Zi	43	208	321	+ 9	161	8	15	14	10	150
mean:		202		+62	359	8	16			

Min: lowest value, NRM (or RM): average value, Max: highest value of remanent magnetization, all in 10^{-5} Gauss.
i: mean inclination and d: mean declination. k: precision parameter. α_{95}: circle of confidence. N: number of specimens. N': number of samples H_{eff}: strength of the demagnetizing field in Oe.
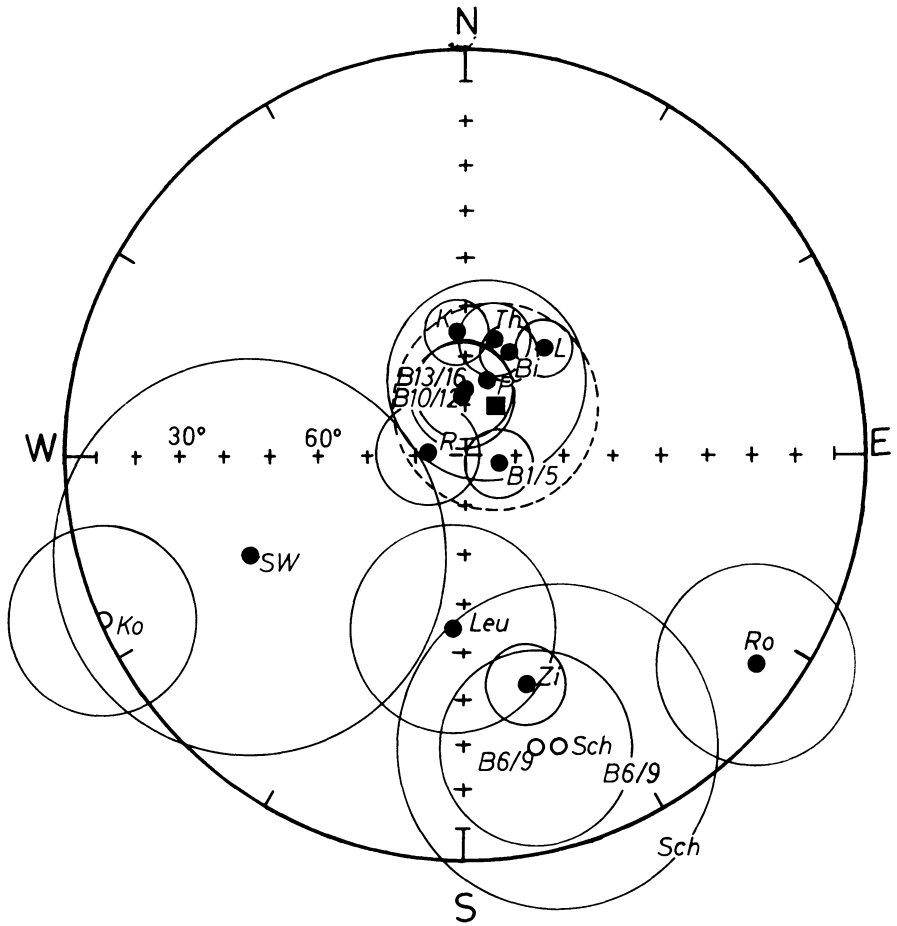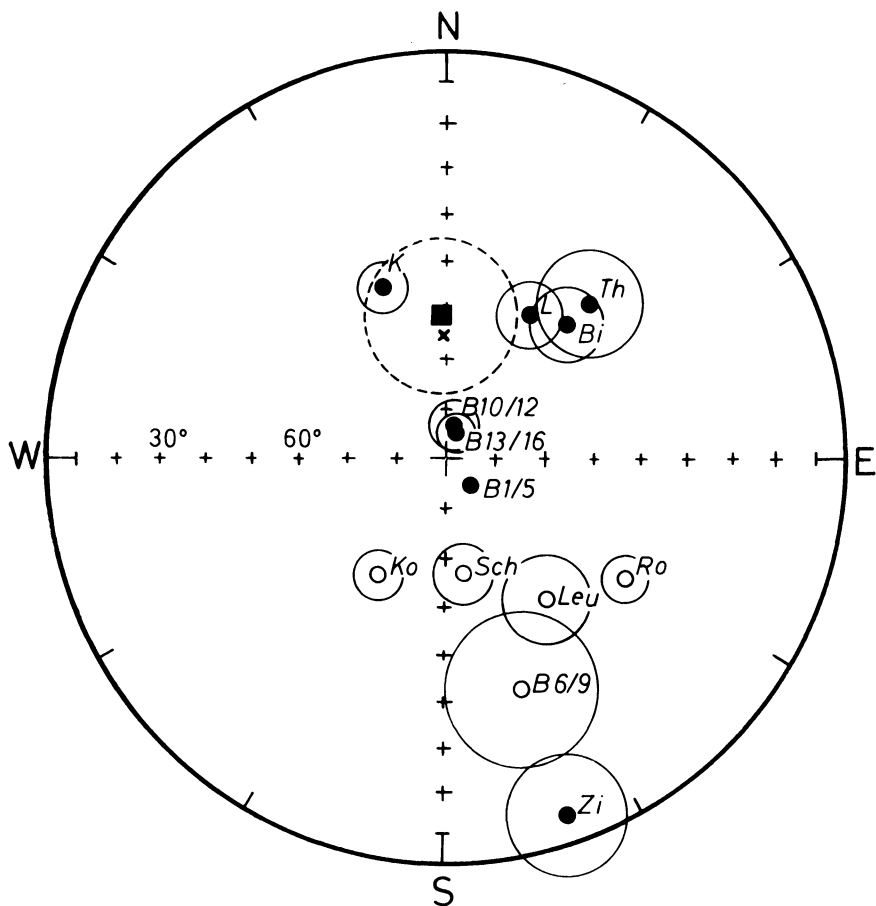
Fig. 1: Directions of remanent magnetization of 16 sites before a. c. demagnetization in equal
     area projection. Closed circles: inclination downward. Open circles: inclination up-
     ward. Square: mean direction of all sites.

mens and N' of the samples.) In some sites the specimen directions of the NRM are
randomly distributed (low k). In most cases the α_{95} are larger than 10^0.

   The stability of the NRM was tested by means of progressive a. c. demagnetization.
This showed that all the basalt specimens carried a viscous remanent magnetization
(VRM) in the direction of the present geomagnetic field. The VRM was removed by
alternating fields between 100 and 200 Oe. Unlike the basalts the remanence of the
phonolites was unstable. No fossil remanent magnetization direction could be ob-
tained after a. c. demagnetization.

Fig. 2: Directions of remanent magnetization of 13 basalt sites after a. c. demagnetization with 100—200 Oe in equal area projection. Closed circles: inclination downward. Open circles: inclination upward. Square: mean direction of all sites. Cross: direction of present geomagnetic field.

Table 2b shows the remanence data for the basalts after a. c. demagnetization with 100—200 Oe. The average intensity of remanent magnetization dropped to $202 \cdot 10^{-5}$ Gauss. Comparing table 2a with 2b as well as Fig. 1 with Fig. 2 it can be seen that a. c. demagnetization produced a better grouping of the remanence directions. α_{95} is in most cases smaller than 10^0.

There seems to be a relation between rock type and direction of the remanent magnetization. The feldspar basalts are all reversely magnetized, while the basanites (with the exception of site Ro) are normally magnetized. The hornblende basalt from
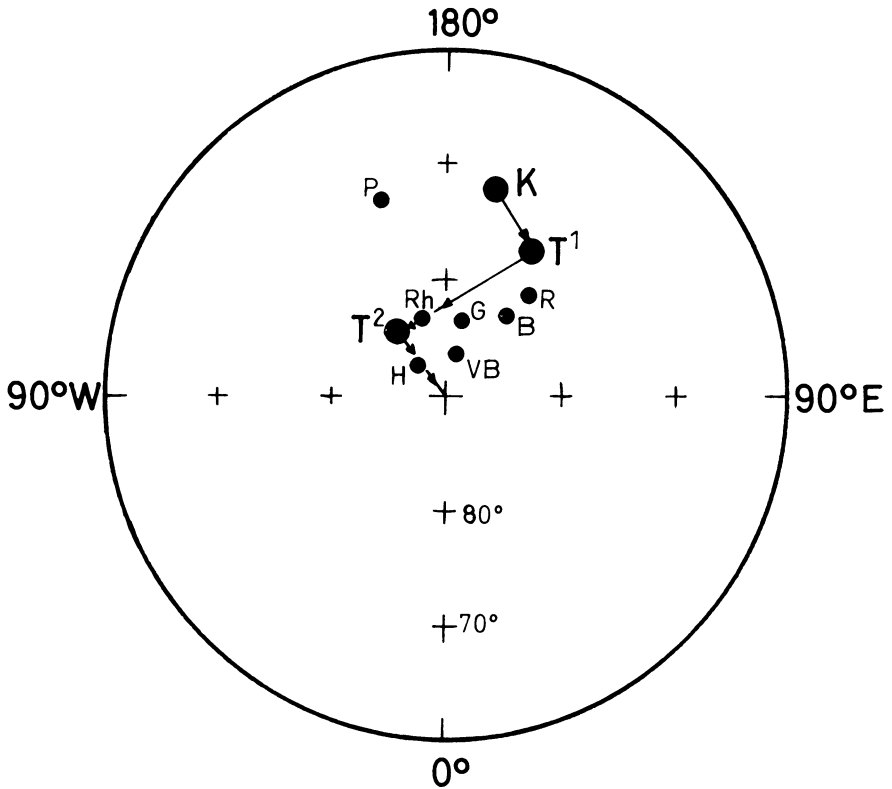
Fig. 3: Part of the polar wandering curve for Europe for Cretaceous (K), Lower Tertiary (T^1) and Upper Tertiary (T^2) according to IRVING (1964). Rh: VGP position of the Rhön basalts. Other Tertiary pole positions (P: Parkstein, B: Siebengebirge near Bonn, G: basalts near Göttingen, H: Habichtswald, R: Ries, VB: Vogelsberg) are cited by SOFFEL and SUPALAK (1968).

Ziegenberg (Zi) displays an intermediate direction and has been dated by geologists between the feldspar basalts of the first eruption period and the basanites of the main eruption.

Paleomagnetic result

The mean direction of the stable component of the remanent magnetization (see table 2b) and the coordinates of the Rhön area ($\lambda = 50,5^0$N, $\Phi = 10^0$E) yield a virtual geomagnetic pole (VGP) with $\lambda' = 83^0$N, $\Phi' = 163^0$W. The error in the declination is $\delta m = 25^0$, the error in the ancient colatitude is $\delta p = 20^0$. The paleomagnetic

result (Fig. 3) is in good agreement with other results from Tertiary in Europe [cited by SOFFEL and SUPALAK 1968 and by MCELHINNY 1970]. According to the polar wandering curve for Europe, the Rhön basalts were formed in late Tertiary, which is in agreement with geological observations.

Acknowledgement

References

BÜCKING, H.: Geologischer Führer durch die Rhön. Borntraeger, Berlin, 1916

FICKE, B.: Petrologische Untersuchungen an tertiären basaltischen bis phonolithischen Vulkaniten der Rhön. Tsch. Miner. Petr. Mitt. Wien, 7, 1961

FISHER, R. A.: Dispersion on a sphere. Proc. Roy. Soc. (London) A 217, 295−305, 1953

IRVING, E.: Paleomagnetism and its Application to Geological and Geophysical Problems· John Wiley and Sons, Inc. New York, 1964

MCELHINNY, M. W.: Notes on Progress in Geophysics, Paleomagnetic Directions and Pole Positions XI. Geophys. J. 20, 417−429, 1970

PHILLIPS, J. D., and A. F. KUCKES: A Spinner Magnetometer. J. Geophys. Res. 72, 2209 to 2212, 1967

SOFFEL, H., and P. SUPALAK: Paläomagnetische Messungen am Basalt vom Parkstein bei Weiden. Z. Geophys. 34, 287−296, 1968

Rockmagnetic Studies on Ophiolites from Montgenevre
(French-Italian Alps)
Preliminary data

J. J. Wagner, Geneva[1])

Summary: Thermomagnetic properties of ophiolites from Montgenèvre (French-Italian Alps) have been investigated. Pillow lavas contain optically homogeneous "titanomagnetite". They have a similarity to a dredged pillow lava from the sea. Serpentinites have irreversible changes in the saturation magnetization; the Curie temperature is near that of pure magnetite.

Zusammenfassung: Es wurden die thermo-magnetischen Eigenschaften von Ophioliten vom Montgenèvre (Französisch-Italienische Alpen) untersucht. Die Pillow-Laven vom Montgenèvre führen optisch homogene Titanomagnetite und zeigen große Ähnlichkeiten mit den in jüngster Zeit vom Meeresboden gesammelten Pillow-Laven. Die Serpentinite besitzen Curie-Temperaturen nahe dem von reinem Magnetit, jedoch treten bei dieser Messung irreversible Änderungen der Sättigungsmagnetisierung auf.

Introduction

The purpose of this investigation is to use rockmagnetic properties in an attempt to make a correlation between the different ophiolite sites. Under the name of ophiolite, the alpine geologist groups basic and ultrabasic rocks of Mesozoic age associated with sediments of the Alpine geosyncline [Vuagnat 1963]. Further, most of these rocks are metamorphic, e. g. green schist and amphibolite facies. We also find a few small masses of ophiolite which are undeformed, with primary structure extremely well preserved; they form a group of apparently non metamorphic ophiolites. Such masses, suitable for rockmagnetic investigation, are found at several places in the Alps. Those of the Montgenèvre Massif are the first to be investigated.

Geological Setting

The Montgenèvre Massif is the largest remnant of apparently non metamorphic ophiolites in the Alps from the Mediterranean Sea to Vienna [Vuagnat 1953]. Geographically, it straddles the French-Italian border between Briançon, in France, and Cesana-Torinese, in Italy. It is important to mention the fact that this massif is a downfaulted block limited on the north and the south by major transverse faults.

---

[1]) Dr. J. J. Wagner, Geophysical Laboratory, University of Geneva, Switzerland.

It is very probably due to this downfaulting that these ophiolites have been preserved undeformed.

Petrology of the Ophiolites

The three usual types of ophiolites are "diabases", gabbros and serpentinites.

"Diabases" are represented by pillow basalts and dikes. The former, which constitute the main part of the massif, are submarine lava flows, but they do not exhibit a strong spilitic character except in one place where we find spilites with hematite. The pillowy flows are cut by coarse grained diabase dikes.

The gabbros are typical alpine gabbros; the most common mineral assemblage is more or less altered plagioclase and diallage. Their grain size changes rapidly from place to place; in the Montgenèvre they are rather coarse. These rocks are also cut by dikes of diabase.

The third type of ophiolite, the serpentinites, is well represented in the eastern part of the massif in Italy. They frequently consist entirely of minerals of the serpentine group. It is certain that they are derived from peridotites; in some of the more massive parts the primary banding is still visible.

Relationship between the Three Groups of Ophiolites

It is very difficult as elsewhere in the Alps, to see existing relationships between the three rock types. However, if diabase dikes in the gabbros are feeder dikes of the lavas, it could seem likely that the basalts flowed out on a basement of consolidated gabbros. The contact between the serpentinites and the other ophiolite types seems always to be tectonic.

Metamorphism

The term "apparently" non metamorphic ophiolites has been used deliberately. In general, in the past, undeformed rocks with preserved fine texture were considered to have escaped the effects of alpine regional metamorphism. The presence of some zeolites, prehnite, epidote and alteration of calcic plagioclase indicates that the ophiolites under study have been affected by low grade metamorphism [PUSZTASZERI 1969].

Origin

The pillow lavas and the diabase dikes are a remnant of an extensive submarine volcanic formation of probable Upper Jurassic to Cretaceous age [VUAGNAT and PUSZTASZERI 1966]. The relationship between gabbros and pillow lavas is still uncertain. Serpentinites are tectonic slices from deepseated ultramafic bodies or maybe from the upper mantle. These ultramafic slices were serpentinized during their ascent in the alpine tectogene.

Problems in Relation to Rockmagnetism

Several problems arise from geological and petrological considerations. As the "diabases" present in the Montgenèvre area are found as pillow lavas or as dikes in pillow lavas and gabbros, it would be interesting to analyze to magnetic properties of these rocks and compare the results to see if they support the proposed correlation. But before we can reach this stage, there are two basic problems.

The first is to investigate the homogeneity of the magnetic data obtained from one pillow and those obtained from a large number of pillows, and the second is to see how low grade metamorphism has affected the primary magnetization of the "diabase".

Lastly, with regard to the serpentinites, it would be interesting to study the magnetic properties and their relation to the serpentinization process and the original banding.

Preliminary Results

Magnetic properties of pillow lavas:

A detailed study from a dredged pillow in the Scotia Sea by WATKINS, PASTER, and ADE-HALL [1970] gives a basis with which to compare the same type of material from the Montgenèvre. They observed several features from the border to the center of a pillow; the titanomagnetites were optically homogeneous, and the grain size increased from below the glassy rim to a maximum in the aphanitic interior. The CURIE temperature varied through the structure, with a mean value around 300^0C; the maximum was reached at the bottom of the aphanitic part. The magnetic stability, deduced from alternating field demagnetization, was high.

The preliminary samples investigated in the Montgenèvre seem to confirm this magnetic behaviour. The thermomagnetic curve (Fig. 1) shows that our specimens underwent irreversible changes on heating in air. The ratio of the saturation magnetization before and after heat treatment is always larger than two. This agrees with the observations of OZIMA, OZIMA and KANEOKA [1968], who noticed a large increase of J_s after heating for submarine basalts. In general, the type of thermomagnetic curves obtained is that of homogeneous titanomagnetite with low CURIE temperature of the order of 300^0C and the development of a new magnetic phase at 450^0C [CREER and PETERSEN 1969; CREER, NOZHAROV, and WAGNER 1970].

Magnetic properties of serpentinites:

SAAD [1969], by pointing out that serpentinized peridotites may have a highly stable chemical remanent magnetization (CRM) and are paleomagnetically reliable, gave us the idea to test some of our serpentinites which were originally peridotites. The CRM is acquired during the process of serpentinization whereby iron atoms, released from silicate structure of paramagnetic olivine and pyroxene, are oxidized to form ferrimagnetic magnetite.
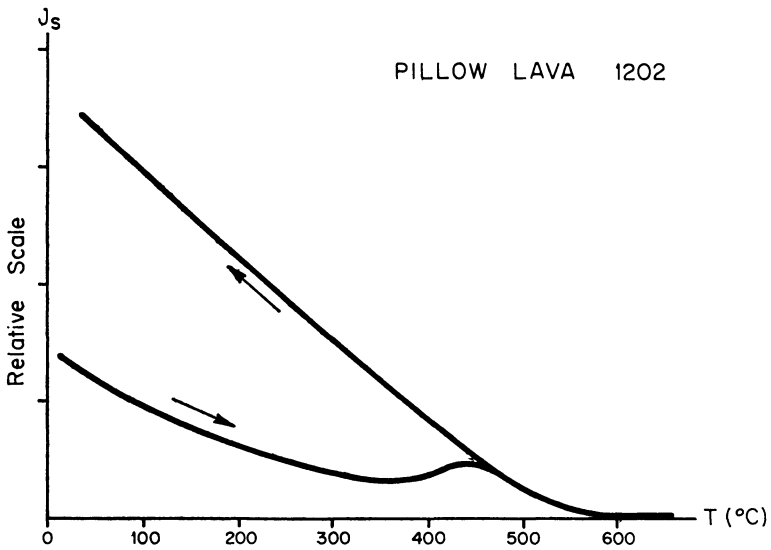
Fig. 1: Typical example of the thermomagnetic behaviour from a basalt pillow during heating and cooling. Magnetization is measured in arbitrary units.
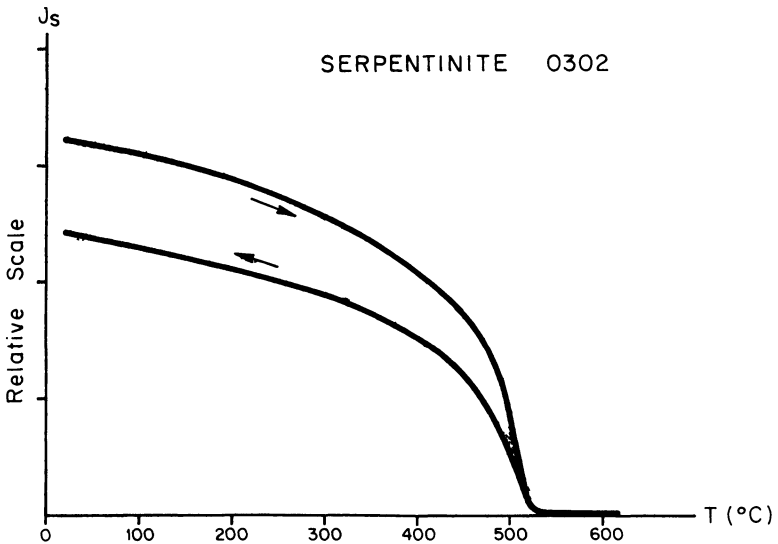

Fig. 2: Thermomagnetic curve during heating and cooling on a serpentinite specimen. Magnetization is measured in arbitrary units.

The development of the serpentinization gives rise to the growth of magnetite grains, and the natural remanent magnetization (NRM) therefore increases but with a loss of stability. Thermomagnetic measurements have been carried out on several samples from different sites. For all, the CURIE temperature is between 525 and 550⁰C, near that of pure magnetite. The thermomagnetic curves are irreversible (Fig. 2); the cooling saturation intensity is lower than the heating one.

Conclusions

As we are at the beginning of a detailed investigation, it is difficult to evaluate results thus far. Nevertheless, one may point out the similarity of the magnetic behaviour of the Montgenèvre pillow lavas with the dredged one from the Scotia Sea, which may confirm the submarine formation of alpine pillowy flows.

In the thermomagnetic work on serpentinites, the CURIE temperatures indicate similar type of nearly pure magnetite at different sites. Whether this indicates more than similar alteration history remains to be seen.

Acknowledgments

References

CREER, K. M., and N. PETERSEN: Thermochemical Magnetization in Basalts. Z. Geophys., 35, 501—516. 1969

CREER, K. M., P. NOZHAROV and J. J. WAGNER: Paleomagnetic and Rock Magnetic Studies on Some Bulgarian Plio-Paleocene Basalts. Pure and Applied Geoph., 82, 1970

OZIMA, M., M. OZIMA and I. KANEOKA: Potassium-Argon ages and magnetic properties of some dredged submarine basalts and their geophysical implication. J. Geophy. Res., 73, 711—723, 1968

PUSZTASZERI, L.: Etude pétrographique du massif du Chenaillet Hautes-Alpes, France, Bull. suisse de Minér. Pétrogr. 49, 426—468, 1969

SAAD, A. H.: Magnetic Properties of Ultramafic Rocks from Red Mountain, California, Geophysics, 34, 974—987, 1969

VUAGNAT, M.: Sur un phénomène de métasomatisme dans les roches vertes du Montgenèvre, Hautes Alpes, Bull. Soc. Franc. Minér. Crist., 76, 438—450, 1953

VUAGNAT, M.: Remarques sur la trilogie serpentinites-gabbros-diabases dans le bassin de la Méditerranée occidental. Geol. Rundsch., 53, 336—358, 1963

VUAGNAT, M., and L. PUSZTASZERI: Réflexion sur la structure et le mode de formation des coulées en coussins du Montgenèvre, Hautes Alpes. Arch. Sc. Genève, 18, 120—123, 1965

WATKINS, N. D., T. PASTER and J. ADE-HALL: Variation of the Magnetic Properties in a single deep-sea pillow basalt. Earth Planet. Sci. Letters, 8, 322—328, 1970

SEISMISCHE MESSUNGEN UNTER TAGE

VORFELDAUFKLÄRUNG IM KOHLEBERGBAU

SALZRAND-BESTIMMUNGEN

ERKUNDUNG VON ERZLAGERSTÄTTEN